The role of annexin II in vesicle traffic.

Christien James Merrifield

Department of Physiology
University College London
Gower Street
London WC1E 6BT

Thesis submitted to the Univerisity of London
for the degree of Doctor of Philosophy

February 1999

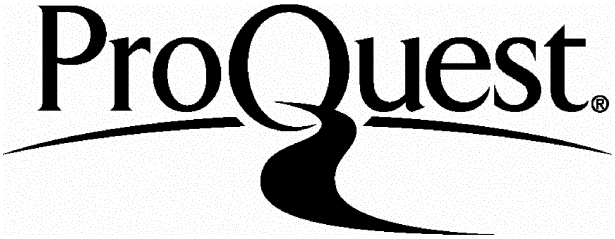

Abstract.

The annexins are a family of proteins that bind acidic phospholipids in the presence of Ca^{2+}. The association of these proteins with the membranes of secretory granules and endosomes indicates these proteins may play a role in membrane trafficking. One member of the family, annexin II, can exist either as a monomer, heterodimer or heterotetramer in conjunction with the S100 protein p11. The ability of annexin II tetramer to bind both membranes and actin in a Ca^{2+}-dependent manner has led to the hypothesis that annexin II may mediate between vesicle and/or plasma membranes and the cortical cytoskeleton. However, despite intensive biochemical characterisation *in vitro*, the function of this protein *in vivo* remains a mystery.

In this study annexin II function in living cells was analysed in several different ways using green fluorescent protein (GFP) in full length annexin II-GFP chimeras and chimeras consisting of fragments of annexin II fused to GFP. Transfection of different cell lines with these annexin II-GFP constructs and fluorescence assisted cell sorting (FACS) allowed the generation of multiclonal cell populations expressing annexin II-GFP fusion proteins. These cell populations were analysed for effects on physiological functions - such as secretion (in the RBL cell line) or differentiation (of the PC12 cell line). This line of investigation did not yield evidence to support a role for annexin II in either of these processes. Using novel forms of microscopy the localisation of a full length annexin II-GFP chimera (NAII-GFP) was followed in single cells under physiological conditions. Under conditions of stress NAII-GFP was found to become incorporated into novel actin based structures, reminiscent of *Listeria* rockets, which propelled pinosomes through the cell interior. This form of vesicle locomotion is dependent on actin polymerisation and may represent a hitherto unrecognised form of vesicle transport.

Table of contents.

List of figures.

List of tables.

Abbreviations.

ABM	actin based motility
AP	alkaline phosphatase
BAPTA-AM	1/2-bis(0-aminophenoxy)ethane-N,N,N',N'-tetraacetic acid tetra(acetoxy-methyl) ester
BSA	bovine serum albumin
CMV	cytomegalovirus
CURL	ompartment of uncoupling of receptor
DIG	detergent-insoluble glycosphingolipid rich membrane domains
DMEM	Dulbecco's modified Eagle medium
DMSO	dimethyl sulfoxide
DTT	dithiothreitol
ECL	enhanced chemi-luminescence
EGF	epidermal growth factor
EGFr	epidermal growth factor receptor
EGTA	ethyleneglycol-bis(β-aminoethylether)-N,N,N',N'-tetraacetic acid
FACS	fluorescence activated cell sorting
FCS	foetal calf serum
FITC	fluoroscein isothyiocyanate
GTP	guanosine 5'-triphosphate
H_2O_2	hydrogen peroxide
HBS	HEPES buffered saline
HBV	Herpes B Virus
HEPES	N-2-hydroxyethylpiperazine-N'-2-ethane sulphonic acid
HRP	horseradish peroxidase
HRP	horseradish peroxidase
HSP 27	heat shock protein 27
IgE	immunoglobulin E
IgG	immunoglobulin G
MAPK	mitogen activated protein kinase
MAPKK	mitogen activated protein kinase kinase
MAPKKK	mitogen activated protein kinase kinase kinase
MTOC	microtubule organising centre
MVB	multi-vesicular body
NGF	nerve growth factor
p120GAP	p120 GTPase activating protein
PAK 1	p21-activated kinase 1

PBS	phosphate-buffered saline
PBS-T	PBS containing 0.05% Tween-20
PCR	polymerase chain reaction
PDGF	platelet derived growth factor
PDGFr	platelet derived growth factor receptor.
PI(3,4,5)P3	phosphatidylinositol-(3,4,5)-triphosphate
PI(4,5)P2	phosphatidylinositol-(4,5)-bisphosphate
PI-PLC	phosphatidylinositol phospholipase C
PI3K	phosphatidylinositol-3-kinase
PIP	phosphatidylinositolphosphate
PKC	protein kinase C
PLA_2	phospholipase A_2
PMA	phorbol 12-myristate 13-acetate
PMA	phorbol-12-myristate-13-acetate
PMSF	phenyl-methyl-sulfonyl-fluoride
PVDF	polyvinyl difluoride
RACK	receptor for activated C kinase
RRC	receptor recycling compartment
SDS	sodium dodecylsulphate
SDS-PAGE	SDS-polyacrylamide gel electrophoresis
SNAP	soluble NSF attachment proteins
SNARE	soluble N-ethylmaleimide-sensitive fusion protein attachment protein receptor
t-PA	tissue plasminogen activator
Tfr	transferrin receptor
Tris	tris(hydroxymethyl)methylamine
TRITC	tetramethylrhodamine isothyocyanate
WASP	Wiskot Aldrich syndrome protein

Acknoweledgements.

I would like to thank Dr. Steven Moss for his supervision and help, and the various members of his group at the Department of Physiology, University College London for their advice and and moral support.

I would also like to thank Prof. Wolfhard Almers, Max Plank Institut fur medezinische forschung, Heidelberg for providing access to the evanescent wave microscope and for being such a hospitable host. Also Thorsten Lang and the other members of the group in Heidelberg for making my stay there so enjoyable and introducing me to German beer.

1. Chapter 1 : Introduction.

1.1 Ca^{2+} - the ubiquitous intracellular messenger.

The first clue that Ca^{2+} might be involved in cellular function came over 100 years ago in 1883 when Sydney Ringer discovered that Ca^{2+} salts in the bathing fluid are essential to maintain contractions in the isolated heart. Since this discovery Ca^{2+} has been found to be involved in almost every facet of cellular life - from control of metabolism to cell locomotion and from control of gene expression to cell adhesion. As might be expected, this plethora of functions implies a corresponding diversity of sensors, effectors and modulators to interpret and act on the Ca^{2+} signals controlling these processes - reflected in the array of Ca^{2+} binding proteins identified to date. Only a fraction of these proteins have a clear function assigned to them. Among those Ca^{2+}-binding proteins whose functions remain enigmatic are the annexins, a discrete multigene family characterised by their ability to interact Ca^{2+}-dependently with membrane phospholipids. Due to their Ca^{2+}-dependent association with both biological and synthetic membranes, and their ability to aggregate membranes and vesicles *in vitro*, annexins have received considerable attention in the drive to elucidate membrane trafficking events *in vivo*. Particular attention has focused on possible roles in both exocytosis and endocytosis and one annexin in particular, annexin II, is now closely linked with both processes.

This introduction aims to familiarise the reader with the annexin family, illuminate those aspects of annexin biology relevant to possible roles in membrane trafficking and evaluate some of the new techniques available to analyse annexin function *in vivo*. Throughout the introduction particular emphasis will be given to annexin II - the subject of this thesis.

1.2 Molecular structure of the annexins.

1.2.1 The annexin core domain.

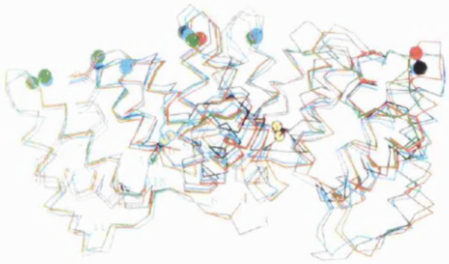

Figure 1.1: Overlaid ribbon diagrams of the core domain of three annexins.

Annexins I (blue), II (black) and V (green: low calcium bound form; red: high Ca^{2+} bound form) seen from the molecule side. The calcium ions are shown as spheres in the colours of the associated proteins. The cystine 297-316 of annexin I and the cystine 133-262 of annexin II are drawn as yellow spheres. Overlay of the four core structures illustrates the conserved topology of the annexin core. (Taken from Liemann and Huber, 1997).

Members of the annexin family are defined by the presence of a characteristic core which is responsible for association with both Ca^{2+} and phospholipids. This core was initially defined by its resistance to proteolysis (Glenney, 1986a; Glenney and Tack, 1985; Johnsson and Weber, 1990) and subsequent sequence analysis revealed the core to consist of four tandemly repeated segments, 70-80 amino acids in length. The conserved annexin repeats show both intramolecular and intermolecular homology (Morgan and Fernandez, 1995). The three dimensional folding of the core domain - revealed by X-ray crystallography - is also highly conserved between annexins V, I, II, III, VI and XII (Burger et al., 1996; Concha et al., 1993; Favier Perron et al., 1996; Huber et al., 1990ab; Lewit Bentley et al., 1992; Luecke et al., 1995; Weng et al., 1993) and forms a characteristic compact, slightly curved disc with the four annexin repeats forming four domains (Figure 1.1).

The domains are arranged in a cyclic array with repeats 1 and 4, and 2 and 3 associating tightly through hydrophobic side chain interactions (see Liemann and Huber, 1997). The centre of the molecule, separating the 1/4 and 2/3 domains is a hydrophilic pore proposed to be an ion conductance channel. This is thought to be the structural basis for the Ca^{2+} channel activity displayed by some annexins *in vitro* (for reviews see Demange et al., 1994; Moss, 1995).

1.2.2 Ca^{2+}-binding and Ca^{2+}-dependent membrane association.

Each annexin repeat consists of five α-helices (a-e) wound in a tight right-handed superhelix. Short loops connect the helices and those extending from the more convex side of the curved disc are involved in Ca^{2+} complexation (see Figure 1.1). Two types of Ca^{2+} binding site have been identified in annexin crystals - termed type II and type III binding sites to distinguish them from EF hand (or type I) Ca^{2+} binding sites of (for example) troponin C (Weng et al., 1993). In the case of annexin II the functionality of these binding sites has been further analysed through mutagenesis (Jost et al., 1992; Jost et al., 1994; Thiel et al., 1992).

Ca^{2+} is coordinated in the type II site by the three carbonyl oxygens of the peptide bonds located in the loop connecting helices a and b to the carboxyl oxygens of an aspartate or glutamate residue found at the loop connecting helices d and e of an annexin repeat. Only three proteinaceous oxygen ligands are present for Ca^{2+} coordination in the type III binding site and these are usually one carbonyl and two nearby carboxylate oxygens. The net result of Ca^{2+} binding is the presentation of four Ca^{2+} ions at the convex face of the annexin core domain which coordinate not only to the protein but also to the phosphoryl moieties of membrane phospholipids. Ca^{2+} -mediated membrane binding does not grossly alter the conformation of the molecule, except in the case of annexin VI which comprises eight annexin repeats in two core domains. Upon membrane binding the two core domains rotate about 90^0 and lie along the plane of the membrane (Benz et al., 1996; Kawasaki et al., 1996). Different members of the annexin family have different calcium sensitivities and phospholipid specificities (see Table 1.1 below).

Table 1.1: The Ca^{2+} concentrations (μM) required to promote half-maximal binding of a variety of annexins to different phospholipids.

	Annexin	***I***	***II(m)***	***II(t)***	***III***	***IV***	***V***	***VI***	***VII***
Lipid									
PS		1.3	0.65	<0.1	8.8	2.4	16	2	-
PA		0.6	0.2	-	1.2	0.95	1.2	0.55	-
PI		2.0	1.3	-	89	4.4	130	34	-
PE		n.b.	n.b.	-	170	5.2	170	33	-

These values have been taken from a single report by Blackwood and Ernst (Blackwood and Ernst, 1990). Abbreviations: PS, phosphatidylserine; PA, phosphatidic acid; PI, phosphatidylinositol; PE, phosphatidylethanolamine; "n.b." denotes no binding.
II(m), annexin II (monomer); II(t), annexin II (tetramer)

The different Ca^{2+} and phospholipid binding affinities of different annexins could be related to the finding that the number and exact location of the individual Ca^{2+} binding sites differ between members of the family (Benz et al., 1996; Burger et al., 1996; Favier Perron et al., 1996; Huber et al., 1990b; Kawasaki et al., 1996; Luecke et al., 1995; Weng et al., 1993). In addition the N-terminal domain of each annexin may also influence the biochemical properties of the core domain through phosphorylation and association with protein ligands, as discussed below.

1.2.3 The N-terminal domain of the annexins

In contrast to the conserved structure of the annexin core, the N-terminal tail domains of different members of the annexin family are highly variable. Such heterogeneity is thought to reflect specificity of function for different members of the family. The N-terminal domain (known as either head or tail) is sensitive to limited proteolysis and differs widely in length from between 12 and 19 amino acids (annexins III, IV, V, VI, X, XII, XIII) to more than 100 amino acids (annexins VII and XI) (for review see Raynal and Pollard, 1994). As well as directly modulating the biochemical properties of the annexin core, the N-terminus may also harbour the binding site for protein ligands (annexin I, annexin II) or post-translational modifications (annexin I, annexin XIII) (see Figure 1.2, overleaf).

Modulation of the properties of core domains' by the N-termini could be due to direct intramolecular interactions between the N-terminal domains and the protein cores in the longer tailed annexins, or reflect conformational modulation of the protein core. For example, removal of the N-terminal domain in annexins I and II leads to an increased affinity for Ca^{2+} and phospholipid (Ando et al., 1989; Liu et al., 1995b; Powell and Glenney, 1987). In the case of annexin I an increase in the affinity of the protein for calcium has also been observed in the presence of an antibody to the N-terminus of the protein (Glenney and Zokas, 1988) whereas such antibodies abrogate annexin I mediated vesicle aggregation (Ernst et al., 1991). Binding of protein ligands to the N-terminus can also modulate the core domain. For instance, binding of p11 to the N-terminus of annexin II and formation of an annexin II_2p11_2 heterotetramer greatly reduces the Ca^{2+} requirement for membrane association (Powell and Glenney, 1987).

As well as modulating the membrane association of the core domain, the N-terminal domain may itself be directly involved in membrane targeting. For instance, Ca^{2+}-independent targeting of annexin II to early endosomes requires residues 15-24 (Jost et al., 1997). These findings hint that at least in some cases annexin/membrane interactions may

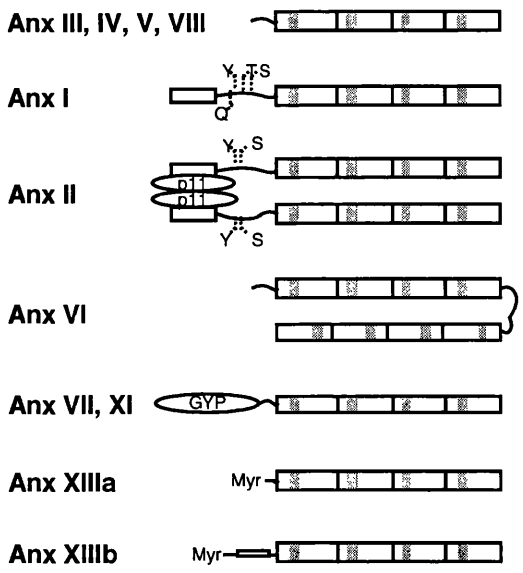

Figure 1.2: Overview of structural organisation of different annexins.

Known vertebrate annexins are classified according to structural characteristics of their N-terminal domains. Annexin repeats are represented by large open repeats while the conserved 17 amino acid endonexin fold is shaded. The small N-terminal boxes for annexins I and II represent the amphipathic α-helical S100 binding sites. Phosphorylation sites for serine (S), threonine (T) and tyrosine (Y) specific kinases, and the glutamine (Q) transglutamination site for annexin I are shown. The GYP domain indicates a glycine-tyrosine-proline rich domain proposed to form a pro-beta helix. Annexin XIII has N-terminal splice variants (a and b) similar to some other annexins but is the only annexin so far to be N-terminally mysitoylated (Taken from Gerke and Moss, 1997).

be more complex than simple Ca^{2+}-dependent association of the core domain with membrane phospholipids, and may involve other (unidentified) protein or lipid moieties (see 1.4 Interaction of annexins with biological and synthetic membranes.).

A further indication that the N-terminal region is important in the regulation of annexins is that this region often harbours phosphorylation sites for protein kinases including protein kinase C (PKC; annexins I and II), epidermal growth factor receptor (EGFr; annexin I) and $pp60^{src}$ (annexin II). Phosphorylation has been shown to have a modulatory effect both on the Ca^{2+}-dependent association of these annexins with membranes, and on the association of annexin II with F-actin (Hubaishy et al., 1995) (see 1.4 Interaction of annexins with biological and synthetic membranes., 1.6 Annexins and the cytoskeleton.). Although the effects of phosphorylation on the biochemical characteristics of these annexins have been extensively documented *in vitro*, the role such modifications play *in vivo* is unclear, with even less known of the interplay between different kinases in annexin function.

As well as phosphorylation other types of post-translational modifications are likely to be of regulatory importance. For example the N-terminal domain of annexin I has a glutamine residue at position 18 which is the site for a transglutaminase cross link to another annexin I chain. The resulting annexin I homodimer has an enhanced sensitivity for phospholipid binding and associates with A431 cellular membranes in a Ca^{2+}-independent manner (Ando et al., 1991; Pepinsky et al., 1989). In the case of annexin XIII Ca^{2+}-independent membrane association is achieved through N-terminal myristoylation (Wice

and Gordon, 1992). Whether myristoylation or the attachment of other lipid moieties is also relevant in the membrane association of other annexin family members remains to be seen.

The amino acid sequences of annexins have yielded important clues to possible annexin function *in vivo*, a feature illustrated by close examination of annexin II (Figure 1.3).

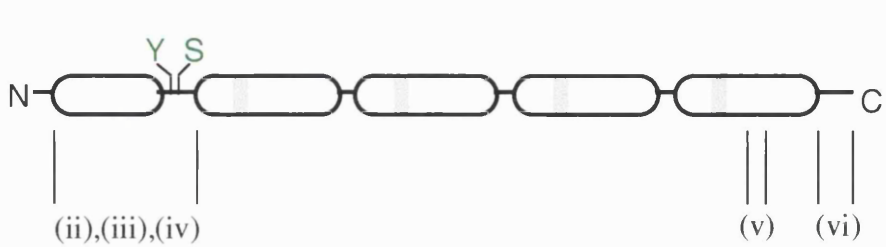

(ii)	S T V H E I L C K L S L E G D H S T P P S A Y G S V K A	
(iii)	S T V H E I L C K L S L E G D H S T P P S A Y G S V K A	
(iv)	A K K T Y D L F K K L L L I G D	Rab 10
	M T S R K K V L L K V I I L G D	Rab 7
	A K T Y D Y Y L F K L L L I G D	Rab 8
	A K T Y D Y Y L F K L L L I G D	Rab 8b
	S T V H E I I L C K L S L E G D	Annexin II
(v)	V L I R I M V S R	
(vi)	K G D Y F R Y L S E V A S G D N	14-3-3 β
	K G D Y Y R Y L A E V A T G E K	14-3-3 γ
	K G D Y H R Y L A E V A T G N D	14-3-3 ε
	K G D Y Y R Y L A E V A A G D D	14-3-3 ζ
	K G D Y Y R Y L A E V A S G E K	14-3-3 η
	K G D Y Q K A L L Y L C G G D D	Annexin II

Figure 1.3: Summary of annexin II structure.

(a)(i) Each repeat of the annexin core contains a 17 amino acid annexin consensus sequence (grey boxes). The core harbors the phospholipid and F-actin binding sites of the molecule. The first 30 residues comprise the amino terminal domain which contains the p11 subunit binding site (red), the serine phosphorylation site for PKC (S)[(1)] and the tyrosine phosphorylation site for pp60$^{c\text{-}src}$ (Y)[(2)]. The N-terminal domain is involved in the regulation of the membrane and F-actin binding and bridging activities of the annexin core. (b) Summary of key binding sites and conserved regions of homology unique to annexin II which have been mapped (see text for references): (ii) N-terminal p11 binding site (residues 1-14)[(3)] (red). (iii) N-terminal domain responsible for Ca^{2+}-independent targeting to early endosomes (residues 15-24)[(4)] (red). (iv) conserved region of homology to the N-terminal of rab proteins in the N-terminal domain (from residues 1-16)[(5)] (blue) (v) C-terminal F-actin binding site (residues 286-294)[(6)] (vi) C-terminal conserved region of homology to 14-3-3 proteins (from residues 323-338, also see Figure 1.6, 33)[(7)] (blue). Sources: [1](Jost and Gerke, 1996), [2](Isacke et al., 1986), [3](Kube et al., 1992), [4](Jost et al., 1997), [5](Upton, 1994), [6](Jones et al., 1992), [7](Roth et al., 1993), [8](Dubois et al., 1996).

At the far C-terminus is a region homologous to a domain in some 14-3-3 proteins (Roth et al., 1993). Interestingly, this domain is also implicated in the binding of annexin I to activated PKC and may be a functional determinant of annexin I as a Receptor for Activated C-Kinase (RACK) (Mochly-Rosen et al., 1991). At the extreme N-terminus are conserved lysine and glycine residues corresponding to invariably conserved residues of the rab family (Upton, 1994). Whether this homology implies a similar target or mode of action for annexin II and (some) members of the rab family is at present unclear.

1.3 Annexin protein ligands.

1.3.1 Annexins bind to a variety of protein ligands.

The range of annexin ligands identified has contributed to the uncertainty surrounding annexin function, and members of the annexin family have been demonstrated to associate with components of the cytoskeleton, extracellular matrix and several enzymes. Of the annexin family, annexin II has been shown to have to most promiscuous binding habits *in vitro* as summarised overleaf (Table 1.2).

Reports of some annexin II/ligand interactions are isolated, and it is difficult to assess the physiological implications of these interactions based on the data available. For instance the binding of annexin II to 3-phosphoglycerate kinase to form a heterodimer has only been reported by one group and awaits independent corroboration (Jindal et al., 1991). However, there are some definite trends. For instance several members of the annexin family bind to cytoskeletal components including F-actin (annexins I and II), G-actin (annexin VI), members of the spectrin superfamily (annexins II and VI) and intermediate filaments (annexin II) fuelling speculation that at least some annexins are involved in modulation of the cytoskeleton (Gerke and Weber, 1984; Ikebuchi and Waisman, 1990; Liu et al., 1987; Regnouf et al., 1991; Tanaka et al., 1994; Watanabe et al., 1994) (see 1.6 Annexins and the cytoskeleton.). Another recurring partnership which has been shown to play key roles in modulating annexin properties *in vitro* and annexin targeting *in vivo* is the association of members of the annexin family with S100 proteins.

Table 1.2: Annexin II protein ligands.

Cytoskeletal ligands	Source
Non-erythroid spectrin (fodrin)	*(Gerke and Weber, 1984)
F-actin	*(Cheney and Willard, 1989)
	*(Glenney, 1986b)
	*(Glenney et al., 1987)
	(Ikebuchi and Waisman, 1990)
	(Regnouf et al., 1991)
	(Jones et al., 1992)
	(Ma et al., 1994b)
Glial Filament Acidic protein	*(Bianchi et al., 1994)
	*(Garbuglia et al., 1995)
Other intracellular ligands	**Source**
p11	(Johnsson et al., 1986)
	(Kube et al., 1992)
3-phosphoglycerate kinase	(Jindal et al., 1991) ?
Cell surface/extracellular ligands	**Source**
Tissue Plasminogen Activation factor (TPA)	(Hajjar et al., 1994)
Fc-γ-receptor	(Kristoffersen et al., 1994)
Human Cytomegalovirus (CMV)	(Wright et al., 1994)
Tenascin C	(Chung and Erickson, 1994)

'*' denotes an association reported to require supra-physiological Ca^{2+} levels. '?' denotes and isolated report. Only key references are shown.

1.3.2 S100 family proteins as annexin ligands.

The S100 family of proteins comprises a subfamily of the EF-hand group of proteins. This superfamily is characterised by a common structural motif, the EF hand, after the E- and F- helices of parvalbumin which selectively bind Ca^{2+} and with high affinity (Kretsinger, 1980; Richard, 1995). The S100 family of proteins was originally characterised as a group of abundant low molecular weight (10-12kDa) acidic proteins that are highly enriched in nervous tissue and are composed of two EF hands flanked by hydrophobic regions at either terminus and separated by a central hinge region. The carboxy terminal EF hand is usually referred to as the canonical Ca^{2+}-binding loop and

encompasses 12 amino acids, whereas the amino terminal loop is formed of 14 amino acids and has a lower affinity for Ca^{2+}. To date some 17 different proteins have been assigned to the S100 family. Two of these, S100A10 (or p11) and S100C, can form complexes with annexin II and annexin I respectively.

Of these these two binding pairs, the most intensively studied is the annexin II_2p11_2 heterotetramer in which a dimer of p11 (S100A10) bridges two annexin II molecules (Erikson et al., 1984; Gerke and Weber, 1984; Gerke and Weber, 1985). Complex formation has profound effects on the biochemical properties of annexin II. Firstly, the calcium requirement for phospholipid binding is drastically reduced (Powell and Glenney, 1987) and secondly the complex formed now possesses two sets of Ca^{2+}/membrane binding core domains and (putative) actin binding domains. This is thought to be the structural basis underlying the enhanced liposome and chromaffin granule aggregating properties of the annexin II_2p11_2 heterotetramer (Drust and Creutz, 1988; Johnstone, 1992; Powell, 1987) and the ability to bundle F-actin (Ikebuchi and Waisman, 1990) (Figure 1.4). Complex formation is Ca^{2+}-independent due to deletion and substitutions within the p11 EF hand loop which render it constitutively available for annexin II binding (Gerke and Weber, 1985).

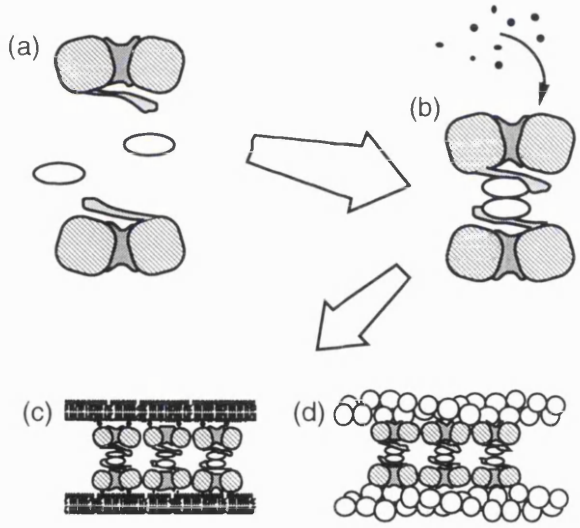

Figure 1.4: Two annexin II monomers and two p11 molecules combine to form a heterotetramer.

(a) Two annexin II monomers (grey) and two p11 molecules (ovals) can combine to form a heterotetramer (b) in the absence of Ca^{2+}. In the presence of Ca^{2+} (black dots) the heterotetramer can potentially cross-link: (c) membranes[1], or (d) F-actin and F-actin[2]. ([1](Blackwood and Ernst, 1990), [2](Ikebuchi and Waisman, 1990))

As well as modulating the biochemical properties of annexin II *in vitro*, annexin II_2p11_2 complex formation also alters the intracellular distribution of annexin II compared to monomeric annexin II, and appears to be necessary for tightly anchoring annexin II in the cortex of fibroblasts and adrenal chromaffin cells (Chasserot Golaz et al., 1996; Thiel et al., 1992; Zokas and Glenney, 1987). The binding sites of annexin II and p11 involved in complex formation map to the N-terminal 14 amino acids of annexin II and to the C-terminal extension of p11 (Johnsson et al., 1988; Kube et al., 1992), and since peptides corresponding to the N-terminus of annexin II successfully interfere with heterotetramer formation, synthetic peptides and fusion proteins encoding this

region have been increasingly used to probe annexin II function *in vivo* (Chasserot Golaz et al., 1996; Harder and Gerke, 1993).

Although reference to p11 function is usually made in the context of research into annexin II function some unexpected and intriguing findings have been made regarding p11 itself. For instance, a yeast two hybrid screen for proteins which interact with a member of the cyclin-dependent kinase (cdk) protein PCTAIRE-1 yielded the eta, theta and zeta isoforms of 14-3-3 proteins as targets, and also p11 (Sladeczek et al., 1997). Biochemical analysis revealed p11 does indeed bind to PCTAIRE-1, though it is not clear whether annexin II can influence PCTAIRE-1 localisation through p11 binding.

Annexin II is not alone in its association with a member of the S100 family of proteins since annexin I can interact with S100C and annexin XI has been found to associate with calcyclin (S100A6) (Mailliard et al., 1996; Naka et al., 1994; Seemann et al., 1996a; Tokumitsu et al., 1993). Unlike the case of annexin II/p11 association, the binding of these annexin to their S100 partners is strictly Ca^{2+}-dependent and little is known of the physiological implications of complex formation. In the case of the annexin I/S100C partnership, annexin I is responsible for the calcium association of S100C with endosomes and may play a role in the association of early endosomes with the cytoskeleton during vesicle traffic.

There is one remaining class of interactions which, at least *in vitro*, may contribute significantly to annexin function. These interactions are between the annexins themselves, since several members of the annexin family have been shown to self associate both in solution and within the plane of membrane surfaces.

1.3.3 Annexin self association.

The earliest example of self association documented for the annexin family was found through analysis of annexin VII mediated chromaffin granule aggregation. This was shown by electron microscopy to coincide with the formation of rod-like structures, similar to those formed by annexin VII in solution, at the junction between aggregated granules (Creutz et al., 1979). Since then other annexins have been shown to form multimers in solution. For instance, annexin XII has been demonstrated, using a chemical cross-linking approach, to form trimers or hexamers (Mailliard et al., 1997). However, attention has largely focused on the ability of annexins to associate laterally when bound to membranes. A number of annexins have been shown to aggregate into planar trimers when bound Ca^{2+}-dependently to the surface of anionic membranes including annexin XII, VI and V (Mailliard et al., 1997; Mosser et al., 1991; Newman et al., 1989). In the case of annexin V at least, analysis using chemical cross-linking to probe aggregation suggests that trimers,

hexamers and higher aggregates form in the presence of Ca^{2+} and anionic phospholipids *in vitro* (Concha et al., 1992). There is also compelling immunoelectron microscopic evidence demonstrating that annexin II_2p11_2, bound in the presence of Ca^{2+} to membrane, laterally associates into two-dimensional plaques between opposing membranes during vesicle aggregation (Lambert et al., 1997). Such plaques present seven electron dense stripes when sectioned corresponding to the outer membrane leaflets (4 stripes in total) and three inner stripes corresponding to the annexin II_2p11_2 heterotetramer (Figure 1.5)

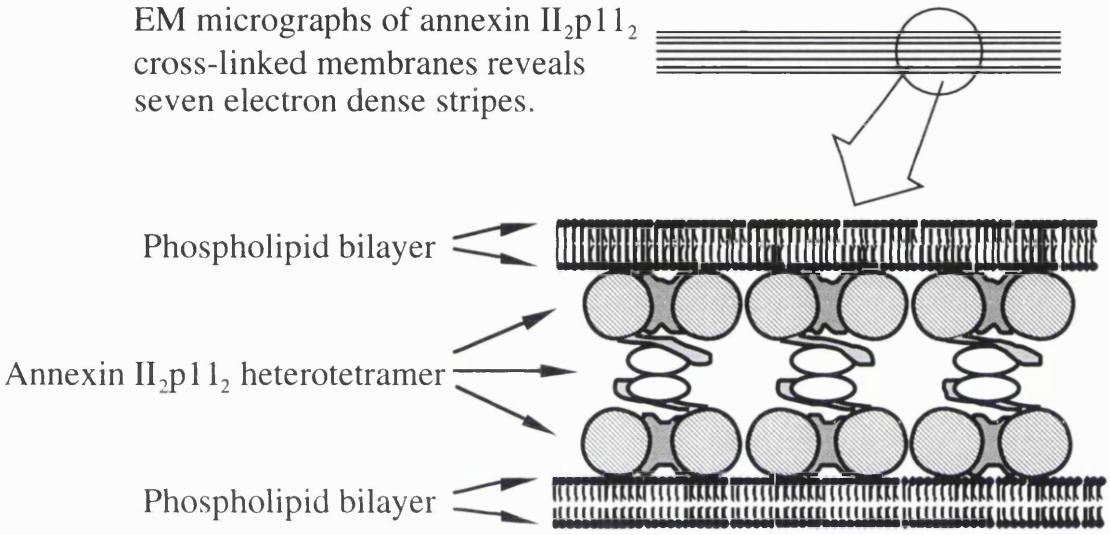

Figure 1.5: Junctional plaques form between membranes aggregated by the annexin II_2p11_2 heterotetramer in the presence of Ca^{2+}.

These junctions appear as 7 electron dense stripes when membrane/membrane interfaces are sectioned and imaged using electron microscopy. The central stripe is thought to correspond to neigbouring p11/p11 dimers while the outer-most four stripes correspond to the leaflets of the cross-linked lipid bilayers. By default the remaining electron dense stripes are thought to correspond to neigbouring, membrane bound annexin II heavy chains. (Modified from Lambert et al., 1997).

What function lateral formation of multimers serves is at present unresolved. Indeed it is not known whether multimers exist outside highly purified and controlled *in vitro* conditions, although there are some indications that annexins may bind to membranes in rafts or plaques *in vivo*. For instance electron micrographs of annexin II bound to the surface of early endosomes in baby bamster kidney (BHK) cells demonstrated that this annexin is localised to the endosomal surface in discrete rafts (Harder et al., 1997). It is interesting to note however that these plaques, visualised in fixed cells, were not localised to inter-membrane junctions but localised to the interface of filamentous elements of the cytoskeleton (see Figure 4.24, p 133).

1.4 Interaction of annexins with biological and synthetic membranes.

1.4.1 Ca^{2+}-dependent association of annexins with membranes.

The annexin family is partly defined by the ability of family members to bind negatively charged phospholipids such as phosphatidic acid, phosphatidylserine or phosphatidylinositol in the presence of Ca^{2+}, and it has been demonstrated that family members show a range of Ca^{2+} sensitivities and phospholipid specificities (see Table 1.1, p 17) (Blackwood and Ernst, 1990; Raynal and Pollard, 1994). Further characterisation of Ca^{2+}-dependent membrane binding *in vitro* has demonstrated membrane binding can modulated by a variety of parameters including local salt concentration, pH and phosphorylation (Jones et al., 1994; Powell and Glenney, 1987) suggesting a variety of control points for membrane binding *in vivo*.

That Ca^{2+} does indeed modulate annexin membrane association *in vivo* is supported by a range of published data. For instance, although annexin II is normally targeted specifically to the inner face of the plasma membrane in fibroblasts, mutation of the type II Ca^{2+}/phospholipid binding sites abolished such targeting. In contrast, mutation of the lower affinity type III Ca^{2+}/phospholipid binding site did not have this effect, suggesting that Ca^{2+} binding is required to initiate normal targeting of annexin II to the inner face of the plasma membrane *in vivo* (Jost et al., 1994; Thiel et al., 1992). Other annexins require higher levels of Ca^{2+} to initiate membrane binding, and this is thought to be the basis of Ca^{2+} dependent translocation of different annexins to the plasma membrane during cell stimulation. Examples include translocation of annexin I to the plasma membrane of neutrophils, of annexin V to the plasma membrane on stimulation of platelets, and of cytosolic annexin II to the plasma membrane in stimulated chromaffin cells (Chasserot Golaz et al., 1996; Kaufman et al., 1996). It is interesting to note however that translocation does not always appear to be reliant on Ca^{2+} alone. For instance in the case of annexin I, translocation to the plasma membrane in neutrophils challenged with opsonized zymogen is only partially mimicked by stimulation with Ca^{2+} and ionophore (Kaufman et al., 1996). Hence another factor(s) is necessary for efficient relocation.

A further perplexing aspect of annexin relocation in response to Ca^{2+} is the basis of targeting specificity, since different annexins can relocate to quite different membranes from the same cell both *in situ* and *in vitro*. The basis of this phenomenon may reside in the location of the relevant annexin to a distinct intracellular organelle prior to stimulation. For example, in human foreskin fibroblasts, SH-SY5Y and MG-63 osteosarcoma cells, nuclear-specific pools of annexins IV and V have been identified which translocate to the

nuclear envelope in response to an increase in intracellular Ca^{2+} (Barwise and Walker, 1996; Blanchard et al., 1996; Mohiti et al., 1995). Membrane specificity in this instance may simply reflect prior nuclear compartmentalisation of these annexins. However, more complex patterns of Ca^{2+}-dependent annexin relocation have been documented. Investigation of Ca^{2+}-dependent translocation of neutrophil annexins *in vitro* suggests that different secretory organelles recruit a distinct mixture of annexins in response to a rise in Ca^{2+}. While annexins I, IV and VI translocate to the plasma membrane, secretory vesicles, neutrophil specific granules and azurophil granules, annexins II and XI distribute unevenly between these membranes and bind only poorly to azurophil granules *in vitro* (Sjolin et al., 1997; Sjolin et al., 1994). Similarly, *in vitro* analysis has demonstrated differential binding of annexins II, VI and VII to secretory granules (Creutz et al., 1992). While Ca^{2+} - dependent binding of annexins VI and VII is similar for both chromaffin and zymogen granules, annexin II shows a marked preference for chromaffin granules.

Taken together these results are difficult to explain if binding of annexins with biological membranes is due to simple association with anionic phospholipids, suggesting other factors are involved. These could include specific protein receptors or interaction with lipid moieties other than anionic phospholipids, as discussed elsewhere.

In conclusion the evidence that annexins associate with, or relocate to membranes under the influence of Ca^{2+} *in vivo* is compelling. What functions they perform on arrival at their target membrane is less clear, and theories have been strongly influenced by the finding that annexin/membrane association can modify the properties of the target membrane in a variety of ways.

1.4.2 Modulation of membrane properties through association of annexins.

While membrane-associated annexins may play an architectural role in the cell, membrane binding by annexins may also have profound effects on the structure and/or character of the membrane itself. For instance channel activity has been been demonstrated for several annexins on *in vitro* association with synthetic membranes (reviewed in Demange et al., 1994; Moss, 1995). The structural basis for such activity remains controversial, and may reside in the possesssion of a central pore in the core domain coupled with 'electroporation' of target membrane on annexin binding or radical reordering of the core domain on membrane insertion (Langen et al., 1998; Rosengarth et al., 1998). A second phenomenon of central importance is the finding that annexins can sequester or "annex" phospholipids within the plane of the membrane (Junker and Creutz, 1994; Junker and Creutz, 1993). Thus annexins can potentially interfere with membrane stability, change

membrane ion permeability or be instrumental in defining lipid microdomains involved in signaling or membrane fusion.

While the relevance of annexin mediated sub-microscopic changes in membrane organisation is poorly understood in terms of function *in vivo*, microscopic changes have been more amenable to study. In particular the ability of annexins to mediate the aggregation and/or fusion of membranes *in vitro* has received considerable attention and constitutes one of the best understood properties of the annexin family.

1.4.3 Ca^{2+}-dependent membrane aggregation and fusion.

The ability of members of the annexin family to aggregate both synthetic and biological vesicles in the presence of Ca^{2+} *in vitro* has been extensively documented and, as might be expected, membrane aggregation varies with annexin, membrane composition and Ca^{2+} concentration. (see Table 1.3 below).

Table 1.3: Summary of vesicle aggregating properties of various annexins (mM required for 50% maximal vesicle aggregation).

	Annexin	*I*	*II(m)*	*II(t)*	*III*	*IV*	*V*	*VI*	*VII*
Vesicle									
NG		750	$>10^3$	-	500	-	-	-	-
CG		213	-	1.8	-	282	n.a.	$>10^5$	200
PS		2	-	0.18	-	$>10^3$	$>10^3$	-	-
PI		15	-	-	-	$>10^3$	$>10^3$	-	-

NG - Neutrophil Granule, CG - Chromaffin Granule, PS - Phosphatidylserine, PI - Phosphatidylinositol, 'n.a.' denotes no aggregation. These figures were taken from Blackwood and Ernst, 1990. II(m), annexin II (monomer); II(t), annexin II (tetramer)

In some instances the molecular basis for vesicle aggregation seems relatively clear, and the Ca^{2+} concentrations required to mediate vesicle aggregation do not preclude a physiological role for this property at global concentrations of Ca^{2+} measured *in vivo* during stimulation. For instance, annexin II_2p11_2 requires only low μM concentrations of Ca^{2+} to promote aggregation of synthetic vesicles composed of phosphatidylserine or purified chromaffin granules while monomeric annexin II requires mM concentrations (Blackwood and Ernst, 1990; Powell and Glenney, 1987). The cross-bridging activity of

the heterotetramer is thought to arise from the "bivalent" conformation, coupled with a lower Ca^{2+} requirement for membrane binding. However, the molecular basis for the vesicle aggregating properties of (for example) annexins I or VII is less clear. In the case of annexin I both the formation of a secondary membrane binding site at the concave face of the molecule and interaction of the N-termini of annexin I monomers bound to opposing membranes have been implicated in vesicle aggregation (de la Fuente and Ossa, 1997; de la Fuente and Parra, 1995; Porte et al., 1996; Wang and Creutz, 1994). Annexin self-association has also been proposed to underlie annexin VII mediated vesicle aggregation through the Ca^{2+} dependent oligomerisation of annexin VII into rod-like structures (Creutz et al., 1979). Since the Ca^{2+} concentrations required to promote vesicle aggregation by these two annexins are relatively high *in vivo* aggregation may only occur in microdomains of high Ca^{2+} proposed to occur adjacent to the plasma membrane and/or Ca^{2+} stores. While microdomains of up to 200-300 μM have been reported to occur in the presynaptic terminal of the giant squid synapse during transmitter release using *n*-aequorin-J as a reporter (Llinas et al., 1992; Sugimori et al., 1994) the sub-plasmalemmal Ca^{2+} dynamics in exocytotic cell models such as chromaffin cells have not been accurately elucidated using similar techniques in intact, actively exocytosing cells. Direct experimental measurements of Ca^{2+} concentrations at the plasma membrane are hindered by the spatial resolution of light microscopy, but comparison of secretion in dialysed cells and intact cells suggests that the concentration of Ca^{2+} at secretory sites can excede 10 μM (Augustine and Neher, 1992). In conclusion it is possible that annexin mediated vesicle aggregation at higher (>10 μM) concentrations of Ca^{2+} is physiologically relevant, but further elaboration would require more accurate estimates of peri-plasma membrane Ca^{2+} concentrations.

In spite of these reservations, the finding that annexins can mediate the Ca^{2+}-dependent aggregation of membranes *in vitro* underpins the proposition that these proteins may play a role in membrane fusion. At least one member of the annexin family has been demonstrated to promote Ca^{2+}-dependent fusion of carefully designed mixtures of synthetic phospholipids at μM concentrations of Ca^{2+}. Thus annexin II_2p11_2 has been shown to promote the fusion of synthetic liposomes composed of phosphatidylserine/ phosphatidylethanolamine (1:3) at only 10 μM free Ca^{2+} (Liu et al., 1995a). This is not the case for biological membranes, where much higher concentrations of Ca^{2+} are required to promote fusion of annexin aggregated vesicles, and typically other factors have been used to reduce the Ca^{2+} concentration required to physiological concentrations. For instance, annexin VII has been shown to promote cis-unsaturated fatty acid mediated fusion of liposomes and chromaffin granules *in vitro* by increasing vesicle aggregation rates (Creutz, 1981; Meers et al., 1988a; Meers et al., 1988b; for review see Zaks and Creutz, 1990) and annexin II has been shown to lower the Ca^{2+} requirement for arachidonic-acid mediated fusion of isolated lammellar bodies and liposomes *in vitro* (Liu et al., 1995a). It has not

been established whether such "biological detergents" play a role in membrane fusion *in vivo*. However, these results do suggest that annexins are not fusogenic themselves at global concentrations of Ca^{2+} found in stimulated cells, but rather may play a role in cross-linking membranes prior to fusion (see 1.7 Annexins and exocytosis.).

While most published data indicate annexins themselves are not fusogenic *per se* there are exceptions, and separate studies have shown both annexins II and VII have fusogenic activities *in vitro*. For instance, annexin II has been demonstrated to mediate fusion of chromaffin granules on phosphorylation by PKC. Since fusion activity was dependent on pre-aggregation of chromaffin granules by annexin II_2p11_2 and subsequent phosphorylation, it was proposed a conformational change in annexin II_2p11_2 led to membrane destabilisation and fusion (Regnouf et al., 1995). As annexin II is phosphorylated by PKC during stimulated secretion in chromaffin cells (but see Waisman, 1995) it was proposed annexin II may play a central role in membrane fusion during exocytosis in these cells.

A quite different picture has emerged from analysis of annexin VII fusogenic activity. Annexin VII was shown to have a Ca^{2+}-dependent GTPase activity and it was found that a combination of GTP, Ca^{2+} and annexin VII could promote vesicle fusion *in vitro* (Caohuy et al., 1996). Since these *in vitro* findings mirror the established Ca^{2+} and GTP requirements of Ca^{2+}-dependent exocytosis it was proposed that annexin VII might integrate Ca^{2+} and GTP mediated signals into membrane/membrane fusion. While several annexins have been shown to bind nucleotides and/or possess nucleotide phosphodiesterase activity (Bandorowicz-Pikula et al., 1997; Calvert et al., 1996), and it has been demonstrated that Ca^{2+}-regulated exocytosis requires GTP (Barrowman et al., 1986; Gomperts et al., 1986; Knight and Baker, 1985) these findings will remain controversial until independently corroborated by other groups.

Reservations surrounding the involvement of various members of the annexin family in the processes of docking and/or fusion in exocytosis and other types of vesicle traffic rest largely on the relatively high concentrations of Ca^{2+} required to promote these interactions. However, given that it is not known precisely how high Ca^{2+} concentrations are at membrane surfaces during fusion *in vivo*, these *in vitro* findings may have some physiological significance. Due to these uncertainties attention has increasingly settled on the annexin II_2p11_2 heterotetramer since this molecule can mediate membrane aggregation at Ca^{2+} concentrations known to occur in stimulated cells. This view has been reinforced by the finding that the membrane binding and aggregating properties of this annexin (and annexin I) are modulated by signaling kinases *in vitro*.

1.4.4 Modulation of annexin membrane and cytoskeletal association by phosphorylation.

Both annexins I and II are substrates for phosphorylation by tyrosine kinases and PKC. In the case of annexin I, phosphorylation by the EGF receptor at Tyr-20 renders the protein susceptible to proteolytic degradation - resulting in modulation of its Ca^{2+} and phospholipid binding and vesicle aggregation properties (for review see Raynal and Pollard, 1994). This effect can be mimicked to some extent by substitution of Tyr-20 with a negatively charged amino acid, resulting in a mutant annexin I with an enhanced Ca^{2+} requirement for vesicle binding and aggregation (Wang and Creutz, 1994). Similar effects were observed when Ser-27, a site for phosphorylation by protein kinase C, is either phosphorylated or is replaced by aspartate or glutamate to mimic phosphorylation (Porte et al., 1996; Wang and Creutz, 1994).

Annexin II is also a major substrate for a variety of tyrosine kinases - a fact recognised some 20 years ago during early investigations of the substrates phosphorylated during cellular transformation. In a series of *in vivo* labeling experiments, Radke, Martin, and Erikson and Erikson (Erikson and Erikson, 1980; Radke et al., 1980; Radke and Martin, 1979) demonstrated that annexin II is phosphorylated on tyrosine residues when chicken embryo fibroblasts are transformed by Rous sarcoma virus. The tyrosine residue targeted by $pp60^{v\text{-}src}$ is located in the N-terminal domain of the molecule and maps to tyr-23 (Isacke et al., 1986). The same site is phosphorylated in cells activated by PDGF (Brambilla et al., 1991; Isacke et al., 1986), and insulin (Biener et al., 1996; Karasik et al., 1988).

Tyrosine phosphorylation decreases the affinity of annexin II_2p11_2 for phospholipid *in vitro* and abolishes chromaffin granule aggregation activity and F-actin bundling activity which normally occur at μM Ca^{2+} levels (Hubaishy et al., 1995; Powell and Glenney, 1987). While tyrosine phosphorylation of annexin II_2p11_2 abolishes chromaffin granule aggregation, both phosphorylated and unphosphorylated annexin II_2p11_2 bind to chromaffin granules with similar affinities (Hubaishy et al., 1995). Since tyrosine phosphorylation greatly increases the Ca^{2+} requirement of annexin II for binding to synthetic membranes composed of phosphatidylserine (Powell and Glenney, 1987) this would suggest that interaction of phosphorylated annexin II_2p11_2 with the chromaffin granule surface is not due to phospholipid binding alone. Thus the loss of chromaffin granule aggregating ability of annexin II_2p11_2 on phosphorylation by $pp60^{v\text{-}src}$ may reflect a switch from membrane binding to interaction with another membrane component(s).

While soluble annexin II is a poor substrate for $pp60^{c\text{-}src}$ in solution, phosphorylation is strongly stimulated by binding of annexin II to negatively-charged phospholipids in the presence of Ca^{2+} (Bellagamba et al., 1997). This suggests that $pp60^{c\text{-}src}$

phosphorylation of annexin II may be functionally relevant at membrane surfaces and might modulate annexin II_2p11_2-mediated membrane/membrane or membrane/cytoskeletal interactions. With this in mind it is worth noting that annexin II_2p11_2 mediated Ca^{2+}-dependent bundling of F-actin *in vitro* is abolished by $pp60^{c\text{-}src}$ phosphorylation of annexin II_2p11_2, and yet annexin II_2p11_2 is only poorly phosphorylated by $pp60^{c\text{-}src}$ when bound to F-actin (Hubaishy et al., 1995). Furthermore both annexin II and $pp60^{c\text{-}src}$ have been located to similar intracellular organelles including caveolae (Song et al., 1997; Stan et al., 1997) and chromaffin granules (Drust and Creutz, 1991; Grandori and Hanafusa, 1988) suggesting $pp60^{c\text{-}src}$ phosphorylation of annexin II might be involved in the function of these structures.

In contrast to phosphorylation by $pp60^{c\text{-}src}$, phosphorylation of annexin II by PKC in the N-terminal domain has little effect on Ca^{2+} -dependent lipid binding but significantly decreases the rate and extent of annexin II_2p11_2 mediated lipid vesicle aggregation (Johnstone et al., 1992; Regnouf et al., 1995). This phenomenon is thought to be caused by the destabilising effect of phosphorylation on the heterotetramer, which dissociates on phosphorylation by PKC (Regnouf et al., 1995).

Of the known sub-classes of PKC, it seems likely that the conventional PKCs, or cPKCs will be the most important in phosphorylating annexin II at membrane surfaces (for review see Dubois et al., 1996). The cPKCs are the only PKCs that possess a Ca^{2+} and phospholipid-binding domain (named C2) which is also found in synaptotagmin, in cytosolic phospholipase A_2, in p120 GTPase activating protein (p120GAP), in phosphatidylinositol phospholipase Cs (PI-PLCs) and in phosphatidylinositol-3-kinase (PI3-kinase) (for review see Nalefski and Falke, 1996). Like annexins cPKCs translocate from the cytosol to negatively charged membrane surfaces upon activation by Ca^{2+} , suggesting that membrane recruitment of cPKCs and annexins may be coordinated.

That phosphorylation of annexin II during Ca^{2+} regulated exocytosis in chromaffin cells may involve phosphorylation by PKC has been inferred from several lines of evidence. Firstly, annexin II is phosphorylated with a similar time course to nicotine stimulated secretion in chromaffin cells (Creutz et al., 1987; Delouche et al., 1997; but see Waisman, 1995). Secondly, while PKC phosphorylation blocks the ability of annexin II_2p11_2 to aggregate lipid vesicles it cannot promote dis-aggregation of annexin II_2p11_2 bound vesicles, and has instead been reported to promote vesicle fusion (Regnouf et al., 1995). However, these findings appear inconsistent with those of Sarafian et al (Sarafian et al., 1991) since the latter show that pre-phosphorylation of annexin II by PKC is necessary to retard run-down in permeabilised chromaffin cells in which PKC has been down-regulated, which would preclude a role for annexin II_2p11_2 (see 1.7 Annexins and exocytosis.).

14-3-3 protein:
KCIP-1 G D Y Y R Y L A E V A T G D D

Annexin:

I			G	D	Y	E	K	I	L	V	A	L	C	G	G	N		
II			G	D	Y	Q	K	A	L	L	Y	L	C	G	G	D	D	
III			G	D	Y	E	I	T	L	L	K	I	C	G	G	D	D	
IV			G	D	Y	R	K	V	L	L	V	L	C	G	G	D	D	
V			G	D	Y	K	K	A	L	L	L	L	C	G	E	D	D	
VI			G	D	F	L	K	A	L	L	A	L	C	G	G	E	D	
VII			G	D	Y	R	R	L	L	L	A	I	V	G	Q			
VIII			G	D	Y	K	N	A	L	L	S	L	V	G	S	D	P	
IX			T	D	Y	G	Y	V	L	V	T	L	T	A	W			
X		T	S	I	D	Y	K	R	A	I	L	T	A	L	L	G	S	A	L
XI			G	D	G	R	K	I	L	L	K	I	C	G	G	N	D	
XII			G	D	Y	K	D	L	L	L	Q	I	T	G	H			
XIII			G	D	F	R	K	L	L	V	A	L	L	H				

Figure 1.6: Homology between annexins and 14-3-3 proteins.

PKC inhibitors such as KCIP-1 bind PKCs and have a 16 amino acid region of homology (blue) with the last 14 amino acids of annexins. In KCIP-1 this region corresponds to residues 127-142 of this 230 amino acid protein (From Dubois et al., 1996).

Of the annexin family only annexins I and II are substrates for PKCs, but the relationship between the annexin family and PKC superfamily could involve multiple members from both families. It has been recognised that endogenous inhibitors of PKC, including KCIP-1 (Aitken et al., 1992) and members of the 14-3-3 family, bind PKC and contain a sequence homologous to the last 14 amino acids of annexins (Figure 1.6, also refer to Figure 1.3, p 20) raising the possibility of a specific interaction between annexins and PKCs (for review see Dubois et al., 1996).

In support of this hypothesis, annexin I has been shown to bind activated PKCs and proposed to be a RACK (Receptor for Activated C Kinase; Mochly-Rosen et al., 1991). A peptide corresponding to this region inhibits binding RACK proteins to PKCs only in the presence of Ca^{2+} and phospholipid (Mochly-Rosen et al., 1991). Thus on one hand PKCs may influence the membrane targeting of annexins I and II through phosphorylation, while on the other a variety of annexins may influence the membrane recruitment of cPKCs themselves. Hence modulation of membrane binding and/or aggregation of annexins I and II may also involve other annexins through PKC targeting.

1.4.5 Ca^{2+}-independent membrane targeting.

Although Ca^{2+}-dependent binding to phospholipids constitutes a fundamental property of the annexin family, annexins I, II, V and VI can interact with biological membranes in the absence of Ca^{2+} (Futter et al., 1993; Harder et al., 1997; Liu et al., 1997; Trotter et al., 1995b). For instance annexin I has been shown to be bound Ca^{2+}-independently to the membranes of multivesicular bodies during EGF receptor internalisation and processing (Futter et al., 1993). Similarly, annexin II associates tightly with biological membranes in a Ca^{2+}-independent, TX-100 insoluble manner in the human neuroblastoma line SH-SY5Y (Blanchard et al., 1996), in stimulated chromaffin cells (Chasserot Golaz et al., 1996; Sagot et al., 1997) and in BHK cells (Harder et al., 1997).

This Ca^{2+}-independent membrane association is extremely tight since it is resistant to high salt and high pH treatments. However, at least in the case of annexin II, it has been suggested that cholesterol may be involved in this type of association since binding is extremely sensitive to cholesterol sequestration. Filipin or digitonin mediated cross-linking of membrane cholesterol leads to the release of a complex consisting of annexin II, α-actinin, ezrin, moesin and membrane-associated actin (Harder et al., 1997). Whether cholesterol plays a role in the membrane-association of other members of the family is not known. Indeed the details of Ca^{2+}-independent annexin membrane binding of annexins I, II V and VI are unclear, a fact reflected in the range of models designed to explain this phenomenon.

1.4.6 Receptors, membrane insertion and other models.

Investigation of the Ca^{2+}-independent association of annexin II with early endosomal membranes has demonstrated that this association is dependent on residues 15 - 24 in the N-terminus (Jost et al., 1997). Mutation of this region abolishes the Ca^{2+}-independent association of annexin II with endosomes, and since this region bears no homology to known membrane binding domains a specific receptor present on endosomes may mediate annexin II binding. With this in mind it is interesting to note that annexin V, bound Ca^{2+}-independently to platelet membranes, has been shown to be closely associated with an unidentified 50 kDa protein using biochemical cross-linking (Trotter et al., 1995a). An array of different receptors could be invoked to explain the different membrane locations of the various annexins. However, if this proves to be the case then the basic question of targeting remains - since the receptors must be delivered to the relevant membranes in the first place. An alternative explanation for Ca^{2+} -independent membrane association could invoke interaction with lipid components of the membrane other than negatively charged phospholipids. As discussed previously, cholesterol may play a role in the Ca^{2+}-independent association of annexin II with target membranes (Harder et al., 1997).

In some respects Ca^{2+}-independent association may be something of a misnomer since, at least in the cases of annexin V and annexin VI, Ca^{2+} is necessary for the initial membrane binding event leading to Ca^{2+}-independent membrane association (Bianchi et al., 1992; Trotter et al., 1995a; Trotter et al., 1995b). Significantly, the concentration of Ca^{2+} required to generate an EGTA resistant pool of annexin V associated with platelet membranes is only 0.8 μm, in contrast to the mM concentration of Ca^{2+} required for maximal Ca^{2+}-dependent binding. Thus, relatively small fluctuations in cytoplasmic Ca^{2+} may have a large effect on the EGTA resistant pool of membrane-associated annexin V. As

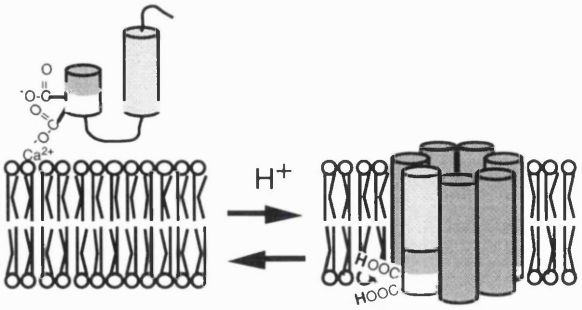

Figure 1.7: Putative model of annexin XII membrane insertion.

Model for the pH-triggered membrane insertion of helices D-E in annexin XII monomer. At neutral pH in solution, or adsorbed to the membrane in the presence of Ca^{2+}, helices D (dark grey/white) and E (pale grey) form a helical hairpin with a short connecting loop. In the surface bound mode Ca^{2+} is jointly coordinated by glutamate 142 and phosphatidylserine (left). When the pH is lowered the carboxylate groups are protonated and insert into the bilayer as a transmembrane helix (right). The grey helices are speculative and are included to represent the remainder of the annexin monomer (From Langen et al., 1998).

this phenomenon is not observed in synthetic membranes composed of phosphatidylserine alone it would appear that it is not an intrinsic property of annexin V but is dependent on other membrane component(s), the identity of which remain unknown.

In all studies of Ca^{2+}-independent membrane association it has been noted that the association is extremely stable, and that annexins behave like integral membrane proteins (Langen et al., 1998). At least in the case of annexin XII evidence exists that this annexin can indeed insert into membrane (Figure 1.7). Using spin labeling, it was shown that at low pH a continuous membrane spanning α-helix is generated from a helix-loop-helix motif in the solution structure (Langen et al., 1998). Since other regions with similar membrane insertion potential were identified on the basis of amino acid sequence it was proposed that the corresponding helices come together to form an aqueous pore, thus explaining the channel activity shown by some annexins *in vitro*.

While these structural findings are likely to be the source of further debate, the finding that annexin XII can associate Ca^{2+}-independently with membranes under conditions of low pH is convincing. It interesting to note that annexin VII mediated fusion of chromaffin granule ghosts has been found to be modulated by pH and maximal fusion was found to occur at pH 4 (Stutzin et al., 1987), coincidently the same pH used by Langen et al (1998) to promote annexin XII membrane insertion. Whether these two observations are related awaits further clarification.

1.4.7 Synopsis of annexin II binding to biological membranes.

In conclusion it has been shown that annexins associate with biological membranes in a variety of ways. While Ca^{2+}-dependent association of annexin II with biological

membranes is fairly well understood, some aspects of Ca^{2+} independent association remain enigmatic, in particular the role of cholesterol and putative protein receptors.

The table below is derived from a survey of literature detailing the different modes of annexin II association with a variety of biological membranes and compartments.

Table 1.4: Characteristics of annexin II association with a variety of biological membranes.

Membrane.	Characteristics	Source
Plasma membrane.	Ca^{2+}-dependent.	(Thiel et al., 1992)
	Ca^{2+}-independent/cholesterol dependent.	(Harder et al., 1997)
Secretory-vesicle membranes.		
Chromaffin granules.	Ca^{2+}-dependent	(Creutz et al., 1987)
Neutrophil specific granules.	Ca^{2+}-dependent.	(Sjolin et al., 1994)
Lamellar bodies.	Ca^{2+}-dependent.	(Liu et al., 1995a)
Endocytic organelles.		
Early endosomes.	Ca^{2+}-independent.	(Jost et al., 1997)
Caveolae.	Ca^{2+}-dependent.	(Parkin et al., 1996)

1.5 Tissue, cellular and intracellular localisation of the annexins.

1.5.1 Overview of annexin distribution.

As a family the annexins are ubiquitous in higher vertebrates, and members have been found in most tissues analysed. However, although broadly expressed at the family level individual members of the family are subject to remarkably controlled expression both spatially and temporally during development. For example, while annexin V is abundant in adult heart there is no evidence of annexin VII expression (van Bilsen et al., 1992) and while expression of annexin II in the fetal pancreas is initially low, expression in the adult pancreas is significantly higher. There is a rich literature demonstrating many examples of such variability in expression. However, since consensus on the function of any one member of the annexin family has not been reached at the cellular level, it is unclear

precisely what the functional basis of this variability is, and in this respect annexin II is no exception.

1.5.2 Annexin II - tissue distribution.

It is difficult to predict the cellular function of annexin II on the basis of tissue distribution alone, although some broad themes are apparant from the numerous studies of annexin II localisation. Annexin II has been reported in avian (Greenberg et al., 1984) and mammalian tissues (Geisow et al., 1984; Glenney et al., 1987; Gould et al., 1984; Pepinsky et al., 1988). The protein is not detectable in heart, smooth muscle, skeletal muscle, liver, platelets and erythrocytes while low levels have been reported in brain and intermediate levels in the spleen, kidney and adrenal gland. It is perhaps significant that the highest concentrations of annexin II have been found in lung, placenta and intestine - tissues notable for their high volume of membrane traffic.

As well as being distributed heterogenously between tissues annexin II concentrations have also been shown to vary in a given cell or tissue type over time. Annexin II has been shown to exhibit transient expression during maturation and differentiation of a variety of cell types (Burgoyne et al., 1989; Eberhard et al., 1994; Reeves et al., 1992). For example, although certain cell types in the adult brain such as reactive astrocytes, ependymocytes and the meningothelium have low concentrations of annexin II, the fetal brain as a whole contains much higher concentrations of annexin II - especially during a period of development corresponding to expansion of radial glia. Other examples where differentiation coincides with increased expression of annexin II include differentiation of embryonic mesenchymal cells into cartilage and connective tissue (Carter et al., 1986) and development of the pancreas. While annexin II is expressed at very low levels in pancreatic islets from 1 week old rats, by adulthood expression levels are high (Ohnishi et al., 1994). An exception to the general rule that differentiation is accompanied by an increase in annexin II expression is found in muscle development since myocytes and myotubes express moderate levels of annexin II, while mature muscle does not (Carter et al., 1986). Although the role(s) of these changes in annexin II expression in tissue function are not clear, suitable tissue culture models exist to investigate this phenomenon at the single cell level since several cell lines are known to show increased expression of annexin II in on differentiation including PC12 cells (Fox et al., 1991), and F9 teratocarcinoma cells (Harder et al., 1993).

In addition to developmental regulation there are several examples where annexin II is absent or at low levels in a healthy adult tissue, but in which expression increases in response to damage or uncontrolled cell proliferation associated with cellular transformation. For example, although not associated with healthy adult brain, annexin II

expression is elevated in several types of neuroblastoma (Reeves et al., 1992; Roseman et al., 1994) and while annexin II is expressed at relatively low levels in adult liver, expression is elevated during regeneration after artificially induced damage (Masaki et al., 1994). Why annexin II levels are elevated under such conditions is unclear. This could be consistent with a role for annexin II in mitogenisis but could also be consistent with a role in adhesion or increased vesicle traffic associated with cellular proliferation.

Although different tissues or cells types may have similar concentrations of annexin II the ratio of monomeric annexin II to heterotetrameric annexin II can vary widely. For example Rous sarcoma virus transformed chicken embryo fibroblasts may have a 50 % excess of monomeric annexin II, while intestinal epithelial cells contain more than 90% in the complexed form (Erikson et al., 1984; Gerke and Weber, 1984). The differences in the ratio of monomeric/heterotetrameric annexin II are due to coordinated expression of annexin II and p11 (Munz et al., 1997) as well as post-translational control (Puisieux et al., 1996) yet the significance of these differences in expression patterns is unclear. The proposed functions of monomeric and complexed annexin II are probably related to the distinct cellular localisations of monomeric and heterotetrameric annexin II as discussed in the following section.

1.5.3 The cellular distribution of annexin II.

The intracellular distribution of annexin II within different cell types has been extensively documented and in general it is associated with the cortical cytoskeleton, specialised cortical structures such as microvilli and caveolae, and a variety of intracellular vesicular compartments including early endosomes and secretory vesicles. The annexin II heterotetrameric and monomeric forms of the protein are do not have the same sub-cellular distribution since annexin II_2p11_2 is found associated with the cortical cytoskeleton while monomeric annexin II is cytoplasmic (Glenney and Zokas, 1987; Thiel et al., 1992).

Although annexin II heterotetramer is normally associated with the sub-plasmalemmal region of the cell it has also been identified in association with the external face of the plasma membrane in a number of cell types including endothelial cells, skin keratinocytes and several types of metastatic and non-metastatic tumour cell (Cesarman et al., 1994; Ma et al., 1994a; Yeatman et al., 1993). The appearance of annexin II on the surface of cells is surprising since the annexins lack a hydrophobic signal sequence that has been characterised for most secreted proteins. Expression of surface bound annexin II_2p11_2 has been associated with binding and internalisation of cytomegalovirus (CMV) (Wright et al., 1995; Wright et al., 1994), binding and activation of tissue plasminogen activator (t-PA) (Cesarman et al., 1994; Hajjar et al., 1994), binding and internalisation of FcγRIII in the syncytiotrophoblast (Kristoffersen, 1996; Kristoffersen and Matre, 1996; Kristoffersen

et al., 1994) and adhesion to a variety of extracellular proteins including heparin (Kassam et al., 1997) and tenascin C (Chung and Erickson, 1994). Why or how one molecule should mediate such a range of interactions at the cell surface and also in the cell interior is unclear.

Annexin II_2p11_2 expression on the cell surface is rare in most normal cells but has been linked with cellular transformation and acquisition of a metastatic phenotype (Tressler et al., 1993; Yeatman et al., 1993). Since annexin II_2p11_2 can potentially mediate between the cell surface and a number of extracellular matrix components it has been proposed that extracellular annexin II_2p11_2 expression may be involved in Ca^{2+}-dependent adhesion of metastatic cells to their target organ(s) and subsequent invasion (Tressler et al., 1993).

Lastly, annexin II has been specifically associated with a number of vesicular intracellular compartments, including early endosomes, vesicles involved in receptor recycling and secretory vesicles (Drust and Creutz, 1991; Emans et al., 1993; Harder et al., 1997; Jost et al., 1997; Pol et al., 1997; van der Goot, 1997). The association of annexin II with these structures has initiated intensive investigation of the role of annexin II in vesicle trafficking, an area of literature discussed in detail elsewhere (see section 1.7 Annexins and exocytosis., 1.8 Annexins and endocytosis., 1.9 Annexins, caveolae and transcytosis.).

1.6 Annexins and the cytoskeleton.

1.6.1 Overview of annexins and the cytoskeleton.

One of the earliest names for members of the annexin family - "calpactin" - was coined in recognition of the Ca^{2+} and actin binding properties of annexins I and II, which were initially referred to as calpactins II and I respectively (Glenney et al., 1987). Both proteins were found to be highly enriched in brush borders and were found to bind and bundle F-actin at mM concentrations of Ca^{2+}. Initially, the high concentrations of Ca^{2+} required to promote F-actin binding and bundling cast some doubt over the physiological relevance of these activities. However subsequent investigations suggested that, at least in the case of annexin II_2p11_2, F-actin binding and bundling can occur at Ca^{2+} concentrations in the μM range (Ikebuchi and Waisman, 1990; Ma et al., 1994b; Regnouf et al., 1991) raising that possibility that this activity may have some physiological function.

More recently a third member of the annexin family, annexin VI, has been found to associate with G-actin *in vitro* (Tanaka et al., 1994) and was found to co-locate with F-actin in stress fibres in immunofluorescence experiments (Hosoya et al., 1992). However these findings seem to contradict experimental evidence derived through investigation of the

interaction of purified annexin VI with rat brain homogenate, as in this study annexin VI was found to associate specifically with calspectin and interfere with the interaction of calspectin and F-actin in the presence of phosphatidylserine (Watanabe et al., 1994). This evidence would seem to implicate annexin VI as a negative regulator of actin/membrane cytoskeleton interactions rather than as a simple linker between membrane surfaces and actin.

As well as being structural components of the cytoskeleton, annexins have also been found to associate with proteins involved in the modulation of actin dynamics. For instance annexin I has been shown to interact with profilin, a phosphatidylinositol 4,5-bisphosphate binding protein implicated in the control of actin polymerisation (Alvarez Martinez et al., 1996; Alvarez Martinez et al., 1997) while annexin II has been shown to form a complex with the actin binding proteins α-actinin, moesin and ezrin (Harder et al., 1997). The implications of these findings are at present unclear, but are consistent with annexins playing a role in actin/membrane dynamics.

Of the three annexins discussed, only annexin II has so far been shown to bind and bundle F-actin at physiological concentrations of Ca^{2+}. These and other findings concerning the interaction of annexin II and the cytoskeleton are discussed below.

1.6.2 Annexin II and the cytoskeleton.

Annexin II has been shown to colocate with F-actin at cortical structures in numerous cell types including brush borders (Kaczan Bourgois et al., 1996; Massey-Harroche et al., 1998), cortical actin in the cell body (Harder and Gerke, 1993) and sites of active membrane protrusion such as ruffles (Diakonova et al., 1997). Immunoelectron microscopic studies have also demonstrated a co-localisation of annexin II and microfilaments, with the localisation of annexin II to discrete patches at the surface of early endosomes, at the interface of microfilaments and the endosome surface (Harder et al., 1997). These immunocytochemical observations indicating an involvement of annexin II in actin dynamics are complemented by compelling *in vitro* data.

Firstly, annexin II_2pI1_2 has been shown to bind and bundle F-actin at physiological Ca^{2+} levels, and the binding sites on annexin II responsible for the interaction with actin have been identified (Jones et al., 1992). Half maximal annexin II_2p11_2 mediated F-actin bundling has been reported to occur at concentrations of Ca^{2+} as low as 0.1-2 μM (Ikebuchi and Waisman, 1990), well within the range of Ca^{2+} concentrations found in cells under physiological conditions. This activity can be specifically inhibited by preincubation of F-actin with a nonapeptide to the putative actin binding site of annexin II at residues 286-294 (Jones et al., 1992). Interestingly, although the nonapeptide inhibits annexin II_2p11_2

dependent F-actin bundling it does so without causing annexin II_2p11_2 dissociation from F-actin. This has lead to the proposition that annexin II_2p11_2 bundles F-actin through self association, which is in turn dependent on a specific conformational change in annexin II_2p11_2 induced by F-actin binding. Abolition of F-actin bundling ability through pre-incubation of F-actin with the nonapeptide could thus be attributed to interference with the conformational change, but not F-actin binding *per se* (Waisman, 1995).

Secondly, annexin II shares some common features with other actin-bundling proteins (Waisman, 1995; and references therein). Half maximal binding of annexin II_2p11_2 occurs near 0.18 μM of free protein which is in the range reported for other bundling proteins such as non muscle alpha-actinin (0.22 μM), fascin (0.53 μM) and the 30 kDa bundling protein from *Dictyostelium* (0.10 μM).

It may be significant that the F-actin bundling activity of annexin II_2p11_2 is modulated by phosphorylation since tyrosine phosporylation by $pp60^{c\text{-}src}$ has been shown to negatively regulate bundling activity (Hubaishy et al., 1995). Interestingly phosphorylation of annexin II_2p11_2 by $pp60^{c\text{-}src}$ occurs poorly in solution, or when annexin II_2p11_2 is bound to F-actin, but is strongly stimulated by the Ca^{2+}-dependent binding of annexin II_2p11_2 to negatively charged phospholipids (Bellagamba et al., 1997). Thus modulation of annexin II_2p11_2 F-actin bundling activity may be influenced by tyrosine phosphorylation, which is itself dependent on Ca^{2+}-dependent membrane binding.

Actin is not the only cortical cytoskeletal element annexin II has been found to bind. In some of the earliest work on annexin II, non-erythroid spectrin (fodrin) was identified as a ligand for annexin II in biochemical extractions and was found to co-localise with annexin II in immunofluorescence studies (Gerke and Weber, 1984). The relevance of this association is questionable since binding depends on relatively high concentrations of Ca^{2+} and may be non-specific (Cheney and Willard, 1989).

Lastly, annexin II has been shown to bind Ca^{2+}-dependently to the intermediate filament protein GFAP (glial fibrillary acidic protein) and to stimulate the assembly of this protein into filaments (Bianchi et al., 1994; Garbuglia et al., 1995). Whether annexin II is involved in assembly of GFAP *in vivo* is unclear, and indeed there are no reports of the two proteins co-locating in immunofluorescence studies.

1.7 Annexins and exocytosis.

1.7.1 Current models of the molecular mechanism of Ca^{2+} regulated exocytosis.

Until quite recently it was suspected that the annexins might play a central, pivotal role in Ca^{2+} regulated exocytosis. Although, as will be discussed later, the annexins may be involved in this process, recent advances have made it clear that the coordinated actions of a large number of unrelated proteins are required for the precise targeting, docking and fusion of exocytic vesicles with the plasma membrane. In particular the role(s) intially proposed for some members of the annexin family are apparently performed by quite different proteins.

Investigation of the molecular mechanisms of Ca^{2+} regulated exocytosis was focused in 1994 by the SNARE (soluble N-ethylmaleimide-sensitive fusion protein attachment protein receptor) hypothesis (for reviews see Linial, 1997; Zheng and Bobich, 1998). The sequence of discoveries leading to the formulation of this hypothesis was initiated by the search for cytosolic proteins involved in vesicular fusion in the Golgi cisternae. These investigations identified N-ethylmaleimide-sensitive fusion protein (NSF) and soluble NSF attachment proteins (SNAPs) (Rothman and Orci, 1992) as proteins involved in vesicle fusion at the Golgi cisternae.

Further work focusing on brain membranes identified membrane specific SNAP receptors (SNAREs) (Sollner et al., 1993b). Specifically one type of SNARE was identified as synaptic vesicle associated membrane protein, VAMP/synaptobrevin (vesicle associated SNARE or v-SNARE) while other types of SNARE, syntaxin and SNAP-25, were found to be specific for the plasma membrane (target-associated SNAREs or t-SNAREs) (Sollner et al., 1993a). The discovery of a stoichiometric complex of a v-SNARE and a t-SNARE, together with the general cytosolic fusion protein SNAP (Clary et al., 1990) and NSF (Block et al., 1988) formed the basis of the SNARE hypothesis (Rothman, 1994). The central tenet of this hypothesis is that that this complex provides a core mechanism for specifically pairing membranes (Figure 1.8, overleaf).

Both v- and t- SNAREs have been characterised in yeast, plants and animals (Bennett, 1995; Linial, 1997; Rothman, 1994). Family members are selectively localised to cellular compartments such as ER and the nuclear envelope, Golgi, endosomes, lysosomes, secretory storage vesicles and apical and basolateral plasma membranes and are required for fusion events that involve the compartments with which they are associated (Bock et al., 1997; Lewis et al., 1997; Pelham et al., 1995; Rothman and Wieland, 1996). As proposed in the intial hypothesis, the v- and t-SNAREs bind each other in a pairwise,

cognate fashion (Bennett et al., 1993; Pevsner et al., 1994; Protopopov et al., 1993; Sogaard et al., 1994) and must reside in opposite membranes for fusion to occur (Nichols et al., 1997).

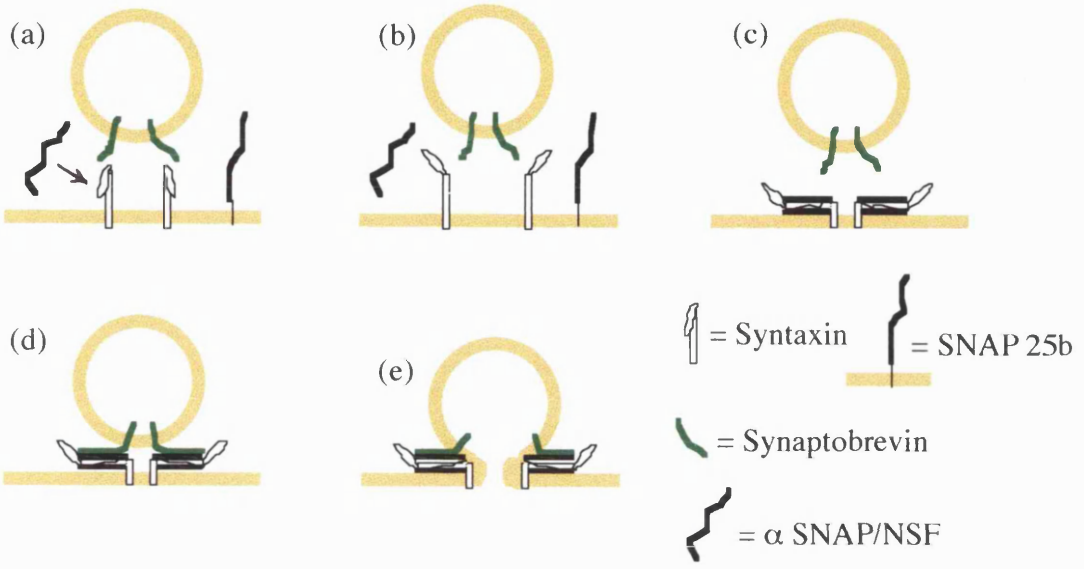

Figure 1.8: Formation of the SNARE complex and its possible role in vesicle fusion.

The core machinery involved in synaptic vesicle/plasma membrane fusion consist of the synaptic vesicle membrane protein synaptobrevin (a vesicle (v-) SNARE) and the plasma membrane proteins syntaxin and the 25 kDa synaptosome associated protein SNAP-25 (two target (t-) SNAREs) which interact to form the SNARE core complex (Sollner et al., 1993a; also see text). During **ACTIVATION** (a - b) two soluble proteins - N- ethylmaleimide sensitive factor (NSF) and soluble NSF attachment protein (α-SNAP) are proposed to disassemble the core complex in preparation for a new round of vesicle fusion (small arrow in (a), note conformational change in syntaxin from (a) to (b)). During **BINARY COMPLEX FORMATION** (b - c) α-SNAP binds to the SNAP receptor (SNAREs) and then binds NSF (not shown in detail). Binary complex formation (docking) is followed by **TERNARY COMPLEX FORMATION** (c-d) which is thought to power **VESICLE FUSION** (e). Modified from Skehel and Wiley, 1998.

Free cognate SNAREs in solution spontaneously assemble into stable complexes (ie assembly is favoured energetically). In solution the free energy released on complex formation is lost as heat while in contrast the formation of v-t-SNARE complexes on adjacent membranes may directly contribute free energy to the process of membrane fusion (Weber et al., 1998). Cognate v- and t-SNAREs bind each other by membrane-proximal heptad repeat regions that are predicted to form coiled-coils or closely related helical bundles. In electron micrographs SNARE complexes are seen to be rods, 13-14 nm long and approximately 2 nm wide, consistent with the formation of such structures (Hanson et al., 1997). Since the membrane anchors of v- and t-SNAREs emerge at the same end of the

rod (Hanson et al., 1997; Lin and Scheller, 1997) this would imply that the rod must lie approximately in the plane of contact between the vesicles paired by a v-t-SNARE complex - the so-called 'SNAREpin'. Formation of SNAREpins could thus be directly involved in 'winching' adjacent membranes together during the process of fusion (for review see Skehel and Wiley, 1998).

There is some evidence that formation of the v-t-SNARE complex may be the minimal machinery required to promote membrane fusion (Weber et al., 1998). However the rate of fusion seen *in vitro* between liposomes charged with cognate SNAREs is low, certainly not within the μs range of Ca^{2+} activated synaptic transmission. How then is SNARE assembly controlled *in vivo*? If the SNARE core complex is instrumental in executing membrane fusion durin Ca^{2+} -regulated exocytosis how is it activated by a rise in intracellular Ca^{2+}?

In view of the interaction of cognate SNAREs on synthetic membranes *in vitro* it comes as little suprise that the assembly of v-t-SNARE complexes *in vivo* appears to be under kinetic control by regulatory proteins (Rothman and Sollner, 1997). Included in this group of proteins are various members of the Rab GTPase family, the Sec1 family, fibrous 'string' proteins (Orci et al., 1998) such as p115 and GM130 (Nakamura et al., 1997) and exocyst complexes (Kee et al., 1997; TerBush et al., 1996). Regulatory proteins can potentially add specificity to v-t-SNARE interaction by locally modulating the rate of SNARE complex assembly.

Searches for a Ca^{2+} sensor to transduce increases in intracellular Ca^{2+} into an exocytic response, via assembly a SNARE complex, have focused largely on synaptotagmin. This 65-kDa integral membrane protein binds to the t-SNARE protein syntaxin and/or negatively charged phospholipids in the presence of Ca^{2+} (Brose et al., 1992; Chapman et al., 1995; Li et al., 1995). All synaptotagmins contain a single transmembrane region, a short N-terminal glycosylated domain within the vesicle lumen and a C-terminal cytoplasmic region. The cytoplasmic region is composed of two homologous C2 domains (homologous to the regulatory region of protein kinase C) known as C2A and C2B. While C2A mediates the interaction between t-SNARE and negatively charged phospholipids the C2B domain has been shown to interact with brain specific β-SNAP (Schiavo et al., 1995) and inositol phosphates (Fukuda et al., 1994; Ibata et al., 1998) and is responsible for the Ca^{2+}-dependent dimerization of synaptotagmin (Chapman et al., 1996). The combination of β-SNAP and synaptotagmin is able to recruit NSF and to assemble a large complex containing α-SNAP and SNAREs (Schiavo et al., 1995). Whether synaptotagmin is indeed the Ca^{2+} sensor in Ca^{2+}-dependent exocytosis is not clear. While synthetic or natural synaptotagmin peptides or anti-synaptotagmin antibodies impair Ca^{2+} triggered exocytosis (Bommert et al., 1993; Elferink et al., 1993) genetic studies have yielded mixed results (Broadie et al., 1995; Geppert et al., 1994), (Littleton et al., 1993;

Shoji-Kasai et al., 1992) possibly due to the existence of mixed synaptotagmin isoforms (Craxton and Goedert, 1995; Sudhof, 1995) with overlapping functions (Ullrich et al., 1994). Uncertainty over how Ca^{2+} and the SNARE complex interact during Ca^{2+} regulated exocytosis has been deepened by recent findings *in vitro*.

Work using sea-urchin egg cortical vesicles (CV) to reconstitute fusion *in vitro* has demonstrated that Ca^{2+} can disrupt the SNARE protein complex without irreversibly blocking fusion (Tahara et al., 1998). It was found that CV SNARE complexes are disrupted by free Ca^{2+} concentrations that triggered maximal fusion. N-ethylmaleimide, which blocks fusion at or before the Ca^{2+}-triggering step blocks complex disruption by Ca^{2+}. However disruption is not blocked by lysophosphatidylcholine (LPC), which transiently arrests a late stage of fusion. Since removal of LPC from Ca^{2+}-treated CV allows fusion, SNARE complex disruption occurs independently from the membrane fusion step. As Ca^{2+} disrupts rather than stabilizes the complex it is hard to reconcile these results with the SNAREpin hypothesis wherein SNARE complex formation is instrumental in driving fusion.

While the original SNARE hypothesis proposed that essentially all membrane fusion events during vesicle traffic are mediated by cognate v- and t- SNARE partners doubts have been raised over the ubiquity of this mechanism by recent findings in *Saccharomyces cerevisiae* (Peters and Mayer, 1998). These results demonstrated that the Ca^{2+} sensor responsible for interpreting a rise in Ca^{2+} into completion of docking and triggering of membrane fusion during vacuole fusion is calmodulin, and not a synaptagmin related protein. Based on these findings a model was proposed in which SNARE complex formation plays a central role in docking, and in which a late stage of docking itself triggers a local rise in Ca^{2+} which is sensed and acted upon by calmodulin.

To conclude, although the potential role of annexins in exocytosis has been largely over shadowed by recent advances, very recent data suggests that the SNARE hypothesis is not applicable to all types of membrane fusion. It is therefor possible that some of the ideas originally proposed for annexin function in membrane fusion might warrant further scrutiny. The evidence for and against an involvement of annexins in Ca^{2+}-regulated exocytosis is discussed in the following section.

1.7.2 The annexins and Ca^{2+} regulated exocytosis.

In the late 1970s, application of the traditional "grind and find" approach of the biochemist led to the purification of annexin VII (synexin) from the adrenal medulla, on the basis of its ability to aggregate chromaffin granules in the presence of Ca^{2+} *in vitro* (Creutz

et al., 1978). The subsequent finding that annexin VII can also aggregate and fuse synthetic liposomes composed of negatively-charged phospholipids in the presence of 10 μM Ca^{2+} suggested aggregation was due to phospholipid binding (Hong et al., 1982; Hong et al., 1981; Ohki and Leonards, 1982). This property suggested that annexin VII could be involved in linking rises in cytoplasmic Ca^{2+} with regulated exocytosis, perhaps playing a role in docking or the fusion process itself. However, two pieces of evidence appeared inconsistent with such a role.

Firstly, the Ca^{2+} concentrations required for annexin VII to mediate half maximal chromaffin aggregation *in vitro* (200μM) appeared too high to occur under physiological conditions since maximal secretion occurs at 1-2 μm free Ca^{2+} in permeabilised chromaffin cells while maximum secretory rate is sustained at <10 μM Ca^{2+} (Augustine and Neher, 1992; Cheek et al., 1989). Secondly, annexin VII is not fusogenic *per se* although fusion of annexin VII aggregated vesicles can be induced by the addition of "biological detergents" such as *cis*-unsaturated fatty acids (Creutz, 1981).

Despite these reservations the hypothesis that annexins are involved in Ca^{2+} regulated exocytosis has received considerable attention, and since the initial findings on annexin VII other members of the family have been implicated in this process in a variety of cell types (see table below).

Table 1.5: Cells types in which annexins have been proposed to play a role in exocytosis.

Annexin	Cell type/secretory vesicle	Source
I	Neutrophils/neutrophil specific granules.	(Meers et al., 1992)
II	Chromaffin cells/chromaffin granuls.	(Creutz et al., 1987)
	Mammary epthilelial/casein(+) vesicles.	(Handel et al., 1991)
	Lung epithelial/lammelar bodies.	(Liu et al., 1996)
	Bovine pulmonery artery endothelial	(Konig et al., 1998)
VII	Chromaffin/chromaffin granules.	(Creutz et al., 1978)

(This table is not a comprehensive review, but indicates the earliest references proposing a role for each given annexin in exocytosis in a range of cell types)

Of those annexins implicated in Ca^{2+}-regulated exocytosis only annexin II aggregates chromaffin granules at physiological Ca^{2+} levels (Drust and Creutz, 1988). Since this discovery attention has focused on annexin II, generating a considerable body of literature.

1.7.3 Annexin II and Ca^{2+}-regulated exocytosis.

Annexin II was identified as a prominent Ca^{2+}-dependent chromaffin granule binding protein (Creutz et al., 1987), and *in vitro* studies demonstrated that the annexin II_2p11_2 heterotetramer could aggregate chromaffin granules at physiologically relevant Ca^{2+} levels (Drust and Creutz, 1988) as well as lamellar bodies from lung epithelial cells (Liu et al., 1995a) and synthetic vesicles (Blackwood and Ernst, 1990). Interestingly, while the annexin II_2p11_2 heterotetramer readily aggregates chromaffin granules it will not aggregate purified zymogen granules indicating specificity in the binding to different classes of secretory vesicle (Creutz et al., 1992). Only annexin II_2p11_2, and not monomeric annexin II, will aggregate vesicles at physiologically relevant Ca^{2+} levels (Drust and Creutz, 1988) presumably because this molecular arrangement provides two Ca^{2+}-dependent membrane binding domains at either end of the complex. Quick freeze deep etch electron microscopy has provided evidence that the crossbridges expected from such a linker indeed exist between annexin II_2p11_2 aggregated granules in vitro (Nakata et al., 1990) and between plasma membrane and granule surfaces in anterior pituatry cells (Senda et al., 1994) and between granule-granule contacts in the cytoplasm (Senda et al., 1998). Definitive evidence that the bridges seen in the cell are indeed annexin II_2p11_2 is lacking, the inference being made on the basis of the localisation of annexin II immunoreactivity to granule-plasma membrane and granule-granule contacts and the size of the cross bridges. Further data on the Ca^{2+}-dependent junctions formed *in vitro* between liposomes by annexin II_2p11_2 has come from cryo-electron microscopic studies (Lambert et al., 1997; see Figure 1.5, 25). These data demonstrate the spontaneous formation of characteristic junctional plaques between the surfaces of neigbouring liposomes in the presence of Ca^{2+} and annexin II_2p11_2 which possesss 7 electron-dense parallel stripes, the three inner stripes of which correspond to the annexin II_2p11_2 cross-bridges. It should be noted that this study also provides evidence that annexin II can cross-bridge membranes in the absence of p11, presumably by a process of self association similar to that proposed for annexin I (Meers et al., 1992).

Although the ability of annexin II to promote Ca^{2+}-dependent membrane/membrane interactions *in vitro* is well characterised, how this property translates into a role in regulated exocytosis is not precisely clear. Attempts to link the membrane cross-bridging properties of annexin II with a physiological function have focused on a putative role in docking and positioning of secretory granules at the plasma membrane in preparation for fusion. A pivotal role in the process of Ca^{2+}-dependent fusion itself has also been proposed based on the finding that annexin II_2p11_2 can lower the Ca^{2+} requirement for fusion of aggregated vesicles *in vitro* in the presence of arachidonic acid (Liu et al., 1995a).

Although this *in vitro* data is extremely suggestive, there is little direct evidence for a role of annexin II in either docking or fusion *in vivo*. The first serious attempts to bridge the gap between the abundant *in vitro* data and living cells, used permeabilised cells to identify proteins involved in regulated exocytosis. Cells permeabilised with digitonin, streptolysin-O, or beta-escin tend to leach soluble proteins into the surrounding medium and concomitantly lose their ability to secrete on stimulation with Ca^{2+} and Mg-ATP (Sarafian et al., 1987). Addition of unfractionated cell cytoplasm to such 'run-down' cells can rescue the secretory phenotype (Sarafian et al., 1987) and, using fractionation techniques, the protein components required to rescue secretion present in the crude cytoplasmic milieu may be identified. Such an approach using digitonin-permeabilised chromaffin cells led to the identification of annexin II as a protein capable of retarding, but not rescuing, the process of run-down in both the heterotetrameric and monomeric forms (Ali and Burgoyne, 1990; Ali et al., 1989) and as a mixture of both forms in alveolar epithelial type II cells (Liu et al., 1996). Half maximal annexin II_2p11_2 mediated chromaffin granule aggregation occurs at 1.8 μM while half maximal secretion from permeabilised chromaffin cells occurs at approximately 1 μM (Morgan and Burgoyne, 1992a) indicating annexin II could be part of the Ca^{2+} sensing machinery in Ca^{2+} regulated exocytosis. Furthermore, retardation of run-down is dependent on the integrity of the annexin II monomer since the annexin II core domain will not retard run-down even in the presence of 200 μM Ca^{2+}, indicating that the N-terminal domain is necessary for the protein's action in exocytosis. While these data argue strongly for an involvement of annexin II in Ca^{2+} regulated secretion it's precise role and importance in the process is unclear. For instance, annexin II cannot rescue the secretory phenotype of chromaffin cells after run-down over prolonged (>60 min) periods (Burgoyne and Morgan, 1990; Sarafian et al., 1991). In contrast, 14-3-3 proteins (Morgan and Burgoyne, 1992a; Morgan and Burgoyne, 1992b; Wu et al., 1992) are capable of stimulating exocytosis from cells which have been run-down over a similar period (70 min). Also, cytosolic extracts depleted of soluble annexin II by immunoadsorption still retard run-down in digitonin permeabilised cells as effectively as complete cytosolic extract (Wu and Wagner, 1991) indicating that annexin II may play only a modulatory role in Ca^{2+} regulated exocytosis. Together these findings have led to the suggestion that the potential of annexin II to retard run-down may reside in the possesssion of a 14-3-3 homology domain (Morgan and Burgoyne, 1992a) (see Figure 1.3, 20, Figure 1.6, p 33). A peptide corresponding to this conserved C-terminal domain acts as a potent inhibitor of exocytosis in permeabilised chromaffin cells (Roth et al., 1993) suggesting the involvement of annexin II in Ca^{2+} regulated secretion may be mediated by this domain of the protein. Stimulation of catecholamine secretion from chromaffin cells by 14-3-3 proteins is thought to be due to reorganisation of the actin cytoskeleton (Roth and Burgoyne, 1995) possibly through increased access of secretory granules to the plasma

membrane. The molecular mechanisms leading to the observed cytoskeletal changes are currently obscure, although it is possible PKC is involved since although both 14-3-3 proteins and PKC can stimulate secretion in run-down chromaffin cells a mixture of the two has a far more potent effect (Morgan and Burgoyne, 1992b). Since 14-3-3 proteins are a poor substrate for PKC this is not thought to be due to direct phosphorylation of the 14-3-3 protein, but would be consistent with 14-3-3 proteins enhancing the efficiency of PKC stimulated secretion - perhaps by influencing PKC targeting or interaction with other target proteins.

With this in mind it is interesting that the 14-3-3 homology domain identified in annexin II is conserved among members of the annexin family (Dubois et al., 1996) and has been implicated in the function of annexin I as a receptor for activated C kinase (RACK) (see Figure 1.6, p 33). A consensus peptide to the conserved region in 14-3-3 proteins inhibits the binding of full length 14-3-3 proteins to PKC (Xiao et al., 1995) while a peptide to the conserved region in annexin I inhibits the binding of PKC to a number of RACKs (Mochly-Rosen et al., 1991). Whether this same domain in annexin II mediates binding of annexin II to PKC has not been elucidated, and it is not known if annexin II also retards run-down through modulation of the actin cytoskeleton.

Some confusion surrounding the possible function of annexin II in Ca^{2+} regulated secretion has arisen through the inconsistent results derived *in vivo* in intact cells, run-down models and *in vitro*. Annexin II is phosphorylated by PKC during stimulated secretion in chromaffin cells with a similar time course to secretion (Creutz et al., 1987; Delouche et al., 1997; but see Waisman, 1995) and it has been established that PKC phosphorylation of annexin II_2p11_2 *in vitro* abolishes the ability of the heterotetramer to aggregate chromaffin granules (Johnstone et al., 1992; Regnouf et al., 1995). These findings would be consistent with PKC phosphorylation of annexin II being involved in the dissociation or disaggregation of membrane surfaces from one another during Ca^{2+} regulated exocytosis. However, Sarafian et al (1991) have shown that after inhibition of PKC in chromaffin cells using staurosporine secretory run-down cannot be retarded by exogenous annexin II unless the annexin II has been phosphorylated by PKC. Since PKC-phosphorylated annexin II_2p11_2 has impaired granule aggregation abilities, this result suggests annexin II performs a role(s) in Ca^{2+} regulated exocytosis independent of membrane aggregation. A direct role in fusion itself has been proposed based on the finding that PKC-dependent phosphorylation of annexin II_2p11_2 involved in chromaffin granule aggregation *in vitro* causes granule/granule fusion (Regnouf et al., 1995). However since fusion activity was dependent on pre-aggregation of chromaffin granules with annexin II_2p11_2 it is unclear how these results relate to those of Sarafian et al (1991).

A second approach to investigate the role of annexin II in secretion in whole cells has been based on microinjection of annexin II homologous peptides into live cells and

subsequent analysis of secretory ability. This approach has been used in conjunction with amperometric measurement of nicotine stimulated secretion in live chromaffin cells (Konig et al., 1998) and with amperometric measurement of secretion followed by subsequent fixation and immunofluorescence analysis of annexin II distribution (Chasserot Golaz et al., 1996). This strategy has provided data showing that microinjection of a peptide corresponding to the N-terminus of annexin II strongly inhibits secretion and concomitantly blocks translocation of annexin II to the subplasmalemmal region (Chasserot Golaz et al., 1996) and that the inhibitory effect on secretion is dependent on the acetylation of the N-terminus (Konig et al., 1998). The findings of these studies - that the N-terminus may be essential for annexin II involvement in secretion - contrast strongly to permeabilisation studies in which a peptide corresponding to the N-terminus of annexin II was found to have no effect on Ca^{2+}-dependent secretion in digitonin permeabilised chromaffin cells (Ali and Burgoyne, 1990). The discrepency between these findings may reside in the different techniques used to access and modulate the cell interior. Since digitonin permeabilises cells through at least partly through sequestration of membrane cholesterol (Rosenqvist et al., 1980), a process known to release a Ca^{2+}-independently bound pool of annexin II (Harder et al., 1997), this could indicate that permeabilisation by-passes a step in exocytosis requiring the N-terminus of annexin II in microinjected cells.

The significance of the translocation of annexin II to a subplasmalemmal domain in relation to Ca^{2+}-dependent secretion is also questionable. Annexin II has been shown to translocate to a subplasmalemmal, detergent-insoluble fraction during stimulated secretion of chromaffin cells (Chasserot Golaz et al., 1996; Sagot et al., 1997) or the neuroblastoma SH-SY5Y cell line (Blanchard et al., 1996). Although annexin II translocation in chromaffin cells could be consistent with a role in Ca^{2+}-dependent exocytosis, in the SH-SY5Y cells annexin II apparently translocates to discrete membrane domains which do not resemble the distribution of synaptic vesicle proteins - arguing against a role for annexin II in membrane fusion in these cells.

The third strategy used for investigating the function of annexin II in a secretory cell line *in vivo* has utilised expression plasmids to manipulate the levels of annexin II in PC12 cells (Graham et al., 1997). Three cell lines were generated in this study: one in which functional annexin II was removed from the cytoplasm using a mutant which aggregates annexin II, a second mixed clonal cell line constitutively overexpressing annexin II and a third cell line which over-expressed annexin II when challenged with sodium butyrate. None of these cell lines showed a significant impairment or enhancement of Ca^{2+}-regulated exocytosis either before or after induction of over expression, arguing against a central role for annexin II in Ca^{2+}-dependent exocytosis in PC12 cells.

In conclusion, the evidence for a central role of annexin II in Ca^{2+}-regulated exocytosis in all cell types where this process occurs is currently inconclusive. However

the evidence that annexin II is involved in Ca^{2+}-regulated secretion in certain cell types - for instance bovine aortic endothelial cells (Konig et al., 1998) - is compelling and perhaps reflects subtle differences in the mechanisms underlying regulated exocytosis in different cells.

1.8 Annexins and endocytosis.

1.8.1 General.

Members of the annexin family have been found in association with most recognised endosomal compartments (Table 1.6). In addition annexins II and VI have been associated with caveolae, but since the function of caveolae in endocytosis and/or signaling is unclear these structures are discussed elsewhere (see 1.9 Annexins, caveolae and transcytosis.).

Table 1.6: Annexins and endocytic compartments.

Compartment.	Annexin.	Source.
Early endosome.	I, II, VI	(Diakonova et al., 1997; Seemann et al., 1996b) (Seemann et al., 1997; Harder et al., 1997) (Jost et al., 1997; van der Goot, 1997) (Aledo et al., 1997; Jackle et al., 1994) (Ortega et al., 1997)
CURL[1]	IV, VI	(Diakonova et al., 1997; Pol et al., 1997)
MVB[2]	I	(Pol et al., 1997; Futter et al., 1993)
RRC[3]	II, VI	(Pol et al., 1997; Jackle et al., 1994)
Late endosome	V	(Diakonova et al., 1997)
Phagosome	I, III, IV, VI	(Harricane et al., 1996; Kaufman et al., 1996) (Diakonova et al., 1997; Desjardins et al., 1994)

(CURL) Compartment of Uncoupling of Receptor/Ligand, (MVB) Multi Vesicular Body, (RRC) Receptor Recycling Compartment

Of those annexins associated with endocytic compartments, annexins I, II and VI have been closely scrutinised and are perhaps the best understood in terms of targeting and possible function. While the evidence for annexin I and II leans towards roles post

internalisation (but see Biener, 1996) - perhaps in vesicle trafficking and/or receptor sorting - annexin VI has been implicated in the very earliest stages of endocytosis in the budding of clathrin coated pits using an *in vitro* assay (Lin et al., 1992). However, any notion that annexin VI plays an essential role in this process is certainly questionable since the A431 cell line - which readily supports clathrin mediated endocytosis - does not possess annexin VI (Smythe et al., 1994) and annexin VI knockout mice are indistinguishable from wild type mice (Hawkins and Moss, unpublished results). It would seem safe to assume that clathrin-mediated endocytosis occurs unhindered in these mice, although this has not been specifically analysed at the time of writing. The remaining evidence for a role of annexin VI in endocytosis is mostly based on association of annexin VI with specific endocytic compartments. For instance, annexin VI has been found to be greatly enriched in an apical early endosomal compartment and in compartments associated with receptor/ligand uncoupling, multivesicular bodies and receptor recycling in hepatocytes (Jackle et al., 1994; Ortega et al., 1998). As annexin VI has been shown to bind actin (Hosoya et al., 1992) it is feasible that annexin VI plays a role in mediating between these compartments and the actin cytoskeleton, though evidence to substantiate this hypothesis is lacking.

As in the case of annexin VI, some controversy surrounds the role of annexin I in endosome dynamics. It has been known for some time that annexin I is a substrate for the EGF receptor (Pepinsky and Sinclair, 1986; Valentine Braun et al., 1987; Varticovski et al., 1988) and experiments have demonstrated that tyrosine phosphorylation occurs within multivesicular bodies during inward vesiculation of these structures, and sorting of the EGF receptor to lysosomes (Futter et al., 1993). These findings have led to the suggestion that annexin I plays a role in these processes, though there is no direct evidence to support this claim, and indeed these results have been questioned. Since the cells used in this study constitutively overexpressed the EGF receptor, chronic EGF stimulation may have overloaded the endocytic system leading to abnormal vesicle trafficking, causing "overspill" of components normally found in early endocytic compartments into later ones. Studies using cells which naturally express the EGF receptor suggested annexin I is in fact associated with early endosomes and not multivesicular bodies (Seemann et al., 1996b). These data, based on immunoelectron microscopy and cell fractionation, further demonstrate the importance of the N-terminal domain in targeting annexin I to early endosomes since truncation of the N-terminal 26 residues of annexin I alters its intracellular distribution to later elements of the endocytic path. However, although details of targeting specificity and the molecular basis of targeting have been clarified, the function of annexin I in early endosome biology is obscure. An important clue may be the ability of annexin I to target S100C to early endosomes (Seemann et al., 1997) and the eventual resolution of annexin I function may reside in the biology of this protein.

In comparison to annexins I and VI, published data implicating annexin II in endosome dynamics is perhaps more consistent and this may be attributed to the use of both *in vitro* and powerful *in vivo* approaches. Attention has largely focused on the association of annexin II and early endosomes, identified through cell fractionation, immunofluorescence and immunoelectron microscopic studies.

1.8.2 Annexin II and endosomal compartments.

Annexin II is phosphorylated during internalisation of insulin receptor (Biener et al., 1996) and it was suggested that annexin II may be involved in the internalisation and/or sorting of this receptor, perhaps in a similar relationship to that between annexin I and the EGF receptor. Stronger evidence that annexin II is involved in early endosome dynamics has come from *in vitro* data and increasingly from intact cell models.

Firstly, annexin II has been implicated in the process of early endosome fusion. By using two distinctly labeled early endosome populations *in vitro* it has been possible to identify proteins involved in endosomal fusion. Using such an approach it was shown annexin II is a major component of fusogenic endosomal fractions and is efficiently transferred from a donor population of early endosomes to an acceptor population during *in vitro* fusion (Emans et al., 1993). Further experiments have demonstrated that Ca^{2+}-dependent fusion of isolated early endosomes can be blocked by addition of an anti-annexin II antibody or annexin II peptide (Mayorga et al., 1994) suggesting a role for annexin II in either fusion itself or aggregation of early endosomal membranes prior to fusion. One could imagine that constitutive early endosome fusion this type role may be central to the maintenance of early endosome architecture *in vivo* since there is evidence the early endosome consists of a continuous network of interconnected tubules, and not isolated vesicles (Tooze and Hollinshead, 1991). However, these *in vitro* experiments, though suggestive, can only reconstitute a subset of the possible interactions annexin II_2p11_2 could potentially mediate *in vivo*. For instance annexin II_2p11_2 could also cross-bridge the surface of early endosomes to cytoskeletal elements such as actin, and thus function either in maintaining overall architecture of the early endosomal system or in an actin-dependent trafficking process.

Evidence is accumulating that annexin II may indeed have an architectural role, anchoring early endosomes to the cortical cytoskeleton of the cell. For example early endosomes in Madine Darby Canine Kidney (MDCK) cells are normally anchored in the periphery of the cell in conjunction with actin, annexin II and p11 (Harder and Gerke, 1993). Incubation of the cells in low Ca^{2+} leads to breakdown of the cortical actin cytoskeleton and redistribution of early endosomes into the cell body suggesting that

maintenance of the cortical cytoskeleton is Ca^{2+} dependent. Crucially, redistribution of early endosomes can also be achieved by ectopic expression of a trans-dominant annexin II-p11 mutant designed to aggregate endogenous annexin II_2p11_2. Aggregation of annexin II_2p11_2 leads to specific co-aggregation of early endosomes within the cell body without affecting the cortical cytoskeleton. Thus annexin II_2p11_2 appears to be essential for locating early endosomes to the cell periphery.

With respect to this finding it is interesting to note that while cortical anchorage of annexin II and early endosomes is Ca^{2+}-dependent the association of annexin II and early endosomes is not. Binding to early endosomal membranes in the absence of Ca^{2+} has been shown to be mediated through residues 15-24 (Jost et al., 1997). Thus the Ca^{2+}-dependent anchorage of early endosomes in the cell cortex, if mediated by annexin II_2p11_2, may reflect the Ca^{2+}-dependent association of annexin II and some other cortical component such as actin rather than a Ca^{2+}-dependent association with membrane.

There is further evidence that annexin II may mediate between membranes and the actin cytoskeleton, and specifically between the surface of early endosomes and the actin cytoskeleton, from immunoelectron microscopic studies. Micrographs show annexin II present at the surface of early endosomes in clearly defined patches at the interface of filamentous components of the cytoskeleton (presumably microfilaments) and the early endosomal surface, consistent with a role for annexin II in linking the two (Harder et al., 1997; see Figure 4.24, 133). Bearing in mind that Ca^{2+} -independently membrane bound annexin II has been associated with α-actinin it is interesting to note that these proteins have been found to be highly enriched at membranes of the receptor recycling compartment (RRC) (Pol et al., 1997). Of the total amount of each protein associated with the entire endosomal system, 84% of actin, 90% of α-actinin and 95% of annexin II was found at the RRC. Taken together these data strongly suggest annexin II plays a role in mediating between the actin cytoskeleton and the surfaces of a subset of endosomal compartments. Whether this is an architectural role - with annexin II acting as an anchor - or a role in vesicle dynamics is at present unclear.

1.9 Annexins, caveolae and transcytosis.

1.9.1 Overview of caveolae structure and function.

Caveolae are cholesterol and sphingolipid enriched membrane domains which form plasma membrane invaginations of regular size and shape in most mammalian cell types (Brown and London, 1997; Hooper, 1998). The precise functions of caveolae have been

difficult to elucidate, one of the reasons being that caveolae are apparently but one specialised type of a broad range of detergent-insoluble glycosphingolipid rich membrane domains (DIGs) (Brown and London, 1997; Hooper, 1998). Since the biochemical methods used to isolate and analyse caveolae rely disruption of native cell membranes it has been feared DIGs of all types are simply an artifactual product of detergent extraction of membranes (Mayor and Maxfield, 1995). This has been somewhat allayed by recent work employing single particle tracking of fluorescently labeled DIG components in the plasma membrane of live cells which suggests phase separation and formation of isolated domains occurs in intact membranes (Sheets et al., 1997). Further evidence phase separation does indeed occur *in vivo* has been provided by studies using fluorescence resonance energy transfer (FRET) to monitor the distribution of glycosylphosphatidylinositol- (GPI-) anchored folate receptor and transmembrane-anchored folate receptor (Varma and Mayor, 1998). It was found that GPI anchored folate receptors became anchored in cholesterol-dependent membrane domains which were probably less 70 nm in diameter and therefor a similar size to caveolae.

Caveolae are particularly numerous in the continuous endothelium of certain microvascular beds (e.g. heart, lung and muscles) in which they have identified as transcytotic vesicle carriers (Predescu et al., 1998; Schnitzer et al., 1995a; Schnitzer et al., 1994). It seems likely that caveolae also perform more complex tasks besides simple transport since they are enriched in numerous signalling molecules such as src family kinases, members of the ras superfamily, heterotrimeric G-proteins, and a variety of receptors including platelet derived growth factor receptor (PDGFr) and epidermal growth factor (EGFr) (see Schlegel et al., 1998 and references therein). Furthermore there is evidence that caveolae have the molecular machinery for vesicle docking and fusion, including VAMP, NSF and SNAP (Schnitzer et al., 1995b). Together these data suggest caveolae have all the molecular machinery necessary act as 'alternative' endocytic organelles and specifically to receive extracellular signals, assemble signaling complexes and transport these complexes deeper into the cell.

Setting aside the questions surrounding the existence of DIGs in general and caveolae in particular, several members of the annexin family have been associated with these structures, including annexins II and VI. Of these annexins it is annexin II which has most often been associated with these structures.

1.9.2 Annexin II and caveolae.

Annexin II has been identified using cell fractionation techniques as a major component of caveolae in rat lung microvasculature beds (Stan et al., 1997), in the

syncytiotrophoblast of the placenta (Kristoffersen, 1996) and in a variety of cell lines including fibroblasts (Fielding and Fielding, 1995) and MDCK cells (Harder and Gerke, 1994). Moreover, both annexin II Ca^{2+}-independent membrane association and caveolae stability show a similar sensitivity to membrane cholesterol. In isolated membranes both annexin II Ca^{2+}-independent membrane association and caveolae are sensitive to low concentrations of the cholesterol sequestering drug filipin (Harder et al., 1997; Kiss and Geuze, 1997) suggesting that at least a portion of annexin II, bound Ca^{2+}-independently to the plasma membrane, resides in caveolae. It should be noted that the association of annexin II with caveolae could also involve Ca^{2+}-dependent binding. This is based on cell fractionation data demonstrating the association of annexin II with caveolae isolated from porcine lung is sensitive to Ca^{2+} sequestration (Parkin et al., 1996).

It may be significant that a number of receptor and non-receptor tyrosine kinases which have been linked directly with annexin II phosphorylation have also been located to caveolae. For instance annexin II is strongly phosphorylated on activation of the platelet derived growth factor receptor (PDGFr) (Brambilla et al., 1991) and insulin receptor (Biener et al., 1996) and both of these receptor tyrosine kinases have been functionally associated with caveolae (Liu et al., 1996; Smith et al., 1998). A novel relation ship may exist between the insulin receptor and annexin II since, somewhat intriguingly, annexin II phosphorylation has been linked with insulin receptor internalisation (Biener et al., 1996). It has not been established which specific kinases mediate annexin II phosphorylation during PDGF or insulin stimulation, and it seems likely that non-receptor tyrosine kinases perform this function. In this context it should be noted that annexin II was originally identified as a major cellular substrate for $pp60^{v\text{-}src}$, and both $pp60^{v\text{-}src}$ and endogenous $pp60^{c\text{-}src}$ are found concentrated in caveolae (Ko et al., 1998; Song et al., 1997). Thus both annexin II and kinases responsible for annexin II phosphorylation reside in the same membrane domain, although the functional significance of this is unclear.

Surprisingly there is no direct evidence that annexin II colocalises with caveolae *in situ*. An exception may be immunofluorescence data linking annexin II to transcytosis of cholestatic bile salts across hepatocytes in isolated hepatocytic couplets (Wilton et al., 1994). Treatment of couplets with lithocholate led to redistribution of annexin II first to the basolateral membrane, then to a perinuclear distribution and finally to an apical location. It is interesting to note that recent work has demonstrated the regulated internalisation of caveolae and relocation to a perinuclear location in fibroblasts (Parton et al., 1994) though whether the endocytic organelles observed by Wilton et al (1994) were caveolae is not known.

To conclude, despite the extensive biochemical data linking annexin II to caveolae, the function annexin II performs in these membrane domains is unclear. Possibilities include stabilisation of membrane domains, recruitment of negatively charged

phospholipids to these domains and interaction with the actin cytoskeleton. Since caveolae appear capable of supporting fission from the plasma membrane, transport, docking and fusion with target membranes (Schnitzer et al., 1995b) it is possible that annexin II is involved in any one of these steps. Thus, while intriguing, the association of annexin II with caveolae provides little insight into annexin II function.

1.10 Annexin II and human disease.

1.10.1 Annexin II and cancer.

Annexin II was originally identified as a major substrate for $pp60^{v\text{-}src}$, and has since been linked to cellular transformation in various studies. Increased annexin II expression *in situ* has been associated with a number of cancers including brain glioblastoma and pancreatic adenocarcinoma (Reeves et al., 1992; Roseman et al., 1994; Vishwanatha et al., 1993) and *in vitro* with a variety of carcinoma derived cell lines (Chiang et al., 1996; Cole et al., 1992; Kumble et al., 1992).

While elevated annexin II expression clearly coincides with cellular transformation in a number of instances, the role the molecule plays in this process is not clear. Theories range from a direct role in the cell cycle, to involvement in cellular adhesion during metastasis (Tressler et al., 1993). However, other roles for annexin II may also be consistent with published data. For instance, activation of a temperature sensitive v-src in fibroblasts is not only associated with a mitogenic response but also with a specific increase in the rate of macro-pinocytosis (Veithen et al., 1996). Thus up-regulation of annexin II expression associated with carcinogenesis could be consistent with up-regulation of a variety of cellular activities.

1.10.2 Annexin II and virus pathogenicity.

To successfully infect a host cell a virus must initially bind to the surface of the cell before triggering or initiating internalisation. To achieve this a range of proteins expressed on the surface of cells have been successfully exploited by viruses, including annexins V and II (de Bruin et al., 1996; Hertogs et al., 1993; Neurath and Strick, 1994; Wright et al., 1995; Wright et al., 1994).

While annexin V has been implicated in the binding and subsequent internalisation of hepatitis B virus (HBV), surface bound annexin II has been identified as a receptor for cytomegalovirus (CMV) in human umbilical vein endothelial cells (Hertogs et al., 1993;

Wright et al., 1994). CMV binds to such endothelial cells in a saturable and Ca^{2+}-dependent manner, and affinity adsorption of surface radiolabeled endothelial cells to virions resulted in the identification of a major cell-derived protein, subsequently identified as annexin II. Further evidence that annexin II is associated with CMV has come from studies on cultured fibroblasts. Annexin II was identified bound to virus particles isolated from CMV infected cells by immunoblotting of purified virions, by peptide mapping of virion associated proteins and by immunocytochemical staining of gradient purified virions (Wright et al., 1995). That annexin II is involved in the initial surface binding of the protein is suggested by the finding that antisera to annexin II inhibit CMV plaque formation in fibroblast monolayers in a concentration dependent manner (Wright et al., 1995). These data indicate that surface bound annexin II plays an important role in the pathogenesis of CMV and in addition are consistent with the presence of annexin II on the surface of cells under physiological conditions.

1.11 Investigation of annexin II function *in vivo*.

To date studies of annexin II function have been dominated by *in vitro* biochemical investigations. While these have yielded a detailed picture of the biochemical properties of this molecule, the precise role of annexin II *in vivo* remains obscure and this is reflected in the array of functions proposed for annexin II. For example (as has been discussed) annexin II has been linked with DNA replication, with vesicle aggregation, with membrane fusion, with mitogenesis and with cell adhesion. While it is theoretically possible that one molecule can perform such a range of functions, it is equally feasible that annexin II simply performs a similar fundamental function in a variety of situations. If so this function awaits elucidation.

In pursuit of this fundamental function(s), and in view of the extensive *in vitro* data published, the aim of this thesis was to investigate annexin II *in vivo* in intact cells using the fluorescent protein tag, Green Fluorescent Protein (GFP).

The use of fluorescently tagged proteins to follow the distribution and/or relocation of a protein in live cells in real time is a powerful and relatively new approach. This technique was originally dependent on the purification and chemical tagging of proteins with appropriate fluorophores *in vitro*, before microinjection into target cells and image analysis. Although still useful, such an approach presents considerable technical problems and is inevitably associated with cell damage either through photodamage (often catalysed by side reactions associated with fluorophore excitation) and/or microinjection. These problems have been partially circumvented with the introduction of fluorescent protein tags derived from the bioluminescent fluoroprotein of the coelenterate *Aquoria victoriana* (Chalfie et al., 1994; Inouye and Tsuji, 1994; Prasher et al., 1992; Wang and Hazelrigg,

1994). The generation of chimeric proteins is achieved through insertion of the cDNA encoding the protein or protein-fragment of interest upstream or downstream of the GFP open reading frame in an appropriate expression cassette. It is then simply a matter of transfecting the construct into cells and waiting for expression to reach the desired level before experimenting.

The usefulness of GFP as an *in vivo* probe is strengthened by the photostability of the fluorophore, and the fact that the residues responsible for fluorescence are tucked away deep inside the barrel-like protein. This latter characteristic effectively shields the fluorophore from fluctuations in the cellular environment such as changes in pH and ionic conditions (see Figure 1.9).

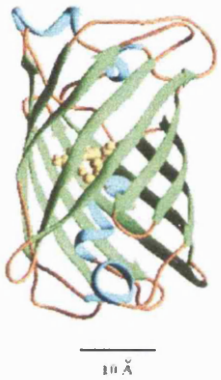

Figure 1.9: GFP forms a tight cylinder.

Eleven strands of β-sheet (green) form the walls of the cylinder. Short segments of helices (blue) cap the top and bottom and also provide a scaffold for the fluorophore (yellow) which is near the geometric centre of the cylinder. The fluorophore consists of an aromatic system made up of Tyr^{66} formed through reduction of its C-C bond coupled with cyclization of the neigbouring glycine and serine residues. Situation of the fluorophores inside the cylinder explains the resistance of the fluorophore to extremes in temperature, pH and ionic conditions.
(After Yang: http://www.bioc.rice.edu/Bioch/Phillips/Papers/gfpbio.html).

Concerns associated with the use of GFP as an *in vivo* tag focus on the possible effects the attachment of a 27 kD tag might have on the target protein. Abolition of protein function is one possible result, but perhaps even worse is modification of protein function leading to erroneous interpretation of results. However the largely successful tagging of proteins such as tubulin and actin (Fischer et al., 1998; Ueda et al., 1997; Yumura and Fukui, 1998) whose sequences are highly conserved, and which are thus thought to be extremely sensitive to modifications, has since illustrated how innocuously GFP can behave in fusion constructs.

However, GFP can sometimes impair the function of its fusion partner. For instance in yeast, GFP-actin cannot rescue a knockout of the single yeast actin gene (Doyle and Botstein, 1996) and in *Dictyostelium*, actin filaments containing more than 30% GFP-actin showed reduced functionality, although GFP-actin fusion proteins have still proved useful in *Dictyostelium* in the elucidation of actin dynamics in live cells (Westphal et al., 1997). Investigations using GFP fusions should therefor involve careful analysis of the properties of fusion proteins made, to pre-empt misinterpretation of results or clarify novel findings.

With respect to the elucidation of annexin II function, GFP enables a range of possible experiments. These include the generation of stable multiclonal cell lines

expressing both full length annexin II-GFP fusion protein and fragments of annexin II fused to GFP, and direct investigation of annexin II distribution at the level of single cells in a variety of physiological situations.

2. Chapter 2 : Materials and methods.

2.1 Cell lines and culture conditions.

RBL: Rat basophilic leukemia cells.

PC12: Rat adrenal phaeochromocytoma cells.

RBL cells were grown in RPMI-1640 medium while PC12 were grown in DMEM. All media were supplemented with 10% foetal calf serum (FCS), penicillin (42 U/ml), streptomycin (42 mg/ml), and glutamine (1.7 mM). Cells were maintained at 37°C, in humidified incubators with 5% CO_2. Cells were frozen at 10^7 cells per ml in freezing medium (90% FCS with 10% DMSO). Vials of cells were initially transferred to a room temperature Stratacooler-cryo (Stratagene) before moving to a -80°C freezer for slow freezing over 24 h. Cells were then transferred to liquid nitrogen for long-term storage. New cell cultures were started every three weeks by defrosting an aliquot slowly to room temperature, washing once in 10 ml medium and transferring to flasks or plates under normal culture conditions. All serum was heat treated at 56°C for 30 minutes to inactivate complement, before aliquoting and freezing.

The medium of RBL and PC12 cells was changed at least every second day (both cell types have doubling times of around 24 h) and were kept sub-confluent. For passage, cells were washed twice in PBS, harvested using Trypsin-EDTA (Gibco), washed in medium and replated at an appropriate density. For microscopy cells were plated onto freshly flamed coverslips.

2.2 Polyacrylamide gel electrophoresis.

For denaturing SDS-polyacrylamide gel electrophoresis, samples were boiled for 5 min before loading. Proteins were loaded onto a discontinuous sodium dodecyl sulphate polyacrylamide gel (Maniatis et al., 1982). The acrylamide:bisacrylamide ratio was 30:0.8% (w/v) (Protogel, National Diagnostics). The concentration of acrylamide was 10% in the resolving gel and 4% in the stacking gel. Gels were run overnight at 65 V, using apparatus Model 400 by Hoefer Scientific Instruments. Pre-stained molecular weight markers were from Gibco, New England Biolabs or BioRad.

2.3 Western Blotting.

Proteins were transferred from the polyacrylamide gel onto PVDF membrane (Immobilon P, Millipore) using the BioRad Electroblot Transfer Apparatus. Transfer was performed at 4^{0}C in blotting buffer (39 mM glycine, 48 mM Tris, 20% methanol), at 0.4 A overnight. The membrane was then blocked for 1 h in PBS containing 0.05% Tween-20 (PBS-T), and 5% defatted skimmed milk.

Membranes were treated with primary antibodies in PBS-T, overnight at 4^{0}C. After the primary incubation, unbound antibody was removed by three fifteen-minute washes in PBS-T, before application of the secondary antibody.

Table 2.1: Antibodies and dilutions used for Western Blotting.

1^0 probe/name	**Target:**	**Source:**	**Host:**	**Dilution:**
PY99	phosphotyrosine	Santa Cruz	Mouse	1/5000
HH7	Annexin II	*	Mouse	1/1000
1^0 probe/name	**Target:**	**Source:**	**Host:**	**Dilution:**
IgG-AP conjugate	Mouse IgG	Promega	NA	1/10000
IgG-HRP conjugate	Mouse IgG	Santa Cruz	NA	1/10000

(* The HH7 antibody, raised against residues 1-18 of human annexin II, was a gift from Prof. V. Gerke, Muenster).

Membranes were washed 3 x in PBS-T to remove unbound secondary antibody. For AP-conjugated secondary antibodies, membranes were developed with Western Blue substrate (a mix of 5-bromo-4-chloro-3-indolyl-1-phosphate and nitro blue tetrazolium, Promega), and excess substrate was removed by multiple washes in tap water. For HRP-conjugated secondary antibodies, bands were visualised by Enhanced ChemiLuminescence (ECL):

Solution 1 : 22.5 mg Luminol (Sigma) was dissolved in 0.5 ml DMSO and added to 50 ml of 0.1 M Tris-HCl pH 8.5. 220 ml of a solution of 37 mg p-Cumaric acid (Sigma) in 2.5 ml DMSO was also added.

Solution 2 : 24.4 ml of a 30.9% stock solution of Hydrogen Peroxide (Sigma) was added to 40 ml of 0.1 M Tris-HCl pH 8.5.

The membrane was bathed in a mix of equal amounts (5 ml) of solutions 1 and 2 for 1 min, and then excess mix was dripped off and the damp membrane was wrapped in Saran wrap and exposed to X-ray film (Kodak) for a period of 5 seconds to 5 minutes.

2.4 Large and small scale preparation of plasmids.

Plasmid-containing bacteria were grown overnight at 37°C in a shaker in Terrific Broth (Gibco), containing the appropriate antibiotic (ampicillin or kanamycin at 50 μg/ml). For small scale preparation of DNA (mini-prep), 3 ml of bacterial culture was used, and plasmid DNA was prepared by alkaline lysis (Maniatis et al., 1982). For larger scale preparation, 50 to 500 ml was grown and plasmids were purified using Wizard Midi- or Maxi-prep kits (Promega). Quantification of nucleic acid solutions was carried out by measuring the absorption at 260 nm (1OD unit = 50 g/ml DNA).

2.5 GFP plasmids.

All GFP plasmids used to generate fusion constructs were acquired from Clontech. Initial attempts to produce fusion constructs using wild-type GFP, or the more fluorescent pS65T mutant proved problematic due to relatively low fluorescence levels. Subsequently all fusion constructs were built using 'enhanced GFP' or pEGFP, a GFP variant which is has both enhanced fluorescence and which has been codon-optimised for mammalian expression (for review of GFP development see Tsien, 1998). Since constructs encoding WT, pS65T and pEGFP have common cloning restriction sites this allowed a limited set of primers to be used for the generation of fusion constructs encoding any one of the three GFP variants.

2.6 PCR Primers and design of annexin II-GFP constructs.

Primers were designed using the programme OLIGO and ordered from Gibco. The primer sequences (sense primers are denoted 'L' and antisense 'R') are shown below.

L	GFPAII (1):	5' tgtcgaagcttagctagcagcaatgtctactgtccacgaaatc 3'
R	GFPAII (2)	5' ctggacaccggtacgtcgtccccaccacacaggta 3'
R	GFPAII (3)	5' catatcggatcctcagtcgtccccaccaccag 3'
R	GFPAII (4)	5' ctggacaccggttcaatgttcaaagcatccctctc 3'

Annexin II fragments were amplified from an expression plasmid in pRc/CMV encoding the entire rat annexin II ORF (pRc/CMV-AII; Upton, 1994). For generation of annexin II fragments in which either Ca^{2+} binding sites I, II and III were ablated, or both the p11 binding site and Ca^{2+} binding sites I, II and III were ablated, fragments were amplified from the expression plasmids CM/AII-CMV or PMCM/AII-M13 respectively (Thiel et al., 1992; kindly provided by Professor Volker Gerke, Muenster).

The diagram overleaf (Figure 2.1) illustrates the predicted PCR products generated from the annexin II ORF using the primer pairs detailed above. Constructs were checked by restriction analysis using unique sites within both the annexin II and GFP ORFs in conjunction with the restriction sites used for cloning of the PCR products.

2.7 Polymerase chain reaction.

PCR was performed using the Expand Long Template PCR or the Expand High Fidelity PCR kit (Boehringer Mannheim) using concentrations of nucleotide, primer and template as recommended by the manufacturer unless otherwise specified in 50 µl reaction volumes. In general buffer 1 or complete buffer with no additional magnesium chloride was used unless otherwise specified. Oligonucleotide primers were purchased from Gibco BRL and kept as 100 mM stocks in Milli-Q water at -80°C and working stocks of 10 mM were made up monthly. Nucleotide solutions were purchased from Boehringer Mannheim. Thin-walled 0.5 ml PCR reaction tubes were from Perkin Elmer. Reactions were set up on ice from master-mix solutions to ensure consistency, and over-laid with mineral oil. Samples were then transferred to a Perkin Elmer DNA thermal cycler pre-heated to 94°C for cycling:

N-terminal fragment of annexin II:

First cycle (x1):	Initial melt at 94°C for 30 s.
Second cycle (x 30):	Anneal/extend at 68°C for 1 s.
	Melt at 94°C for 10 s
Third cycle (x 1):	Anneal/extend at 68°C for 10 s.

Full length annexin II:

First cycle (x1):	Initial melt at 94°C for 60 s.
Second cycle (x 10):	Anneal at 60°C for 30 s.
	Extend at 68°C for 30 s.
	Melt at 94°C for 30 s
Third cycle (x 30):	Anneal at 60°C for 30 s.
	Extend at 68°C for 30 s + 10s per cycle
	Melt at 94°C for 30 s
Fourth cycle (x 1):	Anneal at 60°C for 30 s.
	Extend at 68°C for 120 s.

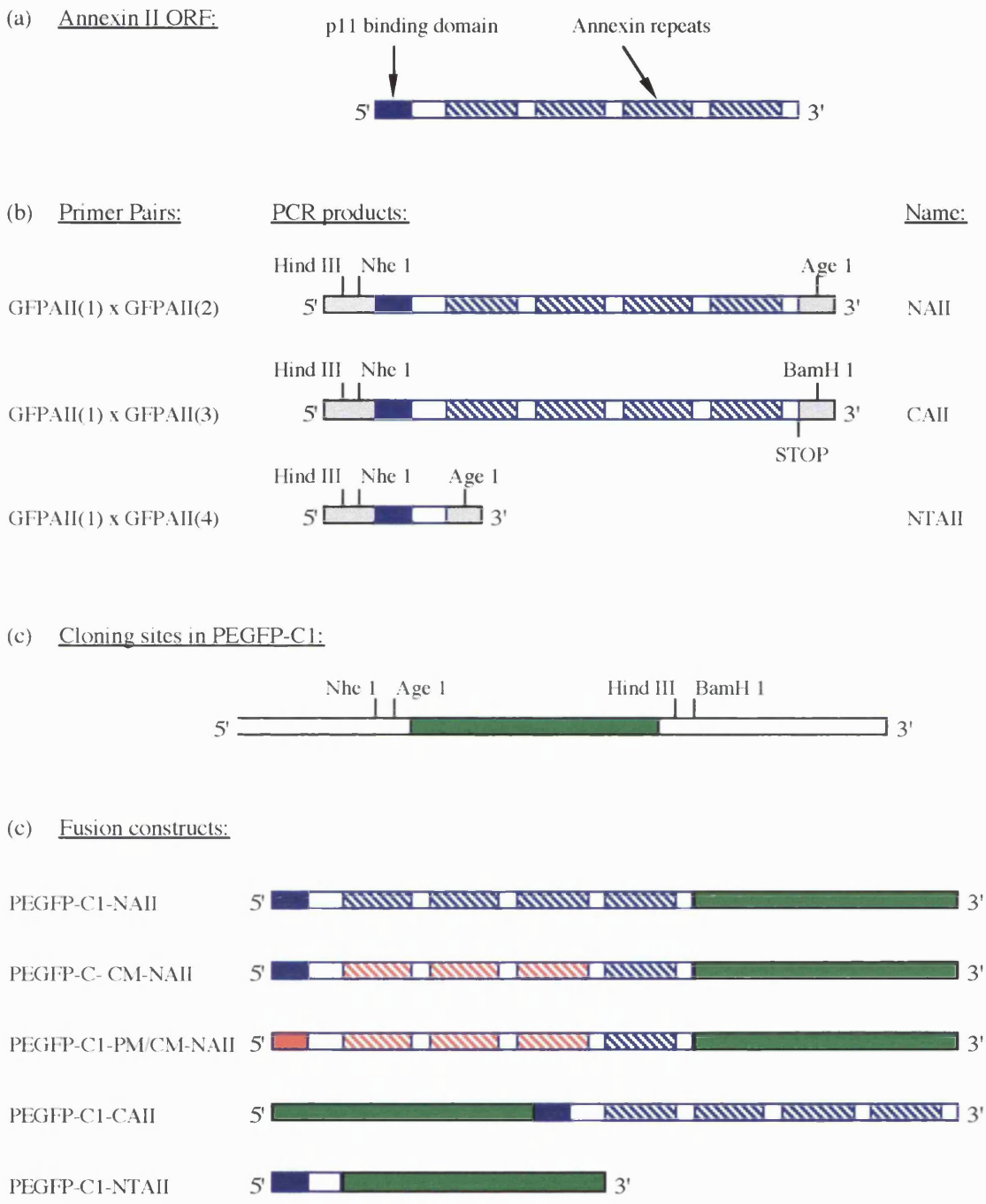

Figure 2.1: Engineering of annexin II-GFP fusion constructs.

The above schematic illustrates the predicted PCR products relative to the annexin II ORF (a). The predicted PCR products (b) have engineered restriction sites in the overhangs generated during PCR (grey). These sites were used to directionally clone the PCR products into PEGFP-C1 using the restriction sites provided (c). Annexin II fragments were cloned either upstream of the GFP ORF (green) to produce N-terminal fusion constructs or downstream of the GFP ORF to produce C-terminal fusion constructs as indicated (d). Red boxes indicate domains of annexin II ablated in mutant annexin II-GFP constructs, CM/NAII-GFP and PMCM/NAII-GFP. See text for details.

Annealing temperatures were determined empirically with an initial estimate of 68^{0}C or 5^{0}C lower than the lowest predicted melting temperature of the oligonucleotides (calculated as 67.5+[34xRGC]-[395/N] in ^{0}C where N is the number of bases and RGC is the ratio of guanine and cytosine residues to total bases), whichever was lower. Extension times were estimated according to the manufacturers instructions based on the expected size of the product. PCR products were analysed by gel electrophoresis.

2.8 DNA manipulation for construction of plasmids.

Restriction enzymes were obtained from New England Biolabs and were used according to the manufacturer's instructions with the appropriate buffer. Approximately 3 µg of DNA was digested with suitable enzymes in a 50 µl volume, and digestion was confirmed by resolution of 5 µl of digest on a 1% agarose gel in 1x TAE buffer (40 mM Tris-acetate pH 7.5, 1 mM EDTA pH 8), staining with ethidium bromide and visualisation under UV illumination (Maniatis et al., 1982). 1 kb DNA ladder from Gibco was used as a marker. Vectors were then further treated with 5 U shrimp alkaline phosphatase (Boehringer Mannheim) to prevent self-ligation, according to the manufacturer's instructions.

Bands were visualised as above but on larger scale preparative gels and using long-wave ultraviolet light (to minimise DNA damage). Bands of interest were excised with a clean scalpel, and placed into pre-treated dialysis tubing with 400 µl of 1x TAE (Maniatis et al., 1982). These were immersed in 1x TAE and the DNA electro-eluted from the gel for 1 hour, before being phenol/chloroform extracted, ethanol-precipitated, washed in 70% ethanol (Maniatis et al., 1982) and resuspended in 10 µl of 1 x Rapid Ligation Kit (Boehringer Mannheim) DNA dilution buffer. Relative DNA levels (insert to vector) were roughly quantified by spotting a range of dilutions of sample and known concentrations of DNA with ethidium bromide onto Saran-Wrap and visualising with ultraviolet light (Maniatis et al., 1982). In general ratios of insert to vector of 4 : 1 gave the most efficient ligations.

Ligations were performed using the Rapid Ligation Kit (Boehringer Mannheim) for 5 minutes at room temperature in a 10 µl volume according to the manufacturers instructions. 1 µl of ligation product was then transformed into E.coli (INVaF', One Shot kit, Invitrogen) according to manufacturer's instructions. Cells were then plated onto L-agar (Gibco) containing the appropriate antibiotic and incubated overnight at 37^{0}C. Colonies were picked, grown up in 3 ml cultures and plasmids were extracted by mini-prep (above) for restriction analysis for those containing the required insert in the correct orientation.

2.9 Transfection of mammalian cells.

RBL cells growing in log phase at 60-70% confluence were harvested by trypsinisation, centrifuged, washed in T-HBS twice (HBS (NaCl 135 mM, KCl 5 mM, $MgCl_2$ 0.4 mM, $CaCl_2$ 1.8 mM, glucose 2 mM, HEPES 20 mM, pH 7.4) and resuspended at a concentration of 2.5 x 10^7 cells/ml. Five minutes prior to transfection 400 µl of cell slurry was transferred to a 2 mm gap electroporation cuvette containing 30 µg of plasmid. Cells and plasmid were mixed by three rounds of trituration using a 200 µl pipette and incubated at room temperature with occasional mixing for a further 10 min. Cells were electroporated with two pulses (with gentle mixing to resuspend clumped cells in between) at 500 V, 125 µF, infinity Ohms using a BioRad GenePulser. After the second pulse 1 ml of fresh medium was immediately transferred to the cuvette and 50% of the transfected cells plated onto a single 90 mm dish (Falcon), with or without coverslips depending on the experiment. By the following morning this gave a 40% confluent population of cells, 10-20% of which routinely expressed the GFP or GFP-chimeric plasmid. If grown on coverslips these were removed to wells of a 6-well plate with 3 ml of fresh medium. For generation of stable cell lines expressing GFP or GPF-chimeras cells were selected with 350 µg/ml neomycin (Gibco) before further selection using FACS. Stable cell lines were maintained in the presence of 175 µg/ml neomycin (Gibco).

PC12 cells were transfected using the same protocol, but with two pulses of 400v, 125 µF and infinity ohms. In general PC12 cells gave transfection efficiencies of 50-70%.

2.10 Investigation of the putative perinuclear endosomal compartment in PC12 cells.

To investigate the effects of endocytic load and temperature block on the size of the perinuclear concentration of NAII-GFP, PC12 cells transiently expressing NAII-GFP were exposed to epidermal growth factor (EGF) under a variety of temperature conditions. Briefly, cells were either fixed straight from the incubator or incubated in HEPES buffered RPMI at 20^{0}C for 20 min in the presence or absence of 100 ng/ml EGF. Cells were then fixed in 3.7% formaldehyde for 10 minutes, briefly permeabilised in 10 µg/ml saponin and mounted for fluorescence microscopy.

To determine the relative size of the perinuclear foci of NAII-GFP, fluorescence confocal slices were taken at the equator of the foci (found by focusing through the specimen). Images were transferred to NIH-Image, calibrated and the cross-sectional area of the foci measured directly. Numerical data were transferred to Excel for processing.

2.11 Assessment of the effects of annexin II-GFP construct expression on differentiation of PC12 cells.

PC12 cells were transiently transfected with the various chimeric GFP constructs and plated onto 20 mm diameter coverslips. To improve cell adhesion coverslips were briefly flamed immediately before plating. PC12 cells were induced to differentiate by supplementing the culture medium with 50 ng/ml nerve growth factor (NGF) 2.5S from mouse submaxillary glands (Boehringer Mannheim) while control cells were grown in medium alone. Cells were fed every morning for three days. At the end of the third day cells were fixed with 3.7% formaldehyde in PBS, washed twice in PBS suplemented with 10 μg/ml saponin before a further two washes in PBS. Excess buffer was removed from coverslips by wicking into tissue, the back of the coverslip was wiped with distilled water and the coverslip inverted onto mountant (90% glycerol, 10% PBS, 0.01% n-propylgallate), blotted and sealed with rubber solution.

To assess the morphological changes induced by NGF challenge fluorescent micrographs were taken of differentiated and undifferentiated cells using the x 63 oil immersion lense of a standard Zeiss Axiovert epifluorescence microscope coupled to an air-cooled CCD camera (Princeton Instruments). Image acquisition was controlled using Lucida software. Images were deliberately saturated to allow neuritic processes to be visualised. To assess the number and length of processes in a given cell images were transferred to NIH-image and all processes longer than 1μM were logged and measured before data collation and analysis in Excel.

2.12 Generation of mixed clonal cell lines expressing GFP or GFP chimeras through FACS.

To generate pure RBL cell lines expressing GFP or GFP chimeras RBL cells were transfected as discussed previously, and the cells from two separate transfections were mixed and plated onto 140 mm diameter petri dishes for selection with neomycin. After three weeks selection each plate was found to harbour upwards of 20 stably transfected colonies. The colonies were harvested using trypsin-EDTA and the resulting suspension of mixed clonal cells sorted by FACS (see Figure 3.6, p 90) to separate cells expressing GFP or GFP chimera from those expressing the selection marker alone. The effectiveness of this strategy was confirmed using epifluorescence microscopy - all the cells sorted in this way were indeed fluorescent (result not shown).

2.13 Secretion experiments in intact RBL cells.

RBL cells were plated overnight in RPMI-1640 in 24 well plates. Each well received 1 ml of RPMI-1640 containing 4.5 x 10^5/ml cells, 1.0 μg/ml anti DNP-IgE (Sigma) and 200 nCi/ml 5-hydroxy[G-^{3}H]tryptamine creatinine sulphate (Amersham). Care was taken to ensure even plating since disturbance of multiwell plates during cell settlement causes cells to accumulate in the centre of each well, leading to erratic results. The following morning wells were washed five times with ice cold HBS (NaCl 135 mM, KCl 5 mM, $MgCl_2$, 0.4 mM, $CaCl_2$ 1.8 mM, BSA 0.5 mg/ml, D-(+)-glucose 1 mM, HEPES 20 mM, pH 7.4) to remove excess [^{3}H]-serotonin and unbound anti-DNP IgE. To stimulate secretion ice-cold HBS supplemented with various concentrations of DNP-albumin was added to the appropriate wells on ice (500 μl) and secretion stimulated by transferring wells to a 37^{0}C water-bath for 20 min. Secretion was rapidly quenched by floating the plate in slush for 2 min. After cooling 400 μl of supernatant from each well was transfered to Eppendorf tubes and spun at 5000 rpm in a benchtop microfuge for 5 min to pellet detached cells. To calculate the amount of [^{3}H]-serotonin secreted 300 μl of supernatant was transferred to 4 ml of ECOSCINT (National Diagnostics), mixed thoroughly, transferred to a scintillation vial for counting using a Packard TRI-CARB 1500 liquid scintillation counter. To calculate the maximum possible secretion wells of [^{3}H]-serotonin loaded cells were lysed into 500 μl of HBS supplemented with 1.0% TX100, and assayed as detailed. All treatments were randomised.

2.14 Investigation of the translocation of annexin II-GFP chimeras to the plasma membrane during stimulated secretion in RBL cells.

RBL cells were transiently transfected with GFP, or NAII-GFP as detailed previously. Cells were immediately plated in RPMI-1640 onto freshly flamed coverslips in 6 well plates for 24 h to allow recovery of transfected cells and plasmid expression. Each well received 3 ml of RPMI-1640 containing 8 x 10^4/ml cells and 1.0 μg/ml anti DNP-IgE. The following morning wells were washed five times in ice cold HBS (NaCl 135 mM, KCl 5 mM, $MgCl_2$ 0.4 mM, $CaCl_2$ 1.8 mM, BSA 0.5 mg/ml, D-(+)-glucose 1 mM, HEPES 20 mM, pH 7.4) to remove unbound anti-DNP IgE. To stimulate secretion ice cold HBS supplemented with 100 ng/ml DNP-albumin was added to the cells on ice and secretion stimulated by transferring wells to a 37^{0}C water-bath for 20 min, at which point the cells were fixed with 3.7% formaldehyde in 1 x PBS. Cells were permeabilised using 10 μg/ml saponin and mounted for fluorescence microscopy as detailed elsewhere. Images of

transfected cells were acquired using confocal microscopy and processed using Adobe Photoshop and NIH Image.

2.15 Fluorescent protein conjugates.

TRITC-(DNP-albumin) was prepared as advised (M.Shipman, personal communication). Briefly, DNP albumin (Sigma) was dissolved in 0.1 M Na_2CO_3, pH 9.0 at a concentration of 2 mg/ml. TRITC (Sigma) was dissolved in DMSO at 1 mg/ml. For each ml of protein solution, 50 µl of dye solution was added very slowly in 5 µl aliquots with continuous stirring at 4^0C. The solution was then left in the dark with gentle stirring for a further 8 h at 4^0C. To quench the reaction NH_4Cl was added to 50 mM and the solution incubated at 4^0C for 2 h. The solution was then dialysed against 0.1 M Na_2CO_3 (5 x 500 ml in 2 h cycles), aliquoted and stored at -80^0C.

For conjugation of Alexa-568 (Molecular Probes) to anti-DNP IgE (Sigma) the protocol as supplied was modified to accommodate the limited amount of antibody available. Briefly, the antibody (original amount 1 ml at 0.5 mg/ml) was concentrated using a Centricon concentrator (Amicon) to 2 mg/ml. The dye (supplied) was suspended in 250 µl of 0.2 M bicarbonate solution and 125 µl placed in an Eppendorf tube with stirrer. The antibody solution (125 µl at 2 mg/ml) was added to the dye solution and the solution mixed quickly by inversion. The entire reaction mix was then forced into the lid of the Eppendorf tube by gently tapping the inverted tube on the bench top, before being placed on a stirrer (in the dark) for 1 h at room temperature. At the end of the incubation the tube was placed in a bench-top centrifuge and spun to 200 g. To quench the reaction 7.5 µl of hydroxylamine (supplied) was added, the tube inverted and the solution forced into the lid as before, ready for 15 min of stirring at room temperature. Conjugated antibody was separated from unbound dye using the gel filtration column supplied and the protein concentration determined using the BioRad protein assay kit, based on the Lowry method of protein quantification. Samples were analysed at 750 nm on a Pharmacia Ultrospec II spectrophotometer and standard protein concentrations prepared using bovine serum albumin, fraction V (Sigma). The IgE-A568 conjugate was aliquoted and stored at -80^0C.

2.16 Investigation of annexin II-GFP chimera distribution in live cells using evanescent wave microscopy.

Evanescent Wave Microscopy (EWM) was performed in Heidelberg using a custom-built microscope designed and built by Dr Jurgen Steyer and Professor Wolfhard Almers, Max Planck Institut Fur Medezinische Forschung, Heidelberg. Since EWM is not

widely used in cell biology the basic principals of this form of microscopy will be briefly explained.

A beam of light undergoing total internal reflection at a glass/water interface will tend to 'tunnel' through the glass and appear in the fluid phase. If light is modeled as a wave this phenomenon is best described as light waves passing through the glass and propagating in the plane of the glass/water interface for a short distance before re-entering the glass. This produces an 'evanescent wave' at the glass/water interface (Figure 2.2, overleaf).

The net result is that the 200 nm of a cell proximal to the coverslip is illuminated by the excitation laser. This arrangement has advantages over both confocal and epifluorescence microscopy. On the one hand EWM allows a thin section of the cell to be imaged close to the plasma membrane - as would be possible using confocal microscopy. However confocal microscopy relies on strong illumination of the entire specimen and fluorescence light collection via a pinhole, an extremely inefficient process which results in over 90% of the fluorescence being discarded. Strong illumination of the specimen inevitably results in photo-damage during prolonged image acquisition. Epifluorescence microscopy similarly relies on illumination of the entire specimen. In contrast EWM relies on selective illumination of a small portion of the cell volume and collection of all the resulting fluorescence via a CCD detector. The cell is exposed to much less light, allowing prolonged image acquisition.

For viewing live cells the microscope was modified to allow the stage and optics to be heated to 37^0C using an AirTherm microprocessor controlled heating unit (WPI). This gave a temperature stability at the stage of +/- 0.1^0C. Unless otherwise stated all images were acquired at 1 frame every 5 s using Metamorph 3.0.

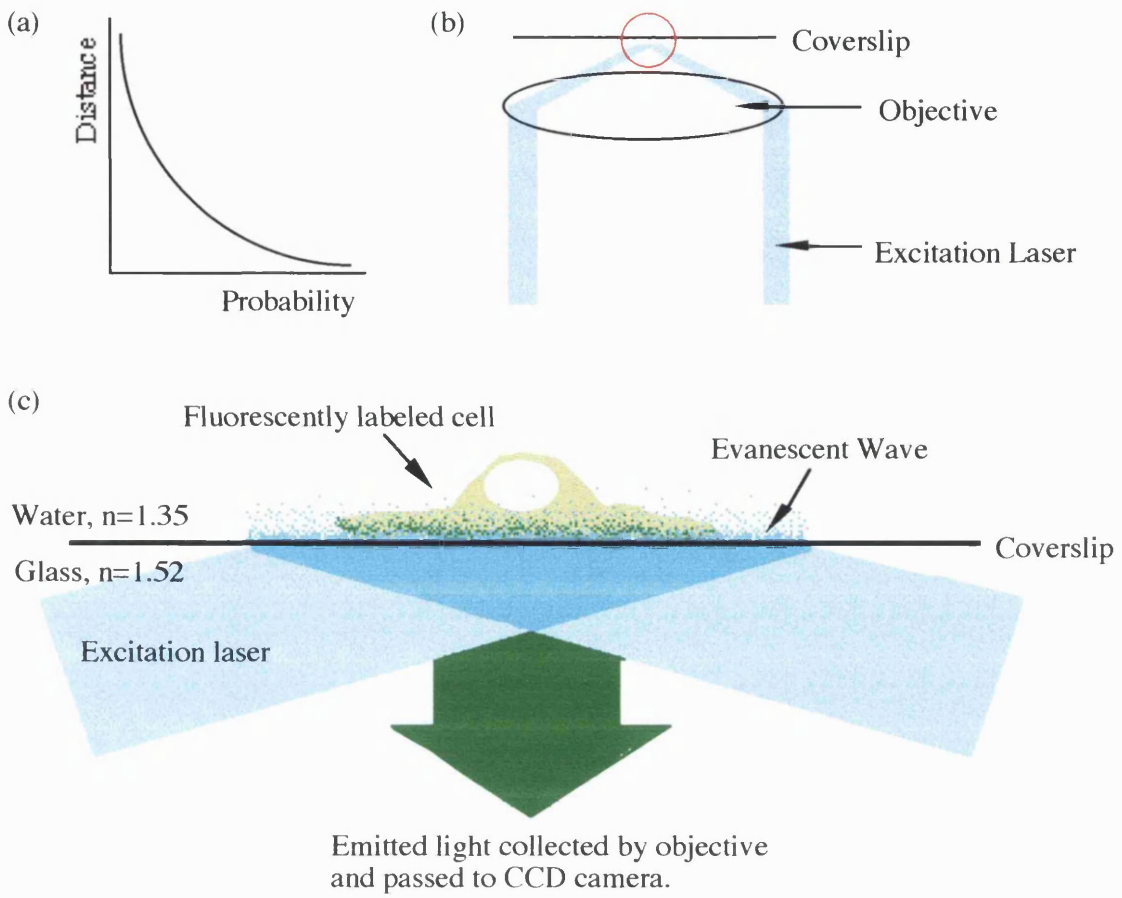

Figure 2.2: Principles of evanescent wave microscopy.

Totally internally reflected light bouncing off of a water/glass interface of a coverslip immersed in buffer will show a tendency to 'tunnel' through the coverslip and appear in the fluid phase*. The probability of a photon appearing at a point above the coverslip decreases exponentially with distance from the coverslip (a). By introducing a hollow cylinder of decoherent laser light into the objective lense of a standard fluorescence microscope an area of total internal reflection automatically occurs at the focal point of the microscope - generating an evanescent wave (area in red circle (b), magnified in (c)). Using laser light of the appropriate wavelength a fluorescently labeled cell in the evanescent wave will be preferentially excited where it is closest to the coverslip generating an image of fluorescence adjacent to the plasma membrane. In the microscope used in this study the maximum penetration depth of excitation laser light is 200-300 nm.

* See (Stout and Axelrod, 1989).

2.17 Induction of actin rockets *in situ* and imaging by evanescent wave microscopy (EWM).

RBL cells were transiently transfected using NAII-GFP or GFP-actin (a kind gift from B.Imhoff, Geneva) as detailed elswhere. To induce the formation of actin rockets in RBL cells, adherent cells on coverslips were initially washed twice in HBS (HBS (NaCl

135 mM, KCl 5 mM, $MgCl_2$ 0.4 mM, $CaCl_2$ 1.8 mM, glucose 1 mM, HEPES 20 mM, pH 7.4) before challenge with HBS + 150 mM sucrose +/- 10 nM PMA +/- 200 μM pervanadate (stimulation buffer). For visualisation of intracellular rocketing in living cells coverslips were washed at room temperature before being transferred to the heated stage (37^0C) in stimulation buffer for 20-40 min to allow the development of intracellular rockets and imaging as described elsewhere.

2.18 Image analysis of EWM image sequences.

For analysis 16-bit greyscale image stacks were analysed using Metamorph 3.0. This software package allows the analysis of average fluorescence in regions of interest in cells over time and the analysis of rocketing pinosome speed and tracks, using a manual tracking facility.

2.19 Generation of QuickTime movies from image sequences acquired using EWM.

To produce QuickTime movies from EWM data 16-bit image sequences were converted to 8-bit in Metamorph 3.0, transferred to NIH-image and saved directly as QuickTime movies.

2.20 Induction of actin rockets, fixation and analysis by immunofluorescence.

For fixation of intracellular rockets prior to immunofluorescent analysis, cells were stimulated as above for 40 min in 6 well plates floating in a 37^0C water bath. At this point stimulation buffer was replaced with pre-heated 3.7% formaldehyde in PBS. The plate was immediately transferred to room temperature for a further 10 min to complete fixation. Coverslips were then washed three times in PBS, permeabilised for 5 min using PBS supplemented with 10-100 μg/ml saponin (depending on probe) and washed a further three times in PBS. Coverslips were then processed for immunofluorescent analysis as detailed elsewhere.

2.21 Immunofluorescence analysis.

Chemically fixed, saponin-permeabilised cells were used for immunofluorescent analysis. In general, for antibody staining a three-tier system was used consisting of

primary antibody, appropriate secondary antibody conjugated to biotin and tertiary streptavidin/fluorophore. This gave optimal amplification of signal and was the most effective strategy when using monoclonal antibodies (such as anti-annexin II HH7) which bind the target molecule with a stoichiometry of 1 and require efficient amplification for visualisation.

The following is a list of primary, secondary and tertiary probes and the concentrations used. All antibodies were titrated individually to assess the optimal working concentration.

Table 2.2: Antibodies used for immunofluorescence analysis.

1^0 probe/name	Target	Source	Host	Dilution
IgG/HH7	annexin II	*	Mouse	1/60
IgG/Sc-7020	phosphotyrosine	Santa Cruz	Mouse	1/500
-	Ezrin	* *	Rabbit	1/400
IgG/A5044	α-actinin	Sigma	Mouse	1/200
IgG/Sc-881	PAK1	Santa Cruz	Rabbit	1/200
IgG/Sc-6437	zyxin	Santa Cruz	Goat	1/200
TRITC-phalloidin	F-actin	Sigma	N/A	1/2000
FITC-phalloidin	F-actin	Sigma	N/A	1/2000
2^0probe/name	Target	Source	Host	Dilution
IgG-biotin/B-7151	mouse IgG	Sigma	Goat	1/200
IgG-biotin/B8895	rabbit IgG	Sigma	Goat	1/800
IgG-biotin/Sc-2042	goat IgG	Santa Cruz	-	1/300
3^0probe/name	Target	Source	Host	Dilution
Streptavidin-FITC	biotin conjugates	Sigma	N/A	1/200
Streptavidin-TRITC	biotin conjugates	Sigma	N/A	1/200

(Other sources: * Professor Volker Gerke, Muenster ; ** Dr Paul Mangeat, Marseille)

Fixed and permeabilised adherent cells on coverslips were processed as follows. After permeabilisation cells were washed twice in PBS, excess buffer was removed through wicking onto tissue paper and the coverslip placed cells uppermost onto parafilm in a moist chamber before addition of 200 µl of PBS + 1^0 probe(s). Cells were incubated overnight at 4^0C to allow adequate time for the 1^0 probe to 'find' the appropriate target. The following morning the coverslips were washed 3 times for 3 min in PBS before incubation with 200 µl of 2^0 probes for an hour at 37^0C in a moist chamber. Coverslips were then

washed again three time for three minutes each in PBS before incubation with 3^0 probes for an hour at 37^0C in a moist chamber. After incubation coverslips were washed a further 3 times for 3 min each in PBS, excess buffer was wicked away and the coverslips were mounted as described previously.

2.22 Confocal analysis of fixed cells.

For confocal imaging of fixed, stained cells Leica TCS-NT, Zeiss LSM or Biorad 600 confocal microscopes were used. Images were processed using Metamorph, NIH-Image and Adobe Photoshop.

2.23 Labeling the vesicle at the tip of actin rockets using endocytic markers.

The protein conjugates used previously to label internalised FcεR1/IgE/antigen clusters (TRITC conjugated DNP-albumin) were found to bleach too quickly for efficient dual wavelength confocal microscopy during labeling of the endocytic vesicle at the tip of actin rockets. For these experiments an IgE/Alexa dye conjugate, IgE-A568, was used to label the FcεR1 receptor directly.

A stainless steel plate (10 x 10 cm, 3 mm gauge) was laid onto ice and coated with saran wrap to produce a cold, hydrophobic surface. Adherent RBL cells, growing on 24 mm diameter coverslips in log phase at 60% confluence were briefly dipped in 4^0C, 1 x PBS to remove dead cells, touched on edge onto tissue paper to remove excess PBS and placed cells uppermost onto the cold plate. A 200 µl aliquot of HBS + 100 ng/ml IgE-A568 was added to the cells, and ice tray covered with foil to protect the coverslips from photobleaching and dust. After 30 min the cells were washed to remove unbound IgE-A568 by dipping and gently swirling in ice cold PBS in 4 x 50ml falcon tubes on ice. Coverslips were then transferred to pre-chilled stimulation buffer in 6 well plates on ice. For stimulation, fixation and subsequent immunofluorescence coverslips were treated as detailed previously.

For pulse labeling of endosomes with a fluid phase marker adherent RBL cells, growing in log phase at 60% confluence were stimulated to produce actin rockets in the presence of 1 mg/ml fixable TexasRed-dextran (Molecular Probes). Prior to fixation coverslips were briefly washed in pre-heated HBS. For fixation and subsequent immunofluorescence coverslips were treated as detailed previously.

Endosomes were labeled *in situ* in live RBL cells by stimulating them to produce actin rockets at 37^0C on the confocal microscope in the presence of 4 mg/ml TexasRed-dextran (Molecular Probes). Alternatively 2 mg/ml FITC-dextran was pulsed onto cells

producing intracellular rockets using a custom perfusion system while being imaged using EWM.

2.24 Dual wavelength imaging of GFP chimeras and TexasRed-dextran in live cells.

For confocal imaging of live cells at 37^{0}C a Leica confocal was modified to allow air heating of the stage and microscope body using an AirTherm microprocessor controlled heating unit (Figure 2.3). These experiments were performed in Heidelberg.

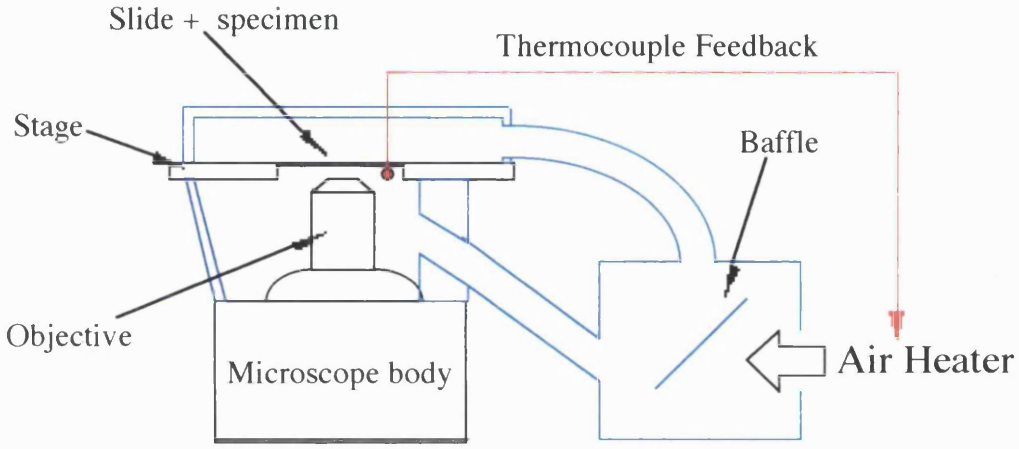

Figure 2.3: Heating of a standard confocal microscope stage using a thermo-couple controlled air heater.

The schematic above represents a section through the microscope body of the Leica confocal used for live cell imaging at 37^{0}C. A series of fabricated insulated walls and conduits (blue) direct the heated air from an AirTherm heater to the stage via a mixing box. Feed-back control is effected via a thermocouple attached to the objective. This simple arrangement gave a temperature control of +/- 0.1^{0}C at the tip of the objective.

Temperature stability at the stage, as measured using thermocouple, was +/- 0.1 ^{0}C. In the absence of a suitable stage coverslips were mounted on slides over a well cut into parafilm and sealed with silicon grease (Figure 2.4, overleaf).

Cells were immediately transferred to the pre-heated stage of the confocal after mounting in this way for 20 min before imaging. Frames were acquired at the lowest practical laser power at a rate of 1 frame every 5 s and image stacks analysed using AdobePhotoshop and Metamorph as detailed below. To simultaneously image GFP chimeras and a fluid-phase endocytic marker cells were mounted as detailed in stimulation buffer supplemented with 4 mg/ml TexasRed-dextran (Molecular Probes).

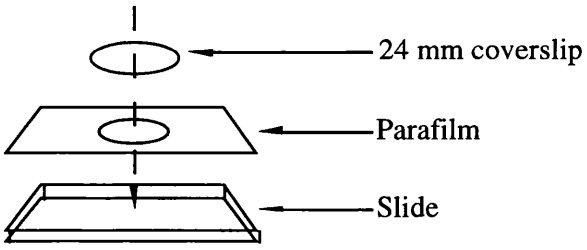

Figure 2.4: Preparation of slides for short-term imaging of live cells using confocal microscopy.

A rectangle of parafilm was cut using a scalpel, and a 20 mm diameter hole cut in the centre using a sharp hole punch. This was stuck firmly to the slide using thin smear of silicone grease. To the well thus formed 100 µl of the appropriate buffer was added, a 24 mm diameter coverslip overlaid and excess fluid wicked away using the edge of a sheet of tissue. The slide was sealed with silcone grease.

2.25 Handling and processing of dual wavelength data and generation of dual colour QuickTime movies.

To generate dual wavelength movies the red and green channel TIF images of each frame of the time sequence were processed in Adobe Photoshop to produce a dual colour image. Briefly, each grey-scale image was indexed to a standardised lookup table for the relevant channel (red or green). These indexed colour images were then transformed to RGB files in Adobe Photoshop and merged to produce a dual colour RGB image for each frame. The resulting sequence of dual colour images was then used to generate a QuickTime movie directly using the shareware programme GraphicConvertor.

2.26 Measurement of fluid phase uptake in RBL cells.

Adherent RBL cells growing in log phase at 60% confluence were harvested using trypsin/EDTA and washed 3 times in ice cold HBS. During the final wash the cells were counted and after the final wash the cell pellet was resuspended at a concentration of $1x10^7$ cells/ml of HBS supplemented with 100 µCi/ml [^{3}H]-dextran (Amersham). Aliquots of 50 µl ($5x10^6$ cells) were transferred to pre-chilled Eppendorf tubes on ice and an equal volume of HBS +/- 300 mM sucrose +/- 20 nM PMA added. After mixing by gentle trituration tubes were transferred to a hotblock at 37^{0}C for 40 min. To quench pinocytosis 1 ml of ice cold HBS +/- 150 mM sucrose was added and the cells immediately transferred to a pre-chilled rotor and pelleted for 5 min at 3000 rpm. Cells were washed a further 4 times with 500 µl HBS +/- 150 mM sucrose at 4^{0}C before being lysed into 100 µl of HBS + 1% TX100. The lysate was transferred to 4 ml of ECOSCINT H (National Diagnostics) and

the amount of [^{3}H]-dextran present measured using a Packard TRI-CARB 1500 liquid scintillation counter. The resulting data (counts per minute - cpm) was transferred to Excel for analysis.

2.27 Measurement of the effects of pervanadate on the incidence of rocketing.

A stock solution of 0.2 M pervanadate was freshly prepared for each experiment by dissolving 0.1 g Na_3VO_4 (Sigma) in 2.71 ml water and adding 30 µl H_20_2 (30% stock by volume, Sigma). Adherent RBL cells, growing in log phase at 60% confluence on coverslips, were stimulated to produce actin rockets with HBS +/- 150 mM sucrose +/- 10nM PMA +/- 200 µM pervandate for 40 min, fixed and stained using TRITC-phalloidin as detailed previously. As an index of the incidence of rocketing the number of cells with 'one or more clearly defined F-actin rockets' was measured. One hundred cells were counted and the number of cells with one or more clearly defined actin rockets scored. This experiment was repeated on three separate days.

2.28 Measurement of the effects of inhibitors on the incidence of rocketing.

Adherent RBL cells, growing in log phase at 60% confluence on coverslips, were incubated +/- inhibitors (Table 2.3, overleaf) before being stimulated to produce actin rockets using HBS + 150 mM sucrose + 200 µM pervanadate for 40 min, fixed and stained using TRITC-phalloidin as described previously. On hundred cells were analysed for clearly defined intracellular rockets after stimulation in the presence of each inhibitor. This experiment was repeated on three separate days.

During the initial screening procedure inhibitors were used at a concentration corresponding to 5 x their published IC_{50} for the desired target. Cells were pre-incubated with each inhibitor for 20 min prior to stimulation and were maintained at the same concentration throughout stimulation, with the exception of Toxin B. Since this toxin is relatively slow-acting a pre-incubation of 2 h was required (A.Hall, personal communication.)

Table 2.3: Inhibitors and stimulants used to probe the mechanism of rocketing: targets, published IC_{50} and suppliers.

Inhibitor	Target (IC_{50})	[Inhibitor]	Source
Chelerythrin Chl.	PKC (600 nM)	3.5 μM	Calbiochem
Herbimycin A	$pp60^{c\text{-}src}$ (900 nM)	4.5 μM	Calbiochem
Lavendustin C	CAM kinase II (200 nM)	2.5 μM	Calbiochem
	$pp60^{c\text{-}src}$ (500 nM)		
Toxin B	Rac-1/Cdc42 (N/A)*	100 ng/ml	* *
LA20190	p38 MAPK	1 μM	Calbiochem
Wortmannin	PI3-kinase (5 nM)	25 nM	Calbiochem
Filipin	cholesterol (N/A)	2 μg/ml	Sigma
Latrunculin B	actin polymerisation (N/A)	5 μM	Calbiochem
BAPTA-AM	Ca^{2+} chelator (N/A)	10 μM	Calbiochem
Stimulants	**Target**	**[Stimulant]**	**Calbiochem**
PMA	PKC	10 nM	Sigma
Pervanadate	phosphotyrosine phosphatases	200 μM	Sigma
Phenylarsine oxide	phosphotyrosine phosphatases	50 μM	Sigma

* (N/A) - Not Applicable.

* * Toxin B was a kind gift from A.Hall, LMCB, London.

3. Chapter 3 : Assessment of GFP as a tool for the investigation of annexin II function *in vivo.*

3.1 Distribution of different annexin II-GFP chimeras in live PC12 cells: role of Ca^{2+} and p11 binding sites.

Annexin II resides in both cytoplasmic and plasma membrane associated pools in a variety of cell types and formation of the annexin II_2p11_2 heterotetramer is thought to be a pre-requisite for successful plasma membrane targeting (Thiel et al., 1992; Zokas and Glenney, 1987). Association of the complex with this region of the cell is probably due to Ca^{2+}-dependent binding to phospholipids and cytoskeletal elements (F-actin and non-erythroid spectrin). This notion is supported by the finding that site-directed mutagenesis of either the p11 binding site or type II Ca^{2+}-binding sites 2, 3 and 4 abolishes plasma membrane targeting of annexin II (Thiel et al., 1992).

To test the functional integrity of the full length, wild type, annexin II-GFP chimera *in vivo*, three additional constructs were used in a comparitive experiment - two full length annexin II-GFP chimeras, one which has mutated Ca^{2+}-binding sites and the other of which has both mutated Ca^{2+} and p11 binding sites, and a truncated annexin II-GFP chimera consisting of the N-terminal domain of annexin II fused to GFP (for details refer to Figure 2.1, p 65).

Undifferentiated PC12 cells express low levels of annexin II (Fox et al., 1991) and over-expression of annexin II leads to redistribution of annexin II immunoreactivity from a cytosolic to cytosolic/plasma membrane distribution (Graham et al., 1997). For these reasons the PC12 cell line was identified as being suitable for investigating the membrane targeting of the different annexin II-GFP constructs *in vivo.*

On expression in PC12 cells only fusion proteins in which the N-terminal domain of annexin II was free were excluded from the nucleus (Figure 3.1). Fusion of GFP to the N-terminus of annexin II (CAII-GFP) destroyed this property, and since the N-terminus of annexin II alone is capable of excluding GFP from the nucleus this suggests the nuclear exclusion signal resides in this domain of the molecule. Nuclear exclusion is independent of p11 binding since a fusion protein consisting of annexin II, with mutated Ca^{2+} and p11 binding sites, fused to GFP also excludes GFP fluorescence from the nucleus. The basis of the nuclear exclusion of annexin II was not investigated further.

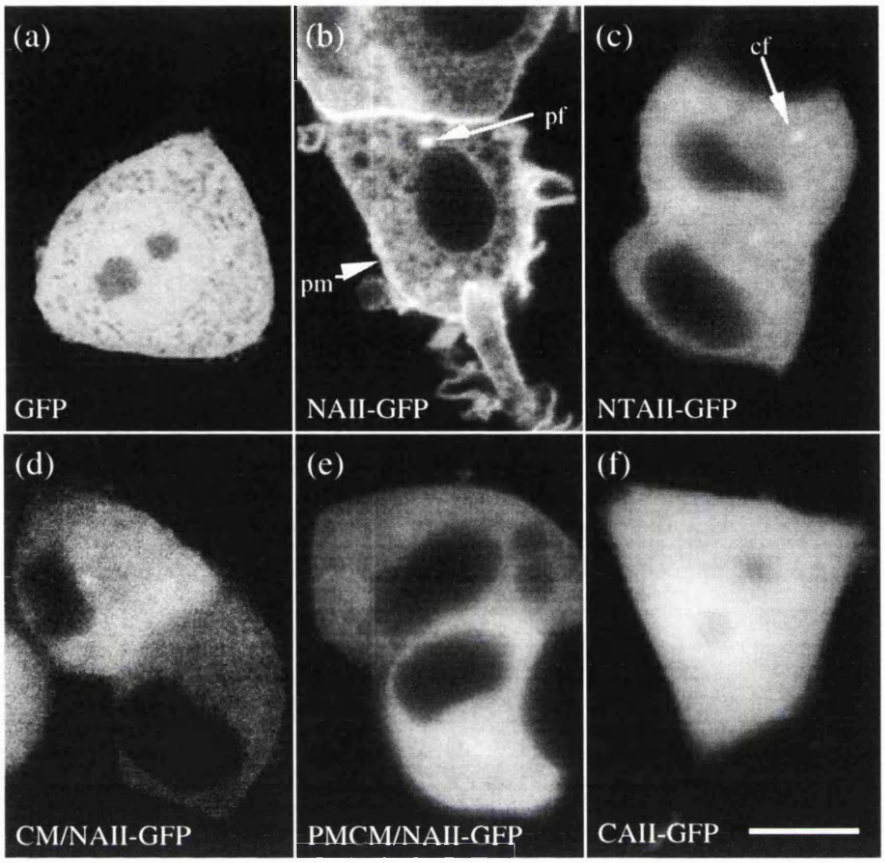

Figure 3.1: Distribution of different annexin II-GFP fusion proteins in living PC12 cells.

PC12 cells were transiently transfected with GFP, NAII-GFP, NTAII-GFP, CM/NAII-GFP, PMCM/NAII-GFP or CAII-GFP (see Figure 2.1, 65) and viewed in HBS by confocal microscopy. GFP fluoresence and fluorescence of a contsruct consisting of GFP fused to the N-terminus of wild type annexin II (CAII-GFP) are homogenous throughout the cell (a)(f). Attachment of GFP to the C-terminus of annexin II targets fluorescence to the plasma membrane (pm) and a bright perinuclear focus (pf) (b). GFP at the C-terminus of the N-terminal domain of annexin II fails to target to the plasma membrane but does concentrate GFP at a cytoplasmic focus (cf) (c). Fusion of GFP to the C-terminus of full length annexin II in which Ca^{2+} binding sites (d) or both Ca^{2+} and p11 binding sites (e) have been mutated fails to target GFP to either the plasma membrane or a distinct cytoplasmic or perinuclear focus. The distribution of a fusion construct in which GFP has been fused to the N-terminus of full length wild-type annexin II is indistinguishable from GFP. These results suggest that the core domain of annexin II is necessary for targeting of fusion proteins to the plasma membrane and that a free N-terminus is necessary for exclusion of fusion proteins from the nucleus (see text for details).

Full length (wild type) annexin II fused to GFP (NAII-GFP) is concentrated at the plasma membrane in live PC12 cells while neither the N-terminus of annexin II fused to GFP (NTAII-GFP) or full length annexin II with mutated Ca^{2+} (CM/NAII-GFP) or both Ca^{2+} and p11 binding sites (PMCM/NAII-GFP) can target GFP fluorescence to the plasma

membrane in live cells (Figure 3.1). This is consistent with published findings (Thiel et al., 1992) and indicates that in the full length (wild type) construct both the p11 binding site and Ca^{2+} binding sites 2, 3 and 4 are intact and functional.

In addition to the plasma membrane, NAII-GFP also targeted GFP fluorescence to discrete perinuclear foci in live cells (Figure 3.1b). Note that NTAII-GFP targets to similar structures (although labeling is less defined) suggesting the motif(s) responsible for this phenomenon are located in the N-terminal domain of annexin II. No such structure was observed in any live PC12 cells expressing GFP alone (Figure 3.1a).

The perinuclear foci of NAII-GFP seen in live PC12 cells might be due to association with a perinuclear endosomal compartment. Various ligand/receptor couples have been demonstrated to relocate to a perinuclear compartment during receptor internalisation and sorting including the epidermal growth factor receptor (EGFr) (Miller et al., 1986) and the transferrin receptor (Tfr) (Hopkins et al., 1990; Hopkins et al., 1994; Martys et al., 1995; Ren et al., 1998; Willingham and Pastan, 1985). Typically, a complex of tubular endosomes has been shown by electron microscopy to envelope the centrioles at the cytocentre which are thought to be involved in receptor recycling (Daro et al., 1996; Ullrich et al., 1996). In at least some instances endosomal markers have been found to relocate to the pericentriolar region within 5 min of internalisation suggesting that the pericentriolar complex of tubules is synonymous with an early endosomal compartment in some cell types (Tooze and Hollinshead, 1991). This compartment was originally defined morphologically but several unique protein markers have recently been identified including cellubrevin (Daro et al., 1996; Teter et al., 1998), rab 11 (Ren et al., 1998; Ullrich et al., 1996) and GDP dissociation inhibitor 2 (GDI-2) (Shisheva et al., 1995).

Since annexin II has been shown to target to early endosomes (Emans et al., 1993; Harder and Gerke, 1993; Harder et al., 1997; Jost et al., 1997; van der Goot, 1997) and endosomes involved in receptor recycling (Pol et al., 1997), localisation of NAII-GFP at a pericentriolar concentration could be consistent with NAII-GFP targeting to these compartments. The finding that NTAII-GFP targets to a similar focus is consistent with this view since Ca^{2+}-independent association of annexin II with early endosomes is mediated by a motif in this domain (Jost et al., 1997). Furthermore, a perinuclear location of annexin II is not without precedent since annexin II has been shown to relocate to this site during transcytosis of glycolithocholate in isolated hepatocyte couplets (Wilton et al., 1994).

Together these published findings suggested that the perinuclear foci of NAII-GFP might be due to association of the fusion protein with an endosomal compartment. However, before examining this further the distribution of the different annexin II-GFP constructs were examined in a different cell line for comparison.

3.2 Distribution of GFP, NAII-GFP, NTAII-GFP, CM/NAII-GFP, PMCM/NAII-GFP and CAII-GFP in live RBL cells.

Confocal microscopy of live RBL cells expressing the N-terminal fusion constructs NAII-GFP, NTAII-GFP, CM/NAII-GFP or PMCM/NAII-GFP revealed different patterns of fluorescence to those seen in PC12 cells. A smooth, homogeneous cytoplasmic distribution with exclusion of signal from the nucleus was seen on expression of these constructs. No concentration of fluorescence was seen either at the plasma membrane or perinuclear foci. As in live PC12 cells both GFP and CAII-GFP fluorescence was evenly distributed throughout the cell, including the nucleus (Figure 3.2).

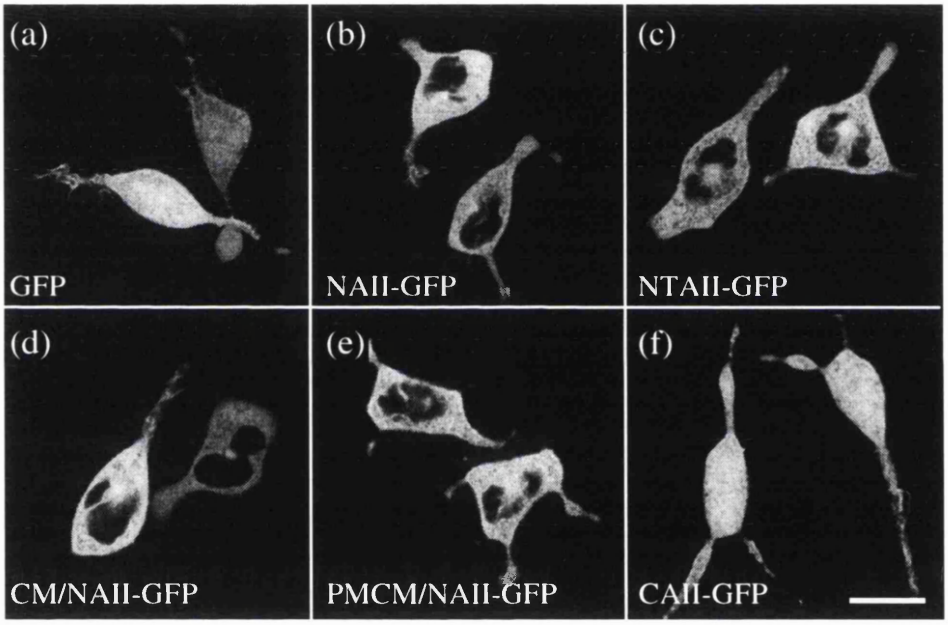

Figure 3.2: Distribution of GFP and annexin II-GFP constructs in live RBL cells.

RBL cells were transiently transfected with GFP, NAII-GFP, NTAII-GFP, CM/NAII-GFP, PMCM/NAII-GFP or CAII-GFP (Figure 2.1) and viewed by confocal microscopy in HBS. GFP while fusion of GFP to the C-terminus of full length wild-type annexin II (b), the N-terminal domain of annexin II (c), full length annexin II with mutated Ca^{2+} binding sites (d) or full length annexin II with mutated Ca^{2+} and p11 binding sites (e) excludes GFP flourescence from the nucleus. The distribution of a fusion construct in which GFP has been fused to the N-terminus of full length wild-type annexin II is indistinguishable from GFP (f) (see text for details).
Scale bar: 10 μm

As in PC12 cells all fusion proteins with the exception of CAII-GFP were excluded from the nucleus. However, in constrast to the distribution in PC12 cells no concentration of any of the fusion proteins was seen at the plasma membrane. Since the annexin II_2p11_2

heterotetramer is preferentially targetted to the cell cortex while the monomer is cytoplasmic (Thiel et al., 1992; Zokas and Glenney, 1987) this could reflect a difference in the ratio of heterotetramer:monomer in these two cell lines. Thus the absence of cortical targeting in RBL cells may simply reflect an excess of monomer over heterotetramer in these cells, although this was not investigated further. The reason for the absence of perinuclear foci in live RBL cells in contrast to live PC12 cells was unclear, and was further complicated by findings in fixed RBL cells as discussed below.

3.3 Distribution of annexin II-GFP constructs in fixed RBL cells.

Expression of GFP constructs allows direct comparisons to be made between the distribution of a protein in both living and fixed cells. Initial experiments investigated the effects of different fixation protocols on GFP fluorescence in RBL cells transiently expressing GFP, NAII-GFP or NTAII-GFP. It was found that GFP flourescence was significantly reduced by fixation using methanol or acetone (results not shown). However chemical fixation using 3.7% formaldehyde followed by permeabilisation with saponin did not significantly affect GFP fluorescence. These results are consistent with the findings of other investigators (M.Shipman, personal communication).

A notable difference to the distribution of constructs in live and chemically fixed RBL cells was the apparent concentration of fluorescence at perinuclear foci in fixed cells, superficially similar to that seen in living PC12 cells. This was most clearly seen in cells expressing NTAII-GFP (Figure 3.3).

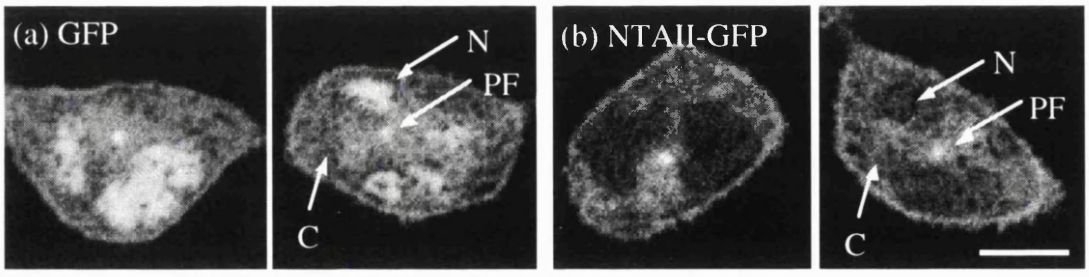

Figure 3.3: GFP is retained in a perinuclear foci in fixed RBL cells.

RBL cells transiently expressing (a) GFP (left panels) or (b) NTAII-GFP (right panels) were fixed with 3.7% formaldehyde in PBS for 15 minutes, permeabilised with 10 µg/ml saponin and mounted for microscopy. GFP fluorescence is washed out of cytoplasm (C) while being preferentially retained in the nucleus (N) and at a single distinct perinuclear focus (PF). Fusion with the N-terminus of annexin II to form NTAII-GFP leads to exclusion of fluorescence from the nucleus and accentuates the perinuclear foci.
Scale bar: 5 µm

It was noted that GFP alone, which was homogenously distributed within live RBL cells (Figure 3.2) became 'concentrated' in both the nucleus and the perinuclear foci in fixed cells. This difference in distribution between living and fixed cells is clearly an artifact and may be explained if the efficiency of chemical-fixation of GFP depends on its location in the cell. Hence GFP will be effectively retained in the nucleus since this environment will tend to retain GFP in a dense mesh of proteins and DNA while GFP free in the cytosol will tend to be lost during permeabilisation and subsequent washes.

This argument can also be used to explain the retention of perinuclear foci of fluorescence. As discussed previously this site is probably the perinuclear microtubule organising centre (MTOC) where a high density of protein is found at the convergence point of microtubules (Cande, 1990). This site would provide ample opportunity for the cross-linking and retention of a soluble protein such as GFP during chemical fixation. However it proved impossible to establish whether or not this perinuclear focus did indeed correspond to the MTOC since the concentrations of detergent necessary to provide access to marker antigens - such as γ tubulin - destroyed GFP fluorescence (data not shown).

These results illustrate that caution is necessary when interpreting the distribution of GFP fusion proteins in fixed cells. In particular a systematic and rigorous comparison between live and fixed cells, those expressing GFP alone and those expressing GFP-chimeras should be performed to separate novel distributions of fluorescence from artifacts. This was especially important in this study where a fixation artifact in RBL cells and novel distribution in live PC12 cells appeared very similar. Since perinuclear foci of NAII-GFP (and NTAII-GFP) were seen in live PC12 cells, while GFP alone did not concentrate in this region, this distribution was considered to be a genuine result of annexin II targeting and was investigated in more detail.

3.4 Further investigation of the perinuclear foci of NAII-GFP in PC12 cells.

Based on published evidence, the discrete perinuclear foci of NAII-GFP seen in live PC12 cells are most likely to be either an extension of the early endosome system and/or recycling compartment. If these foci represent such a compartment, an increase in endocytic traffic might lead to a change in the size and morphology of perinuclear foci. To test this hypothesis, the effects of temperature blocks in conjunction with an increase in receptor mediated endocytosis was examined. Previous studies have demonstrated that reduction to 20^0C blocks endocytic vesicle traffic at a perinuclear compartment and leads to an accumulation of endosomes in this region of the cell in a variety of cell types (Miller et al., 1986).

Since PC12 cells express the EGF receptor and bind and internalise this receptor on challenge with EGF (Chandler and Herschman, 1983) this growth factor was used to induce endocytic traffic in PC12 cells.

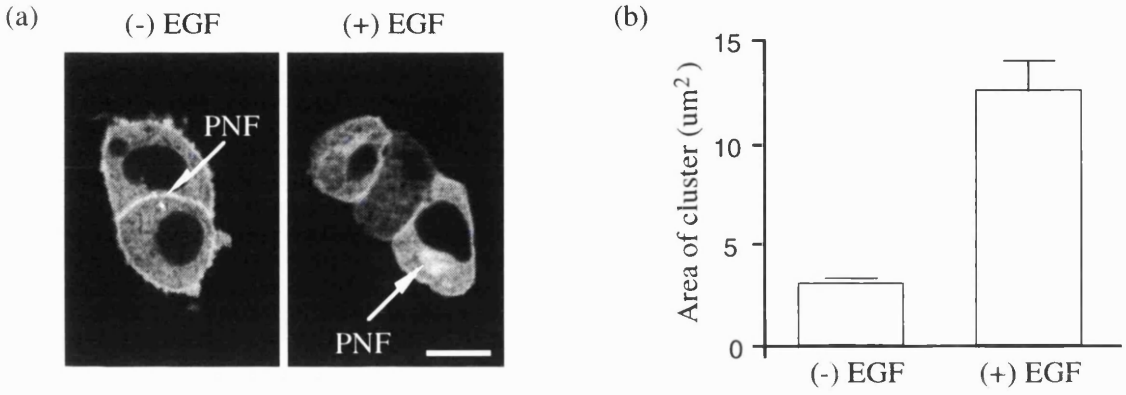

Figure 3.4: Effects of temperature block +/- EGF on the perinuclear foci of NAII-GFP in PC12 cells.

(a) Transiently transfected PC12 cells expressing annexin II-GFP possess a perinuclear foci of NAII-GFP (PNF). Cells were incubated in HEPES-buffered medium in the absence or presence of 100 ng/ml EGF for 20 minutes at 20^{0}C. (b) Fixed cells were analysed by confocal microscopy and the mean cross-sectional area of the perinuclear foci of annexin II-GFP calculated in NIHimage 1.6pcc (n= 20). In the presence of EGF and a 20^{0}C temperature block the perinuclear foci of NAII-GFP significantly increases in size. Scale bar: 10 μm

The result shown in Figure 3.4 is consistent with the perinuclear foci of NAII-GFP fluorescence seen in live PC12 cells being due to association of this chimera with an early endocytic and/or receptor recycling compartment. Attempts to further identify this compartment met with little success for the following reasons.

Firstly, it was not possible localise commercially available EGF-fluorophore conjugates in live cells due to their low fluorescence. Secondly, attempts to co-localise NAII-GFP and internalised receptor using immunofluorescence were unsuccessful since the concentrations of detergent required to allow efficient access of antibodies to the cell interior destroyed GFP fluorescence. Thirdly although the perinuclear concentration of NAII-GFP may be due to accumulation of endocytic vesicles no individual vesicular structures could be visualised moving through the cytosol in live cells using time lapse confocal or evanescent wave microscopy, even though the perinuclear concentration of NAII-GFP was clearly visible using confocal microscopy. These findings may be explained if the putative endosomal vesicles labeled by NAII-GFP are simply too small to be resolved by light microscopy.

A practical way to identify the perinuclear compartment would have been to use electron microscopy in conjunction with horseradish peroxidase-conjugated endosomal markers. However this was seen as a retrograde step since the aim of this project was to investigate the distribution and function of annexin II in live cells.

With this in mind the next series of experiments were designed to find out whether expression of annexin II-GFP fusion constructs had any modulatory effect on events triggered by stimulation of PC12 cells with an alternative growth factor, nerve growth factor (NGF). Stimulation with NGF induces distinct cellular process in PC12 cells and development of a neuronal phenotype (Greene and Tischler, 1976) and annexin II has been implicated in this process (Fox et al., 1991).

3.5 Expression of GFP, NAII-GFP or NTAII-GFP has no effect on PC12 cell differentiation.

The phaeochromocytoma cell line PC12 can be induced to differentiate into a neuronal like phenotype in tissue culture by exposure to NGF (Greene and Tischler, 1976). Culture in the presence of NGF results in the development of characteristic neurites and the concomitant induction of both annexin II and p11 (Fox et al., 1991). While p11 expression is induced 5 fold, annexin II expression shows an even greater increase - up to 13 fold - an observation which has prompted the suggestion that p11 and/or annexin II might play a role in PC12 cell differentiation. This view has been strengthened by the finding that expression of an expression vector encoding p11 induces undifferentiated PC12 cells to produce characteristic processes normally associated with differentiation (Masiakowski and Shooter, 1990).

To determine whether or not overexpression of NAII-GFP or NTAII-GFP influenced the process of differentiation these constructs were transiently transfected into undifferentiated PC12 cells which were then challenged with NGF for three days (see Materials and Methods). A similar strategy has recently been used to identify a role for the serine/threonine kinase PAK (p21-activated kinase) in PC12 neurite outgrowth during differentiation (Daniels et al., 1998).

As controls, both wild-type mock-transfected and GFP-transfected cells were induced to differentiate under the same conditions. After chemical fixation and permeabilisation transfected cells were identified by epifluorescence microscopy and images acquired using either epifluorescence microscopy (transfected cells) or phase constrast microscopy (wild-type cells). Images were analysed and the number and length of processes on individual cells scored (Figure 3.5, overleaf).

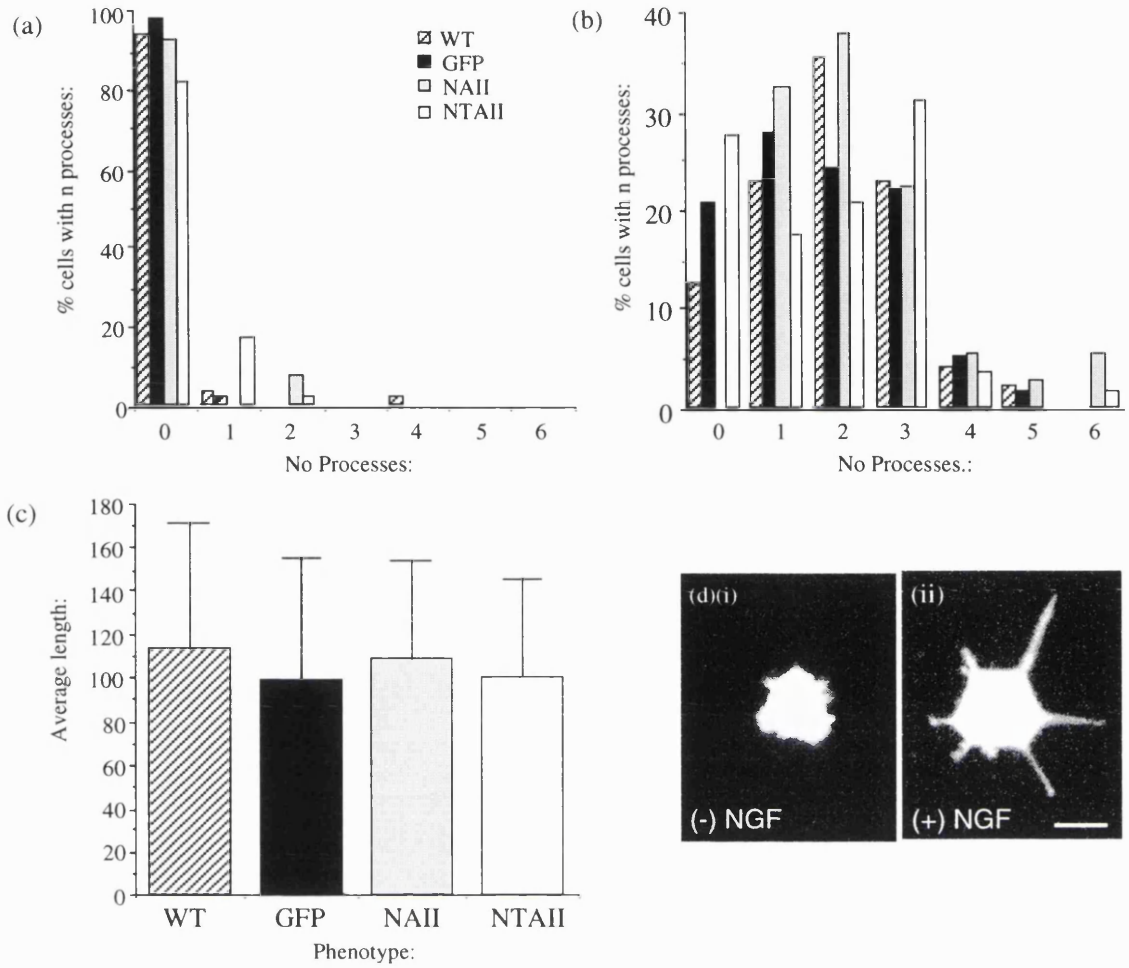

Figure 3.5: Annexin II-GFP constructs do not affect the process of NGF induced PC12 differentiation.

PC12 cells were transiently transfected with GFP, NAII-GFP and NTAII-GFP. Cells were grown with NGF for three days with or without NGF before fixation and microscopic analysis to assess the morphological changes associated with differentiation. (a) Undifferentiated wild type cells, or cells expressing GFP constructs, rarely showed processes. (b) Stimulation with NGF for three days induces process formation in wild-type cells and cells expressing any of the GFP constructs. (c) There is no significant difference between the average lengths of processes formed in wild type cells or cells expressing any of the GFP constructs (average +/- S.E.M.). (d) Example cells expressing GFP grown under normal conditions (i) or challenged with NGF for three days (ii). A process was defined as any fine cell extension > 1 μm.
Scale bar: 10 μm

Neither expression of GFP, NAII-GFP, nor NTAII-GFP had any effect on the morphological changes associated with PC12 differentiation (Figure 3.5). These results demonstrate that, although NAII-GFP targets to the plasma membrane and a perinuclear (possibly) endocytic compartment it does not interfere with the process of NGF-mediated differentiation suggesting that this construct is an innocuous probe *in vivo*.

Since annexin II has been implicated in Ca^{2+} regulated exocytosis the next set of experiments were designed to assess the effects of expression of GFP, NAII-GFP or NTAII-GFP on stimulated secretion in RBL cells. This cell line was chosen for several reasons.

Firstly, intact RBL cells can be stimulated to secrete *in vitro* by cross-linking of surface FcεR1 receptor-bound IgE with antigen though a well characterised signaling pathway (Beaven and Baumgartner, 1996). Secondly, cross linked receptors are rapidly internalised (Isersky et al., 1983) and migrate to a perinuclear location (Pfeiffer et al., 1985) which can be readily followed by labeling either antigen or IgE (Pfeiffer et al., 1985; Ra et al., 1989). Thirdly, FcεR1 stimulated secretion is accompanied by extensive and well characterised cytoskeletal changes. Thus, while Ca^{2+}-regulated secretion is the main focus of this part of the investigation a variety of 'ancillary' cellular events could also be monitored.

The first stage of this investigation required the generation of mixed clonal cell lines expressing GFP, NAII-GFP and NTAII-GFP to high levels. The expression of GFP proved useful in the isolation such cell lines by FACS as discussed in the next section.

3.6 Investigation of stimulated secretion in RBL cells: generation of RBL cell lines through FACS.

Traditional transfection and antibiotic selection for resistant clones generates cell lines with variable levels of expression, and investigation of the effects of construct expression requires the comparison of a number of clones. However the expression of GFP and GFP chimeras provides a convenient 'handle' with which cells expressing the required construct may be isolated using FACS (Mazurier et al., 1998; Meyer et al., 1998).

This technique was exploited in the investigation of the effects of GFP, NAII-GFP and NTAII-GFP on stimulated secretion in RBL cells. Briefly, RBL cells were transfected with GFP, NAII-GFP or NTAII-GFP and selected for four weeks in large (14 cm diameter) culture dishes. Microscopic examination revealed that each plate harboured between 10 and 20 fluorescent clones after four weeks of selection (results not shown). By pooling all the resistant clones from triplicate transfections and sorting to isolate fluorescent cells, pure, mixed clonal populations of cells expressing either GFP, NAII-GFP or NTAII-GFP were generated (Figure 3.6, overleaf). This proved to be a powerful approach for the rapid generation of mixed clonal populations of cells and eliminated the problems associated with clonal variation.

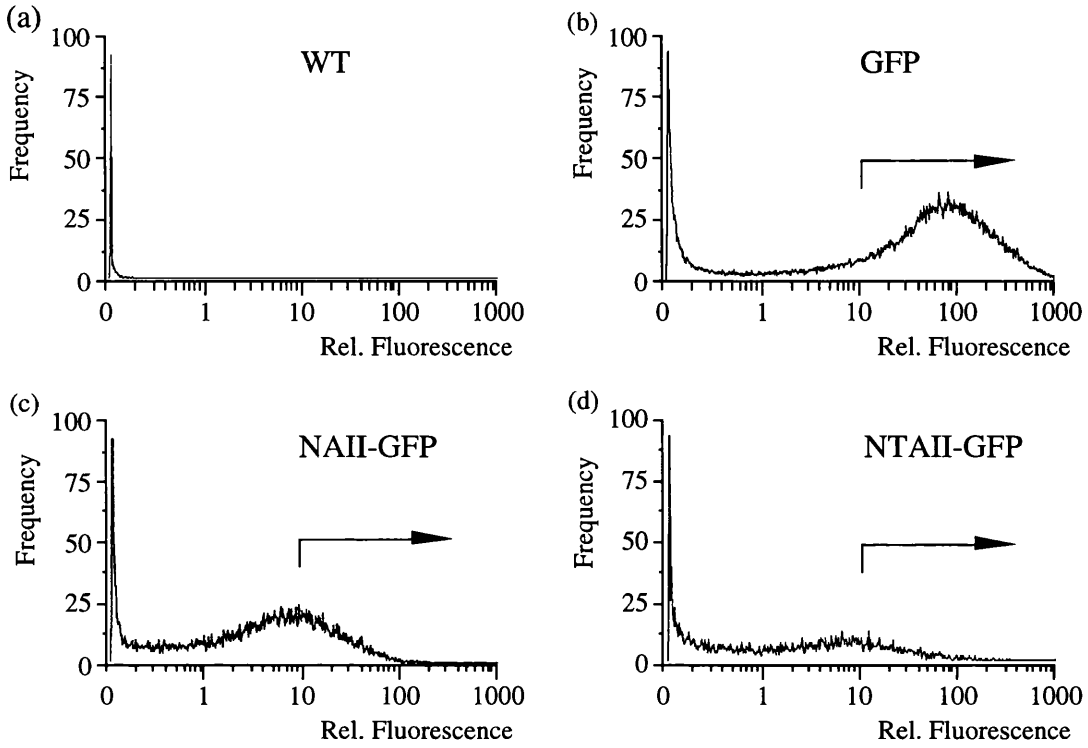

Figure 3.6: Isolation of mixed clonal populations of RBL cells expressing GFP or annexin II-GFP fusion proteins using FACS.

RBL cells were transfected with: (b) GFP, (c) NAII-GFP and (d) NTAII-GFP. (a) No fluorescent cells are seen in untransfected wild type cells. (b-d) Populations of fluorescent cells expressing GFP, NAII-GFP or NTAII-GFP were selected using the gate parameters indicated (arrows).

Examination of the FACS plots revealed that cells expressing the fusion constructs were less fluorescent than cells expressing GFP alone (Figure 3.6). The reason why this occurs is not clear. Conjugation of proteins with chemical fluorophores has been reported to induce partial fluorescence quenching compared to free fluorophore (Schauenstein et al., 1978) although this seems unlikely in the case of GFP since the residues responsible for fluorescence are tucked deep inside the barrel-like GFP protein (Tsien, 1998).

To confirm that the selected cells were producing the correct fusion proteins, whole cell lysates from each population of cells were blotted and probed using an anti annexin-II monoclonal antibody (HH7). Since this antibody recognises a motif comprising the first N-terminal 18 residues of annexin II (Jost and Gerke, 1996) it was expected this antibody would recognise both NAII-GFP, NTAII-GFP and endogenous annexin II (Figure 3.7)

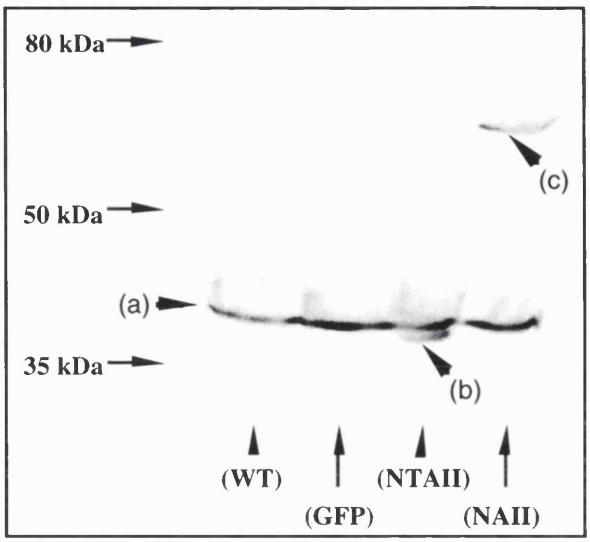

Figure 3.7: Western blot of RBL cells expressing annexin II-GFP fusion proteins.

Mixed clonal RBL cell lines expressing GFP, NAII-GFP or NTAII-GFP were generated as described previously. Whole cell lysates were analysed by SDS-PAGE and western blotting using a monoclonal anti-annexin II antibody. All cell lines express a protein of 36 kDa corresponding to endogenous annexin II (a). Cells expressing NTAII-GFP have an additional band at approximately 35.5 kDa (b) corresponding to the fusion protein (GFP + N-terminal domain of annexin II) while cells expressing NAII-GFP have an additional band at approximately 70 kDa corresponding to the fusion protein (GFP + wt annexin II).

This result confirmed that the selected cells expressed fusion proteins of the predicted molecular weights. It also confirmed directly that the N-terminal domain of annexin II was intact in the fusion proteins since the epitope recognised by the monoclonal antibody used (HH7) spans the p11 binding domain (Jost and Gerke, 1996).

3.7 Investigation of stimulated secretion in RBL cells: GFP, NAII-GFP and NTAII-GFP have no effect on stimulated secretion.

The release of histamine, serotonin and other inflammatory mediators is an early event in a variety of acute allergic, asthmatic and inflammatory reactions which can be modeled *in vitro* using the RBL cell line (Beaven et al., 1987). Binding of multi-valent antigen to FcεR1 receptor bound IgE causes receptor aggregation and initiates a signaling cascade resulting in the release of cellular serotonin, histamine, β-hexosaminidase (Ortega et al., 1989) and a dramatic reorganisation of the actin cytoskeleton and cell spreading (Pfeiffer et al., 1985).

There is extensive evidence that secretion of serotonin and other inflammatory mediators from RBL cells stimulated by FcεR1 clustering is Ca^{2+}-dependent. Receptor clustering leads to elevated intracellular Ca^{2+} which correlates with secretion (Beaven et al., 1984) and a combination of Ca^{2+} and the Ca^{2+} ionophore A23187 specifically stimulates secretion (Pfeiffer et al., 1985), but not the cytoskeletal changes associated with stimulation through FcεR1 clustering, which are mediated through PKC (Pfeiffer et al., 1985). Perhaps the most compelling evidence has come studies on single RBL cells which demonstrated that serotonin release, measured using a carbon electrode, corresponds precisely with induced increases in cytoplasmic Ca^{2+} (Kim et al., 1997).

To investigate the effects of GFP, NAII-GFP and NTAII-GFP on stimulated secretion, sorted, mixed clonal populations of stably transfected cells were simultaneously loaded with [^{3}H]-serotonin and sensitized with anti-DNP-IgE for 16 h prior to the secretion assay. Measurement of [^{3}H]-serotonin release from these intact cells, challenged with a physiological stimulus, revealed that neither NAII-GFP nor NTAII-GFP expression had a significant inhibitory or stimulatory effect on secretion compared to cells expressing GFP alone (Figure 3.8, overleaf). All transfected cells showed a slight decrease in the extent of stimulated secretion compared with wild type cells - possibly due to the impact of plasmid expression and selection on cell health.

These results with RBL cells are consistent with published results demonstrating that in PC12 cells, over-expressing annexin II or an inhibitory annexin II-p11 chimera, did not influence secretion (Graham et al., 1997) and with findings in permeabilised chromaffin cells which demonstrated that an N-terminal annexin II peptide had no effect on Ca^{2+}-dependent secretion (Ali and Burgoyne, 1990). However these findings are not consistent with microinjection studies which showed that an N-terminal annexin II peptide inhibits Ca^{2+}-dependent secretion in both chromaffin cells and bovine aortic endothelial cells (Chasserot Golaz et al., 1996; Konig et al., 1998).

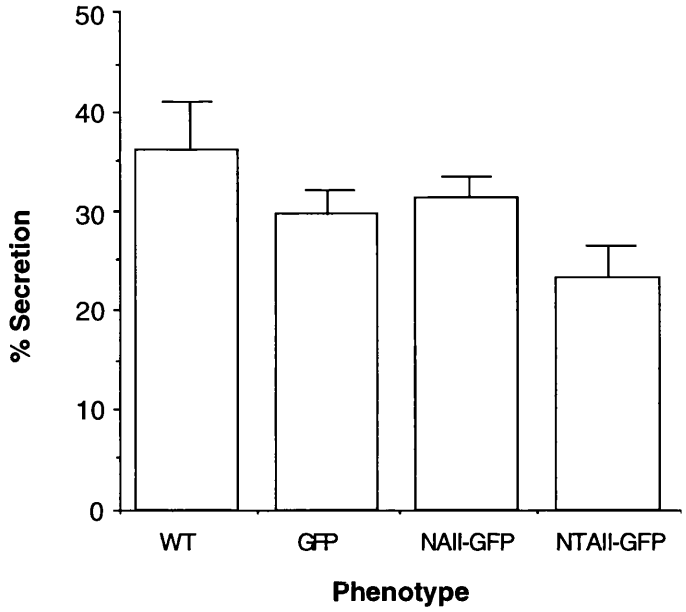

Figure 3.8: Effects of annexin II-GFP constructs on stimulated secretion in intact RBL cells.

Stable mixed clonal populations of cells (isolated by FACS of neomycin resistant cells) were plated overnight in randomly allocated wells in 24 well plates in the presence of anti-DNP IgE (1.0 μg/ml) and [^{3}H]-serotonin (500 nCi/ml). The following morning cells were washed extensively with HBS, stimulated with DNP-albumin (100 ng/ml) for 20 min before recovery of supernatant and measurement of [^{3}H]-serotonin release. Expression of GFP, full length annexin II-GFP (NAII-GFP) or the N-terminus of annexin II fused to GFP (NTAII-GFP) has no significant effect on the extent of stimulated secretion in intact RBL cells (values shown are average +/- S.E.M., n= 5, data shown is representative of multiple replicates).

3.8 Translocation of NAII-GFP but not NTAII-GFP to the cell cortex during stimulated secretion.

Previous studies in chromaffin cells have demonstrated that annexin II translocates to the plasma-membrane during stimulated exocytosis (Chasserot Golaz et al., 1996; Sagot et al., 1997). To find out if NAII-GFP translocated to the plasma membrane during IgE/antigen stimulated exocytosis in RBL cells, transiently transfected RBL cells were stimulated to secrete using anti DNP IgE/DNP-albumin before chemical fixation, permeabilisation and analysis by confocal microscopy (Figure 3.9, overleaf).

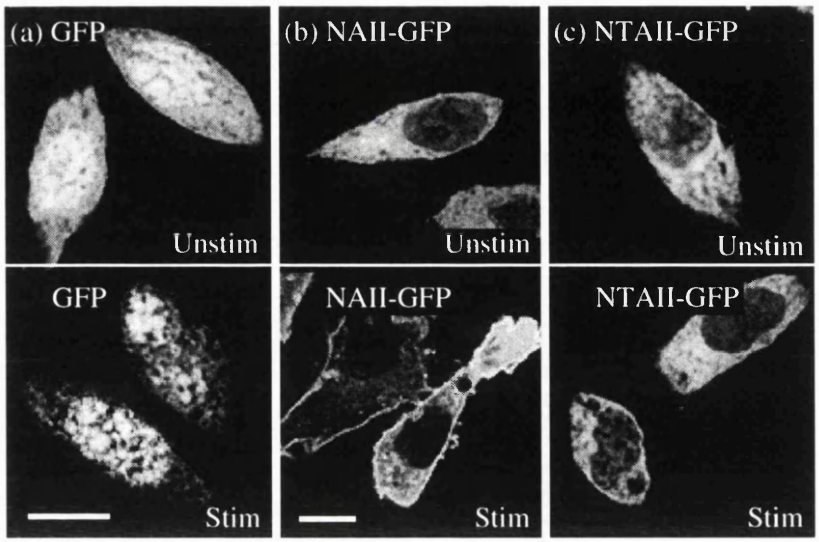

Figure 3.9: NAII-GFP but not NTAII-GFP becomes associated with the plasma membrane on stimulation of exocytosis in RBL cells.

RBL cells were transiently transfected with GFP, NAII-GFP or NTAII-GFP, sensitised with anti-DNP IgE and stimulated with DNP-albumin for 20 minutes (see Figure 2.1, Materials and Methods). Cells were fixed in 3.7% formaldehyde and imaged using confocal microscopy. Stimulation of cells expressing GFP alone causes an apparent loss of GFP fluorescence from the cytoplasm, which makes the nucleus appear strikingly bright (a). In contrast NAII-GFP shifts from a cytosolic to a predominantly plasma membrane distribution (b). While full length annexin II is able to target GFP to the plasma membrane in stimulated cells the N-terminal domain alone remains cytosolic (c). (See text for details.) Scale bars: 10 μm, note lower frame in (b) is at a lower magnification.

These results agree with previously published results in chromaffin cells which used chemical fixation and immunoflourescence analysis to demonstrate the translocation of annexin II to the plasma membrane during stimulated exocytosis (Chasserot Golaz et al., 1996). Membrane association of GFP fluorescence is dependent on the core domain of annexin II since NTAII-GFP (the N-terminal domain of annexin II fused to GFP) does not become membrane associated under these conditions. Comparison of the fluorescence profile of the plasma membrane in unstimulated and stimulated cells expressing NAII-GFP demonstrates the apparant translocation of NAII-GFP to the plasma membrane more clearly (Figure 3.10, overleaf).

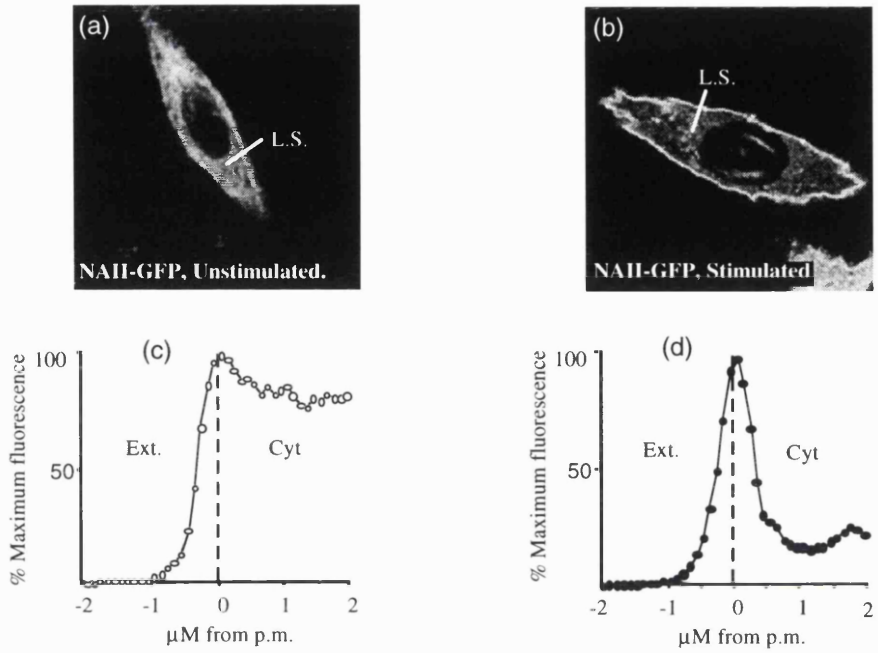

Figure 3.10: Semi-quantitative comparison of trans-plasma membrane fluorescence profiles in unstimulated and stimulated RBL cells expressing NAII-GFP.

Confocal micrographs of (a) unstimulated and (b) IgE/DNP-albumin stimulated RBL cells expressing NAII-GFP were analysed using NIH Image. Briefly, a 4 µm linescan was taken for each cell across the plasma membrane from the cell exterior (Ext) into the cell cytoplasm (Cyt) as indicated as indicated by the lines, L.S. (drawn twice actual size, 8 µm) (c)(d). The resulting numerical data were standardised to peak and background levels and averaged (n= 10). The fluorescence profile in the region of the plasma membrane changes dramatically on stimulation (compare (c) and (d)) and suggests NAII-GFP becomes associated with the plasma membrane on stimulation of RBL cells with IgE/DNP-albumin (see text for details). Error bars have been omitted for clarity.

While these data were consistent with published data and indicated NAII-GFP became associated with the plasma membrane as a consequence of IgE/DNP stimulation, these fixed cell data could not be used for a quantitative analysis of NAII-GFP translocation to the plasma membrane. This is for the following reasons. Although linescan data (Figure 3.10) indicate there has been a dramatic change in the ratio of plasma membrane:cytosolic fluorescence signal of NAII-GFP it is unclear whether NAII-GFP became concentrated at the plasma membrane above levels of soluble NAII-GFP free in the cytoplasm in live cells. This is because loss of soluble NAII-GFP may have occured during fixation, effectively changing the ratio of plasma membrane:cytosolic fluorescence. Such an effect is not unlikely since it has been reported that chemical fixation can result in the redistribution of soluble proteins through differential extraction (Melan and Sluder, 1992). It should be

noted that GFP also becomes apparently 'concentrated' in the nucleus on stimulation (Figure 3.9, 94) which would be consistent with this theory.

Could chemical fixation have different effects on unstimulated and stimulated cells? Stimulation of RBL cells with IgE/antigen causes dramatic changes in the mechanical properties of the plasma membrane (Dai et al., 1997) and actin cytoskeleton (Liu et al., 1987) which may alter susceptibility to permeabilisation (by the fixative) and loss of unfixed, soluble proteins. There is some experimental evidence to substantiate this argument since it has previously been shown that stimulation of exocytosis in sea-urchin eggs renders the plasma membrane vulnerable to damage by chemical fixation (Chandler, 1984). To investigate the stimulation-dependent association of NAII-GFP with the plasma membrane further, experiments were designed to investigate this phenomenon in live cells (see section 3.10 Investigation of NAII-GFP distribution during stimulation of secretion in live RBL cells., p 98).

3.9 Partial colocalisation of NAII-GFP and early endocytic compartments in stimulated RBL cells.

During experiments investigating the translocation of NAII-GFP in RBL cells it was noted that NAII-GFP in stimulated cells is often seen to decorate large (1-2 μm) vesicular structures. These were often found close to the plasma membrane (Figure 3.11).

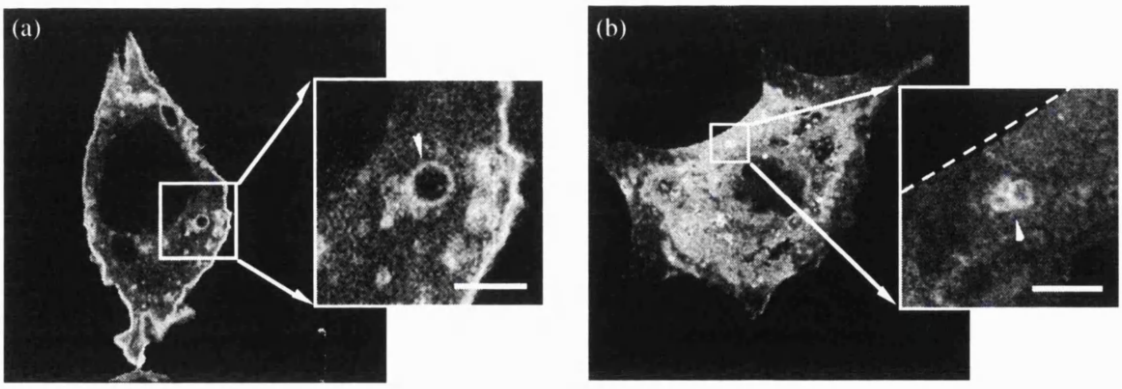

Figure 3.11: In IgE/antigen stimulated cells NAII-GFP is often associated with large vesicular structures in the cytoplasm.

RBL cells were transiently transfected with NAII-GFP, sensitised with anti-DNP IgE and stimulated with DNP-albumin for 20 min as detailed in Materials and Methods. On stimulation annexin II-GFP becomes associated with the plasma-membrane (a) and large vesicles in the cytoplasm (arrow, inset). Confocal slices taken close to the plasma-membrane at the lower surface of stimulated cells (b) reveals clusters of NAII-GFP decorated vesicles (arrow, inset) adjacent to the plasma membrane.
Scale bar: 2 μm.

Since the secretory structures in RBL cells are relatively large (up to 1.5 μm) (Spudich and Braunstein, 1995) the vesicles observed in Figure 3.11 could be associated with exocytosis. On the other hand, given that annexin II has been associated with number of endocytic compartments (Harder et al., 1997; Pol et al., 1997) and the fact that IgE/antigen stimulation leads to an increase in both receptor mediated endocytosis and pinocytosis (Pfeiffer et al., 1985) these structures could also be associated with endocytosis.

To find out if these vesicular structures are a type of endosome, RBL cells expressing annexin II-GFP were stimulated using a TexasRed-DNP-albumin conjugate before fixation. FcεR1-mediated secretion is stimulated by clustering of the FcεR1/IgE through cross-linking of bound IgE by the cognate antigen (Isersky et al., 1983), and clustered FcεR1/IgE/antigen complexes are rapidly removed from the cell surface via both clathrin-mediated endocytosis and clathrin-independent endocytosis (Pfeiffer et al., 1985; Ra et al., 1989). Thus labeled antigen would be expected to specifically tag activated FcεR1/IgE/antigen complexes and be rapidly endocytosed (Figure 3.12).

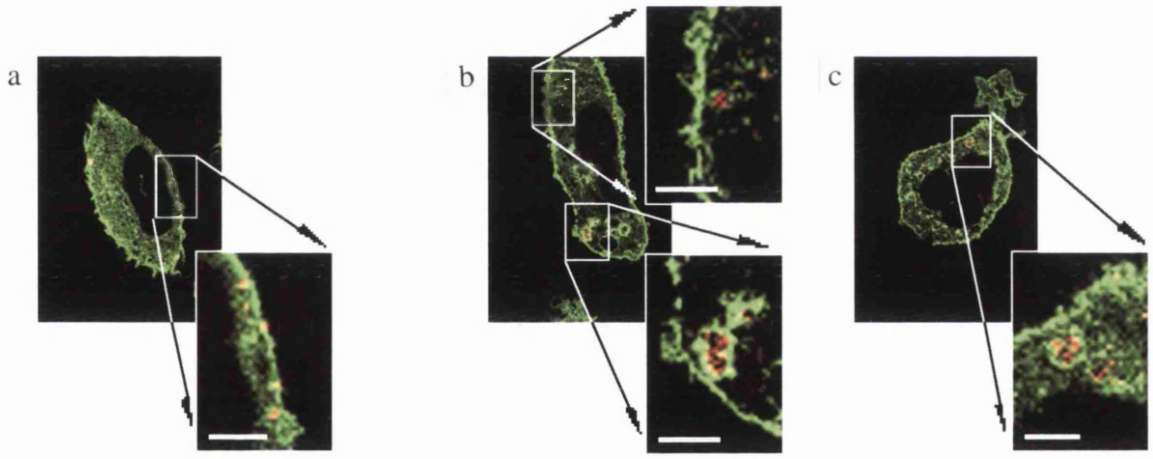

Figure 3.12: NAII-GFP partially colocates with large endocytic vesicles adjacent to the plasma membrane.

RBL cells were transiently transfected with NAII-GFP and sensitised with anti-DNP-IgE as detailed in Materials and Methods. Cells were incubated for 30 min at 4°C with 200 ng/ml rhodamine conjugated DNP-albumin and either (a) immediately fixed or (b)(c) incubated for 20 min at 37°C to promote receptor aggregation and internalisation. Incubation at 4°C allows TRITC-DNP-albumin binding to the surface of sensitised RBL cells which remains at or adjacent to the surface of the cell (red dots). In contrast warming to 37°C allows internalisation of TRITC-DNP-albumin in large aggregates some of which are coated in NAII-GFP ((b)(c) inset).
Scale bar: 2 μm.

Although this experiment revealed that at least some of the vesicles seen are of endocytic origin the precise identity of these vesicles remains obscure. The problem of identifying these structures was compounded by the recent discovery that a portion of IgE prebound to surface FcεR1 receptors becomes localised to secretory vesicles, which in RBL cells are a modified type of lysosome (Xu et al., 1998). Although not confirmed this raises the possibility that endocytic markers (such as labeled antigen) might become concentrated in secretory vesicles during the time course of a secretion assay. However in light of data generated in later experiments (see Chapter 4.0) it is possible that these structures were macro-pinosomes although this was not investigated further.

3.10 Investigation of NAII-GFP distribution during stimulation of secretion in live RBL cells.

In view of the results obtained using fixed cells, the redistribution of NAII-GFP in live, fully intact cells was investigated during stimulated secretion. Data suggesting NAII-GFP becomes tightly associated with the plasma membrane during stimulated secretion using chemical fixation and confocal microscopy agreed with published results (Chasserot Golaz et al., 1996) and indicated that a portion of cytoplasmic NAII-GFP becomes tightly associated with the subplasmalemma on stimulation. Furthermore NAII-GFP was seen to be associated with vesicular structures adjacent to the plasma membrane in stimulated cells. Evanescent Wave Microscopy (EWM - see Figure 2.2) was used to investigate NAII-GFP plasma membrane association, and the vesicular structures, in live cells. EWM allows measurement of fluorescence at the base of a cell in a thin, peri-plasmalemmal layer illuminated by the evanescent wave. One would predict that translocation of NAII-GFP to the plasma membrane would lead to an increase in the concentration of GFP molecules in the evanescent wave and a corresponding increase in fluorescence.

RBL cells transiently expressing either GFP or NAII-GFP and sensitised with anti-DNP IgE were mounted for EWM at 37^{0}C and stimulated *in situ* with 100 ng/ml DNP-albumin. Images were acquired at 1 frame every 6 s and analysis of the resulting image sequences revealed numerous dark vesicles backlit against NAII-GFP in the cytoplasm (data not shown). NAII-GFP was not concentrated around these vesicles, and so the identity of the peri-plasma membrane vesicles seen in fixed IgE/antigen stimulated cells remains unknown. The image sequences generated were subsequently analysed to quantify changes both in area and fluorescence (Figure 3.13, overleaf).

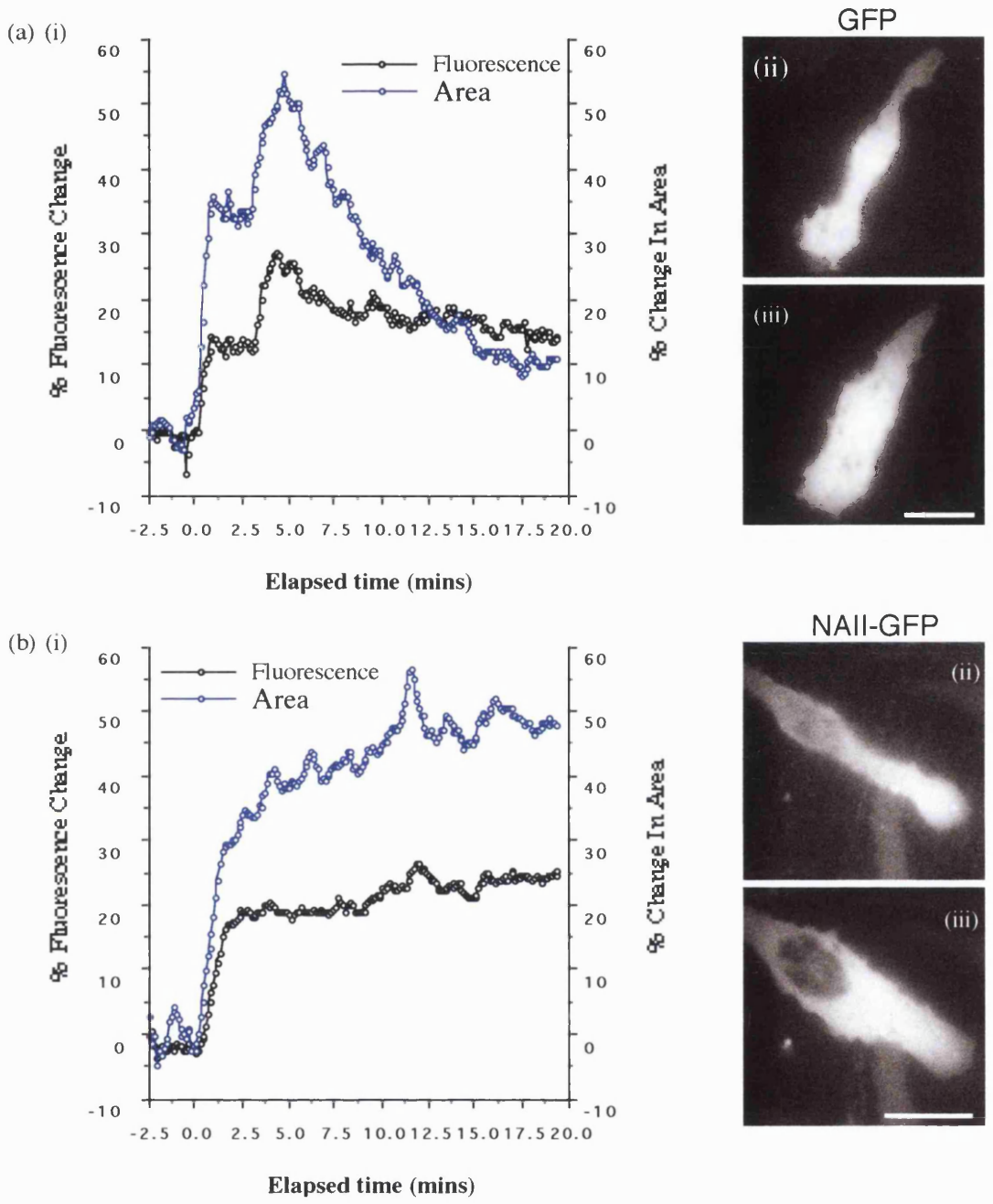

Figure 3.13: Stimulation of GFP(+) or NAII-GFP(+) RBL cells with IgE/DNP-albumin leads to cell spreading and an increase in average fluorescence.

RBL cells expressing either GFP or NAII-GFP were sensitised with IgE, imaged at 37^{0}C using EWM and stimulated *in situ* with 100 ng/ml DNP-albumin. (a)(i) Plot of the average fluorescence of an example cell expressing GFP illustrates that both area and average fluorescence increase on stimulation. (b)(i) Similar increases in area and average fluorescence are seen in cells expressing annexin II-GFP. In both (a) and (b) example frames prior to stimulation (ii) and 1 minute after stimulation (iii) illustrate the morphological changes triggered by addition of DNP-albumin at T= 0. (Scale bar = 20 μm)

These data (Figure 3.13) yielded two pieces of information. Firstly, cells expressing GFP or NAII-GFP increased the size of their 'footprint' when stimulated with IgE/DNP-albumin, as reported previously for untransfected RBL cells (Pfeiffer et al., 1985; Spudich, 1994). Expression of GFP or NAII-GFP did not appear to have any gross effect on the morphological changes elicited by stimulation.

Secondly, cells expressing NAII-GFP or GFP both showed an increase in fluorescence when stimulated (Figure 3.14, overleaf). Unlike NAII-GFP, GFP alone was never seen to associate with membranes under any conditions in either live or fixed cells, hence the observed increase in fluorescence was not due to membrane translocation of either GFP or NAII-GFP.

Initially there appeared to be two explanations for the measured increase in cellular fluorescence. Firstly, and most simply, an increase in fluorescence could be explained through closer adhesion of stimulated cells to the coverslip since this would effectively introduce more fluorophore into the brightest part of the evanescent wave, immediately adjacent to the glass. A second, perhaps more intriguing explanation, is that the cells may undergo a volume change on stimulation. Using the soluble cytoplasmic fluorophore calcein, it has been possible to accurately measure volume changes in single N1E1-115 neuroblastoma cells (Crowe et al., 1995) and show that a decrease in cell volume is elicited by both hyperosmotic shock or high intracellular free Ca^{2+}.

The fluorescence changes seen on stimulation of GFP and NAII-GFP expressing cells would thus be consistent with a decrease in cell volume. Such volume changes have previously been suggested to occur, since stimulation of RBL cells with IgE/DNP leads to a decrease in plasma membrane tension consistent with a decrease in cell volume (Dai et al., 1997). Furthermore recent data demonstrated that an increase in membrane tension in chromaffin cells causes a dramatic decrease in exocytosis (70 fold) without irreversibly impairing secretory capability (Solsona et al., 1998). Together these results suggest that membrane tension might play key role in modulating exocytosis, which could be influenced by membrane addition (exocytosis), membrane retrieval (endocytosis) and volume changes.

To test the hypothesis that the observed increases in fluorescence could be explained by cell shrinkage, RBL cells expressing NAII-GFP were imaged using EWM during challenge with HBS supplemented with 150 mM sucrose (Figure 3.14, overleaf).

As expected, challenge with mildly hyperosmotic HBS induced a similar (though more rapid) increase in fluorescence as seen in stimulated cells, without inducing any morphological changes (data not shown). Although these preliminary experiments proved inconclusive in themselves, the investigation of hyperosmolarity induced volume changes led directly to the discovery of a second, unprecedented phenomenon induced by

hyperosmotic challenge. This was the appearance of a novel class of motile vesicle, as discussed in Chapter 4.

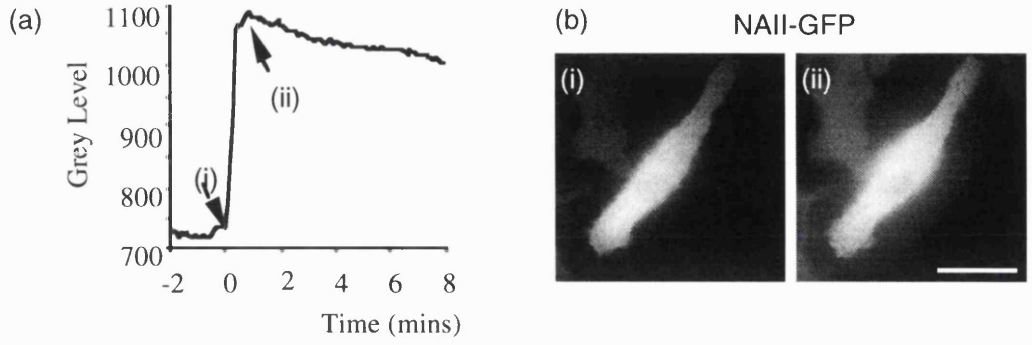

Figure 3.14: The fluorescence increase seen in NAII-GFP(+) RBL cells when stimulated to secrete can be mimiced by hyperosmotic shock.

To test whether the increase in fluorescence seen in stimulated cells might be caused by a decrease in cell volume, RBL cells expressing NAII-GFP, were stimulated with HBS + 150 mM sucrose at 37^{0}C to induce cell shrinkage. Cells were imaged using EWM (1 frame every 6s) and challenged with hyperosmolar HBS after 2 min. (a) Measurement of the average fluorescence of an example cell demonstrates that a rapid increase in fluorescence, consistent with cell shrinkage, is seen on challenge with hyperosmolar HBS. (b) Example frames from the image sequence immediately before challenge (i) and 1 min post challenge (ii) illustrate that no radical change in morphology occurs immediately after challenge with hyperosmolar HBS.
Scale bar: 20 μm.

3.11 Conclusions.

Initial experiments established that expression of a variety of annexin II-GFP chimeras in either PC12 or RBL cells has little impact on cell viability, and it was shown using western blotting that fusion proteins of the appropriate molecular weights are expressed. Analysis of the distribution of annexin II-GFP constructs *in vivo* revealed that only one fusion construct, NAII-GFP (in which GFP is fused to the C-terminus of annexin II) is targeted to the cell cortex in live PC12 cells. This is consistent with the previously reported localisation of exogenously over-expressed annexin II in this cell line (Graham et al., 1997). Further investigation of cortical targeting of NAII-GFP confirmed this process is dependent on intact Ca^{2+} and p11 binding sites, consistent with previously published results (Thiel et al., 1992). Taken together these results indicate that NAII-GFP, but not CAII-GFP is a valid probe for annexin II distribution *in vivo*.

The reasons for the unexpected localisation of NAII-GFP and NTAII-GFP to perinuclear foci were less clear. While there was indirect evidence that these foci might

represent an endocytic compartment, findings in fixed RBL cells confused this issue. Specifically, chemical fixation and confocal microscopic analysis of RBL cells expressing GFP or NTAII-GFP revealed bright perinuclear foci which were superficially similar to the foci seen in live PC12 cells. Since the fluorescence signal of GFP and NTAII-GFP is homogeneous throughout the nucleus and cytoplasm, and throughout the cytoplasm respectively, in live RBL cells, this indicates that chemical fixation can modulate the apparent 'concentration' of a protein in different cellular locations.

Further confusion between data in chemically fixed cells and living cells emerged through analysis of the distribution of NAII-GFP in resting RBL cells and RBL cells stimulated with IgE/antigen. While NAII-GFP appeared to have translocated to the plasma membrane in fixed cells, careful analysis of live cells failed to corroborate this result. The observed association of NAII-GFP with the plasma membrane after stimulation appeared specific since GFP or NTAII-GFP did not show comparable changes in distribution. However, it is difficult to make accurate quantitative measurements of the putative 'translocation' using fixed cells. To make a meaningful comparison between randomly sampled images of unstimulated and stimulated cells would require prohibitively large samples to be gathered since transfected RBL cells express NAII-GFP to varying degrees (see for example the FACS plot in Figure 3.6). This problem is compounded by the fact that it is unclear how chemical fixation might contribute to the observed differences in distribution of NAII-GFP between unstimulated and stimulated cells. This was graphically illustrated by analysis of cells expressing GFP alone since GFP alone appeared 'concentrated' in the nucleus after stimulation of cells followed by chemical fixation and processing for confocal microscopy (see Figure 3.9). Thus, while a portion of NAII-GFP might become tightly associated with the plasma membrane on stimulation of RBL cells, this might not be seen in live cells if masked by a high background concentration of soluble NAII-GFP.

It seems likely that the only way to differentiate between these possibilities would be to observe RBL cells expressing NAII-GFP through the entire manipulation of stimulation, fixation and permeabilisation *in situ* using confocal microscopy. Comparison of the cortical fluorescence signal before and after the experimental manipulations would confirm whether NAII-GFP had genuinely translocated to the cell cortex on stimulation, or whether this effect was influenced by chemical fixation. In addition it might reveal whether stimulation can modulate the way in which cells respond to chemical fixatives. Stimulation initiates dramatic changes in the mechanical properties of the plasma membrane (Dai et al., 1997) and the actin cytoskeleton (Liu et al., 1987) both of which might influence the extent of cell damage and loss of soluble proteins during fixation.

In addition to the apparent translocation of NAII-GFP to the plasma membrane it was also noted that NAII-GFP coated relatively large vesicles near to the plasma

membrane. Although some of these vesicles contain an endocytic marker, the identity of these structures remained obscure. No similar structures were seen in live RBL cells expressing NAII-GFP and stimulated with IgE-antigen. However, as for the plasma membrane, the localisation of NAII-GFP to these structures might only become apparent during fixation and permeabilisation.

As well as being a useful tool for cellular localisation experiments it was also established that NAII-GFP is suitable for investigating a variety of physiological processes in which annexin II has been implicated. Firstly the transient expression of fusion proteins allowed the effects of these constructs on the differentiation of PC12 cells to be analysed. No significant effect on differentiation was found, arguing against the role for annexin II in this process which has been previously proposed (Fox et al., 1991). Secondly it was established that GFP can be used as a convenient 'handle' to isolate pure, multiclonal cell lines expressing the fusion construct of interest using FACS. Subsequent analysis of IgE/antigen stimulated exocytosis in RBL cell lines generated in this way, expressing a variety of annexin II-GFP constructs showed that annexin II-GFP constructs had no significant impact on IgE/antigen stimulated exocytosis. These results corroborate previous findings which established that overexpression of annexin II in PC12 cells failed to modulate stimulated exocytosis (Graham et al., 1997). In particular the finding that the N-terminus of annexin II, fused to GFP, has no effect on stimulated exocytosis in intact RBL cells was striking. It has been shown previously by several groups that N-terminal peptides of annexin II can inhibit stimulated secretion (Chasserot Golaz et al., 1996; Konig et al., 1998) while other investigators found no such effect (Ali and Burgoyne, 1990). The results of the present study agree with the latter finding. Furthermore, the cells used in the present study were intact.

Investigation of fluorescence changes in intact RBL cells expressing GFP or NAII-GFP led directly to the discovery of a novel class of motile vesicle. This phenomenon is discussed in detail in the following chapter.

4. Chapter 4 : Investigation of vesicle rocketing *in vivo.*

4.1 NAII-GFP forms a tail behind mobile, fusogenic vesicles.

In a minority of RBL cells expressing NAII-GFP, challenge with hyperosmolar HBS led to the appearance of a novel class of mobile vesicles. These vesicles ranged in size from sub-resolution (visible via the associated tail) to 2 μm, moved on curving trajectories through the cytoplasm and were trailed by brightly fluorescent NAII-GFP tails (Figure 4.1).

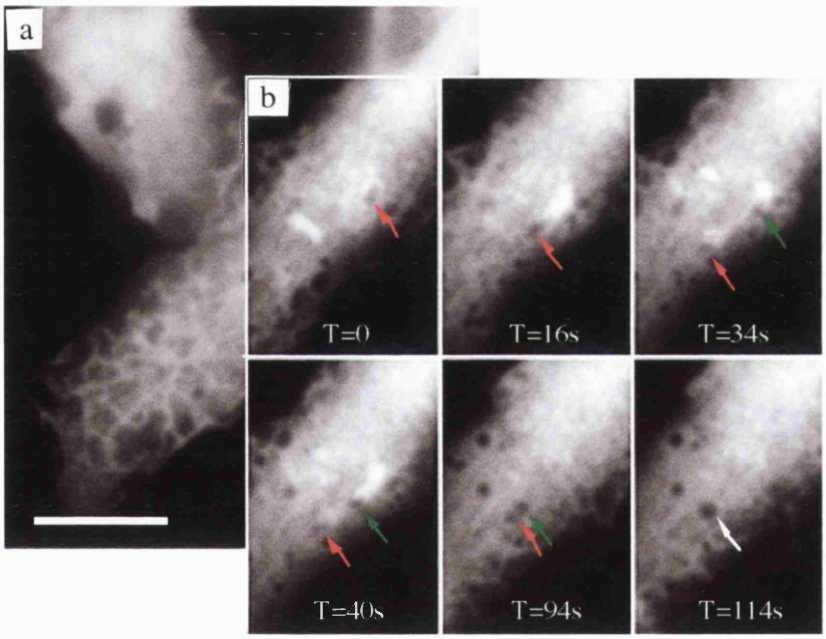

Figure 4.1: NAII-GFP is associated with mobile, fusogenic vesicles.

RBL cells, transiently expressing NAII-GFP, were challenged with HBS + 150 mM sucrose for 30 min at 37°C and imaged by EWM. (a) Overview of example cell producing rocketing vesicles. (b) Time resolved montage of area highlighted in (a). At T=0 s a vesicle appeared from deeper in the cell (red arrow) and moved in the plane of the membrane (T=0 s to T=34 s) before stopping. A second rocketing vesicle (green arrow) appeared at the same point, moved along the same path and stopped adjacent to the first rocket (T=94 s). The two vesicles then fused to form one larger vesicle (white arrow). Note that NAII-GFP is associated with the vesicles while they are mobile, but is not enriched between the vesicles prior to fusion. (For full sequence refer to Movie 4.1 on the accompanying CD).
Scale bar: 10 μm.

Since no such tails were observed in any cells expressing GFP alone (not shown) this phenomenon was clearly dependent on the attachment of annexin II to GFP. As

annexin II has frequently been linked to vesicle aggregation and fusion (see Chapter 1, Introduction) it was interesting to note that NAII-GFP was not concentrated at the surface of vesicles when they were closely apposed prior to fusion, and was concentrated in the vicinity of vesicles only when these vesicles were mobile. Specifically, NAII-GFP was found concentrated in a polarised plume in the wake of mobile vesicles which disappeared concomitantly with termination of vesicle motion.

A thorough search of the literature revealed that nothing had been published which resembled these findings, although there is a considerable literature concerning similar structures associated with the intracellular bacteria *Listeria* (Theriot et al., 1992), *Shigella* (Bernardini et al., 1989) and *Rickettsia* (Hackstadt, 1996; Sanders and Theriot, 1996) and the intracellular virus *Vaccinia* (Cudmore et al., 1995; Cudmore et al., 1996). All four pathogens have been shown to coerce the actin cytoskeleton into forming polarised tails which are thought to propel them through the cytoplasm.

This raised a number of questions. Firstly, are the tails behind rocketing vesicles actin-based? Secondly, what are the vesicles? Lastly, why is NAII-GFP associated with the tail? These questions, and others, were addressed in the following experiments.

4.2 Targeting of GFP-actin to rocketing vesicles in hyperosmotically shocked RBL cells.

Analysis of the distribution of GFP-actin in resting RBL cells demonstrated that it is incorporated into actin-based structures in this cell line in a comparable manner to endogenous actin (Figure 4.2, overleaf).

Since the distribution of GFP-actin and endogenous actin was indistinguishable in resting RBL cells, as demonstrated previously for fibroblasts (Ballestrem et al., 1998), this GFP construct was used to assess whether GFP-actin is incorporated into rocket tails in hyperosmotically shocked RBL cells. RBL cells, transiently expressing GFP-actin, were challenged with HBS supplemented with 150 mM sucrose while being imaged by EWM (Figure 4.3, overleaf).

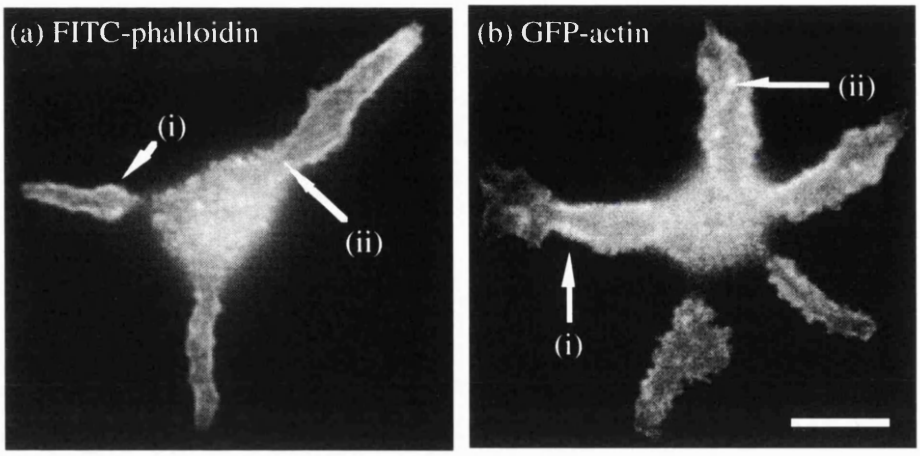

Figure 4.2: GFP-actin has the same distribution as native actin stained by FITC-Phalloidin in RBL cells.

The distribution of F-actin in fixed phalloidin stained wild type cells (a) is indistinguishable from the distribution of GFP-actin in live cells (b) when viewed by EWM. F-actin is present in the cell cortex (i) and in foci (ii) in both live and fixed cells. The live cell in (b) features in Movie 4.2, appending CD. Scale bar: 10 μm

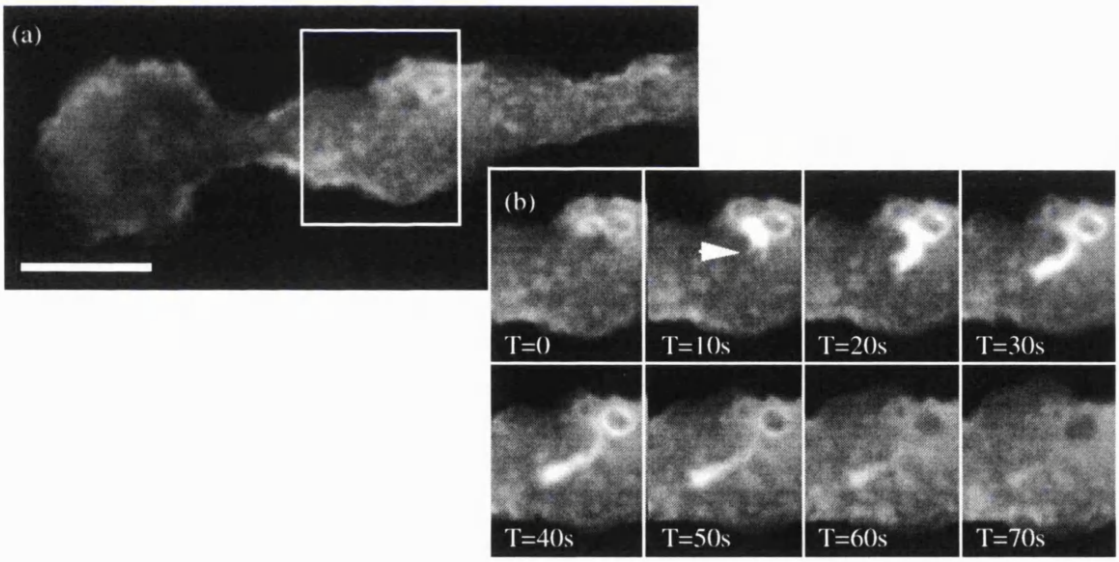

Figure 4.3: GFP-actin is incorporated into rocket tails behind unidentified vesicles in hyperosmotically shocked RBL cells.

RBL cells, transiently expressing GFP-actin, were challenged with hyperosmotic HBS (HBS+150 mM sucrose) for 20 min at 37^{0}C *in situ* using EWM. (a) Example cell. (b) Time resolved montage of boxed region in (a) follows a brightly fluorescent GFP-actin rocket (arrow) appearing in the evanescent wave and traveling briefly in the plane of the membrane before fading. For full movie sequence see Movie 4.3, accompanying CD.
Scale bar: 10 μm

Since GFP-actin was incorporated into rocket tails behind mobile vesicles in a similar fashion to NAII-GFP, and given the similarities with the movement of *Listeria*, *Shigella* and *Vaccinia*, this result demonstrated that the rocket tails seen behind moving vesicles were actin based and might be involved in propulsion of the unidentified vesicles.

Although hyperosmotic shock alone could consistently be used to generate rocketing vesicles, the incidence of events, judged empirically, was low. Therefore, ways of enhancing the production of rocketing vesicles were investigated. If this could be achieved it would facilitate analysis of the mechanism(s) of rocket formation, aid the identification of rocketing vesicles and allow the design of more formal experiments to identify the vesicles responsible for rocket generation.

Since the vesicles at the head of rocket tails are similar in size to macro-pinosomes (Casey et al., 1986) and phorbol ester stimulates macro-pinocytosis in a variety of cell types including neutrophils (Keller, 1990), macrophages (Phaire-Washington et al., 1980) and RBL cells (this study, Figure 5.1, p 137), the effects of phorbol myristic acid (PMA) and a combination of PMA and hyperosmotic shock on rocket generation were investigated. Firstly the effects of PMA alone on cells expressing NAII-GFP or GFP-actin were analysed (Figure 4.4).

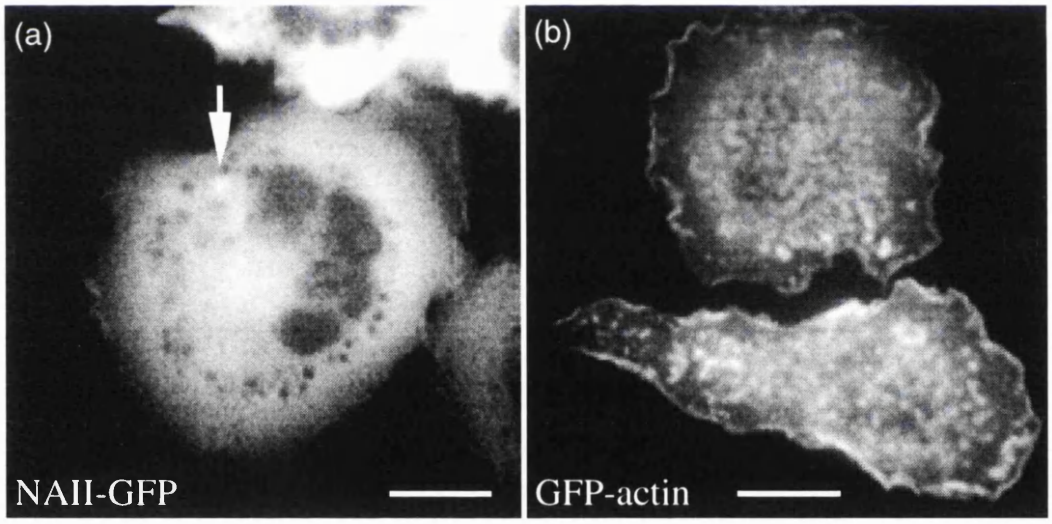

Figure 4.4: The effects of PMA on RBL cells expressing NAII-GFP or GFP-actin.

RBL cells transiently expressing NAII-GFP (a) or GFP-actin (b) were stimulated with 10 nM PMA for 30 min before imaging using EWM. Cells spread characteristically as reported previously (see text). (a) NAII-GFP fluroescence is relatively uniform, and occasional minor rocketing events are seen (arrow). (b) In contrast GFP-actin is localised at numerous foci at the lower surface of cells, and appears to 'scintillate'. The cells above feature in (a) Movie 4.4a and (b) Movie 4.4b.
Scale bar: 10 μm

As reported previously PMA alone stimulates cell spreading (Pfeiffer et al., 1985), though does not by itself stimulate prolific rocketing. Interestingly, while NAII-GFP fluorescence remains homogeneous (see Movie 4.4a, supplementary data) actin-GFP fluorescence 'scintillated' (see Movie 4.4b, supplementary data) as though complex waves of GFP-actin polymerisation were occurring close to the plasma membrane at the lower surface of the cell. Indeed, on rare occasions the scintillation of fluorescence resolved into waves (data not shown). The nature of these actin waves was not investigated further, though it was noted that they superficially resemble published data illustrating Ca^{2+} waves (Bootman and Berridge, 1996).

Since PMA does not strongly stimulate the production of NAII-GFP or GFP-actin rockets the effects of a combination of PMA and hyperosmotic shock were investigated (Figure 4.5 and Figure 4.6).

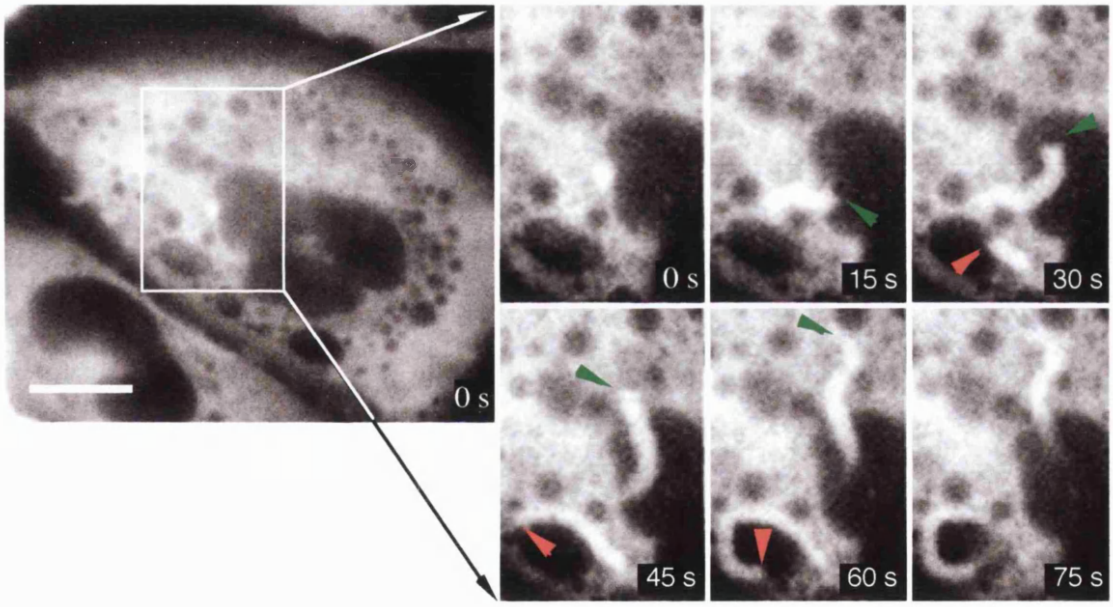

Figure 4.5: Co-stimulation of RBL cells expressing NAII-GFP with PMA and hyperosmotic shock induces prolific NAII-GFP rocketing.

RBL cells transiently expressing annexin II-GFP were stimulated to produce rocketing vesicles using 10 nM PMA and hyperosmotic shock (+ 150 mM sucrose) and imaged using EWM. Co-stimulation with PMA and hyperosmotic shock induces numerous rocketing vesicles (green and red arrows). For full movie sequence see Movie 4.5, supplementary data. Scale bar: 10 μm

To check that the NAII-GFP decorated rockets induced through co-stimulation with PMA and hyperosmotic shock were actin-based the experiment was repeated using RBL cells transiently expressing GFP-actin (Figure 4.6).

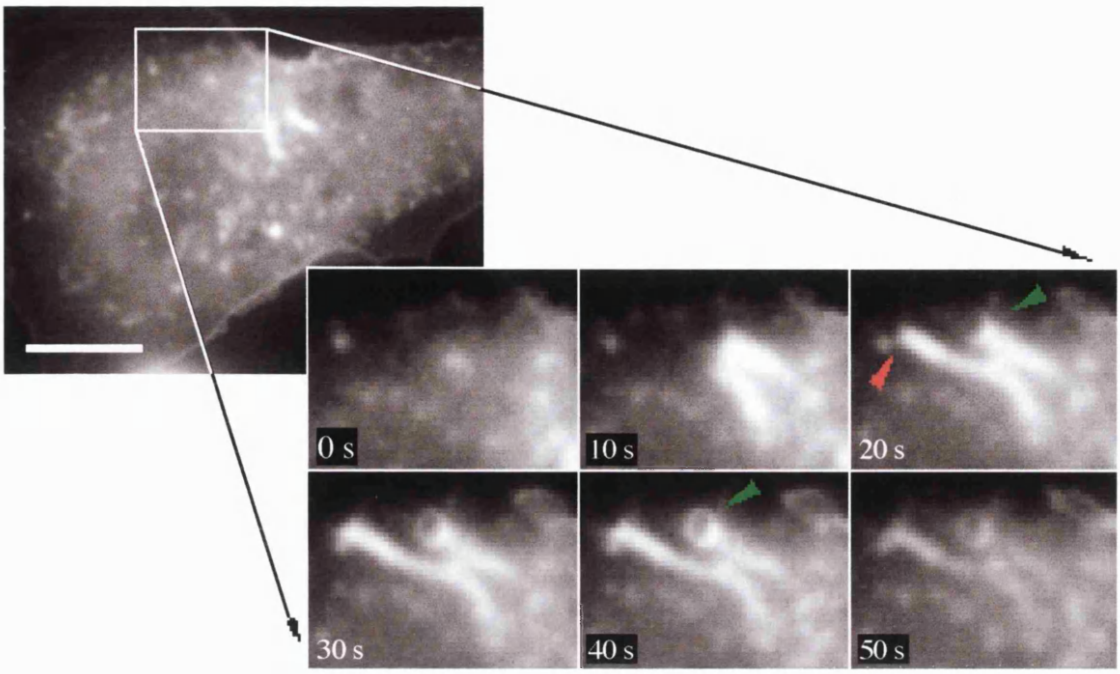

Figure 4.6: Co-stimulation of RBL cells expressing GFP-actin with PMA and hyperosmotic shock induces prolific GFP-actin rocketing.

RBL cells transiently expressing GFP-actin were stimulated to produce rocketing vesicles using 10 nM PMA and hyperosmotic shock (+ 150 mM sucrose) and imaged using EWM. Co-stimulation with PMA and hyperosmotic shock induces numerous rocketing vesicles (green and red arrows). Note that when the rocketing vesicles terminate the vesicle at the tip of the GFP-actin rocket occasionally becomes 'haloed' in GFP-actin (green arrow, T=40 s) For full movie sequence see Movie 4.6, supplementary data.
Scale bar: 10 μm

Quite clearly, a combination of PMA and hyperosmotic shock is far more effective at stimulating the generation of both NAII-GFP rockets (see Movie 4.5, supplementary data) and GFP-actin rockets (see Movie 4.6, supplementary data). This discovery allowed further experiments to be designed to investigate the identity, the kinetics and ultimately the molecular basis of vesicle rocketing. Once these goals had been achieved it was hoped that this would generate a mechanistic frame-work which might clarify the data obtained using NAII-GFP, and ultimately reveal the function of annexin II.

4.3 Identity of the rocketing vesicles.

The vesicle at the tip of NAII-GFP and GFP-actin labeled rocket tips could belong to any of a number of classes of intracellular vesicle. Given the fact that both annexin II and actin have been shown to associate with both secretory vesicles (for references see Table 1.5) and endosomal compartments (for references see Table 1.6) these seemed the most

likely candidates. While secretory vesicles in most cell types are relatively small (for example c.10-12 nm for the dense core granules of chromaffin cells; Kryvi et al., 1979) the secretory granules of RBL cells are considerably larger, up to 1.5 μm (Spudich and Braunstein, 1995), and are thought to represent a specialized form of secretory lysosome (Xu et al., 1998). Furthermore since intergranule fusion had been observed under the experimental conditions employed it was possible that extremely large secretory vesicles had been generated. These vesicles could also have endosomal origins since endosomal compartments range in size from 70-100 nm (clathrin coated vesicles) (Bomsel et al., 1988) through to 1 μm or more (macro-pinosomes) (Casey et al., 1986) and, significantly, the incidence of vesicle generation was found to be strongly stimulated by PMA.

To identify the vesicles at the tips of rockets this part of the investigation progressed in several stages. Firstly, given that fixation and staining of cells enables a much greater range of probes to be used, the preservation of rocket tails was investigated following fixation. Since GFP-actin heavily labels rocket tails in live cells, and given the precedent set by actin tails associated with *Listeria*, *Shigella*, *Rickettsia* and *Vaccinia* it was likely tails would stain for F-actin in fixed specimens. This assumption was used as the basis to test a variety of fixation/permeabilisation protocols. Chemical fixation preserved actin tails which could be subsequently stained using rhodamine-phalloidin while methanol, acetone or ethanol fixation did not preserve these structures (data not shown). Subsequent refinement of the chemical fixation protocol demonstrated that introduction of fixative to the specimen at 37^{0}C, followed by rapid cooling to room temperature gave the most consistent results.

Since it is considerably easier to specifically label endosomes than secretory vesicles, the first experiments were designed to eliminate this class of compartment from the investigation. RBL cells express the FcεR1 receptor for IgE at high levels and fluorescently labeled IgE can be prebound to this receptor at the membrane surface and used to follow endocytosis stimulated by PMA (Ra et al., 1989). By labeling IgE with a suitable marker (Alexa 568, Molecular Probes) and staining F-actin with FITC-phalloidin both endosomes and F-actin could be visualised in single cells stimulated to produce rockets (Figure 4.7).

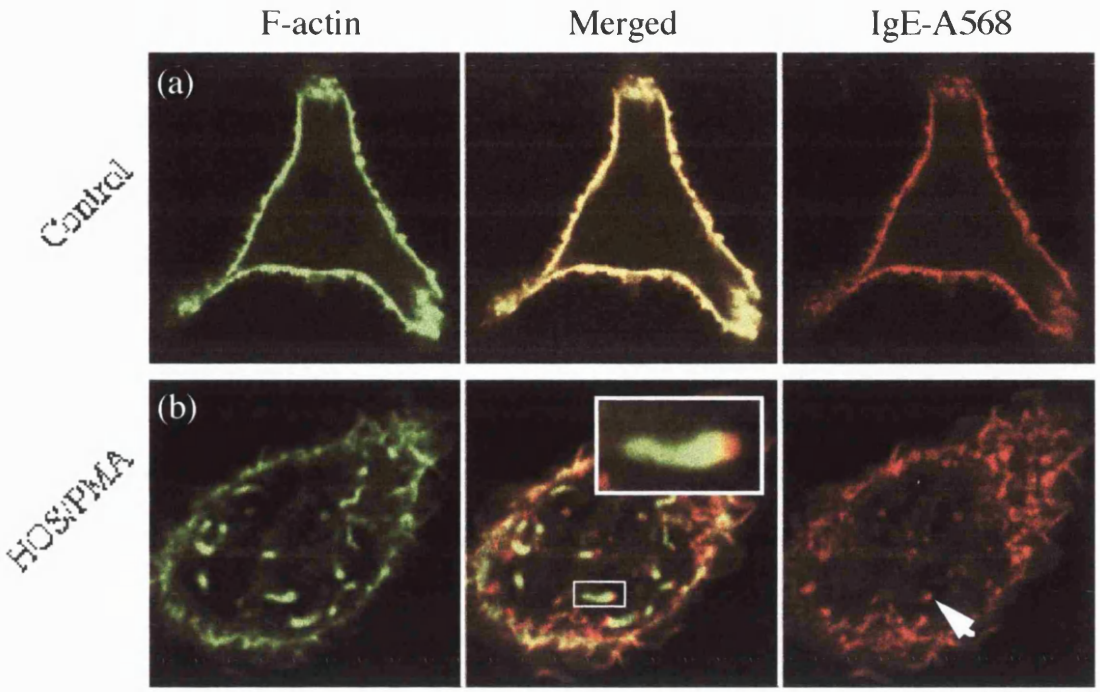

Figure 4.7: Rockets are composed of F-actin and are nucleated at the surface of endosomes.

RBL cells were incubated with IgE-A568 to label the FCεR1 receptor at the plasma membrane surface. (a) At the resolution of the confocal microscope IgE-A568 fluorescence colocalises with F-actin at the cell cortex and is not found deeper in the cell cytoplasm. (b) On stimulation with (+)150 mM sucrose and 10 nM PMA (HOS/PMA) for 45 min IgE-A568 is internalised in endosomal strucutures (arrow) while the actin cytoskeleton reorganises into "comet tails" trailing behind IgE-A568 labeled endosomes (inset). These structures are found dispersed throughout the cell cytoplasm.

This result illustrates two points. Firstly the vesicles at the tips of rocket tails are a type of endosome (probably of pinocytic origin). Secondly, the actin in the tail is polymerised into filaments since it is stained by phalloidin (Lengsfeld et al., 1974) and phalloidin does not bind other forms of polymerised actin such as actin paracrystals which form previously described 'actin rods' (Nishida et al., 1987).

To confirm that all rocket tails were nucleated at the surface of endosomes a number of IgE-A568 labeled, stimulated, fixed and FITC-phalloidin stained cells were imaged using confocal microscopy. Of 80 rockets seen in 50 cells 98% were associated with clearly labeled endosomes confirming F-actin rocket tails are nucleated at the surface of endosomes. The small percentage of unlabeled rocket tips may be due to the dynamics of PMA induced FcεR1/IgE-A568 internalisation. With time, the relative concentration of FcεR1/IgE-A568 at the cell surface will decrease, reducing the amount of label associated with newly formed endosomes. Indeed it was noted that apparently unlabeled rocket tips

were seen in cells with unusually low plasma membrane FcεR1/IgE fluorescence (data not shown).

Although these results demonstrate that the vesicles seen at the tips of rockets are endosomes it does not provide information concerning the relative age of these endosomes or demonstrate where during endocytosis the rocket tails are formed. These two questions were addressed in the following experiments.

4.4 Investigation of rocketing half-life.

Although the results using IgE-A568 demonstrated conclusively that an endocytic compartment initiates F-actin rockets this method of labeling does not give any clues as to the age of the compartment since it takes at least 20 minutes for cells to initiate rocketing (data not shown). To resolve this question a series of experiments were designed to investigate the uptake and incorporation of fluid phase markers into rocketing endosomes.

Initially a fixable lysine-substituted dextran was used as a fluid phase marker to label endosomes. Cells were pulsed for variable times, washed in buffer, fixed and stained for F-actin. Although this protocol labeled endocytic compartments in stimulated cells no colocalisation between the marker and F-actin labeled tails was seen irrespective of the incubation time with fluid phase marker (Figure 4.8). However, it was noted that this protocol introduces a brief interval between labeling of even the 'youngest' endosomes and fixation, since the specimen was washed clean of dextran before fixation, a process taking several minutes. Hence any endosomes younger than this interval would not be labeled.

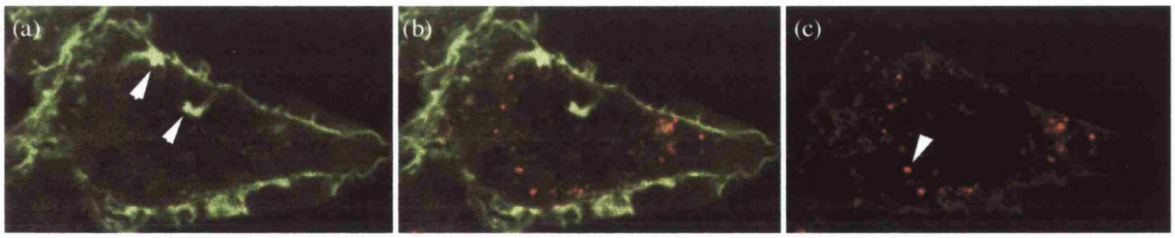

Figure 4.8: Rapid pulse labeling of endocytic compartments followed by chemical fixation fails to label rocketing pinosomes.

Wild-type RBL cells were stimulated to produce rocketing endosomes using HBS supplemented with 150 mM sucrose and 10 nM PMA for 20 min. For the last 5 min cells were exposed to 4 mg/ml lysin substituted TRITC-dextran. After a 2 minwash cells were fixed in 3.7% formaldehyde and stained for F-actin with FITC-phall. before imaging by confocal microscopy. (a) F-actin rockets (arrows) are visible in the cytoplasm of this representative cell. (b)(c) TRITC-dextran is retained in intracellular early-endocytic compartments but does not colocate to the tips of F-actin rockets (b).

To reduce this time interval live RBL cells expressing NAII-GFP were stimulated to induce rocketing vesicles on the EWM and then pulse labeled with FITC-dextran *in situ* using rapid perfusion. Since the vesicles at the tips of rockets normally appear black against the fluorescence of NAII-GFP in the cytoplasm any FITC-dextran labeled vesicles should be differentiated from unlabeled vesicles on the basis of their bright fluorescence. This technique does indeed label endocytic compartments, which are presumed to be macro-pinosomes on the basis of size and confinement to actively ruffling domains of the cell (Figure 4.9). FITC-dextran does not generally label the vesicle at the tips of rockets even though rockets consistently appear shortly after wash-out of the fluid phase marker. Despite the fact that this experiment was repeated twenty times, only three (possible) labeled rocket tips were seen within 60 s of wash-out.

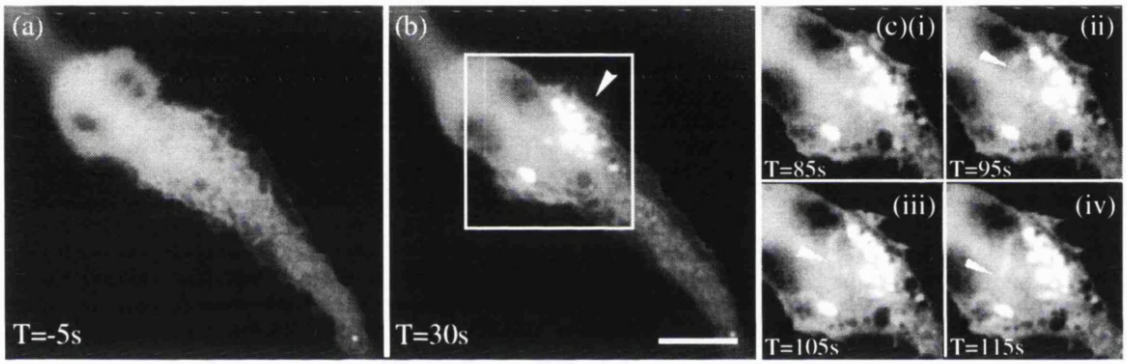

Figure 4.9: Rapid pulse labeling *in situ* with FITC-dextran does not generally label the tips of rocketing vesicles.

RBL cells, transiently expressing NAII-GFP, were stimulated to produce rocketing pinsomes *in situ* by hyperosmotic shock. (a) A cell was chosen, pulsed with 2 mg/ml FITC-dextran for 30 s before switching perfusion stream to HBS/sucrose at T=0 s to wash away external FITC-dextran. (b) 30 s after switching streams fluorescence background is low enough to visualise the NAII-GFP and newly labeled endocytic compartments (arrow). These are presumed to be macro-pinosomes on the basis of size, speed of appearance and confinement to actively ruffling domains of the cell. (c) A short time later rockets appear (arrow) in this region of the cell. The tips of these rockets are not labeled with FITC-dextran and hence these rocketing endosomes must have formed within the last 95s.
Scale bar: 10 μm

Together these results suggested that the vesicles at the tips of rockets were either generally older than five minutes, or younger than a minute. To completely eliminate the interval between exposure to fluid phase marker and visualisation of rocketing endosomes a dual channel experiment was designed to image labeled pinosomes and GFP-actin labeled rocket tails *in situ*. Cells expressing GFP-actin were stimulated to produce rockets on the

stage of a confocal microscope in the presence of 4 mg/ml TRITC dextran. This allowed the visualisation of all labeled pinosomes, irrespective of their age (Figure 4.10).

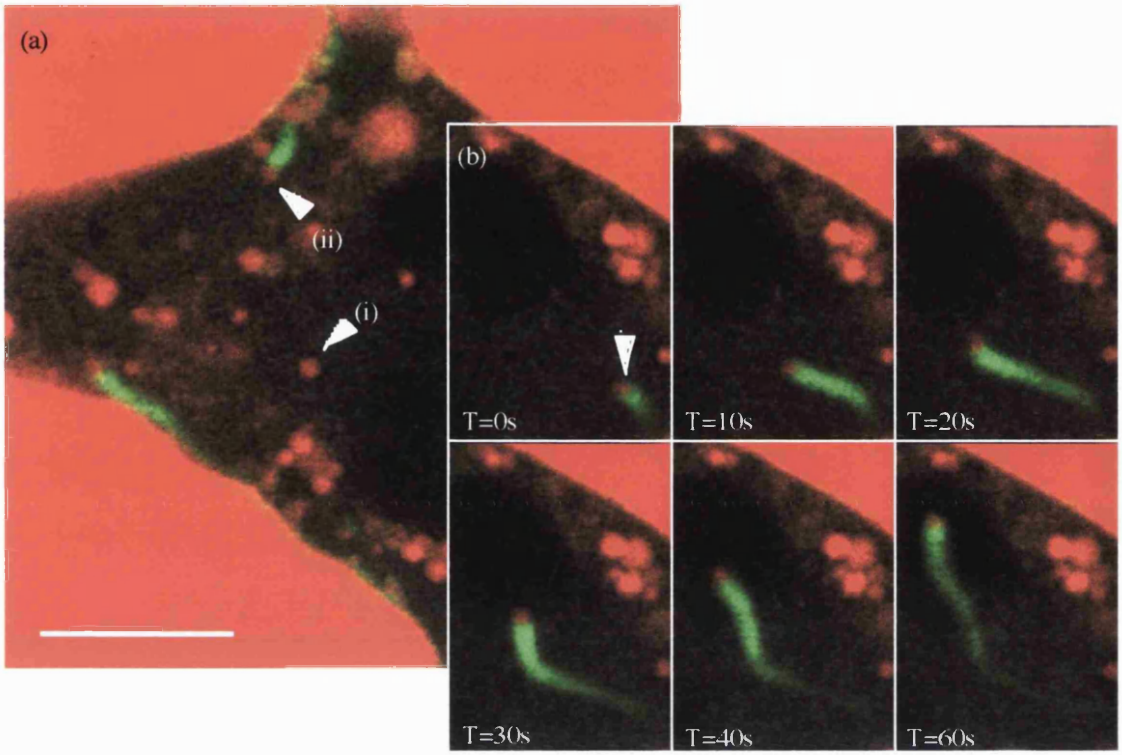

Figure 4.10: Dual wavelength imaging of GFP-actin and TexasRed dextran in living RBL cells stimulated to produce rocketing pinosomes.

RBL cells, transiently expressing GFP-actin, were stimulated to produce rocketing pinosomes by challenging with HBS supplemented with 150 mM sucrose and 10 nM PMA at 37^{0}C for 20 min. Endosomes were labeled *in situ* using 4 mg/ml TRITC-dextran. (a)(i) Labeled pinosomes appear as red dots against a dark cytoplasmic background. (ii) Rocketing pinosomes trailing a bright fluorescent plume of GFP-actin can be seen migrating through the cytoplasm. (b) Time resolved montage of a single rocketing endosome caught moving in the confocal plane. For full sequence see Movie 4.10, accompanying CD.
Scale bar: 10 μm

By labeling endosomes with a fluid phase marker in this way it was found that essentially all rocketing endosomes were labeled (62 rocket tips labeled out of 69 rockets imaged in 7 cells). A number of rockets were scored as 'unlabeled' since no tip was clearly imaged. This was to be expected since at the acquisition rate of one frame every five seconds there is ample opportunity for the pinosome at the tip of a rocket to pass through the confocal plane without being imaged while the longer and persistent tail will be recorded. Rocketing pinsosomes comprised a minority of the total population of labeled pinosomes (20.4% +/- 6.2%) consistent with their short half-life.

Taken together these results using fluid phase markers and a variety of labeling protocols suggest that rocketing endosomes are a very 'early' endocytic compartment, generally less than 90 seconds old. This is consistent with the observation that individual rockets have not been imaged for longer than 3 min by EWM crawling around adjacent to the plasma membrane in the plane of the coverslip. On the basis of size, the fact that the incidence of rocketing endosomes is strongly stimulated by PMA and their labeling with a fluid phase marker it was proposed that a more precise definition of rocketing endosome would be 'rocketing macro-pinosome'. This view was substantiated by direct visualisation of the initiation of rocketing endosomes at the plasma membrane, as described in the following section.

4.5 The initiation of endocytic rocketing and rocket polarity.

Dual colour imaging of fluid phase marker and GFP-actin *in situ* revealed important clues as to the 'ignition' point of rockets. Deconvolution of dual colour image sequences allowed rocket formation to be followed through cup formation through to rocket initiation (Figure 4.11).

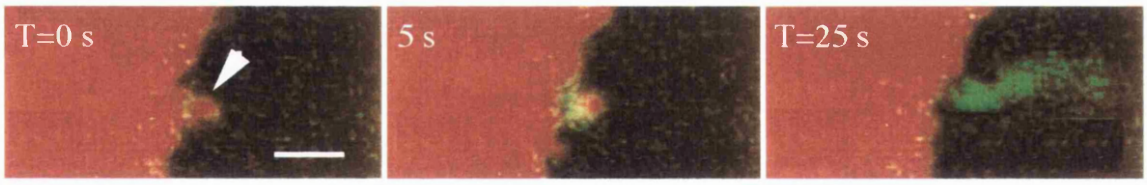

Figure 4.11: Actin rockets ignite during pinosome formation.

Deconvolution of time resolved confocal image sequences revealed that GFP-actin is recruited to the surface of newly formed macro-pinosomes during macro-pinocytosis at the plasma membrane. (a) A pinocytic cup (arrow) is seen in section engulfing a portion of TRITC-dextran labeled buffer (red). (b) During budding, or immediately after, GFP-actin (green) is recruited to one pole of the newly formed macro-pinosome. (c) Sustained actin polymerisation launches the pinosome into the cytoplasm leaving a characteristic rocket tail (arrow).
Scale bar: 1μm

The formation and closure of a relatively large cup, engulfing fluid at the membrane surface is diagnostic of macro-pinocytosis (see Araki et al. (1996) and references therein) affirming the previous assumption. Critically, this result clearly demonstrates that the initiation of rocketing occurs at, or immediately after, macro-pinocytic cup closure. To confirm these *in vivo* findings the orientation of fixed and stained rocket tails in cells labeled with IgE-A568 was investigated. If rockets ignited deep in the cell one would

expect them to impact at the plasma membrane at random angles, whereas if they ignite at the plasma membrane they should be oriented with the posterior end of the tail addressing the plasma membrane at angles closer to 90^0. To test this hypothesis the angles rocket tails make with the plasma membrane were measured for 50 cells (Figure 4.12).

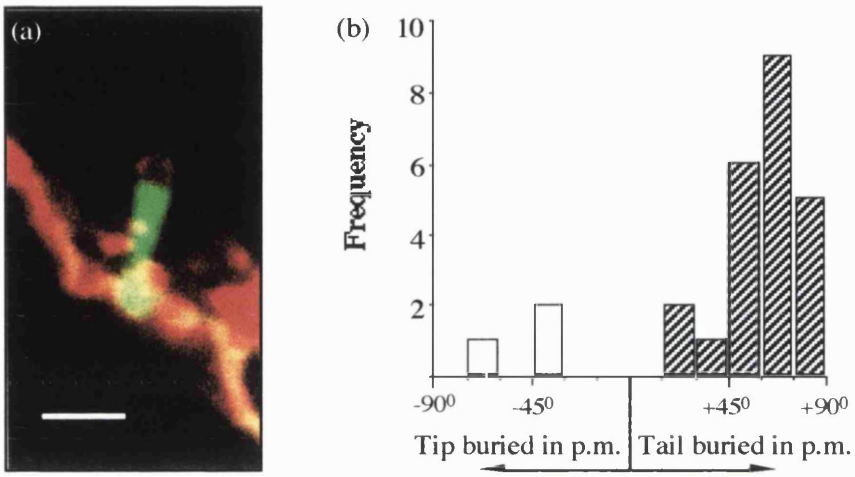

Figure 4.12: The angles made by rocket tails and the plasma membrane.

(a) Wild-type RBL cells were sensitised with IgE-A568 (red) before being stimulated to produce rocketing macro-pinosomes using a combination of hyperosmotic shock and PMA. Cells were chemically fixed and counterstained for F-actin (green) and analysed by confocal microscopy (see Materials and Methods). (b) The angle made between the long axis of the rocket tail and the plasma membrane was scored for all rocket tails clearly contacting the cell surface. In 50 cells analysed 78 out of 84 actin tails were clearly tipped by labeled pinosomes of which 29 were found contacting the plasma membrane. The majority of rocket tails contacting the plasma membrane are oriented pointing away from the plasma membrane at angles close to 90^0, as though they had just launched.
Scale bar: 2 μm

This result demonstrates that rocket tails are most often oriented as if they have just left the plasma membrane, confirming the results *in vivo* and suggesting that rockets 'ignite' at the plasma membrane and launch newly formed pinosomes deeper into the cell. A better idea of the trajectories taken by rocketing pinosomes was gained by 3-D image reconstruction of rhodamine-phalloidin labeled rocket tails in fixed cells. This suggested that rocketing pinosomes imaged by EWM descend into the evanescent wave before crawling along the base of the cell in the plane of the coverslip (Figure 4.13, overleaf).

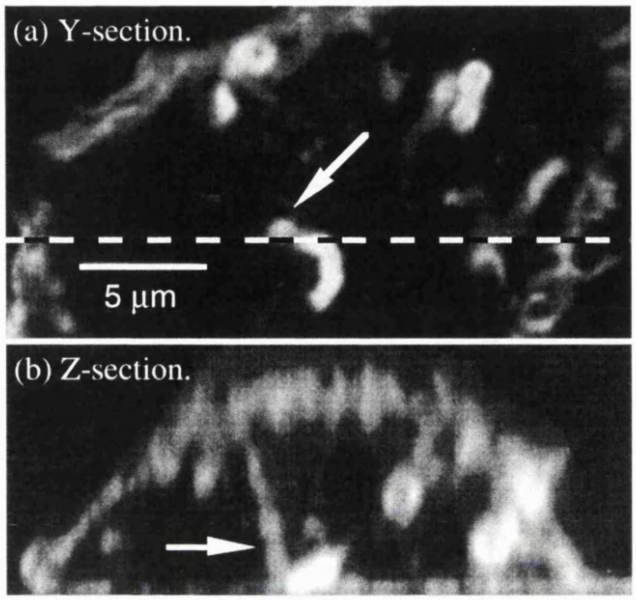

Figure 4.13: 3-D image reconstruction of tail trajectory in fixed cells.

Wild-type RBL cells were stimulated to generate rocketing macro-pinosomes using hyperosmotic shock and PMA, fixed and stained for F-actin using TRITC-phalloidin. (a) Y-section 1 µm above the lower surface of the cell shows F-actin rocket oriented in the plane of the coverslip. (b) Z-section along dashed line in (a) reconstructed from the corresponding stack (63 optical sections made at 200 nm intervals). The arrow indicates the F-actin tail in (a).

Taken together these observations lend some weight to the hypothesis that rocketing is initiated at the surface of the cell and propels the newly formed pinosome from the cell surface deeper into the cytoplasm. Furthermore these data provide insight into the mechanism responsible for macro-pinocytic rocketing.

The polarity of rocketing *Listeria* is thought to arise through cell division leading to unequal distribution of factor(s) necessary for the nucleation of actin on the surface of the bacteria (Smith et al., 1995; Tilney et al., 1992). This cannot apply to rocketing pinosomes or other rocketing vesicles where polarity must arise through some other mechanism. On the strength of previous findings it seems likely that rocketing pinosomes derive their polarity from the process of budding at the plasma membrane. In this model the actin polymerisation machinery driving the lips of the pinocytic cup close is deposited at the navel of the newly formed pinosome where it organises an actin tail (Figure 4.14, overleaf).

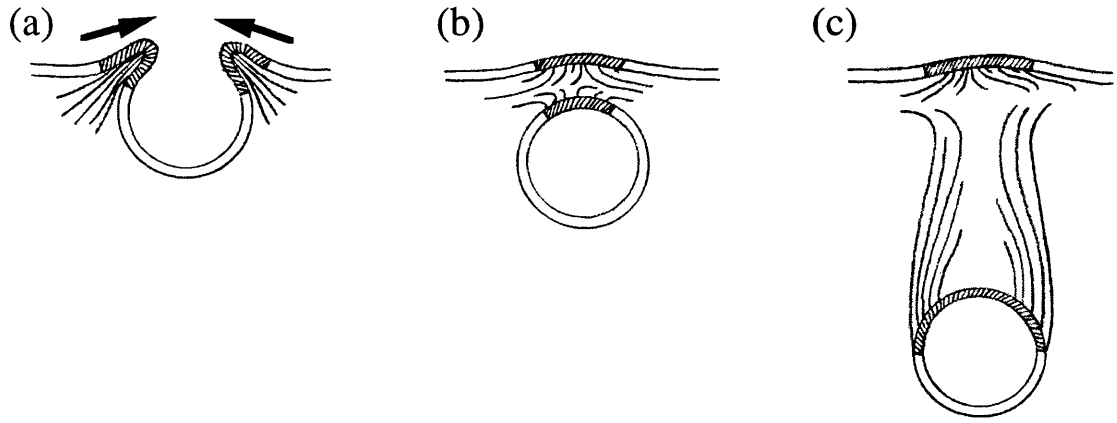

Figure 4.14: How macro-pinocytic rockets might be formed during macro-pinosome formation.

A circular ruffle forms by controlled actin polymerisation. This engulfs a volume of fluid as actin polymerisation, nucleated at the crest of the ruffle (hatched) drives the neck of the cup closed (a). As the neck of the newly formed pinosome pinches close, the molecular machinery driving actin polymerisation is passed on to the newly formed pinosome at one pole (b). Continued actin polymerisation at the pinosome surface results in the organisation of a polarised rocket tail (e).

Since several protein and lipid kinases have been implicated in the process of macro-pinocytic cup formation and closure it was possible to test this model directly (Keller, 1990; Phaire-Washington et al., 1980; Swanson, 1989; Swanson et al., 1999). This is explored in more detail in Chapter 5. It should be noted that although the majority of rocketing macro-pinosomes apparently initiate shortly after formation, exceptions were recorded. Two types of episode were observed. In the first type of episode newly formed pinosomes recruited GFP-actin to their surface shortly after formation but fail to form rocket tails (not shown). In the second type of episode, macro-pinosomes, seen as separate entities in the cytoplasm, had recruited GFP-actin to their surface in an un-polarised halo, but apparently polarised and formed rocket tails spontaneously (for instance see Figure 4.18, p 125). Thus, while this working model (Figure 4.14) might explain the origins of most rocketing vesicles, there are qualifications.

4.6 Kinetic analysis (I): The speed of rocketing pinosomes.

To characterize the motion of rocketing macro-pinosomes, image sequences showing GFP-actin labeled rocket tails were recorded using EWM and analysed using Metamorph 3.0. Rocketing macro-pinosomes moved at 0.24 μm/s +/- 0.10 μm/s at 37^{0}C (+/- SD, 699 measurements on 126 actin tails in 9 cells), and a frequency plot of instantaneous speeds showed a peak at 0.2 - 0.25 μm/s (Figure 4.15). Comparable values

have been published for Listeria (0.23 μm/s, 37°C; Smith et al., 1996) and Shigella (0.1 μm/s, 37°C; Zeile et al., 1996) demonstrating that actin tails propel cargo at similar speeds in different cells, whether they be macro-pinosomes or intracellular viral or bacterial pathogens.

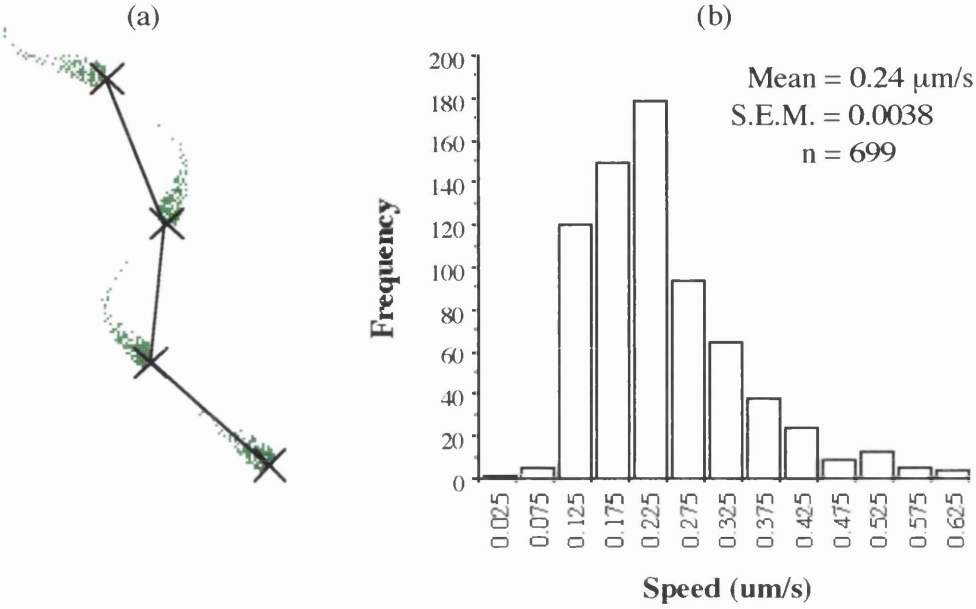

Figure 4.15: Rocketing pinosomes move at similar speeds to intracellular bacterial pathogens.

RBL cells were transiently transfected with GFP-actin and stimulated to produce rocketing pinosomes using HBS (+)150 mM sucrose and 10 nM PMA at 37°C on the Evanescent Wave Microscope. Images were acquired every 5 s. (a) Using the tracking facility in Metamorph the linear displacement of the tip of rocketing pinosomes between successive images in an image stack was measured. Speed is calculated simply as linear displacement/frame rate. Note that this analysis will tend to underestimate the speed of rocketing pinosomes which move on curved trajectories. (b) All non zero values were pooled and plotted. The modal speed of rocketing pinosomes coincides with the published average speed of rocketing *Listeria* at 0.23 μm/s. A minority of pinosomes show exceptionally rapid displacements of up to 0.6 μm/s.

The similarity between the speeds of intracellular bacteria and rocketing pinosomes suggests that the mechanism of actin polymerisation driven motion is similar in both instances. However, some characteristics of macro-pinocytic rocketing appear to be unique, such as 'actin puffs' occasionally associated with the termination of rocketing.

4.7 Termination of rocketing and actin puffs.

While rocketing macro-pinosomes and *Listeria* are kinetically indistinguishable in terms of speed, there is one notable difference between the two phenomena. While *Listeria* have been recorded rocketing for up to 30 minutes *in vivo* (Nanavati et al., 1994) rocketing macro-pinosomes clearly stop as though the machinery responsible for actin polymerisation was suddenly switched off (for instance see Figure 4.1, p 104). A novel phenomenon was observed in relation to this process. On stopping, a minority of GFP-actin decorated rocketing pinosomes stop, grow dim and form the epicentre for a diffuse 'puff' of GFP-actin accumulation (Figure 4.16, overleaf).

The basis of this phenomenon is not known. The appearance of GFP-actin accumulation during tail formation and the formation of actin puffs were distinctly different and hint that different mechanisms underlie the two phenomena. Recent investigations using GFP-actin in live cells have also reported 'actin clouds' (Ballestrem et al., 1998) which are superficially similar to actin puffs, though there are no reports associating actin clouds with intracellular vesicles. A speculative explanation is that actin puffs represent the discharge of macro-pinosome luminal Ca^{2+}. Although this was not investigated further it is not unlikely, since biochemical investigations have demonstrated fluid-phase endocytosis may contribute up to 20% of Ca^{2+} uptake into cells (Fernando and Barritt, 1996).

In conclusion, while *Listeria* and macro-pinocytic rockets are indistinguishable in terms of speed, there are aspects of the latter phenomenon which appear to be unique. To make an informed comparison of the two phenomena required additional information. For instance there is good evidence that the actin polymerisation at the surface of *Listeria* and formation of an associated tail is responsible for force generation and bacterial propulsion (for review see Cossart, 1998). Can the same be said of macro-pinocytic rockets?

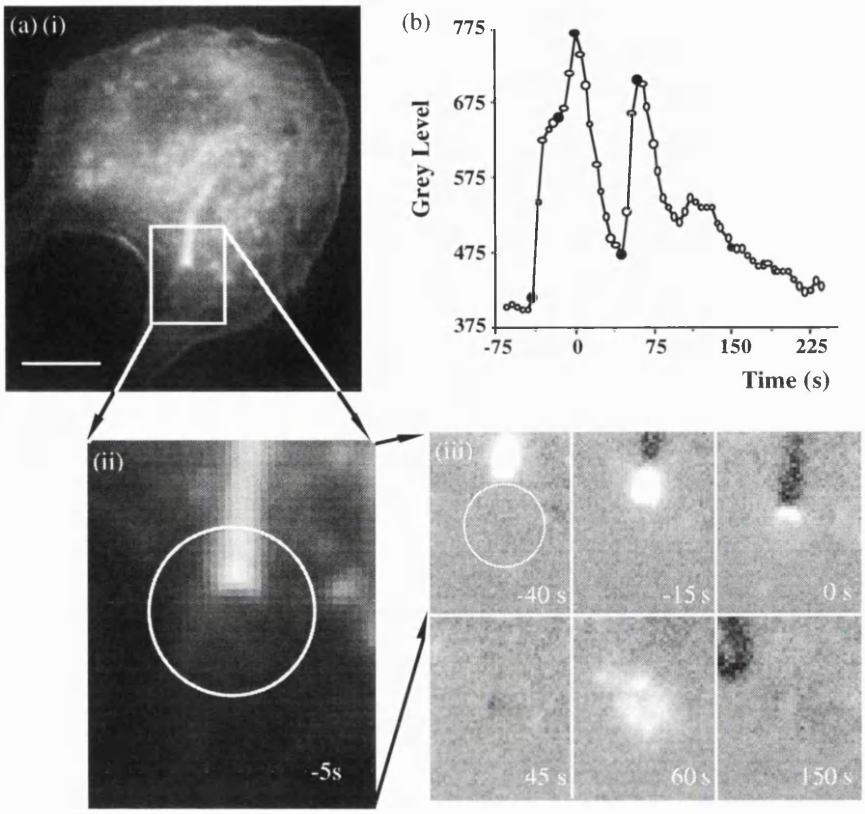

Figure 4.16: A burst of actin polymerisation may follow arrested rocketing.

(a) Pinosome rocketing was stimulated in cells transiently expressing GFP-actin using hyperosmotic shock and PMA and images acquired using EWM at an acquisition rate of 1 fram every 5 s. (i). A rocket which came to rest in a relatively clear area of cytoplasm has been chosen for analysis (ii). The image sequence of this area was processed to produce a differential image sequence* to emphasise fluctuations in fluorescence levels (iii). Arrival of the rocketing pinosome in the region of interest (white circle in (a)(ii)) at T=0 s produced an inital peak in average fluorescence in this area (b) followed by decay of the polarised actin tail as the pinosome draws to a halt. A transient, unpolarised burst of actin polymerisation occurs 60 s later around the now static pinosome (white cloud in at T=60 s in (a)(iii), second peak in (b)). Filled circles in (b) correspond to frames in (iii). Refer to Movie 4.16 for full sequence, appending CD.
Scale bar: 10 μm,

* **Differential images** show the difference in fluorescence between two successive images of a sequence. Pixels with a neutral grey value (mid-tone) have changed relatively little between successive frames, pixels with higher values (white) have become brighter and images with lower values (dark) have become dimmer.

4.8 Evidence that rocketing generates the force for motion.

Elegant studies on the life cycle of *Listeria* have demonstrated that vectorial intercellular migration occurs through formation of protruberances at the cell surface of infected cells, tipped by a single bacteria, which becomes engulfed by neigbouring cells (Temm Grove et al., 1994). This phenomenon is dependent on actin polymerisation since an isogenic *Listeria* mutant that is unable to recruit actin filaments cannot colonize polarised epithelial cell layers (Temm Grove et al., 1994). Since the plasma membrane is under tension (Dai et al., 1997) the ability of *Listeria* to to evaginate the plasma membrane after impact at an appropriate angle is consistent with actin polymerisation delivering an axial force to the bacteria.

A similar argument for force generation can be applied to rocketing pinosomes since these can also evaginate the plasma membrane when they impact at an angle close to 90^0 (Figure 4.17). No such thick, actin rich filapodia were seen in the absence of rocketing macro-pinosomes.

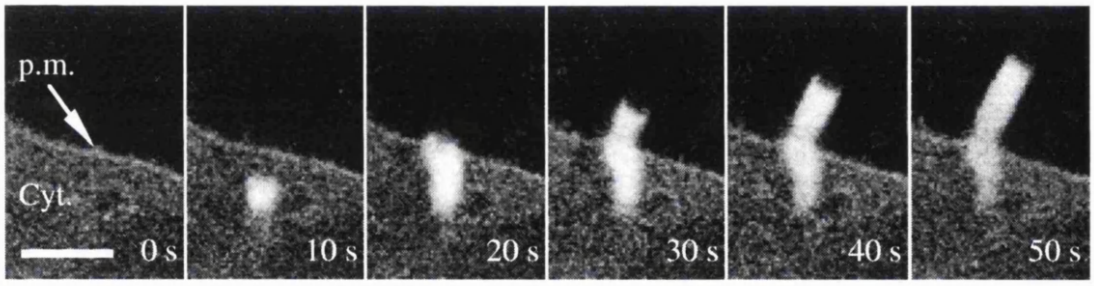

Figure 4.17: Rocketing generates sufficient force to evaginate the plasma membrane.

RBL cells, transiently transfected with GFP-actin, were imaged using confocal microscopy at 37^0C as detailed in Materials and Methods and stimulated with hyperosmotic shock and PMA to generate intracellular rockets. A minority of rockets moving through the cytoplasm (cyt) strike the plasma membrane (p.m.) at angles close to 90^0 forming a projection. This suggests that the vesicle at the tip of the rocket is being driven with a significant force.

The kinetics of *Listeria* and endosomal rocketing appear to be very similar and it seems highly probable that actin polymerisation plays a central role in force generation in both systems. However, how actin polymerisation can be transduced into an axial force is not clear - a feature made apparent by an examination of current models designed to explain actin polymerisation dependent locomotion.

4.9 Models to explain actin polymerisation driven locomotion.

Investigation of the actin based locomotion of intracellular pathogens has provided valuable insight into the molecular mechanisms underlying the induction of actin polymerisation and motility. Common themes have become apparent in the mechanisms employed by these organisms to control actin polymerisation (for example, see Purich and Southwick, 1997). *Listeria* is perhaps the best understood system where a series of actin-binding proteins including ActA, VASP, profilin and Arp2/3 interact in a cascade to sequester, concentrate and polymerise monomeric actin at the bacterial surface (Cossart, 1998). Although it is clear that these interactions serve to promote actin polymerisation at the surface of *Listeria* they provide little insight into the mechanism by which actin polymerisation is actually transduced into movement.

The problem of harnessing actin polymerisation into useful work is illustrated by the following paradox. To add a monomer to the tip of a growing actin filament there must be sufficient gap to accommodate the monomer, suggesting the cargo must move away from the tip of the actin filament before the filament can grow. Yet to move force must be delivered to the cargo, which is presumed to arise through actin polymerisation. Recent attempts to tackle this problem are embodied in the so called "Brownian ratchet model".

In its earliest form this model proposed that a polymer, by adding monomers to its growing tip, could rectify the free diffusive motions of an object in front of it (Peskin et al., 1993). This process produced an axial force by employing the free energy of polymerization to render unidirectional the otherwise random thermal fluctuations of the cargo. The model assumed that the collinear polymer was infinitely stiff, and so the Brownian motion of the load alone created a gap sufficient for monomers to intercalate between the tip and the load. Consequently this model predicts that velocity will depend on the size of the load through its diffusive coefficient. However, *Listeria*, *Shigella* and pinosomes move at similar speeds despite their very different sizes. Also, actin filaments do not address loads as collinear arrays in biological situations. For example, the actin network at the leading edge of lamellipodia is organized into an approximately orthogonal network (Small et al., 1995; Stossel et al., 1984).

Refinement of the Brownian ratchet model by Mogilner et al (1996) sought to address this problem. In particular, generalization of the Brownian ratchet model allowed inclusion of the elasticity of the polymer and relaxation of the collinear structure of growing tips. In this "elastic Brownian motion" model thermal fluctuation of the actin filaments (rather than the cargo) is rectified by addition of monomers, transmitting a small amount of force to the cargo. Increasing cargo size is accommodated by an increase in the number of attendant actin filaments, explaining why very different sized cargoes can be propelled at similar speeds. An important feature of this model is the finding that the angle at which the growing actin filaments address the cargo is critical. In particular, if too close to

perpendicular there will be insufficient tip displacement to allow monomer addition thus accomodating the orthoganol arrangement of actin filaments at membrane surfaces. It was interesting to note that some aspects of macro-pinocytic architecture are not readily explained by this model, as discussed in the following section.

4.10 Substructure of rocket tails.

On occasion, exceptionally large diameter rocket tails were visualised forming in cells expressing GFP-actin using confocal microscopy. Pinosomes were labeled using TRITC-dextran and the resulting sequences revealed two architectural features which would have otherwise gone un-noticed. Firstly during tail formation and the initiation of rocketing it was noted that the pinosome at the tip of GFP-actin rockets became deformed as though being squeezed by the attendant tail. Secondly it was found that the actin tails trailing behind rocketing pinosomes were hollow (Figure 4.18, overleaf). Although only rarely seen in living cells this seemed to be a general feature of tail architecture since large diameter rocket tails observed using confocal microscopy in fixed, phalloidin stained cells were also hollow (result not shown).

The observation that large pinosomes become deformed as though being squeezed by actin tail was surprising. This finding has been partially clarified by recent investigations of the forces generated in rocketing *Listeria* (Gerbal, personal communication). This investigation employed direct micromanipulations to deliver defined loads to actively rocketing bacterium and their actin tails *in vitro*. Quantitative analysis of the resulting image sequences established an unexpected feature of *Listeria* rocketing. In contrast to theoretical predictions of 'Brownian ratchet' models the *Listeria* at the tip of an actin rocket was found to be firmly attached to its tail. A firmly attached actin meshwork would not be capable of delivering a force through thermally rectifying Brownian motion of either the cargo or actin filaments and would only be able to exert an elastic force on the bacteria. From these findings Gerbal et al concluded that a force, generated via actin polymerisation, compresses the actin meshwork at the surface of (and exerts a stress on) rocketing *Listeria*. As this force encounters the curved tail end of the bacteria this compressive force is translated into an axial force. Since the zone of compression itself will advance with continued actin polymerisation the result is smooth directed locomotion. While *Listeria* would not deform since they possess a rigid bacterial wall, a similar mechanism would explain the deformations observed in large rocketing pinosomes (Figure 4.19, overleaf). A good analogy of this mechanism is that of squeezing a (wet) soap bar - the compressive load of grasping is very quickly translated into motion of the soap. In the model proposed by Gerbal et al the force responsible for deforming the actin mesh at the surface of *Listeria* is proposed to come from actin polymerisation. How this occurs is not clear. An additional

possibility, not suggested by Gerbal et al, is that remodelling of the actin meshwork itself is responsible for generating this force and that actin polymerisation does not generate force directly at all.

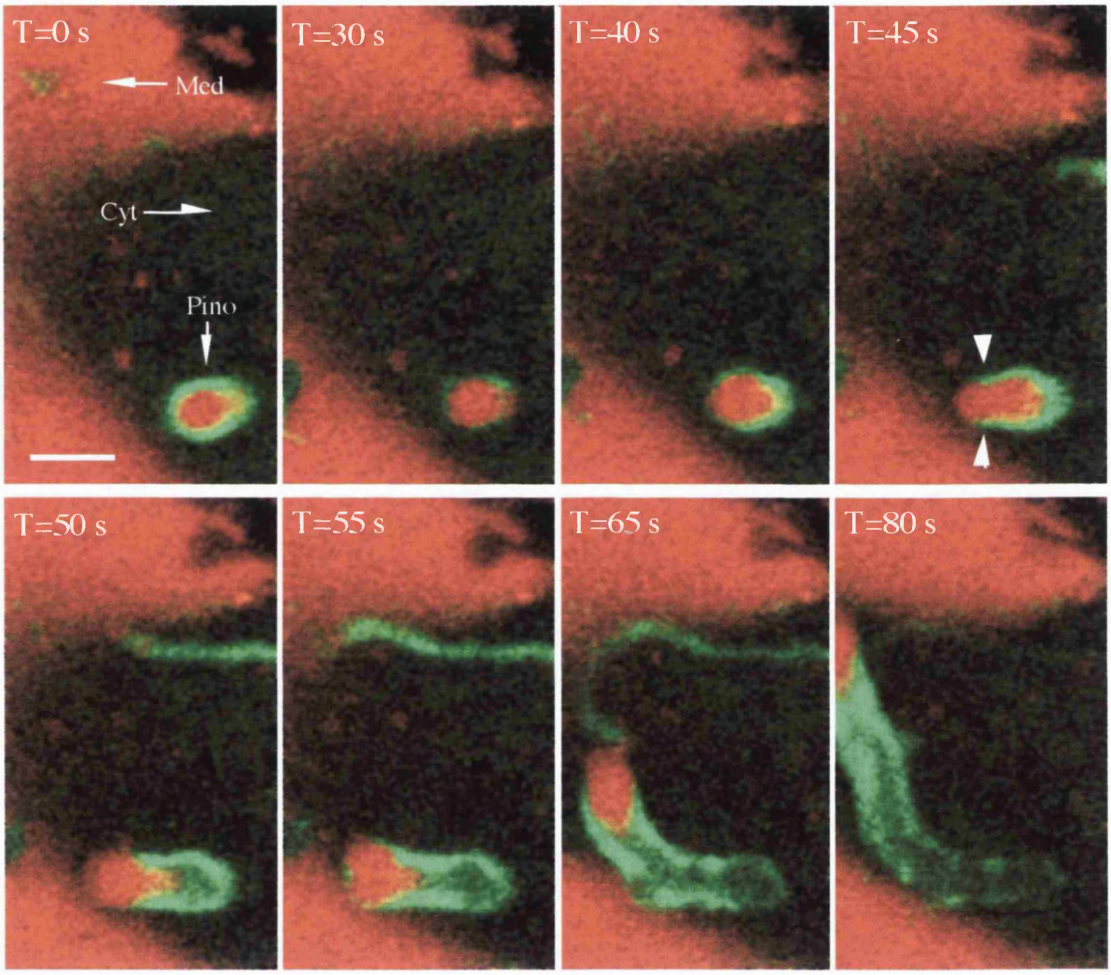

Figure 4.18: Rocket tails can be hollow.

RBL cells expressing GFP-actin were stimulated to form rocket tails in the presence of 4 mg/ml TRITC-dextran and simultaneously imaged by confocal microscopy. The surrounding medium (Med) fluoresces strongly red as do labeled pinosomes (Pino.) while the cell cytoplasm (Cyt) appears dark. GFP-actin is associated with the surface of an exceptionally large (2 μm) pinosome in an unpolarised halo (T=0 s). After briefly dimming GFP-actin polymerisation recommences at one pole of the pinosome, generating a hollow tail. During the initiation of actin polymerisation (T=40 to T=45 s) the tail end of the pinosome is deformed as though being squeezed (arrows). This suggests the force delivered to the pinosome by the actin tail is not a simple axial load (see text for details). For full movie sequence refer to Movie 4.18 in the accompanying CD.
Scale bar: 2.5 μm

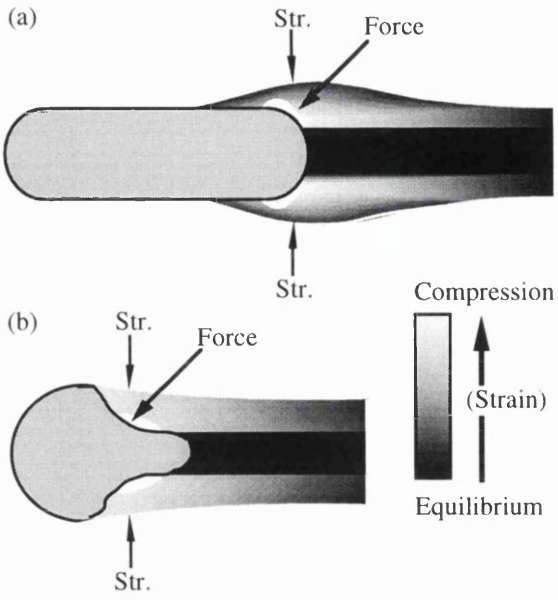

Figure 4.19: Compression and actin polymerisation driven locomotion.

During actin-polymerisation driven locomotion of (a) Listeria or (b) rocketing macro-pinosomes newly formed actin meshwork exerts a compressive stress (Str.) on the cargo. This compressive load is translated into an axial force driving locomotion through the geometry of the cargo and continued tail extension.

The second finding, namely the formation of hollow actin tails, is not without precedence since *Listeria* have also been reported to generate hollow tails (Tilney et al., 1992). These results were based on immuno-electron microscopic studies, and have been the subject of some dispute since other groups report that *Listeria* generated tails are in fact homogeneous in section (Zhukarev et al., 1995). Discrepancy between the results of several groups may have arisen through differences in fixation and/or preparation of specimens for electron microscopy, since rough handling may cause *Listeria* tails to collapse. This issue has not been clarified by visualisation of *Listeria* tails in living cells, probably because the tails have a relatively small diameter. Since the presence of hollow tails associated with rocketing pinosomes *in vivo* has now been recorded in real time this phenomenon cannot be dismissed as artefactual. Why should the actin tail be hollow? Tilney et al proposed that this may simply be dictated by the geometry of the cargo being propelled (see Figures 5, 6 and 7; Tilney et al., 1992) and argued as follows. If actin filaments elongated from the surface of a single *Listeria* without cross-links they would tend to grow radially. If on the other hand the filaments are cross-linked together as they elongate from the surface of the bacteria by cross-bridges of equal length, the filaments will aggregate. Since actin only nucleates on one half of a given bacterium, and fails to nucleate on newly septated wall, the cross-bridged filaments will tend to pull the meshwork of filaments distally. In this way the filaments can elongate from the bacteria while still maintaining the cross-links in the meshwork and thus generate the tail seen extending from the distal end of the bacterium. This argument may also apply to rocketing pinosomes.

4.11 Kinetic analysis (II): Comparison of the decay rates of GFP-actin and NAII-GFP in the tails of rocketing pinosomes.

The classic "comet tail" appearance of *Listeria* actin tails arises from the rapid incorporation of actin at the bacterial end of the tail followed by slower tail disassembly, giving tails their characteristic tapered shape (Theriot et al., 1992). Tail disassembly is thought to occur through F-actin depolymerisation, and cofilin has been shown to facilitate this process (Rosenblatt et al., 1997). Incorporation of fluorescently labeled actin (Nanavati et al., 1994; Theriot et al., 1992) and α-actinin (Nanavati et al., 1994) into *Listeria* tails both *in vitro* and *in vivo* has allowed the kinetics of tail disassembly to be analysed. This approach was adopted in the analysis of both GFP-actin and NAII-GFP decorated rockets and allowed a direct comparison of the kinetics of dissociation of these probes from macro-pinocytic rocket tails (Figure 4.20).

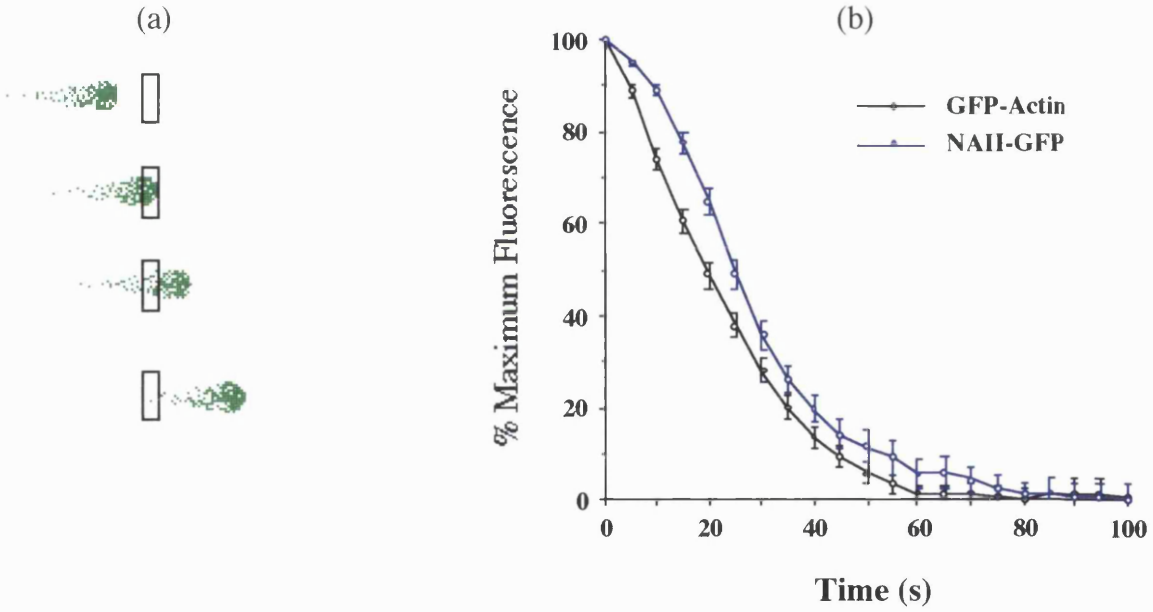

Figure 4.20: Comparison of fluorescence decay of GFP-actin and NAII-GFP labeled rocket tails.

Cells transiently transfected with either GFP-actin or NAII-GFP were stimulated to induce rocketing pinosomes using hyperosmotic shock and PMA at 37°C and images acquired using evanescent wave microscopy at a rate of one frame every 5 s. (a) To measure the changes in fluorescence within a rocket tail a region of interest (rectangle) was defined in the path of a rocketing pinosome and the average fluorescence within the region measured in successive frames. The resulting decay curves were then standardised to local background (as 0%) and peak fluorescence (as 100%) and averaged to give the plot above (b). Tails labeled with NAII-GFP show an initial delay in the onset of fluorescence decay (compare the initial slopes of the two lines). (n=25, points are average +/- S.E.M.)

In contrast to the variable results published for the decay rates of *Listeria* actin tails (Nanavati et al., 1994; Theriot et al., 1992), the decay rates of rocketing pinosome tails as measured using EWM are remarkably constant. This is probably due to the high signal:noise ratio of EWM images.

Comparison of the decay profiles of GFP-actin and NAII-GFP revealed that the two proteins dissociate from the tail with slightly different kinetics (t1/2 for GFP-actin = 21 s, t1/2 for annexin II-GFP = 26 s). In particular there is a slight but definite lag in the onset of NAII-GFP fluorescence decay. This could be for several reasons. Firstly it could indicate that NAII-GFP over-expression leads to modulation of the stability of the tail and retards (initial) disassembly. An alternative explanation is that NAII-GFP dissociation from the tail occurs through a different mechanism to that of actin, and that NAII-GFP is perhaps associated with another (cytoplasmic?) component. In theory these alternative models could be differentiated using simultaneous dual wavelength analysis of suitable fluorescent actin and annexin II probes in the same macro-pinocytic rocket tail. This would be technically challenging and was not pursued further.

4.12 The recruitment of NAII-GFP to rocket tails.

One of the most interesting questions regarding NAII-GFP targeting to macro-pinocytic rocket tails is that of recruitment. It could be that NAII-GFP association with the tails behind rocketing pinosomes simply reflects promiscuous actin binding by NAII-GFP. There are several reasons for disagreeing with this view. Firstly, in resting RBL cells F-actin forms a dense cortex and yet NAII-GFP was not enriched in the cortex of live RBL cells (Figure 3.2, p 83). Secondly, imaging of live RBL cells expressing GFP-actin using EWM revealed focal adhesions closely apposed to the plasma membrane, and yet similar structures were not seen in resting cells expressing NAII-GFP (compare micrograph (a)(ii), Figure 3.13, p 99, and micrograph (b), Figure 4.2, 106). Thirdly, cells expressing GFP-actin stimulated with PMA formed characteristic dense peri-plasmalemmal actin aggregates, as do wild type cells stimulated, fixed and stained with rhodamine phalloidin (not shown). Cells expressing NAII-GFP were never seen to form fluorescently labeled filaments or aggregates under the same conditions (compare micrographs (a) and (b), Figure 4.4, p 107).

At present there are several possible explanations for the concentration of NAII-GFP in the tails of rocketing pinosomes in living cells. The simplest explanation is that annexin II has a structural role, perhaps under the influence of Ca^{2+} since annexin II_2p11_2 requires μM Ca^{2+} to bundle F-actin *in vitro* (Hubaishy et al., 1995; Ikebuchi and Waisman, 1990; Jones et al., 1992). In this model annexin II is recruited to and cross-links newly formed filaments near the surface of the rocketing pinosome. Fluorescence decay of tail-

associated NAII-GFP reflects dissociation of NAII-GFP from F-actin during tail disassembly.

An alternative explanation is that the NAII-GFP seen in the tail may in fact be 'redundant', is not bound to actin at all and is simply confined in a dense meshwork of actin. In this model NAII-GFP is recruited to the macro-pinosome surface, is subsequently released and is left in the wake of the moving pinosome embedded in a dense meshwork of actin. Recruitment to the macro-pinosome surface could involve Ca^{2+}-dependent membrane binding, while dissociation from the membrane surface and actin might involve tyrosine phosphorylation (Figure 4.21).

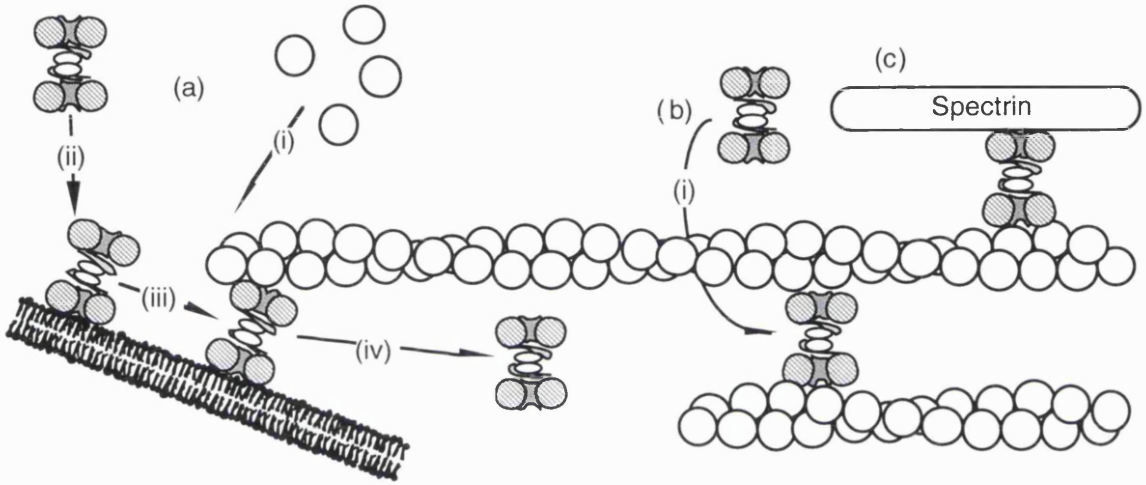

Figure 4.21: Possible role(s) of annexin II in actin tail biogenesis.

(a)(i) In an actively rocketing macro-pinosome actin continuously polymerises at the interface of the tail and pinosome surface. (ii) Annexin II tetramer could be recruited to the pinosome surface where it transiently binds newly polymerised actin (iii) and anchors it to the membrane. This link formed by the annexin II-tetramer between F-actin and the membrane surface is sensitive to phosphorylation by tyrosine kinases, which causes the annexin II tetramer to disengage from the membrane surface (iv), allowing actin polymerisation to drive the membrane away from the (static) actin tail in a nucleation/release mechanism. (b) In an alternative model annexin II may be recruited directly to the actin tail (i) and be involved in the internal stabilisation of the structure. (c) Alternatively annexin II could form a crossbridge between the outer shell of the actin tail and other cellular components, such as non-erythroid spectrin anchoring the tail within the local cytoplasm.

It is not entirely clear whether annexin II_2p11_2 could be recruited as indicated, since it is thought to be tightly anchored to the cortical cytoskeleton but this model (Figure 4.21) would be consistent with the *in vitro* findings that Ca^{2+}-dependent membrane- and actin-binding is abolished on tyrosine phosphorylation of annexin II (Hubaishy et al., 1995). Furthermore tyrosine phosphorylation of annexin II_2p11_2 is strongly stimulated by Ca^{2+}-

dependent membrane binding (Bellagamba et al., 1997; Glenney, 1985) suggesting a mechanism wherein annexin II could mediate the association and dissociation of F-actin and a membrane surface through sequential Ca^{2+}-dependent binding and tyrosine phosphorylation. Loss of NAII-GFP fluorescence from the tail would correspond to meshwork dissociation and release of NAII-GFP into the cytosol. An alternative scenario, not illustrated in Figure 4.21, would involve monomeric NAII-GFP being recruited to actin tails either Ca^{2+}-dependently or independently. However, since monomeric annexin II and F-actin have not been linked this seems less likely based on published evidence and it is not clear what role monomeric annexin II could perform in tail formation.

With this model in mind it is interesting that recent findings have established *Vaccinia* actin-dependent locomotion, but not *Listeria* or *Shigella* locomotion, is dependent on tyrosine phosphorylation (Frischknecht et al., 1999). Microinjection of an anti-phosphotyrosine antibody significantly reduced the incidence of *Vaccinia* nucleated F-actin rockets and was found to bind to the tips of actin tails, probably at the interface of the*Vaccinia* and actin. The identity of the tyrosine phosphorylated protein(s) located at the head of*Vaccinia* tails is currently unknown.

How can the models proposed in Figure 4.21 be differentiated? Employment of a chemical cross-linking assay *in situ* may provide clues. If NAII-GFP was firmly attached to F-actin in the tail then one might expect cross-linking to lead to retention of NAII-GFP in these structures. Alternatively, if NAII-GFP was only closely associated with other proteins at the tip of the rocketing pinosome (consistent with a 'recruitment-release' model) then one would expect the concentration of NAII-GFP to be higher at the macro-pinosome than in the tail.

Since chemical fixation with formaldehyde is extremely sensitive to intermolecular distance (Schwendeman et al., 1995) simple chemical fixation, permeabilisation and counterstaining of F-actin to identify tails might help differentiate between these alternative models (Figure 4.22).

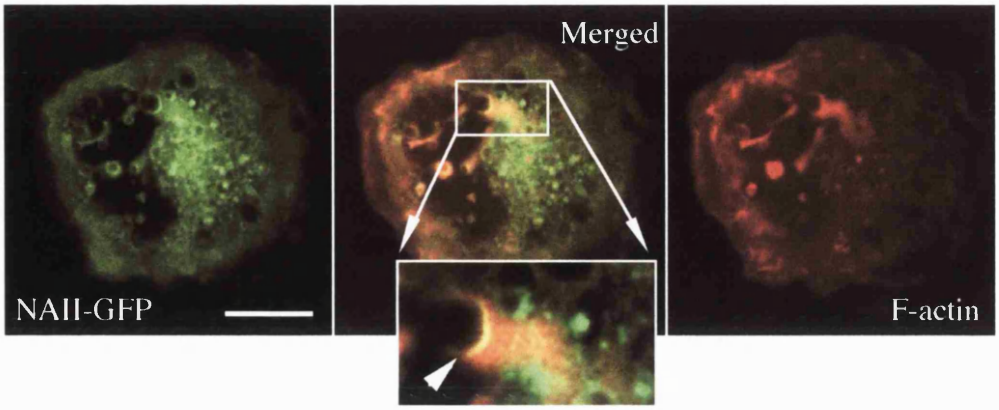

Figure 4.22: Distribution of NAII-GFP in cells stimulated to produce rocketing pinosomes prior to chemical fixation.

RBL cells were transiently transfected with NAII-GFP, stimulated to produce rocketing macro-pinosomes before fixation in 3.7% formaldehyde and permeabilisation with 10 μg/ml saponin (see Materials and Methods). NAII-GFP is not concentrated in rhodamine-phalloidin stained F-actin tails but is found concentrated at the interface of stained F-actin rocket tails and the attendant macro-pinosome (yellow ring, indicated by arrow).
Scale bar: 10 μm

This result (Figure 4.22) supported the proposed model since NAII-GFP appeared concentrated at the tips of rocketing pinosomes, rather than the F-actin tail. To confirm that NAII-GFP and endogenous annexin II have a similar distribution, RBL cells were stimulated to produce rockets, fixed and stained for annexin II using a monoclonal antibody and F-actin using rhodamine phalloidin (Figure 4.23). Both fixed NAII-GFP expressing and wild-type cells gave similar results - neither endogenous annexin II nor NAII-GFP were concentrated within the tail itself but were instead enriched at the surface of the macro-pinosome at the head of rockets. This result is consistent with a close association of both endogenous annexin and NAII-GFP with other proteinaceous membrane components resulting in efficient chemical fixation at the membrane surface. These findings favour a 'membrane recruitment - release' model (Figure 4.22a) rather than direct recruitment from the cytoplasm into the newly formed tail.

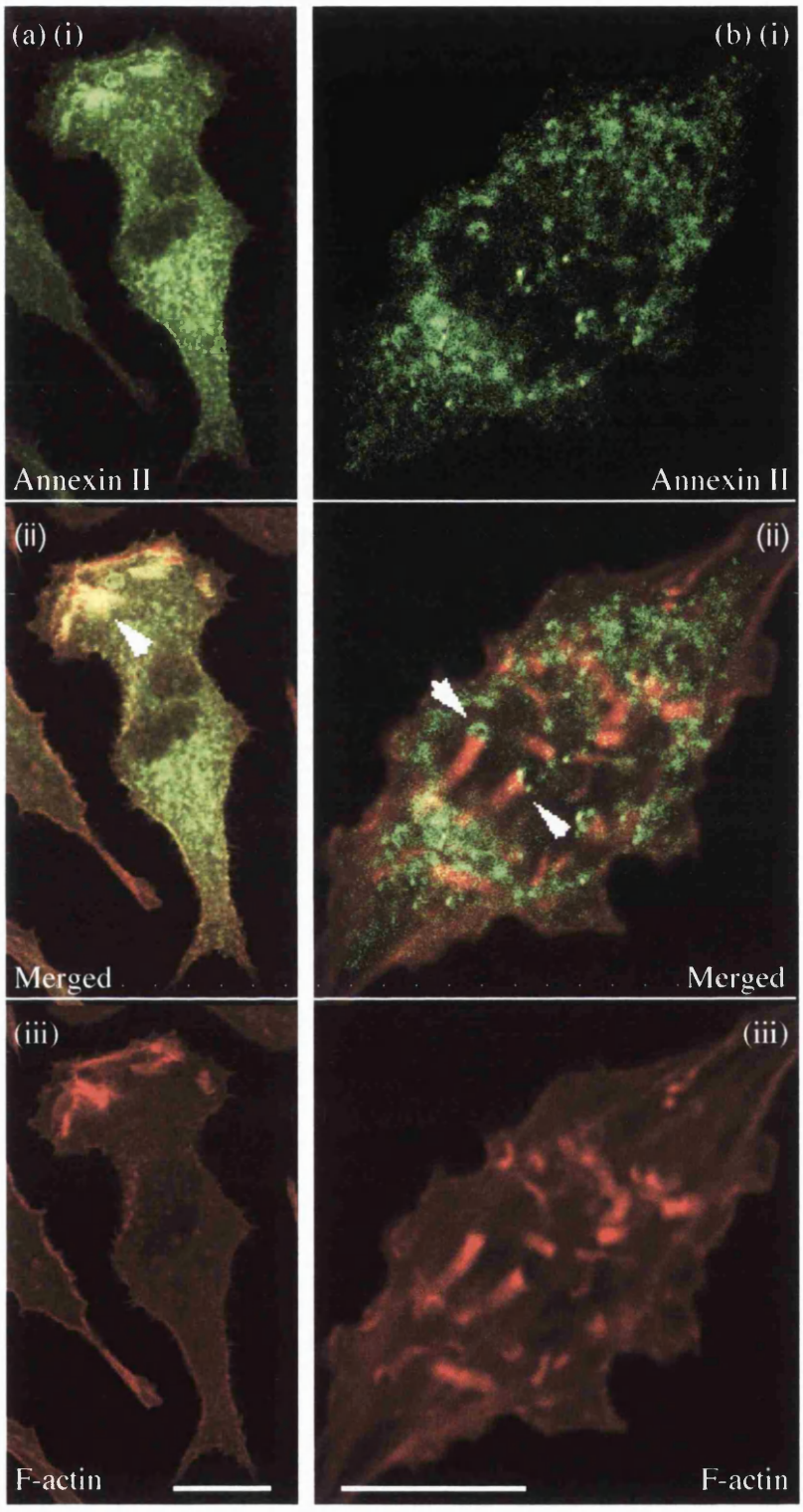

Figure 4.23: Endogenous annexin II locates to the tip of rocketing pinosomes.

Resting (a) or stimulated (b) WT-RBL cells were fixed, permeabilised and stained for annexin II (green) and actin (red). Annexin II in resting cells is distributed evenly through the cytoplasm, and colocalises with F-actin at ruffles (arrow, (a)(ii)). In cells stimulated with hyperosmotic shock and PMA the F-actin cytoskeleton reorganises into rocket tails (b). Endogenous annexin II is not present in the tail, but is concentrated at the rocket tip (arrows, (b)(ii)). Scale bar: 10 μm

4.13 Published data suggests endogenous vesicles might rocket *in vivo*.

In light of new data on macro-pinocytic rockets, and the known colocation of endogenous annexin II and NAII-GFP with these structures, it was interesting to note that published data suggests that endogenous vesicles might form F-actin rockets under physiological conditions. Firstly, immunoelectron micrographs show structures which might be interpreted as rocketing early endosomes (Harder et al., 1997; reproduced in Figure 4.24). In these structures immuno-gold labeled endogenous annexin II was found in close association with the surface of labeled early endosomes, and was often found to extend away from the surface of early endosomes into the cytoplasm. Furthermore, filamentous elements, probably F-actin, were associated with aggregates of annexin II at the surface of early endosomes.

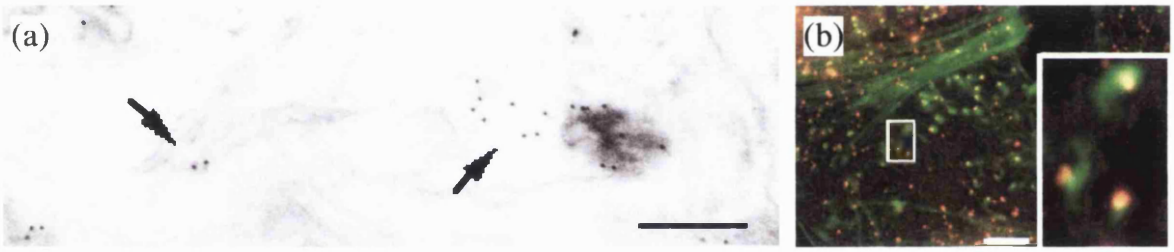

Figure 4.24: Annexin II immunoreactivity extends behind early endosomes in polarised plumes.

This immunoelectron micrograph (a), taken from (Harder et al., 1997), shows a gold labeled annexin II 'rocket tail' extending from the surface of an HRP labeled early endosome in a BHK cell (arrows). The authors noted that annexin II immunoreactivity "... extends for some distance from the early endosomal surface ... " and that filamentous elements, most probably F-actin, often colocate with clustered annexin II immunoreactivity at the surface of early endosomes (Scale bar: 30 nm). The fluorescence micrograph (b) taken from (Frischknecht et al., 1999) shows a cluster of little actin tails (LATs) consisting of an F-actin tail (green) and clathrin stained tip (red) in HeLa cells suggesting clathrin coated vesicles can form actin rockets *in vivo*, under physiological conditions (Scale bar: 5 μm). See text for details.

A second piece of published information provides further evidence that vesicle rocketing might occur *in vivo* under physiological conditions. During investigation of the tyrosine phosphorylation dependence of *Vaccinia* locomotion (Frischknecht et al., 1999) smaller, *Vaccinia*-independent rocket tails were discovered by immunofluorescence microscopy. These 'little actin tails' (LATs) consisted of a short F-actin tail, stained by phalloidin, and a head region which stained for both phosphotyrosine and clathrin. This

would suggest that clathrin-coated vesicles can rocket under physiological conditions. Whether annexin II also locates to the head of LATs is not currently known, although recent work using cell fractionation has demonstrated that annexin II associated Ca^{2+}-independently with clathrin-coated vesicles (Turpin et al., 1998). However it seems unlikely that LATs are of endocytic origin since they did not stain for transferrin receptor, and it was proposed that they may be derived from the Golgi apparatus. Since LATs could not be induced by a variety of manipulations and specific markers have not been found for LATs the nature of these structures is currently obscure.

To conclude, it seemed possible that rocketing macro-pinosomes represent one type of a hitherto neglected class of mobile intracellular vesicle. To gain further insight into the possible role(s) annexin II might perform in tail biogenesis, macro-pinocytic rocketing required further characterisation. In particular the roles of Ca^{2+}, and signal transducing lipid and protein kinases were examined.

4.14 Conclusions.

These results demonstrate that hyperosmotic shock can induce the appearance of a novel class of mobile macro-pinosome. Macro-pinocytic rockets are generated, for reasons which are presently obscure, when a nascent macro-pinosome formed at the plasma membrane recruits actin to its surface in an exaggerated fashion, and is driven away from the plasma membrane at an angle close to 90^0. Although macro-pinocytic rockets were indistinguishable from rocketing *Listeria* in kinetic terms, there are phenomena associated with these structures which appeared to be unique (for instance actin puffs), the origins of which were unclear. Furthermore, unlike *Listeria*, macro-pinocytic rockets showed elements of tight control with regard to actin polymerisation. For instance, macro-pinocytic rockets formed at the plasma membrane in less than 5 seconds, and could stop with a similar time course at the lower surface of the cell. The molecular cues responsible for initiating and terminating macro-pinocytic rocketing are unclear, and constitute one of the most interesting aspects of this phenomenon.

Other observations of rocketing macro-pinosomes *in vivo* have hinted at dynamic forces acting at the cargo/actin tail interface which are not easily explained by contemporary models of actin-polymerisation driven force generation. In particular the apparent constriction of large macro-pinosomes during rocket formation bears striking resonance with recent (unpublished) findings in *Listeria*. These have shown that the force for propulsion, possibly generated directly through actin polymerisation, is delivered indirectly to the surface of rocketing *Listeria* via elastic loads. The analysis of rocketing macro-pinosomes should help to clarify this model further since macro-pinosomes, unlike

Listeria, would be expected to deform under stress, yielding clues as to the dynamic forces acting on their surface. Preliminary observations made in this study substantiate this view.

The finding that NAII-GFP is enriched in the actin tails behind rocketing macro-pinosomes *in vivo* is suprising. Although annexin II was originally characterised as a Ca^{2+} and actin- binding protein (calpactin) doubts were raised over the Ca^{2+}-dependent association of annexin II and F-actin due to the relatively high concentrations of Ca^{2+} required for this process (Gerke and Weber, 1984). However more recent findings have suggested that annexin II_2p11_2 can bind and bundle F-actin at physiological Ca^{2+} concentrations (Ikebuchi and Waisman, 1990). Although a possible role for annexin II_2p11_2 in mediating between F-actin and membrane surfaces has not been formally tested *in vitro,* it has been noted that annexin II immunoreactivity locates to 'regions of membrane protrusion' (Diakonova et al., 1997), and that annexin II, a limited set of actin binding proteins and actin itself form a cholesterol-dependent complex that associates with cellular membranes (Harder et al., 1997). The findings in the present study constitute the first evidence of annexin II in association with an actin based structure *in vivo*, although the basis of this interaction has not been dissected.

It is interesting to note that a role for annexin II in actin dynamics has been previously dismissed since annexin II does not specifically colocate with actin based structures such as stress fibres (Zokas and Glenney, 1987). However, actin tails and actin stress fibres are quite different entities. While the former are highly dynamic structures, formed from continued recruitment and polymerisation of actin at a membrane surface, the latter structures are relatively stable and show only limited turnover of actin monomer (Suzuki et al., 1998). Although it is not presently clear whether the association of NAII-GFP with macro-pinocytic rockets reflects an involvement in actin polymerisation at the macro-pinosome surface, observations in chemically fixed cells suggest that both endogenous annexin II and NAII-GFP are intimately associated with the macro-pinosome and not the F-actin tail of macro-pinocytic rockets. These findings are consistent with a role for annexin II in actin/membrane interactions during macro-pinocytic rocketing, rather than simple cross-linking in the F-actin tail.

Perhaps one of the most intriguing questions raised by theses experiments concerns the role(s) actin polymerisation might play in vesicle traffic *in vivo*. Harder et al (Harder et al., 1997) have published immuno-electron microscopic evidence that annexin II forms rafts at the surface of early endosomes and extends away from these vesicles in plumes. Even more intriguing is the recent discovery of 'LATs' (Little Actin Tails) during investigation of the tyrosine-phosphorylation dependence of *Vaccinia* locomotion (Frischknecht et al., 1999). These structure resemble tiny rocketing macro-pinosomes and consist of a clathrin (+)/phospho-tyrosine (+) head, and F-actin tail. It was proposed that LATs might be rocketing endosomes. However the head of LATs failed to label with

transferrin suggesting an alternative origin, perhaps from the Golgi apparatus. With these recent data in mind it seems feasible that actin polymerisation could propel vesicles *in vivo* under physiological conditions and constitute a hitherto neglected form of vesicle propulsion.

5. Chapter 5 : Investigation of the molecular basis of macro-pinosome rocketing.

5.1 Hyperosmotic shock, cell signaling and macro-pinocytosis.

To begin the investigation of the molecular mechanism of macro-pinocytic rocketing the effects of hyperosmotic shock on macro-pinocytosis were analysed. This experiment was aimed to establish whether the phenomenon of macro-pinocytic rocketing might be explained by up-regulation of the entire macro-pinocytic process on stimulation with hyperosmotic shock (Figure 5.1).

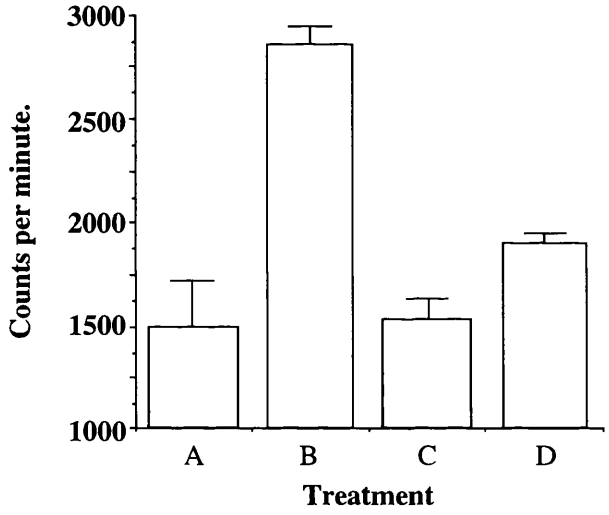

Treatments:

(A) - HBS

(B) - HBS + PMA

(C) - HBS + HOS

(D) - HBS + HOS + PMA

Figure 5.1: Hyperosmotic shock inhibits PMA stimulated macro-pinocytosis.

Fluid phase endocytosis was measured using [^{3}H]-dextran in wild-type RBL cells challenged with HBS +/- 150 mM sucrose, +/- 10 nM PMA (indicated above). Challenge with hyperosmotic shock has little effect on the amount of [^{3}H]-dextran associated with cells while challenge with PMA leads to a dramatic increase in fluid phase endocytosis. The increase in fluid phase endocytosis induced by PMA is inhibited by costimulation with hyperosmotic shock (see text for details). Values shown are average +/- S.E.M. and are representative of triplicate experiments.

Hyperosmotic shock clearly interferes with efficient macro-pinocytosis and yet data data in the previous chapter strongly links hyperosmotic shock and macro-pinocytic rocketing. A model based on microscopic observations was previously formulated suggesting that rocketing arises through the exaggeration of a step(s) which are normally required for macro-pinocytosis. How might this occur? One possible mechanism would

invoke the interaction of signaling pathways stimulated by hyperosmotic shock and the molecular mechanism of macro-pinocytosis. Specifically, if macro-pinocytosis and anisosmolarity-induced signaling have common molecular components, one might expect hyperosmotic shock to directly exaggerate specific steps in macro-pinocytosis. This theme was explored in the following sets of experiments.

5.2 Possible links between anisosmotic induced signaling and macro-pinocytic rocketing.

The maintenance of a constant cell volume is a fundamental property of cells from such evolutionarily divergent organisms as *Saccharomcyes cerevisiae* and *Homo sapiens* and the mechanisms responsible for sensing and responding to changes in extracellular osmolarity are correspondingly conserved. Analysis and identification of proteins phosphorylated in response to osmotic shock in *S.cerevisiae* led to the discovery of HOG-1 (high osmolarity glycerol response 1) (Brewster et al., 1993; Maeda et al., 1995), a member of the mitogen activated protein kinase (MAPK) family. HOG-1 is rapidly tyrosine phosphorylated in response to hyperosmotic shock (Brewster et al., 1993) and is instrumental in triggering transcription of stress response genes (Marquez et al., 1998) and modulation of specific enzymes (Reynolds et al., 1998).

The discovery of HOG-1 was swiftly followed by the identification and cloning of the mammalian homologue p38, first purified as a macrophage polypeptide that becomes tyr-phosphorylated and activated *in situ* in response to bacterial lipopolysaccharides and hyperosmotic shock (Galcheva-Gargova et al., 1994; Han et al., 1994). In common with (SAPK) pathways in general, small GTP binding proteins of the Ras superfamily have been implicated in the regulation of proximal components of the p38 pathway (for brief review see Kyriakis and Avruch, 1996). In particular the Rho family GTPases Rac1 and Cdc42 strongly activate p38 upon cotransfection and have been shown to regulate p38 through the downstream mediator p21 activated kinase 1 (PAK1) (Zhang et al., 1995).

PAKs are 60-70 kDa proteins whose C-terminus is 60-70% identical to S.cerevisiae Ste20p and whose N-terminal domain contains a Rac1/Cdc42 binding domain (Bagrodia et al., 1995; Manser et al., 1994; Martin et al., 1995; Teo et al., 1995). Like Ste20p, the PAKs are activated directly upon interaction with the GTP-bound form of Rac1/Cdc42 *in vitro* (Bagrodia et al., 1995; Manser et al., 1994; Martin et al., 1995; Teo et al., 1995) while dominant negative PAK1 mutants abolish Rac1/Cdc42 mediated activation of p38 (Zhang et al., 1995). Lastly PAK1 has been shown to be activated directly by hyperosmotic shock in mammalian cells (Clerk and Sugden, 1997) which correlates well with its proposed position in the p38 path. However the effectors mediating between PAK1 and p38 have not been identified.

These proximal components of the hyperosmolarity-activated p38 pathway (Figure 5.2) are intriguing since they have been demonstrated to directly influence the actin cytoskeleton. In addition a downstream effector of p38, Hsp27 has also been shown to modulate actin dynamics *in vivo* (reviewed in (Landry and Huot, 1995).

The proximal components, Rac1, Cdc42 and PAK1 are particularly interesting with respect to macro-pinocytic rocketing since they have been implicated in the initiation and control of polarised actin polymerisation. In addition Rac1 and Cdc42 have been implicated in phagocytosis in RBL cells (Massol et al., 1998). Although a link between either GTPase and pinocytosis has not been established it seems likely that that the molecular mechanism responsible for cup closure in phagocytosis and macro-pinocytosis are similar since 'spacious' phagocytic cups can form without guidance from a particle surface, in an analagous way to macro-pinosomes (Swanson et al., 1999).

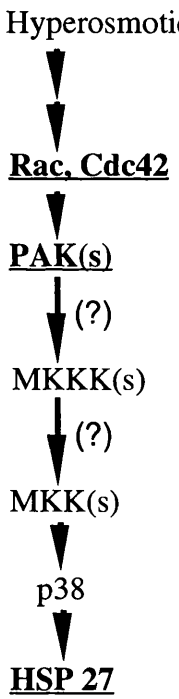

Figure 5.2: The p38 MAPK pathway.

The diagram illustrates the proposed signal transduction pathway for activation of the stress-regulated p38 pathway. Components which have been shown to directly modulate the actin cytoskeleton are in bold type (See text for details. *MKK*, MAP kinase kinase; *MKKK*, MAP kinase kinase kinase) (Figure modified from Zhang et al., 1995)

The second component of the p38 pathway which may contribute to rocketing *in vivo* is PAK1. Membrane targeting of PAK1 stimulates actin polymerisation and neurite outgrowth in PC12 cells (Daniels et al., 1998) and this serine/threonine kinase is activated by hyperosmotic shock (Clerk and Sugden, 1997). Critically, PAK1 has recently been found to locate to macro-pinosomes in fibroblasts (Dharmawardhane et al., 1997) suggesting PAK1 could act as a link between the two ingredients needed for macro-pinocytic rocketing: polarised actin polymerisation and macro-pinosomes.

The last component of the p38 pathway which may modulate the actin cytoskeleton in response to hyperosmotic shock is HSP27. This downstream effector of p38 MAPK was first identified as one of the heat-shock proteins that accumulates to high levels in cells in response to elevated temperature (for review see Landry and Huot, 1995). In motile cells HSP27 is concentrated in motile cell protrusions such as

lamellipodia, filapodia and membrane ruffles (Lavoie et al., 1993). Cell lines overexpressing HSP27 have more cortical actin, fewer stress fibres and show an increase in pinocytosis as compared to control cells (Lavoie et al., 1993). In contrast stable lines expressing a non-phosphorylatable mutant of HSP27 show reduced pinocytosis compared to control cells.

In conclusion there are (at least) three components involved in the p38 pathway which could potentially be involved directly in the process of macro-pinocytic rocketing and which are worthy of further investigation. The experimental approaches formulated to investigate the molecular mechanism of macro-pinocytic rocketing were strongly influenced by the timely publication of data describing vesicle rocketing *in vitro* (Ma et al., 1998a; Moreau and Way, 1998). These data, implicating Cdc42 in the formation of F-actin rockets in *Xenopus* extracts are discussed in detail below.

5.3 Vesicle rocketing *in vitro.*

Recent findings *in vitro* have described actin based rocketing of both unidentified vesicles (Moreau and Way, 1998) and synthetic vesicles (Ma et al., 1998a) in *Xenopus* egg extracts. These investigations have provided several key pieces of data. Firstly, rocketing *in vitro* was strongly stimulated by pervanadate and GTPγS and this was shown to be based on an absolute requirement for the small GTP-binding protein Cdc42. Secondly it was found that pervanadate also strongly stimulates rocketing *in vitro* (Ma et al., 1998a; Moreau and Way, 1998). Thirdly it was found that the membrane composition of synthetic vesicles modulated their recruitment of actin and organisation of an actin tail. Specifically it was found that incorporation of phosphatidylinositol (4,5) bisphosphate ($PI(4,5)P_2$) or phosphatidylinositol (3,4,5) triphosphate ($PI(3,4,5)P_3$) into synthetic vesicle membranes relieved the requirement for GTPγS to promote rocketing (Ma et al., 1998a). It was not clear in this study whether the apparently equal effectiveness of $PI(4,5)P_2$ and $PI(3,4,5)P_3$ at initiating vesicle rocketing was due to the interconversion of one to the other in the vesicle membrane through the action of PI3-kinase(s) or PI3-phosphatase(s).

These results *in vitro* may help to clarify some aspects of macro-pinocytic rocketing *in vivo*. In particular the finding that rocketing *in vitro* has an absolute requirement for Cdc42 was striking since, as discussed previously, this small GTP-binding protein has been implicated in the p38 MAPK pathway. Also, the finding that pervanadate strongly stimulates rocketing *in vitro* was intriguing. If pervanadate, a potent protein tyrosine phosphatase inhibitor, stimulates vesicle rocketing this would imply that tyrosine phosphorylation may play a role in this phenomenon. If this is the case then tyrosine phosphorylation of which substrate(s) and by which tyrosine kinases(s)?

5.4 The molecular basis of macro-pinosome rocketing (I): Investigation of macro-pinosome rocketing induction

Experiments were performed to investigate the effects of pervanadate on macro-pinosome rocketing in intact RBL cells (Figure 5.3). GTP analogues were not used in these preliminary experiments as they are not cell permeable, though the involvement of the small GTP binding proteins Rac and Cdc42 were investigated in later experiments using the inhibitor toxin B (results discussed elsewhere).

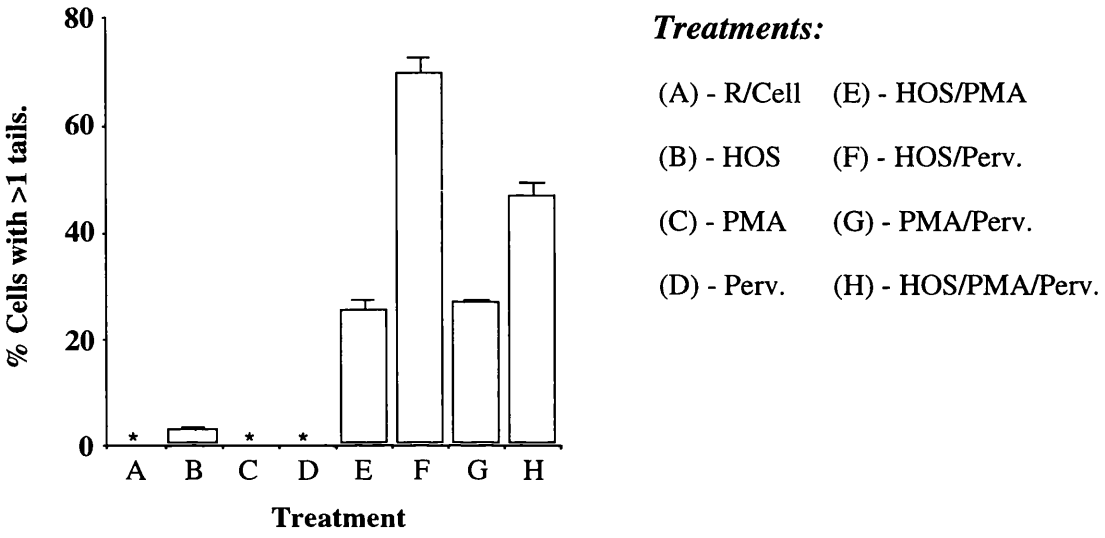

Figure 5.3: Quantification of the effects of hyperosmotic shock +/- PMA +/- pervanadate on the incidence of hyperosmolarity induced rocketing.

RBL cells, 40-50% confluent, were stimulated with HBS +/- 150 mM sucrose (HOS), +/- 10 nM PMA (PMA) and +/- 200 μM pervanadate (Perv) as indicated. Cells were fixed in 3.7% formaldehyde, permeabilised and stained for F-actin with rhodamine-phalloidin. Random fields of cells were viewed by epifluorescence microscopy and the number of cells with one or more rocketing pinosomes in each field counted (100 cells per coverslip, 3 separate experiments). Rocketing pinosomes are not seen in resting cells, nor cells stimulated with either PMA or pervanadate alone (*). Challenge with hyperosmolar HBS causes a small fraction of cells to generate rocketing pinosomes. Inclusion of PMA or pervanadate dramatically increases the incidence of rocketing, with pervanadate being the more effective of the two. While induction of rocketing pinosomes with either PMA or pervanadate alone is strictly dependent on the inclusion of hyperosmotic shock, a combination of PMA and pervanadate can also induce rocketing (see text for details).

This result demonstrated that hyperosmotically induced macro-pinosome rocketing is strongly stimulated by pervanadate in a similar way to vesicle rocketing *in vitro* (Ma et al., 1998a; Moreau and Way, 1998). Furthermore the previously described effect of PMA on this phenomenon was confirmed and quantified. However, although both PMA and pervanadate stimulated the production of macro-pinocytic rockets it seems unlikely that they

act in the same way. Specifically, it was noted that induction of rocketing pinosomes with either PMA or pervanadate is strictly dependent on co-stimulation with hyperosmotic shock - yet a combination of PMA and pervanadate can by-pass this requirement. This result is graphically illustrated by an examination of the F-actin cytoskeleton after challenge with these different combinations of agonists (Figure 5.4).

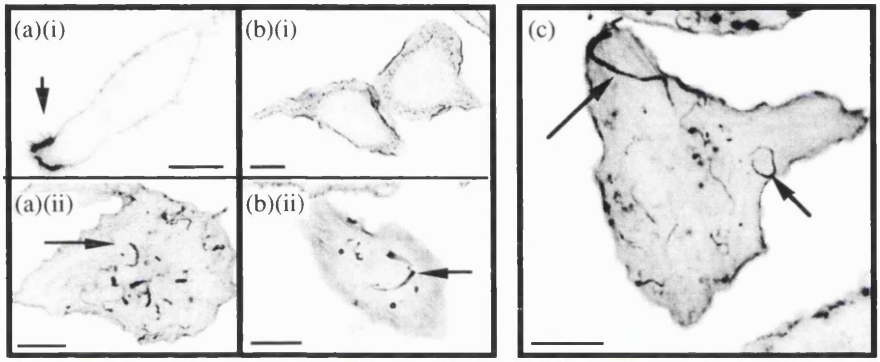

Figure 5.4: Stimulation of RBL cells with different combinations of PMA, pervanadate and hyperosmotic shock leads to characteristic changes in the actin cytoskeleton.

RBL cells were stimulated for 45 min with HBS supplemented with (a)(i) 200 μM pervanadate, (a)(ii) 200 μM pervanadate + 150 mM sucrose, (b)(i) 10 nM PMA, (b)(ii) 10 nM PMA + 150 mM sucrose, (c) 200 μM pervanadate + 10 nM PMA. Stimulation with pervanadate leads to the generation of a tight, polarised F-actin cap ((a)(i) arrow) while costimulation with hyperosmotic shock leads to the generation of characteristic F-actin rockets ((a)(ii) arrow). Stimulation with PMA leads to cells spreading (b)(i) while costimulation with hyperosmotic shock leads to generation of rockets ((b)(ii) arrow). Costimulation with PMA and pervanadate leads to cell spreading and generation of rockets in the absence of hyperosmotic shock ((c) arrow) (see text for details).
Scale bar: 10 μm F-actin was visualised using FITC-phalloidin

In light of the published *in vitro* data one possible explanation is that both agonists induce rocketing at least in part through stimulation of phosphatidylinositolphosphate (PIP) production. In RBL cells challenge with PMA has been shown to induce production of PI(4)P and $PI(4,5)P_2$ (Apgar, 1994) while challenge of a variety of cells types with pervanadate has been shown to induce production of a variety of PIPs (Helgadottir et al., 1997). Significantly, hyperosmolarity can apparently modulate the type of PIPs produced by cells stimulated with pervanadate since co-stimulation of HEK-293 cells with 0.5 M sorbitol and 0.1 mM pervanadate led to the specific accumulation of $PI(3,4,5)P_3$ (Meier et al., 1998). It is not known whether RBL cells co-stimulated with hyperosmotic shock and either PMA or pervanadate accumulate $PI(4,5)P_2$ or $PI(3,4,5)P_3$ although this appears probable in the light of published evidence. A working hypothesis to explain macro-pinocytic rocketing would invoke $PI(3,4,5)P_3$ over-production at some stage during macro-

pinocytosis which 'charges' the newly formed pinosome. Nascent macro-pinosomes would then rocket by a similar mechanism to rocketing vesicles *in vitro*.

The finding that PMA and pervanadate in combination can induce the formation of macro-pinocytic rockets suggests there are at least two possible routes leading to the formation of macro-pinosome rockets - one stimulated by PMA and the other stimulated by tyrosine phosphorylation (Figure 5.5).

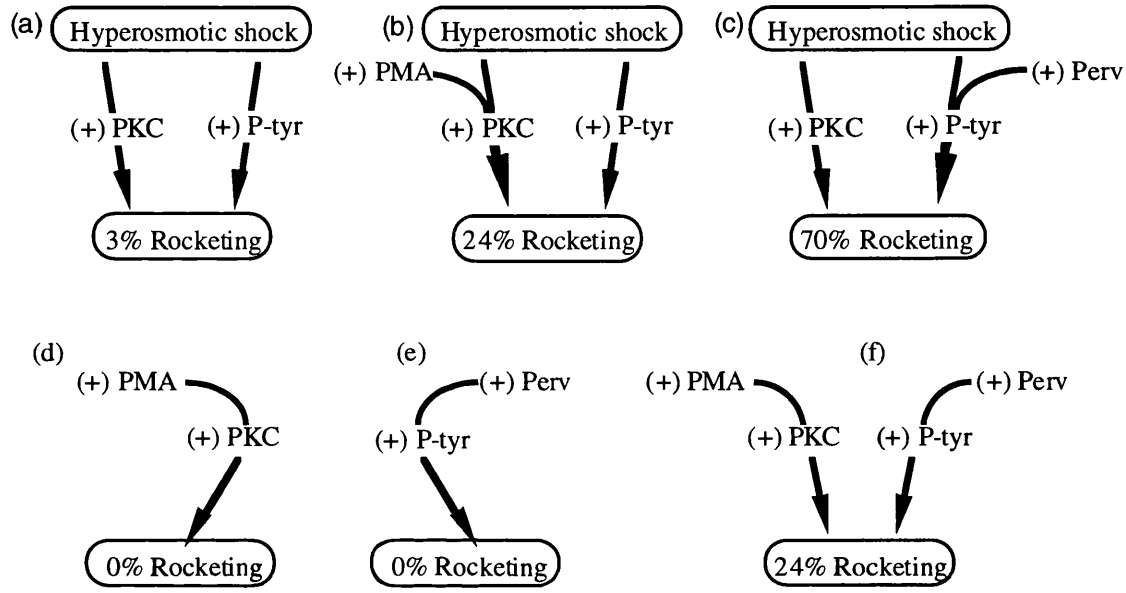

Figure 5.5: Model to explain the synergistic effect of PMA and pervanadate on macro-pinosome rocketing.

(a) Under conditions of hyperosmotic shock two pathways may become activated which are involved in the formation of rocketing pinosomes, one involving PKC and the other involving tyrosine phosphorylation. Activation of both pathways is required to induce pinosome rocketing. (b)(c) Under conditions of hyperosmotic shock up-regulation of either pathway leads to an increase in the incidence of rocketing. The other pathway required to stimulate rocketing is still activated by hyperosmotic shock. (d)(e) Activation of either pathway alone in the absence of hyperosmotic shock using PMA or pervanadate cannot stimulate rocketing as the alternate pathway is inactive. (f) Activation of both pathways using a combination of PMA and pervanadate in the absence of hyperosmotic shock stimulates the production of rockets.

In an attempt to untangle the signaling events leading to macro-pincocytic rocketing further and test aspects of the working hypothesis the next stage of the investigation involved screening inhibitors that would disrupt specific components of the pathway. Since stimulation of cells with a combination of pervanadate and hyperosmotic shock proved so potent at inducing macro-pinocytic rockets cells were stimulated using this combination of agonists in the presence of a variety of different inhibitors and the incidence of rocketing analysed.

5.5 The molecular basis of macro-pinosome rocketing (II): The effects of potential inhibitors and stimulants on macro-pinosome rocketing.

RBL cells were stimulated to produce F-actin rockets using hyperosmotic shock and pervanadate in the presence of a variety of inhibitors (Table 5.1). Cells were fixed and stained for F-actin and the number of cells in the population with one or more clearly defined rockets counted. In this preliminary screen inhibitors were used at 5 x their published IC_{50}. Due to the prolonged time course of the experiment and potential for non-specific effects on macro-pinocytosis through cell damage inhibitors were not considered to have had a specific effect on rocketing unless two criteria were met: firstly cells showed complete abolition of macro-pinosome rocketing and secondly there was no obvious extensive cell mortality or gross effects on cell morphology which might have indirectly affected the process of macro-pinocytosis. Only one novel potential stimulant, phenylarsine oxide, was tested. The incubation protocols used are detailed in Materials and Methods.

Table 5.1: Effects of inhibitors on macro-pinocytic rocketing.

Inhibitor	Target (IC_{50})	Conc. used.	Rocketing?
Chelerythrin Chl.	PKC (660 nM)	3.3 μM	Yes
Herbimycin A	$pp60^{c\text{-}src}$ (900 nM)	4.5 μM	Yes
Lavendustin C	CAM kinase II (200 nM)	2.5 μM	Yes
	$pp60^{c\text{-}src}$ (500 nM)		
Toxin B	Rac-1/Cdc42 (?)	100 ng/ml	Yes
SB202190	p38 MAPK (350 nM)		Yes
Wortmannin	PI3-kinase (5 nM)	25 nM	No
Filipin	cholesterol (N/A)	2 μg/ml	Yes
Latrunculin B	actin polymerisation (N/A)	5 μM	No
BAPTA-AM	Ca^{2+} chelator	10 μM	No
Stimulants	**Target**		
PMA	PKC	10 nM	Yes
Pervanadate	phosphotyrosine phosphatases (N/A)	200 μM	Yes
Phenylarsine oxide	phosphotyrosine phosphatases (N/A)	50 μM	No

Of the inhibitors screened only three abolished macro-pinocytic rocketing: wortmannin, latrunculin B and BAPTA-AM. To investigate the observed effects of these agonists further, titrations were performed to find the lowest concentration of each which completely abolishes rocketing (detailed below).

The effects of each inhibitor screened in both control cells and cells stimulated to produce macro-pinocytic rockets are discussed below. Images of the actin cytoskeleton are printed in negative contrast since the human eye is more sensitive to detail (such as F-actin rockets) rendered in black against a white background.

---

1. Chelerythrin chloride.

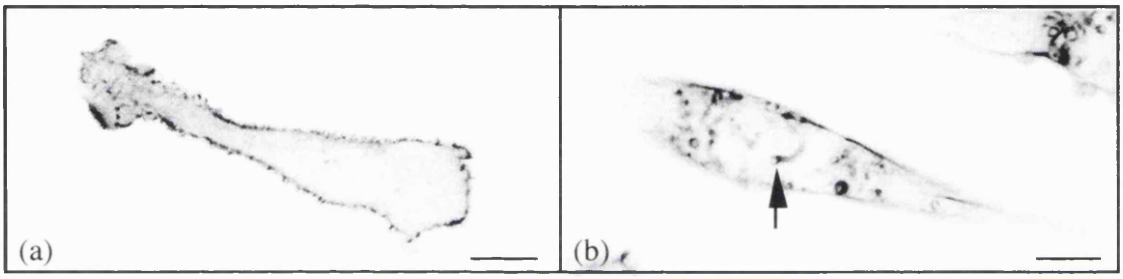

Figure 5.6: The effects of chelerythrin chloride on resting RBLs and RBLs stimulated to produce macro-pinocytic rockets.

RBL cells were pre-treated with 3.3 μM chelerythrin chloride for 20 min before incubation with (a) HBS or (b) (HBS + HOS + Perv) for a further 45 min. Cells were fixed using formaldehyde, stained for F-actin and viewed by confocal microscopy. Chelerythrin chloride does not completely inhibit the formation of F-actin rocket tails (arrow in (b)).
Scale bar: 10 μm

Published data has implicated PKC in macro-pinocytosis and has demonstrated that this form of endocytosis is strongly stimulated by PMA in a variety of cell types (Keller, 1990; Phaire-Washington et al., 1980; Swanson, 1989; Swanson et al., 1985) and is repressed by PKC inhibitors (Keller and Niggli, 1993; Keller and Niggli, 1994). The fact that chelerythrin chloride, a potent PKC inhibitor, did not abolish macro-pinocytic rocketing would suggest that PKC does not play a direct role in this phenomenon (Figure 5.6). However it has already been established in this study that PMA strongly stimulates pinocytosis and hyperosmolarity induced macro-pinocytic rocketing in RBL cells (see Chapter 4.0, also Figure 5.1, Figure 5.3). A simple explanation could be that only very low levels of PKC activity are required for efficient macro-pinocytic rocketing, and that the concentration of inhibitor used is insufficient to completely abolish PKC activity in the face of the powerful stimuli used.

2. Herbimycin A and Lavendustin C.

Since pervanadate is a potent stimulus of macro-pinocytic rocketing tyrosine phosphorylation may play a central role in this phenomenon. With the model proposed for annexin II function in rocketing in mind (see Figure 4.21, p 129) particular attention was paid to inhibitors of $pp60^{c\text{-}src}$. Previous sudies have shown that transformation of fibroblasts with $pp60^{v\text{-}src}$ specifically up-regulates macro-pinocytosis while having no effect on receptor mediated endocytosis, suggesting that $pp60^{src}$ may be involved in this process (Veithen et al., 1996). However neither herbimycin A nor lavendustin C showed significant inhibition of hyperosmolarity/pervanadate induced macro-pinocytic rocketing (Figure 5.7). This would suggest that this kinase is not directly involved in macro-pinocytic rocketing. However, since pervanadate is a potent protein tyrosine phosphatase inhibitor this data must be viewed with some caution. It is possible that residual levels of tyrosine kinase activity would be sufficient to promote significant phosphorylation of target proteins in the absence of active phosphatases.

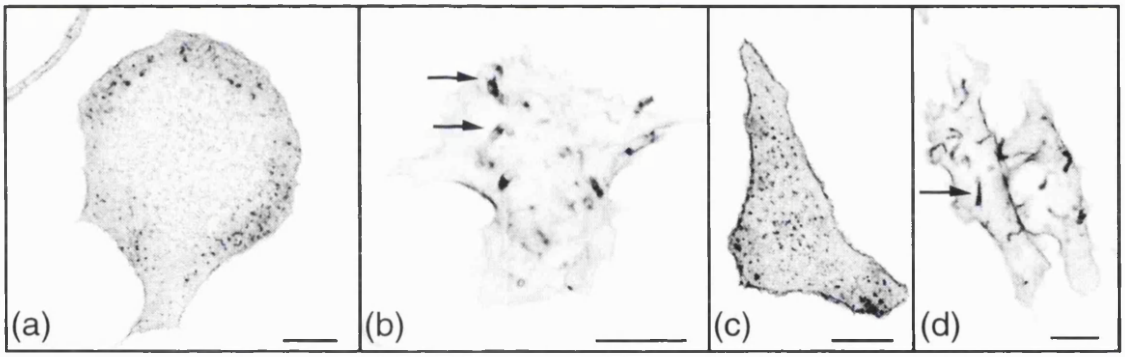

Figure 5.7: The effects of Herbimycin A or Lavendustin C on resting RBLs and RBLs stimulated to produce macro-pinocytic rockets.

RBL cells were pre-treated with (a)(b) 4.5 µM Herbimycin A or (c)(d) 2.5 µM Lavendustin C for 20 min before incubation with either (a)/(c) HBS or (b)/(d) (HBS + HOS + Perv) for a further 45 min. Cells were fixed and stained for F-actin and viewed by confocal microscopy. Both Herbimycin A and Lavendustin C cause unstimulated RBL cells to spread. Neither inhibitor has a significant effect on macro-pinocytic rocketing. Scale bar: 10 µm

3. Toxin B.

Toxin B is a potent inhibitor of both Rac-1 and Cdc42 (Dillon et al., 1995; Prepens et al., 1996). It has previously been shown to inhibit phagocytosis in macrophage and RBL cells (Massol et al., 1998; Siffert et al., 1993) - a process similar to macro-pinocytosis in

its requirement for membrane protrusion and the formation of an actin-rich cup (Swanson et al., 1999). The effects of toxin B on macro-pinocytosis are not known and it is not known if Cdc42 is involved in this process although given recent data highlighting the similarities between phagocytosis and macro-pinocytosis it is possible that Cdc42 could play a role in the latter process (Swanson et al., 1999). Furthermore, as discussed, vesicle rocketing *in vitro* has an absolute requirement for Cdc42 (Ma et al., 1998ab; Moreau and Way, 1998). Thus the finding toxin B had no effect on the incidence of macro-pinocytic rocketing *in vivo* was unexpected (Figure 5.8).

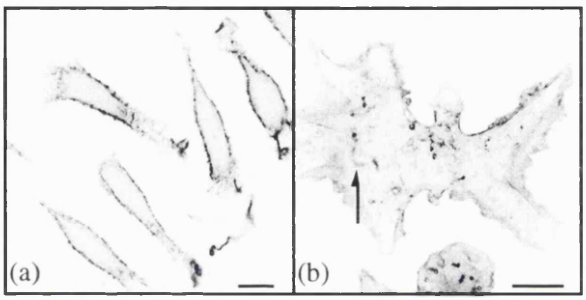

Figure 5.8: The effects of Toxin B on resting RBL cells and RBL cells stimulated to produce macro-pinocytic rockets.

RBL cells were pre-treated with 100 nM Toxin B for 2 h and incubated for a further 45 min in either (a) HBS or (b) (HBS + HOS + Perv). Cells were fixed and stained for F-actin and viewed by confocal microscopy. Treatment with Toxin B has no visible effect on the cytoskeleton of either resting RBL cells or RBL cells stimulated to produce macro-pinocytic rockets (see text for details).
Scale bar: 10 μm

There is reason to treat this result with caution since it was also found that toxin B had little effect on the actin cytoskeleton in resting RBL cells - quite unlike the previously reported effects of toxin B on other cell types (Fiorentini et al., 1989; Malorni et al., 1990; Mitchell et al., 1987; Ottlinger and Lin, 1988; Siffert et al., 1993). It was noted that in a recent study of receptor-mediated phagocytosis in RBL cells which showed that toxin B inhibits phagocytosis in this cell line, relatively high concentrations of toxin B (100 ng/ml) and prolonged incubation times (16 h) were used (Massol et al., 1998). The experiments performed in this study were based on previous experiments in macrophages which used much shorter incubation times (2 hours). Further experiments to investigate the effects of toxin B on macro-pinocytic rocketing would thus require much longer pre-incubation times with the toxin.

4. SB202190.

SB202190 is a specific inhibitor of p38 MAPK (Young et al., 1997) and would be expected to interfere with macro-pinocytic rocketing if effectors of p38 (such as HSP27) were directly involved in this process. SB202190 does not have a significant effect on macro-pinocytic rocketing or the actin skeleton in resting cells (Figure 5.9), suggesting that HSP27 is not a key element in this phenomenon.

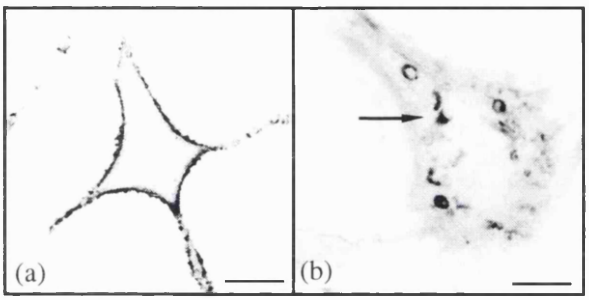

Figure 5.9: The effects of SB202190 on resting RBL cells and RBL cells stimulated to produce macro-pinocytic rockets.

RBL cells were pre-treated with 1.75 μM SB202190 and incubated for a further 45 min in either (a) HBS or (b) (HBS + HOS + Perv). Cells were fixed and stained for F-actin and viewed by confocal microscopy. Treatment with SB202190 has no visible effect on the cytoskeleton of either resting RBL cells or RBL cells stimulated to produce macro-pinocytic rockets.
Scale bar: 10 μm

5. Filipin.

Recent data has demonstrated a cholesterol-dependent mode of annexin II-membrane association in conjunction with actin and specific actin-binding proteins (Harder et al., 1997). Furthermore fluid phase endocytosis, mediated by caveolae (or related structures) is sensitive to cholesterol sequestration using filipin (Kiss and Geuze, 1997). Although moderate concentrations of filipin caused significant changes in cell morphology and the actin cytoskeleton (Figure 5.10, overleaf) these did not abolish rocketing, suggesting that this phenomenon is not sensitive to cholesterol sequestration.

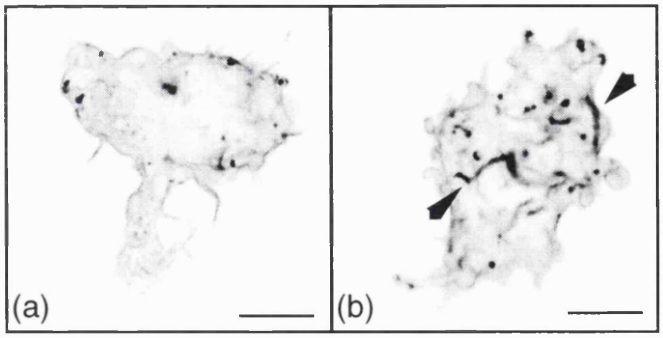

Figure 5.10: The effects of filipin on resting RBLs and RBLs stimulated to produce macro-pinocytic rockets.

RBL cells were pre-treated with 2 µg/ml filipin and incubated for a further 45 min in either (a) HBS or (b) (HBS + HOS + Perv). Cells were fixed, stained for F-actin and viewed by confocal microscopy. Although treatment with this concentration of filipin causes gross cell damage it does not completely inhibit the formation of F-actin rocket tails (arrow in (b)).
Scale bar: 10 µm

6. Latrunculin B.

Latrunculin B is a potent cell permeable inhibitor of actin polymerisation (Spector et al., 1989) derived from the marine sponge *Latrunculia magnifica*. Pre-incubation of RBL cells with latrunculin B completely abolished macro-pinocytic vesicle rocketing. Previous studies have shown that macro-pinocytosis requires active actin polymerisation since this process is sensitive to cytochalasins (Phaire-Washington et al., 1980).

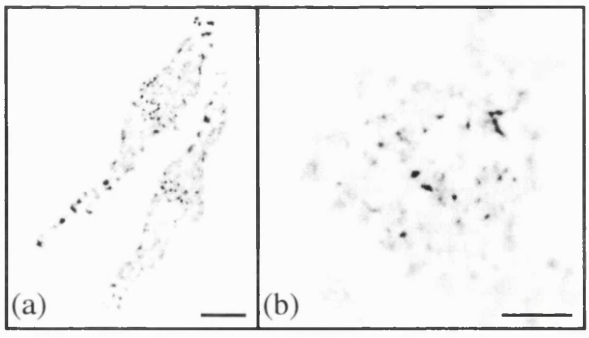

Figure 5.11: The effects of Latrunculin B on resting RBLs and RBLs stimulated to produce macro-pinocytic rockets.

RBL cells were pre-treated with 1 µM Latrunculin B and incubated for a further 45 min in either (a) HBS or (b) (HBS + HOS + Perv). Cells were fixed and stained for F-actin before viewing by confocal microscopy. Latrunculin B causes characteristic reorganisation of the F-actin cytoskeleton into fragmented foci in unstimulated and stimulated cells.
Scale bar: 10 µm

In view of published evidence and data obtained in this study it seemed likely that macro-pinocytic rocketing would be sensitive to latrunculin B, a view confirmed by this finding.

7. Wortmannin.

Wortmannin is a potent and selective inhibitor of PI3-kinases at nM concentrations (Arcaro and Wymann, 1993; Wymann and Arcaro, 1994). Since it has been shown that wormannin inhibits macro-pinocytosis at similar concentrations to PI3-kinase inhibition in RBL cells (Barker et al., 1995) and macrophages (Araki et al., 1996) it is thought that PI3-kinase is required for this process. There is compelling evidence to suggest that PI3-kinase is required at the very last stages of macro-pinocytosis during cup closure. Both immunofluorescence and video microscopy of macrophages treated with wortmannin revealed that the successfully formation pinocytic cups which failed to pinch close and form a pinosome, and which instead receded into the cytoplasm (Araki et al., 1996). Published data on vesicle rocketing *in vitro* reported that this phenomenon was insensitive to wortmannin (Ma et al., 1998a; Moreau and Way, 1998). Titration of wortmannin revealed that this inhibitor completely abolished rocketing at concentrations as low as 2 nM (triplicate experiment). Cortical actin and ruffling in cells treated with wortmannin appears little different to controls (Figure 5.12) indicating that inhibition of PI3-kinase does not inhibit recruitment of F-actin to the plasma membrane *per se*.

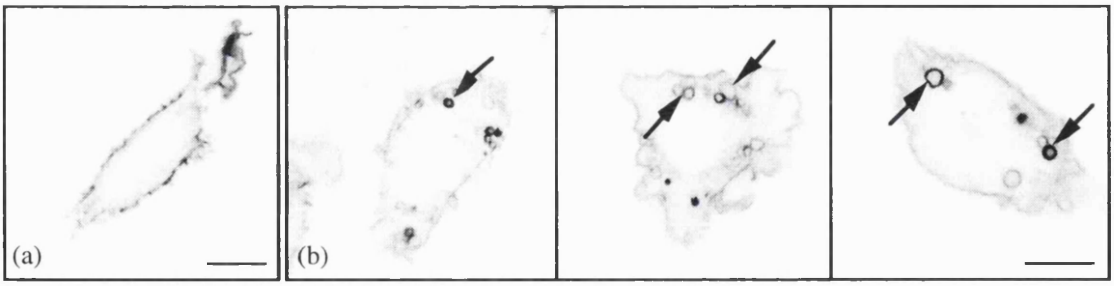

Figure 5.12: The effects of wortmannin on resting RBLs and RBLs stimulated to produce macro-pinocytic rockets.

RBL cells were ptre-treated with 2 nM wortmannin for 20 min before incubation with either (a) HBS or (b)(c)(d) (HBS + HOS + Perv) for a further 45 mins. Cells were fixed, stained for F-actin and viewed by confocal microscopy. Wortmannin does not abolish ruffling in un-stimulated cells (a). In cells stimulated with (HBS + HOS + Perv) the typical macro-pinocytic rockets are absent. Instead cells have numerous F-actin decorated vesicles (arrows in (b)).
Scale bar: 10 μm

Phosphoinositides, and in particular $PI(4,5)P_2$, are implicated in the formation of ruffles and the recruitment of F-actin to the plasma membrane through numerous lines of evidence (for review see Janmey, 1994). The finding that wortmannin does not inhibit ruffling, but specifically inhibits the formation of macro-pinocytic rockets suggests that the only the latter process is dependent on a 3-phosphorylated phosphatidylinositol phosphate. It is not presently known whether the strongly F-actin (+) vesicles seen in RBL cells in which rocketing has been inhibited with wortmannin represent macro-pinosomes which have failed to polarise. This would be a priority for future experiments.

7. BAPTA-AM.

In view of the association of NAII-GFP with rocketing macropinosomes, and the established biochemical properties of annexin II, a model was described previously postulating that annexin II may be involved in macro-pinocytic rocketing in a Ca^{2+}-dependent manner (Figure 4.21). This experiment was thus designed to establish whether macro-pinocytic rocketing was dependent on intracellular Ca^{2+}.

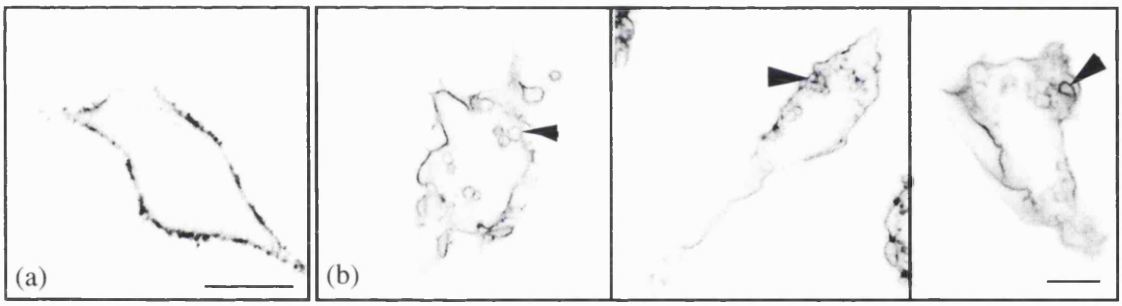

Figure 5.13: The effects of BAPTA-AM on resting RBLs and RBLs stimulated to produce macro-pinocytic rockets.

RBL cells were pre-treated with 1 μM BAPTA-AM for 20 min before incubation with either (a) HBS or (b) (HBS + HOS + Perv) for a further 45 min. Loading with BAPTA-AM has little effect on the cortical cytoskeleton in resting cells (a). In cells stimulated with (HBS + HOS + Perv) no F-actin rocket tails are seen in any cells. Instead cells show numerous F-actin decorated vesicles (arrows in (b)).
Scale bar: 10 μm

BAPTA-AM enters cells where it is cleaved by cytosolic esterases and trapped intracellularly as the active Ca^{2+} chelator BAPTA. Treatment of RBL cells with 10 μM BAPTA-AM completely abolished macro-pinocytic rocketing. Subsequent titration revealed that concentrations as low as 1 μM completely abolish rocketing (Figure 5.13). Analysis of the F-actin cytoskeleton in cells treated with HOS/Perv/BAPTA revealed a striking similarity to the F-actin cytoskeleton in cells treated with HOS/Perv/wortmannin. Rather

than the characteristic F-actin rockets, cells were found to contain numerous F-actin decorated vesicles which were often found clustered close to the plasma membrane. Whether these were 'aborted' rockets or not is not at present clear, and their identification would be a priority experiment for future studies *in vivo*.

8. Phenylarsine oxide.

Phenylarsine oxide (PAO) is a membrane permeant phosphotyrosine phosphatase inhibitor and was tested as a substitute for pervanadate. Surprisingly a combination of hyperosmolarity and PAO did not induce macro-pinocytic rocketing but did induce distinctive changes in the F-actin cytoskeleton (Figure 5.14). This can be explained if the specificities of PAO and pervanadate for phosphotyrosine phosphatases do not coincide.

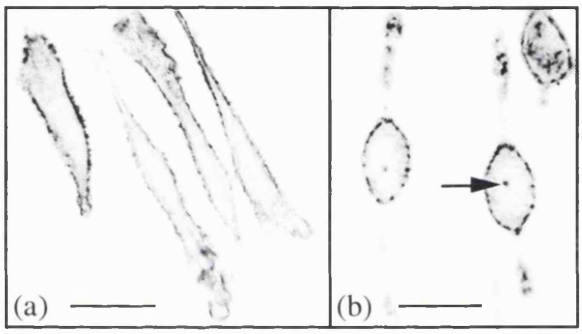

Figure 5.14: The effects of phenylarsine oxide (PAO) on resting RBLs and RBLs stimulated to produce macro-pinocytic rockets.

RBL cells were incubated with (a) HBS/HOS or (b) HBS/HOS + 50 μM PAO for 45 min. Co-stimulation with hyperosmotic shock and PAO does not induce macro-pinocytic rocketing, but induces the accumulation of F-actin in characteristic perinuclear foci (arrow in (b).
Scale bar: 20 μm

The accumulation of F-actin at perinuclear foci elicited by a combination of hyperosmolarity and PAO was unexpected. Interestingly, a previous report has demonstrated that accumulation of caveolae in perinuclear foci can be triggered using a combination of hyperosmolarity and the serine/threonine phosphatase inhibitor okadaic acid (Parton et al., 1994). F-actin was involved in this process since it was found to be sensitive to cytochalasin D. This present observation was not pursued further.

These experiments established several key points. Firstly the finding that latrunculin B totally inhibits macro-pinocytic rocketing confirms that this phenomenon is dependent on

actin polymerisation. Secondly these experiments indicate that macro-pinocytic rocketing requires PI3-kinase and hence a 3-phosphorylated PIP. This would be consistent with a possible role for $PI(3,4,5)P_3$ in macro-pinocytic rocketing since this PIP has been shown to accumulate in mammalian cells stimulated with hyperosmotic shock and pervanadate (Meier et al., 1998) and strongly stimulates rocketing of synthetic vesicles *in vitro* (Ma et al., 1998a). This finding also supports the model proposed in Chapter 4, suggesting that macro-pinocytic rocketing arises through exaggeration of a step during macro-pinocytic cup closure (Figure 4.14, p 118), a process known to be sensitive to low levels of wortmannin (Araki et al., 1996). Thirdly it was established that macro-pinocytic rocketing is Ca^{2+}-dependent.

These last two findings may be significant in the context of annexin II biology given that the biochemical hallmark of annexin II is Ca^{2+}-dependent association with negatively charged phospholipids (for review see Raynal and Pollard, 1994). While it has been established that annexin II shows moderate Ca^{2+}-dependent binding to phosphatidylinositol *in vitro* (Blackwood and Ernst, 1990) a thorough search of the literature failed to uncover any evidence that Ca^{2+}-dependent binding to phosphatidylinositol phosphates has been analysed for this annexin. The Ca^{2+} requirements for half maximal binding of annexin II and annexin II_2p11_2 to a variety of phosphatidylinositol phosphates would be a useful set of data in assessing the feasibility of the proposed role of annexin II in macro-pinocytic rocketing.

Other findings in this preliminary investigation need clarification. While substantial inhibition of macro-pinocytic rocketing may be significant, lack of inhibition does not effectively prove anything. This is especially true in the present study since inhibitors might not effectively work in the face of the massive stimulus dealt by pervanadate, and matters are further complicated by the varying specificities and side-effects of the different inhibitors used. To clarify these preliminary findings multiple approaches will need to be used to analyse each effector in isolation in the future.

Since a thorough and systematic analysis of the molecular basis of macro-pinocytic rocketing through the use of inhibitors was beyond the scope of this investigation a second approach was explored. It was reasoned that immunofluorescence might allow macro-pinocytic rockets to be screened *in situ* for the association of a variety of candidate proteins. These experiments are discussed below.

5.6 The molecular basis of macro-pinosome rocketing (III): Immunofluorescence analysis of macro-pinocytic rockets.

Earlier immunofluorescence analysis had established that endogenous annexin II is located at head of rocketing macro-pinosomes in stimulated cells (Figure 4.23, p 132). The

following experiments used the same experimental protocol to probe for the association of a variety of candidate proteins with macro-pinocytic rockets. Since a combination of HBS+HOS/PMA had been used to generate macro-pinocytic rockets during the initial kinetic characterisation of macro-pinocytic rockets and immunofluorescence analysis this combination of stimuli was used in the following experiments.

α-actinin and ezrin. Published data has established that membrane associated actin, annexin II, ezrin and moesin form a cholesterol-dependent complex associated with cellular membranes (Harder et al., 1997). Furthermore both α-actinin and ezrin have been found to associate with the actin tails produced by *Listeria* (Nanavati et al., 1994; Sechi et al., 1997; Temm Grove et al., 1994) and α-actinin is essential for *Listeria* rocketing (Dold et al., 1994). The association of ezrin with macro-pinocytic rockets was analysed by immunofluorescence and revealed that this molecule does not concentrate at either the macro-pinosome responsible for rocket formation or the associated F-actin tail (Figure 5.15).

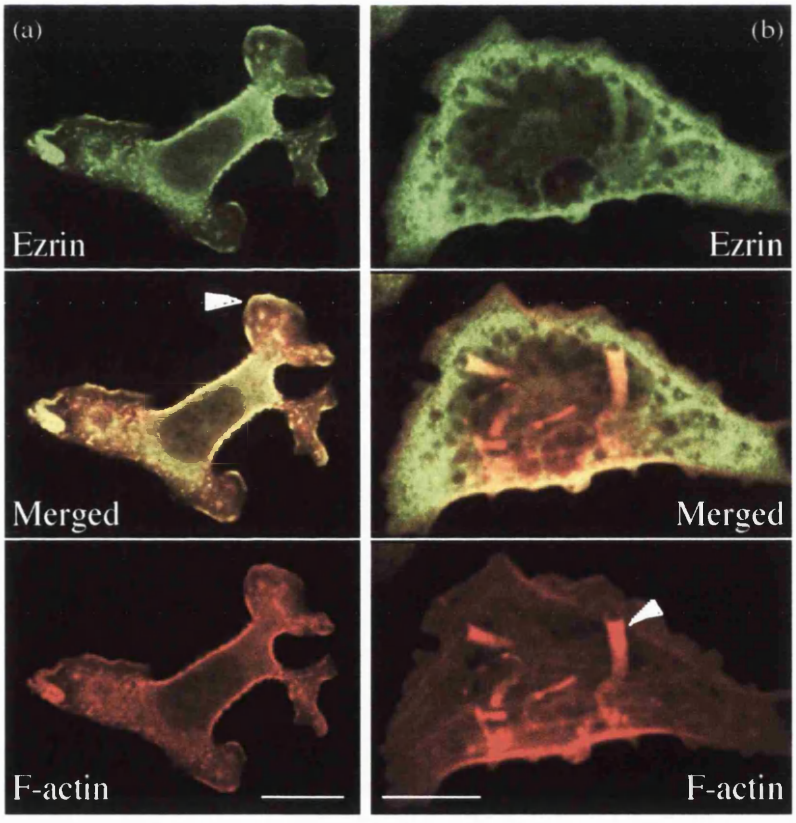

Figure 5.15: Localisation of ezrin in resting and stimulated RBL cells.

(a) In resting RBL cells ezrin colocates with F-actin at ruffles (arrow) and at the cell cortex. (b) On stimulation with HOS/PMA (see Materials and Methods) F-actin reorganises into characteristic macro-pinocytic rocket tails (arrow). Ezrin is not specifically associated with these structures (see text for details).
Scale bar: (a) 20 μm, (b) 10 μm

Earlier experiments established that macro-pinocytic rocketing was not sensitive to filipin, suggesting the annexin II/ezrin/moesin/actin complex documented by Harder et al (1997) does not play a role in macro-pinocytic rocketing. Analysis of α-actinin distribution proved inconclusive, attributable in part to the antibodies used (results not shown). It should be noted that the results of the present study do not rule out a possible association of either protein with rocketing macro-pinosomes since only one primary antibody for each protein was used.

Zyxin. Investigations into the actin dependent rocketing of *Listeria*, *Shigella* and *Vaccinia* have demonstrated the importance of poly-proline rich proteins in the mechanism of actin recruitment and tail formation (for review see Purich and Southwick, 1997; Zeile et al., 1998). Comparison of the ActA oligoproline sequence with known endogenous actin regulatory proteins has led to the identification of two consensus homology sequences designated actin based motility sequences 1 and 2 (ABM-1 and ABM-2) (Table 5.2; modified from Purich and Southwick, 1997).

Table 5.2: Endogenous cellular proteins possesssing ABM-1 or ABM-2 domains.

	Actin regulatory proteins with ABM-1 domains.
Protein.	**Comments.**
ActA	ActA is essential for actin based *Listeria monocytogenes* motility and a synthetic peptide analogue to domain ActA-2 inhibits both *Listeria* and *Shigella* motility at 20-200 nM.
Vinculin	Locates to focal contacts and has binding sites for F-actin and VASP.
Zyxin	Binds to other actin regulatory proteins including VASP.
iActa	*Listeria ivanovi* expresses a homolog of ActA, iActA which performs a similar function.

	Actin regulatory proteins with ABM-2 domains.
Protein	**Comments.**
VASP	Peptide corresponding to the repeat GPPPP motif of this protein inhibits intracellular *Listeria* and *Shigella* motility.
WASP	Mutant forms of this protein result in Wiscott-Aldrich syndrome. Required for *Shigella flexnerii* actin based motility.
N-WASP	A neuronal Grb/ASH-binding protein with 50% homology to WASP.
Ena	Shares other homology domains with VASP.
Mena	Neuronal protein sharing VASP homology domains.

Of these proteins zyxin and VASP are good candidates for an involvement in macro-pinocytic rocketing since they both possess the conserved ABM-1 sequence. Furthermore *Listeria* ActA surface protein has significant sequence homology with both proteins (Cossart, 1998). Immunofluorescence analysis revealed there was no colocation of zyxin with macro-pinocytic rockets (Figure 5.16, p157). The possible association of other candidate proteins possesssing ABM-1/ABM-2 domains with rocketing macro-pinosomes was not investigated and would be a priority in further investigations.

PAK1. As discussed previously, the serine/threonine kinase PAK1 is a good candidate for involvement in macro-pinocytic rocketing although the precise role PAK1 plays in stimulating actin polymerisation has not been established. In view of this and the published data linking Cdc42 and vesicle rocketing *in vitro*,, the possible association of macro-pinocytic rockets and PAK1 was investigated (Figure 5.17, p 158).

In stimulated cells PAK1 was found to locate to the head of rocketing macro-pinosomes where it may be involved in promoting actin polymerisation. It is interesting to note that previous studies *in vitro* have dismissed the involvement of PAK1 in vesicle rocketing since vesicle rocketing *in vitro* is not sensitive to the moderate concentrations of wortmannin which have been shown to inhibit PAK1 activity (Moreau and Way, 1998).

An intriguing and currently inexplicable feature of the association of PAK1 and the head of rocketing pinosomes is the finding that immunoreactivity was located to single, off-set foci at the tips of the F-actin rockets. Whether this is functionally significant or simply reflects a fixation artefact is unclear. Since recent results have demonstrated that dominant negative PAK1 mutants are effective at suppressing endogenous PAK1 activity (Qiu et al., 1995) these might prove useful in future experiments designed to establish if PAK1 is necessary for macro-pinocytic vesicle rocketing *in vivo*.

Phosphotyrosine. Pervanadate was found to strongly stimulate hyperosmolarity induced macro-pinosome rocketing in intact cells and has previously been shown to stimulate vesicle rocketing *in vitro* (Ma et al., 1998a; Moreau and Way, 1998). This suggests that tyrosine phosphorylation could be involved in macro-pinocytic rocketing. Furthermore recent findings have demonstrated phosphotyrosine immunoreactivity is specifically located to the head of *Vaccinia* , clathrin coated vesicle F-actin rockets and rocket tails formed in *Xenopus* oocyte extract by unidentified vesicles (Frischknecht et al., 1999). In contrast to these results analysis of the distribution of phosphotyrosine immunoreactivity in stimulated RBL cells revealed phosphotyrosine immunoreactivity was absent from the surfaces of rocketing macro-pinosomes but concentrated at the plasma membrane (Figure 5.18, p 159). However, it should be noted that different monoclonal anti-phosphotyrosine antibodies were used in the present study and the study by

Frischknecht et al and that monoclonal anti-phosphotyrosine antibodies vary in the tyrosine phosphorylated eptitopes they recognise (S.Moss, personal communication). Since rocketing macro-pinosomes have only recently been derived from the plasma membrane a difference the observed difference in phosphotyrosine immunoreactivity between suggested that molecular reorganisation involving tyrosine phosphorylation and/or dephosphorylation occurs during formation of macro-pinosome rockets.

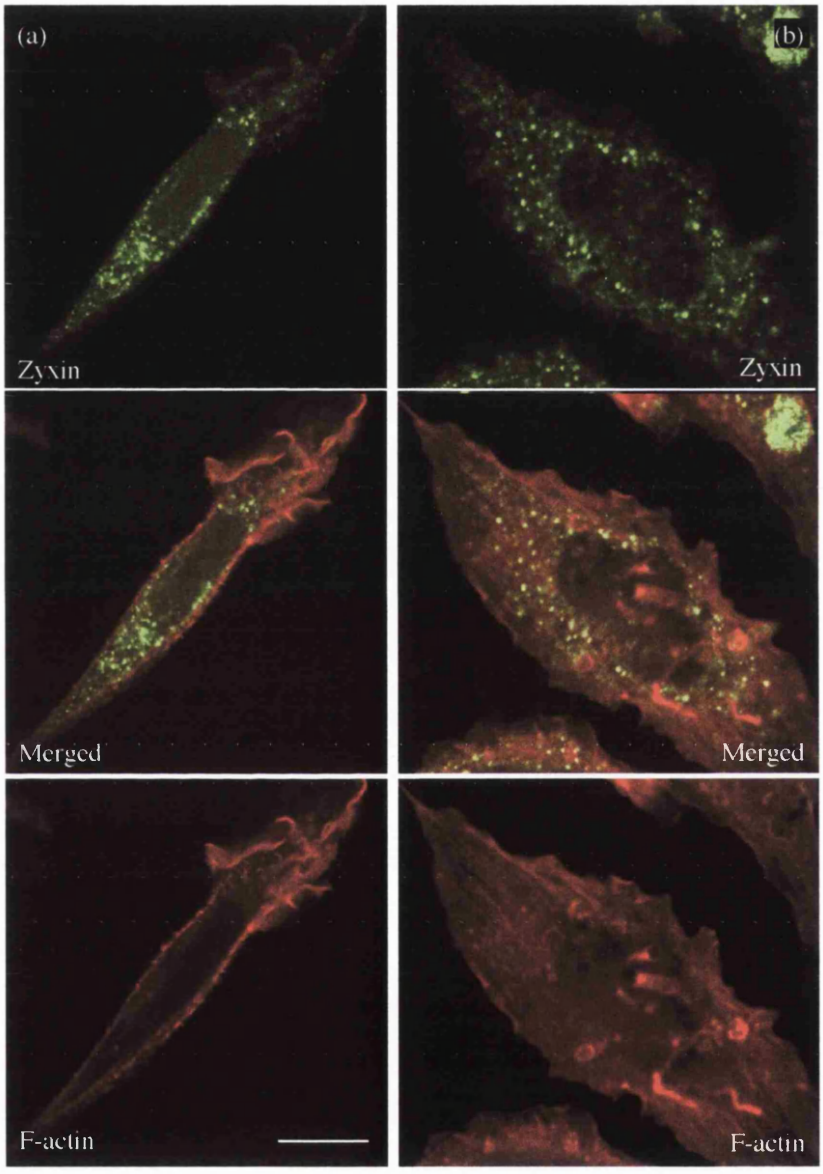

Figure 5.16: Localisation of zyxin in resting and stimulated RBL cells.

A commercially available monoclonal antibody to zyxin was used to locate zyxin in unstimulated and stimulated cells. (a) In resting RBL cells zyxin is located in discrete foci in the cytoplasm. F-actin is located at the cell cortex and in ruffles. (b) On stimulation with HOS/PMA F-actin reorganises into characteristic macro-pinocytic rocket tails. Zyxin is not associated with these structures (see text for details).
Scale bar: 10 μm

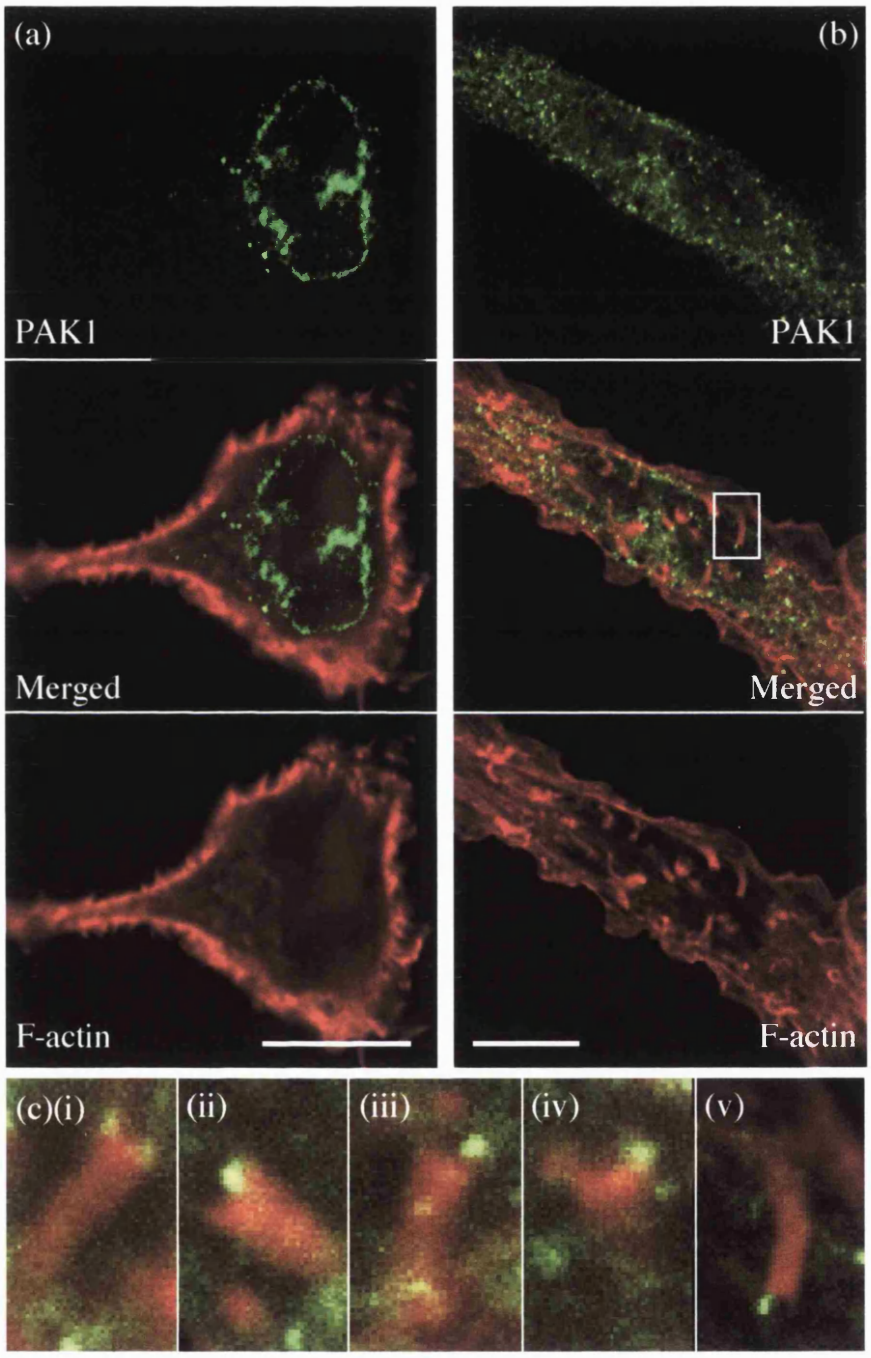

Figure 5.17: Localisation of PAK1 in resting and stimulated cells.

(a) PAK1 is found predominantly in a perinuclear location in unstimulated cells. (b) Stimulation with HOS/PMA leads to generation of characteristic rocket tails with PAK1 immunoreactivity localised to the rocket tip. (c) Close examination of a number of rocket tails shows that PAK1 immunoreactivity is often localised to a single foci at the tip of actin tails, offset from the central axis of the rocket tail ((c)(v) corresponds to boxed region in (b)(ii)).

Scale bar: 10 μm

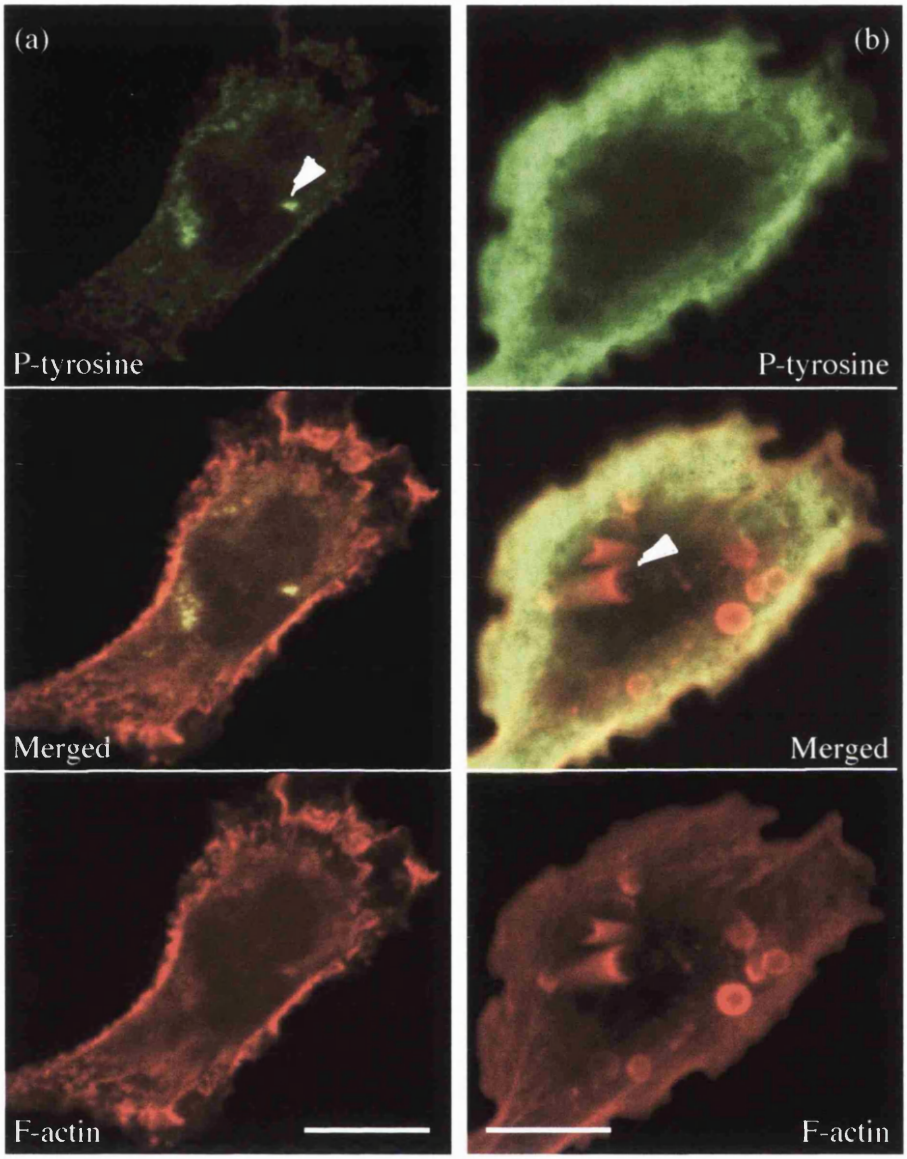

Figure 5.18: Localisation of phosphotyrosine immunoreactivity in resting and stimulated cells.

(a) In unstimulated cells immunoreactivity is restricted to punctate structures deep in the cytoplasm, often in a perinuclear location (arrow). (b) In cells stimulated with HOS/PMA phosphotyorosine immunoreactivity is restricted entirely to the plasma membrane. The antibody does not stain either the rocket tail or the newly formed macropinosome at the tip of the F-actin rocket, indicating that the plasma membrane and macropinosomes can be differentiated on the basis of phosphotyrosine immunoreactivity (see text for details).
Scale bar: 10 μm

5.7 Model of the molecular mechanism responsible for the formation of macro-pinocytic rockets.

The data from the previous experiments, evidence from microscopic observations *in vivo* (see Chapter 4) and published data on vesicle rocketing *in vitro* has been integrated in a theoretical model for the mechanism of macro-pinocytic rocketing (Figure 5.19). Also included are known interactions between components.

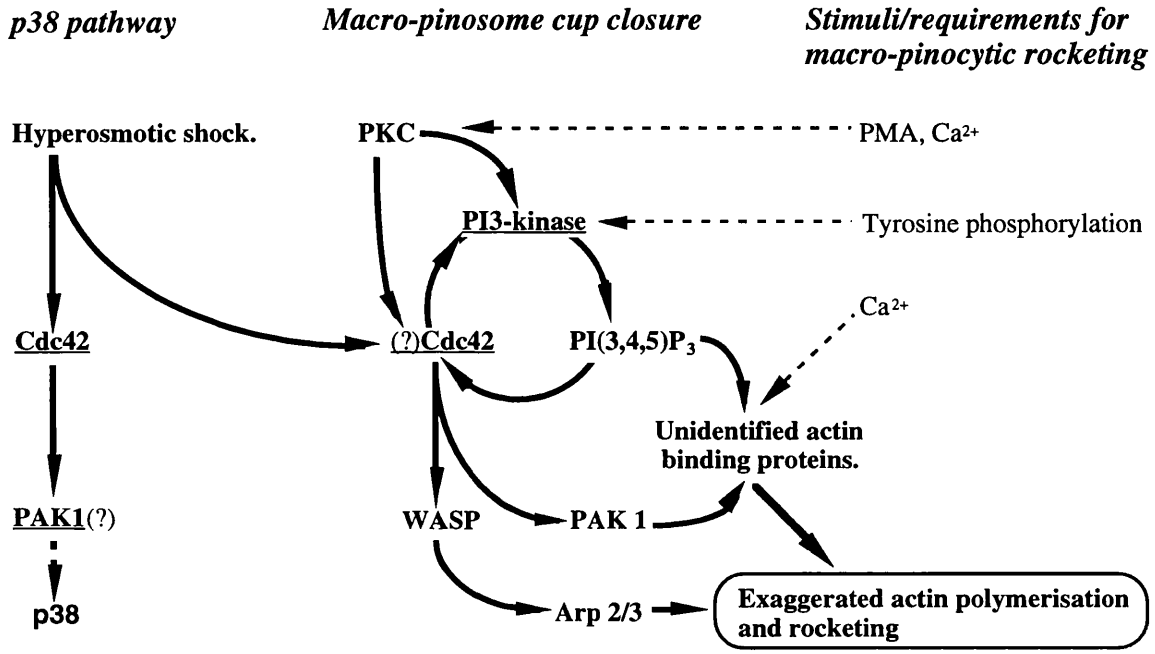

Figure 5.19: Theoretical model for the molecular mechanism responsible for the formation of rocketing macro-pinosomes.

In this theoretical model hyperosmotic shock activates the p38 MAPK pathway, components of which (such as Cdc42) are common to both the p38 MAPK path and the mechanism responsible for cup closure during macro-pinocytosis. Over-activation of Cdc42 leads to exaggerated actin polymerisation during cup closure and at the nascent macro-pinosome surface through direct interaction with actin binding proteins such as WASP[1] and Arp2/Arp3 complex[2], or indirectly through PAK1[3] (and unidentified effectors). Since it has been demonstrated that Cdc42 can directly activate PI3-kinase[4] and that $PI(3,4,5)P_3$ acts upstream of Cdc42 in promoting actin polymerisation at the surface of rocketing synthetic vesicles[5], a positive feedback loop could maintain continued actin polymerisation (see text for details). Since PMA stimulates macro-pinocytosis, PKC acts upstream of either PI3-kinase or Cdc42. A combination of hyperosmolarity and pervanadate activates the production of $PI(3,4,5)P_3$ through PI3-kinase[6]. A requirement for Ca^{2+} could act at the level of PKC recruitment or at the level of unidentified membrane/actin binding proteins involved in actin polymerisation at the membrane surface. (Refs: [1](Symons et al., 1996), [2](Ma et al., 1998b; Machesky and Insall, 1998), [3](Daniels et al., 1998; Dharmawardhane et al., 1997; Zhang et al., 1995), [4](Zheng et al., 1994), [5](Ma et al., 1998a), [6](Meier et al., 1998)).

This theoretical model has some interesting properties. While researching components which might be involved in macro-pinocytic rocketing (both implicated and proposed) it was noted that a positive feedback loop could exist at the centre of the mechanism responsible for macro-pinocytic rocketing. This hypothesis is based on the published findings that Cdc42 can bind to and activate PI3-kinase (Zheng et al., 1994) and that $PI(3,4,5)P_3$ acts upstream of Cdc42 in promoting actin polymerisation at the surface of rocketing synthetic vesicles (Ma et al., 1998a). Thus activation of PI3-kinase by Cdc42 would lead to increased levels of $PI(3,4,5)P_3$ at the pinosome surface, which would result in increased Cdc42 activation, which would complete the loop by activating PI3-kinase. The notion of a positive feedback loop is attractive since it could help explain the observed rapid initiation and termination of macro-pinocytic rocketing. Initiation of the loop would lead to rapid amplification of actin recruitment and tail formation, while breaking the loop would lead to a rapid termination of actin polymerisation and consequently vesicle locomotion.

It was also noted that the poly-proline rich Wiskot-Aldrich sydrome protein (WASP) is an attractive candidate for an ABM-2 domain protein in macro-pinocytic rocketing. WASP is necessary for actin polymerisation propelled locomotion of *Shigella flexnerii* (Suzuki et al., 1998) and is a known effector of Cdc42 (Symons et al., 1996) and can directly activate Arp2/3 (Machesky and Insall, 1998). Immunocytochemical analysis of WASP in RBL cells stimulated to produce rocketing macro-pinosomes would be a interesting experiment for future studies.

Interestingly it was also noted that both WASP and PAK1 have been shown to interact directly with the Src homology domain 2 and 3 (SH2 and SH3) containing adaptor protein Nck. PAK1 binds to the second N-terminal Src homology 3 (SH3) domain of Nck (Bokoch et al., 1996) and Nck can mediate the relocation and activation of PAK1 (Lu et al., 1997) while WASP can bind to the C-terminal SH3 domain of Nck (Rivero-Lezcano et al., 1995). This would suggest that Nck could serve to colocate PAK1 and WASP.

5.8 Conclusions.

It has been shown that while macro-pinocytosis is not stimulated by hyperosmotic shock, the phenomenon of macro-pinocytic rocketing is directly related to this cellular stress. Specifically while PMA or pervanadate alone do not elicit macro-pinocytic rockets, co-stimulation using either agonist and hyperosmotic shock does. There is some evidence to suggest that there are (at least) two branches involved in the stimulation of this phenomenon - one involving PKC and one involving tyrosine phosphorylation - since costimulation of cells with PMA and pervanadate can elicit macro-pinocytic rockets in the absence of hyperosmotic shock.

Since hyperosmotic shock has been shown to activate highly conserved MAPK pathways in a variety of mammalian cells - the p38 MAPK pathway - it was suggested that interaction of this path and macro-pinocytosis might conspire to form macro-pinocytic rockets. In particular three known proximal components of the pathway (Rac1, Cdc42 and PAK1) and one downstream component (HSP27) are candidate effectors which may contribute to this phenomenon. In preliminary experiments the p38 inhibitor SB202190 did not affect rocketing, suggesting that HSP27 is not involved in this process. Furthermore it was found that Toxin B did not affect the incidence of macro-pinocytic rocketing either suggesting that Rac1 and Cdc42 are not involved. This finding was qualified by immunofluorescence results which demonstrated that the Cdc42 effector PAK1 locates to the head of rocketing macro-pinosomes. Since PAK1 is an effector of Cdc42 this would indirectly implicate Cdc42 in the process of macro-pinocytic rocketing.

The recent description of a Cdc42-dependent form of vesicle rocketing *in vitro* (Ma et al., 1998a; Moreau and Way, 1998) - a phenomenon strikingly similar to macro-pinocytic rocketing - lends significant weight to the idea that this small GTPase could be involved in macro-pinocytic rocketing *in vivo*. This view has been strengthened by previous results suggesting a role for Cdc42 in cup closure during phagocytosis (Massol et al., 1998), a process which is closely related to cup closure during macro-pinocytosis (Swanson et al., 1999). This is relevant to macro-pinocytic rocketing since the latter process has been proposed to be the initiation point for macro-pinocytic rocketing (this project).

Unlike vesicle rocketing *in vitro*, macro-pinocytic rocketing *in situ* is extremely sensitive to the PI3-kinase inhibitor wortmannin suggesting the involvement of a 3-phosphorylated PIP in this process. Since a direct interaction between PI3-kinase and Cdc42 has been demonstrated previously (Zheng et al., 1994) and PI3-kinase is involved in cup closure during phagocytosis and macro-pinocytosis (Araki et al., 1996) it is possible that these two effectors act in concert in the process of macro-pinocytic rocketing.

Although the Ca^{2+} requirement of vesicle rocketing *in vitro* has not (apparently) been formally analysed, it was found in the present study that macro-pinocytic rocketing is abolished by chelation of intracellular Ca^{2+}. The level at which Ca^{2+} sequestration acts is unclear, although there are several components which might be affected. Firstly, it might act at a level proximal to actin polymerisation or actin/macro-pinosome interaction. Ca^{2+} sequestration could, for instance, act at the level of PKC isoforms possesssing a C2 domain responsible for Ca^{2+}-dependent association with negatively charged phospholipids (Nalefski and Falke, 1996). Alternatively Ca^{2+} sequestration might act downstream at the level of actin/macro-pinosome interaction during actin recruitment and/or release at the macro-pinosome surface. With this in mind it is notable that the fluorescent marker with

which macro-pinocytic rockets were discovered (NAII-GFP) was a GFP chimera based on the Ca^{2+}-dependent membrane and F-actin binding protein, annexin II.

Thus far there are no apparent parallels between rocketing macro-pinosomes and rocketing intracellular bacteria with respect to the molecular mechanism of F-actin tail formation. Initial immunofluorescent analysis failed to locate a candidate poly-proline rich protein (zyxin). However there are other candidate poly-proline rich proteins whose location with respect to macro-pinocytic rockets should be analysed by immunofluorescence microscopy. Of these one of the most attractive candidates is WASP since this is a known effector of Cdc42 (Symons et al., 1996) and has recently been shown to directly activate the Arp2/3 complex (Machesky and Insall, 1998). Furthermore both WASP and the Cdc42 effector PAK1, which is known to locate to the head of macro-pinocytic rockets, bind the adaptor protein Nck, suggesting a potential mechanism by which the two proteins might be functionally linked (Bokoch et al., 1996; Rivero-Lezcano et al., 1995).

Lastly the finding that pervanadate strongly stimulates macro-pinosome rocketing is intriguing, although it is not clear at which level tyrosine phosphorylation might be involved in promoting macro-pinocytic rocketing. A recent report has revealed that co-stimulation of HEK-293 cells with pervandate and hyperosmotic shock leads to a marked accumulation of $PI(3,4,5)P_3$ through the activation of PI3-kinase(s) (Meier et al., 1998). It was noted there was an apparent synergy between hyperosmotic shock and pervanadate treatment in the accumulation of $PI(3,4,5)P_3$, although the basis of this was unclear. It is possible that tyrosine phosphorylation, stimulated by pervanadate treatment, could contribute to activation of PI3-kinase via the p85 subunit (reviewed in Fruman et al., 1998) since binding of SH2 domains of the p85 regulatory subunit of PI3-kinase with tyrosine phosphorylated target motifs increases the catalytic activity of the associated p110 subunit two to three fold (Backer et al., 1992; Carpenter et al., 1993).

Further evidence that tyrosine phosphorylation may play an active role in macro-pinosome biogenesis has come from immunofluroescence analysis using a monoclonal anti-phosphotyrosine antibody (SC-19) which revealed that a distinct difference in the distribution of tyr-phosphorylation immunoreactivity at the plasma membrane and the surface of rocketing macro-pinosomes. The surface of the latter structures are not labeled at all, suggesting that tyr-phosphorylated epitopes recognised by the antibody used (SC-19) became masked (through protein/protein interaction?) or de-phosphorylated during macro-pinocytic rocket formation. Interestingly it has recently been demonstrated that an alternative anti-phosphotyrosine antibody (4G10) specifically recognises a tyrosine phosphorylated protein(s) at the head of rocketing*Vaccinia* and clathrin coated vesicles (Frischknecht et al., 1999). Monoclonal anti-phosphotyrosine antibodies are notoriously variable in their recognition of tyrosine phosphorylated epitopes (S.Moss, personal

communication) and significantly, five other monoclonal anti-phosphotyrosine antibodies tested in the latter study did not target to the heads of rocketing *Vaccinia* (Frischknecht et al., 1999). Thus the apparent absence of tyrosine phosphorylated proteins at the surface of rocketing macro-pinosomes may be misleading, and these structures should be probed with 4G10 in the future. In a broader context rocketing macro-pinosomes may be a useful model for investigating the role of tyrosine phosphorylation in controlling actin polymerisation in the future.

6. Chapter 6 : Discussion.

6.1 Actin, annexin II and vesicle rocketing.

The aim of this project was to explore the function of annexin II in living, intact cells using GFP fusion proteins. The initial strategy was designed to explore some of the proposed functions of annexin II during Ca^{2+}-regulated exocytosis in a mast cell line and differentiation of a neuroendocrine cell line. It was established that NAII-GFP was a valid probe for annexin II since the chimera associated with the plasma membrane in intact, living PC12 cells and this property showed the same sensitivity to mutation as wild-type annexin II. However, no evidence was found to support a role for annexin II in either PC12 differentiation or stimulated exocytosis in RBL cells. Furthermore, although NAII-GFP behaved like wild-type annexin II in its requirements for plasma membrane association in intact PC12 cells, observations made in resting and stimulated RBL cells were confusing. Similar to previous observations of endogenous annexin II in chromaffin cells (Chasserot Golaz et al., 1996) NAII-GFP apparently translocated to the plasma membrane after cells were stimulated, chemically fixed and processed for fluorescence microscopy. However there was no evidence to suggest that NAII-GFP translocated to the plasma membrane in living cells.

This finding has broader implications. Immunofluorescence is one of the most widely used techniques in cell biology yet it is acknowledged that chemical fixation and subsequent permeabilisation can produce artefacts (Chandler, 1984; Melan and Sluder, 1992; Morgenstern, 1991; Robinson et al., 1996). Thus the differences between results in intact, fixed cells and live cells observed in this project may reflect properties of fixation as well as real biological phenomena. A practical way to resolve these problems would be to image NAII-GFP expressing cells throughout the entire experimental manipulation of stimulation, chemical fixation and permeabilisation *in situ*. This would allow the effects of each step in the experiment to be correlated with the observed localisation of NAII-GFP.

While the initial goals of this project were to explore some of the well established ideas about annexin II biology, the finding that NAII-GFP associates with the actin tails of rocketing vesicles *in vivo* was surprising. This finding is consistent in several ways with the biochemical hallmarks and established sub-cellular distribution of annexin II. Firstly it demonstrates the association of annexin II with an early endocytic compartment, secondly it demonstrates the association of annexin II with an actin-based structure and thirdly the process itself is Ca^{2+}-dependent.

Whether actin polymerisation plays a central role in vesicle traffic *in vivo* under physiological conditions is not clear. Classical views of transport mechanisms in vesicle traffic have been based on 'motors and tracks'. To get a vesicle from point 'a' to point 'b'

cytoskeletal trackways - either actin or tubulin - are proposed to exist between the two points. Directed transport is achieved by attaching the appropriate motors to the cargo which is then dragged along the appropriate sequence of tracks (Huang et al., 1999). The number of organelle-specific motors identified to date is consistent with this view (Goodson et al., 1997), but it remains difficult to explain how cargo finds its way to the relevant track in the first place. One could speculate that actin-polymerisation driven locomotion of vesicular compartments might be utilised in short excursions, perhaps only over distances of a few tens or hundreds of nanometers under normal physiological conditions, while longer distances are serviced by more familiar motor driven processes. In this context it is notable that published electron micrographs of annexin II and early endosomes *in situ* revealed possible annexin II 'tails' (Harder et al., 1997) hinting that early endosomes might rocket *in vivo*. Secondly a variety of actin-binding proteins including α-actinin, profilin and annexin II - all of which have now been associated with rocket tails of either vesicles or intracellular pathogens - have been located to a sub-set of endocytic compartments including early and recycling endosomes (Pol et al., 1997; Witke et al., 1998). Thirdly it has been established clathrin-coated vesicles can nucleate actin polymerisation (Kohtz et al., 1990) and more recent data showed clathrin-coated vesicles can form F-actin rocket tails *in situ* (Frischknecht et al., 1999). It appears that data is slowly accumulating to support a role for actin polymerisation in the transport of certain types of intracellular vesicle, though this will be difficult to test directly. As a first stage in further investigations the recently descibed *in vitro* system, using *Xenopus* egg extract (Ma et al., 1998a; Moreau and Way, 1998), appears particularly attractive since the rocketing capabilities of purified cellular compartments could be tested in isolation.

In addition to actual vesicle transport actin polymeriation may also be involved directly in the initial formation of these compartments. It is established that actin polymerisation plays a central role in macro-pinocytosis (Keller and Niggli, 1995) and there is evidence that both actin and annexin II are involved in other types of endocytosis. For example clathrin-mediated endocytosis in yeast requires actin (Kubler and Riezman, 1993; Munn et al., 1995; Penalver et al., 1997) as does clathrin-mediated endocytosis in some mammalian cells (Durrbach et al., 1996; Gottlieb et al., 1993; Lamaze et al., 1997) and annexin II has been implicated in endocytosis of activated insulin receptor (Biener et al., 1996). The requirement for actin remodelling in clathrin-mediated endocytosis is particularly intriguing. It has been shown that coated endosomes require actin polymerisation for fission from the apical, but not basolateral, surface of polarised epithelial cells (Gottlieb et al., 1993). Treatment with cytochalasin D caused the accumulation of coated vesicles at the apical surface of the cell, a significant proportion of which were found attached to the plasma membrane by a thin neck of membrane as though they had failed to bud. Although the process of clathrin vesicle fission has recently been

attributed to the GTPase dynamin (reveiwed in McNiven, 1998) it has been predicted the actin cytoskeleton facilitates dynamin-mediated vesicle fission by exerting a force on the newly formed endosome, thus facilitating dynamin mediated compression and severing of the membrane umbilicus (McNiven, 1998). The phenomenon of actin polymerisation powered 'vesicle launch' from the plasma membrane (this study) would be ideally suited to this function. Firstly a force would be symmetrically delivered to the nascent endosome and transmitted as a tensile load to the umbilicus, facilitating dynamin-mediated fission. Secondly, since it is known that F-actin rocket tails are hollow (this study), this propulsive mechanism would accommodate the umbilicus during the earliest stages vesicle fission. Thirdly, continued actin polymerisation would propel the newly formed endosome deeper into the cell, initiating the first step of polarised vesicle transport. This hypothesis would place vesicle rocketing at the heart of endosome fission, and indeed recent findings have demonstrated that proteins controlling actin polymerisation are essential for endocytosis in yeast, including a component of the Arp2/3 complex (Moreau et al., 1997) and the yeast homologue of WASP (Naqvi et al., 1998). It will be interesting to see whether these separate lines of investigation converge on a role for actin polymerisation in endocytosis and early endosome dynamics in the future.

Although it is feasible that annexin II might play a modulatory role in some types of endocytosis, it should be noted that studies in our laboratory have established annexin II is not essential for receptor mediated endocytosis *per se*. Thus, internalisation of the B-cell receptor (this study, data not shown) or internalisation and recycling of the transferrin receptor (Professor V.Gerke, personal communication) proceeded unhindered in annexin II-/- DT40 cells, which were indistinguishable from wild type DT40 in these experiments. Somewhat surprisingly, preliminary results using electron microscopic analysis indicate DT40 annexin II-/- cells have a 30% reduction in fluid phase endocytosis (Professor V.Gerke, personal communication) although the basis of this finding is unclear.

It is tempting to speculate that the discovery of NAII-GFP labeled macro-pinocytic rockets could have implications for other proposed functions of annexin II. One of the longest standing notions has been that annexin II is involved in Ca^{2+}-regulated exocytosis, the evidence for which is discussed elsewhere. Would involvement of annexin II in membrane/actin interactions be consistent with a role in exocytosis? There are several reasons for believing that this may be possible.

Although the precise role of the actin cortex in Ca^{2+} regulated exocytosis is unclear it was established some time ago that the actin cortex disassembles prior to exocytosis (Koffer et al., 1990; Sontag et al., 1988). This prompted the proposal that cortical actin disassembly, controlled by actin severing proteins (Borovikov et al., 1995; Zhang et al., 1996) and GTP binding proteins (Norman et al., 1994), is a pre-requisite for efficient exocytosis as it allows secretory granules to access docking sites at the plasma membrane

(the so called 'barrier hypothesis' - (Koffer et al., 1990; Sontag et al., 1988; Vitale et al., 1995) but see (Norman et al., 1996). However, while actin remodelling certainly coincides with Ca^{2+} regulated exocytosis the dynamic events responsible for delivering secretory granules to the plasma membrane are not fully understood. In particular it is not clear whether transport of granules to the plasma membrane requires active transport, perhaps by granule-associated myosin (Burridge and Phillips, 1975).

With this in mind it is interesting that chromaffin granules can nucleate actin polymerisation *in vitro* (Miyamoto et al., 1993) and may be surrounded by an actin cage *in vivo* (Miyamoto et al., 1993; Nielsen, 1990). Secondly chromaffin granules are enriched in the actin-binding proteins annexin II (Drust and Creutz, 1991) and α-actinin (Bader and Aunis, 1983) both of which have been associated with rocketing vesicles or intracellular pathogens. Thirdly the proposed function of annexin II in Ca^{2+} regulated exocytosis may reside in the possession of a 14-3-3 homology domain (Morgan and Burgoyne, 1992a) and 14-3-3 proteins are thought to be involved in remodelling of the actin cytoskeleton during secretion (Roth and Burgoyne, 1995) though it is not known whether annexin II also modulates the actin cytoskeleton. It seems unlikely chromaffin granules form fully developed F-actin rockets during exocytosis, a related form of locomotion could occur *in vivo* during vesicle transport to the plasma membrane. This would be more analagous to 'melting' through the actin cortex, like a hot ball-bearing through ice, rather than fully developed rocketing, but would still be dependent on polarised dissassembly and assembly of F-actin, and might involve components of vesicle rocketing. However this would imply a requirement for actin polymerisation during sustained exocytosis - a notion which may be either supported (Muallem et al., 1995) or dismissed (Norman et al., 1996) according to published data. Although expression of various annexin II-GFP constructs in this study had no significant effect on stimulated exocytosis in RBL cells, it should be noted that the kinetics of secretion were not analysed in detail and so potential effects on the rates of exocytosis at different times post-stimulation may have been overlooked.

To conclude there are several aspects of annexin II biology which would be interesting to investigate further based on findings in this study. An obvious question to address concerns the molecular basis of the association of NAII-GFP with the F-actin tails of rocketing macro-pinosomes. Although mutant NAII-GFP chimeras were available for part of this project, this did not coincide with availability of the evanescent wave microscope and therefor the association of these mutants with that F-actin tail of macro-pinocytic rockets was not tested. Preliminary experiments in fixed cells indicated that none of the various annexin II-GFP chimeras suppressed the generation of rocketing macro-pinosomes (data not shown) although by examining the association of mutant annexin II-GFP chimeras with these structures *in vivo*, the domain(s) involved in binding to the F-actin tail *in vivo* might be identified. It is also possible that over-expression of mutant

annexin II-GFP chimeras might modulate other characteristics of the phenomenon (for example speed, decay rate of tail etc) in novel ways. With this in mind a dominant negative annexin II-p11 chimera has recently been shown to be effective at targeting annexin II function *in situ* (Harder and Gerke, 1993). This might prove a useful tool for probing annexin II function in the process of macro-pinocytic rocketing in the future.

6.2 Rocketing macro-pinosomes as an experimental system for studying actin/membrane interactions in the future.

More than 50 actin-binding proteins have been identified to date that directly interact with the actin cytoskeleton (see Ayscough, 1998 and references therein). These have been grouped into six functional families: monomer sequestering, filament capping, filament severing, nucleating, cross-linking and bundling. While *in vitro* data can rapidly yield information on how a given protein might interact with the actin cytoskeleton in isolation, it is difficult to reveal the cascades of interactions which undoubtedly occur *in vivo*. Even less is known about the ways in which these networks of interactions relate to extracellular signaling cues that promote actin assembly/disassembly at precise locations in the cell.

In recent years the *Listeria* system has provided a powerful *in vivo* and *in vitro* model system in which actin/membrane interactions might be modeled and systematically analysed. Since the first description of this system (Tilney and Portnoy, 1989) some 150 papers have been published on *Listeria* locomotion, indicating the high degree of interest in *Listeria* locomotion. Although the *Listeria* system has provided considerable insight into the control of actin polymerisation it possesses intrinsic limitations. Central to these limitations is the fact that *Listeria* is a highly evolved pathogen, and evolution has taylored its control over actin polymerisation to its own peculiar lifecycle. This is exemplified by the finding that actin polymerisation is dependent on one bacterially encoded protein (ActA) which has no closely related endogenous homolog for its entire sequence. It seems more likely that ActA represents a pastiche of domains (Beckerle, 1998; Cossart, 1998), combined in one molecule that can mimic the function(s) of a number of endogenous proteins. A related finding is that *Listeria* locomotion lacks some fundamental aspects of control which one would expect endogenous actin polymerisation to demonstrate *in vivo*. For instance, once moving *Listeria* continue moving for up to 30 minutes and do not appear to be under any form of cellular constraint (Nanavati et al., 1994).

A potentially more powerful strategy to study membrane/actin interactions has recently emerged in the form of an *in vitro* system utilising *Xenopus* oocyte extracts and either synthetic or unidentified (*Xenopus* oocyte) rocketing vesicles (Ma et al., 1998a; Ma et al., 1998b; Moreau and Way, 1998). This has only recently been established, and has already provided new insights into the role(s) of PIPs, the small GTPase Cdc42 and the

Arp2/3 complex in controlling actin polymerisation at membrane surfaces. With these established experimental systems in mind perhaps the most significant result of this project has been the development of a new approach for investigating actin/membrane interactions *in vivo*. This system compliments both the *Listeria* system and the *in vitro* system described previously. It allows the quantitive investigation of actin polymerisation at the surface of characterised cellular compartment *in vivo*, in mammalian cells. In future studies, macro-pinocytic rocketing *in vivo* could be used to test theories formulated using either *Listeria* or vesicle rockets *in vitro*. Preliminary experiments in this study have demonstrated that macro-pinocytic rockets can be used for direct *in vivo* kinetic analysis of actin polymerisation, immunoflourescence screening for proteins involved in this process and for screening inhibitors which might target actin polymerisation. A particularly attractive approach which has not been explored thus far would be to investigate the effects of specific dominant negative inhibitors on the phenomenon of macro-pinocytic rocketing. By co-transfecting RBL cells with GFP-actin and the appropriate constructs it should be possible to investigate the effects of dominant negative Rac1 and Cdc42 (Zhang et al., 1995), PAK1 (Daniels et al., 1998) and different PI3-kinase isoforms (Auer et al., 1998; Jiang et al., 1998) on macro-pinocytic rocketing *in vivo*. This would provide a powerful and highly specific strategy for dissecting out the molecular interactions responsible for actin recruitment to a defined biological membrane.

To conlude, there are unique characteristics of macro-pinocytic rocketing which might prove superior to established systems. The initiation of macro-pinocytic rockets occurs in less than 5 seconds, and the cessation of rocketing occurs in a similar time frame. In contrast both *Listeria* and *in vitro* vesicle rockets take at least several minutes to initiate tail formation (Moreau and Way, 1998; Nanavati et al., 1994). It is this aspect of tight control over the initiation and termination of actin polymerisation which may make macro-pinocytic rockets particularly attractive for future studies.

Appendix: Supplementary digital movies.

The following is a list of digital movies in the appending CD. For more details and scale bars please refer to the relevant figure legend in the main text (complimentary movies and figures share the same index number). All image sequences were acquired at 1 frame every 5 s unless stated otherwise in the relevant figure legend and replay at a frame rate of 10 frames/s (50 x real time). The appending CD is formatted for PC computers and will be read by any Power PC Macintosh or higher. All movies are in the QuickTime format and will be supported by any Macintosh Power PC or higher. For PC users who have not installed QuickTime the software is available free at the following web address:

http://www.apple.com/quicktime/download/index.html

These movies do not supply any information additional to that recorded in the main text of this thesis. However, it is difficult to reproduce the fluid changes in cell morphology and protein localisation which occur in live cells using static images and morphometric measurements and it is hoped these movies will ammend this shortcoming.

Movie:	Title:
Movie 4.1	NAII-GFP is associated with mobile, fusogenic vesicles.
Movie 4.2	GFP-actin dynamics in a resting RBL cell.
Movie 4.3	GFP-actin is incorporated into rocket tails behind unidentified vesicles in hyperosmotically shocked RBL cells.
Movie 4.4a	NAII-GFP dynamics in a RBL stimulated with PMA.
Movie 4.4b	GFP-actin dynamics in a RBL cell stimulated with PMA.
Movie 4.5	Co-stimulation of RBL cells expressing NAII-GFP with PMA and hyperosmotic shock induces prolific NAII-GFP rocketing.
Movie 4.6	Co-stimulation of RBL cells expressing GFP-actin with PMA and hyperosmotic shock induces prolific GFP-actin rocketing.
Movie 4.10	Dual wavelength imaging of GFP-actin and TexasRed dextran in living RBL cells stimulated to produce rocketing endosomes.
Movie 4.16a	A burst of actin polymerisation may follow arrested rocketing (overview of cell).
Movie 4.16b	A burst of actin polymerisation may follow arrested rocketing (magnified region of interest).
Movie 4.18	Rocket tails may be hollow.

References.

Aitken, A., Amess, B., Howell, S., Jones, D., Martin, H., Patel, Y., Robinson, K., and Toker, A. (1992). The role of specific isoforms of 14-3-3 protein in regulating protein kinase activity in the brain. Biochem Soc Trans *20*, 607-11.

Aledo, J. C., Lavoie, L., Volchuk, A., Keller, S. R., Klip, A., and Hundal, H. S. (1997). Identification and characterization of two distinct intracellular GLUT4 pools in rat skeletal muscle: evidence for an endosomal and an insulin-sensitive GLUT4 compartment. Biochem-J *325*, 727-32

Ali, S. M., and Burgoyne, R. D. (1990). The stimulatory effect of calpactin (annexin II) on calcium-dependent exocytosis in chromaffin cells: requirement for both the N-terminal and core domains of p36 and ATP. Cell Signal *2*, 265-76.

Ali, S. M., Geisow, M. J., and Burgoyne, R. D. (1989). A role for calpactin in calcium-dependent exocytosis in adrenal chromaffin cells. Nature *340*, 313-5

Alvarez Martinez, M. T., Mani, J. C., Porte, F., Faivre Sarrailh, C., Liautard, J. P., and Sri Widada, J. (1996). Characterization of the interaction between annexin I and profilin. Eur-J-Biochem *238*, 777-84

Alvarez Martinez, M. T., Porte, F., Liautard, J. P., and Sri Widada, J. (1997). Effects of profilin-annexin I association on some properties of both profilin and annexin I: modification of the inhibitory activity of profilin on actin polymerization and inhibition of the self-association of annexin I and its interactions with liposomes. Biochim-Biophys-Acta *1339*, 331-40

Ando, Y., Imamura, S., Hong, Y. M., Owada, M. K., Kakunaga, T., and Kannagi, R. (1989). Enhancement of calcium sensitivity of lipocortin I in phospholipid binding induced by limited proteolysis and phosphorylation at the amino terminus as analyzed by phospholipid affinity column chromatography. J-Biol-Chem *264*, 6948-55

Ando, Y., Imamura, S., Owada, M. K., and Kannagi, R. (1991). Calcium-induced intracellular cross-linking of lipocortin I by tissue transglutaminase in A431 cells. Augmentation by membrane phospholipids. J-Biol-Chem *266*, 1101-8

Apgar, J. R. (1994). Polymerization of actin in RBL-2H3 cells can be triggered through either the IgE receptor or the adenosine receptor but different signaling pathways are used. Mol Biol Cell *5*, 313-22.

Araki, N., Johnson, M. T., and Swanson, J. A. (1996). A role for phosphoinositide 3-kinase in the completion of macropinocytosis and phagocytosis by macrophages. J Cell Biol *135*, 1249-60.

Arcaro, A., and Wymann, M. P. (1993). Wortmannin is a potent phosphatidylinositol 3-kinase inhibitor: the role of phosphatidylinositol 3,4,5-trisphosphate in neutrophil responses. Biochem J *296*, 297-301.

Auer, K. L., Contessa, J., Brenz-Verca, S., Pirola, L., Rusconi, S., Cooper, G., Abo, A., Wymann, M. P., Davis, R. J., Birrer, M., and Dent, P. (1998). The Ras/Rac1/Cdc42/SEK/JNK/c-Jun cascade is a key pathway by which agonists stimulate DNA synthesis in primary cultures of rat hepatocytes. Mol Biol Cell *9*, 561-73.

Augustine, G. J., and Neher, E. (1992). Calcium requirements for secretion in bovine chromaffin cells. J Physiol *450*, 247-71.

Ayscough, K. R. (1998). In vivo functions of actin-binding proteins. Curr Opin Cell Biol *10*, 102-11.

Backer, J. M., Myers, M. G., Jr., Shoelson, S. E., Chin, D. J., Sun, X. J., Miralpeix, M., Hu, P., Margolis, B., Skolnik, E. Y., Schlessinger, J., and et al. (1992). Phosphatidylinositol 3'-kinase is activated by association with IRS-1 during insulin stimulation. Embo J *11*, 3469-79.

Bader, M. F., and Aunis, D. (1983). The 97-kD alpha-actinin-like protein in chromaffin granule membranes from adrenal medulla: evidence for localization on the cytoplasmic surface and for binding to actin filaments. Neuroscience *8*, 165-81.

Bagrodia, S., Taylor, S. J., Creasy, C. L., Chernoff, J., and Cerione, R. A. (1995). Identification of a mouse p21Cdc42/Rac activated kinase [published erratum appears in J Biol Chem 1996 Jan 12;271(2):1250]. J Biol Chem *270*, 22731-7.

Ballestrem, C., Wehrle-Haller, B., and Imhof, B. A. (1998). Actin dynamics in living mammalian cells [In Process Citation]. J Cell Sci *111*, 1649-58.

Bandorowicz-Pikula, J., Wrzosek, A., Pikula, S., and Awasthi, Y. C. (1997). Fluorescence spectroscopic studies on interactions between liver. Eur J Biochem *248*, 238-44.

Barker, S. A., Caldwell, K. K., Hall, A., Martinez, A. M., Pfeiffer, J. R., Oliver, J. M., and Wilson, B. S. (1995). Wortmannin blocks lipid and protein kinase activities associated with PI 3-kinase and inhibits a subset of responses induced by Fc epsilon R1 cross-linking. Mol Biol Cell *6*, 1145-58.

Barrowman, M. M., Cockcroft, S., and Gomperts, B. D. (1986). Two roles for guanine nucleotides in the stimulus-secretion sequence of neutrophils. Nature *319*, 504-7.

Barwise, J. L., and Walker, J. H. (1996). Annexins II, IV, V and VI relocate in response to rises in intracellular calcium in human foreskin fibroblasts. J-Cell-Sci *109*, 247-55

Beaven, M. A., and Baumgartner, R. A. (1996). Downstream signals initiated in mast cells by Fc epsilon RI and other receptors. Curr Opin Immunol *8*, 766-72.

Beaven, M. A., Maeyama, K., Wolde-Mussie, E., Lo, T. N., Ali, H., and Cunha-Melo, J. R. (1987). Mechanism of signal transduction in mast cells and basophils: studies with RBL-2H3 cells. Agents Actions *20*, 137-45.

Beaven, M. A., Rogers, J., Moore, J. P., Hesketh, T. R., Smith, G. A., and Metcalfe, J. C. (1984). The mechanism of the calcium signal and correlation with histamine release in 2H3 cells. J Biol Chem *259*, 7129-36.

Beckerle, M. C. (1998). Spatial control of actin filament assembly: lessons from Listeria. Cell *95*, 741-8.

Bellagamba, C., Hubaishy, I., Bjorge, J. D., Fitzpatrick, S. L., Fujita, D. J., and Waisman, D. M. (1997). Tyrosine phosphorylation of annexin II tetramer is stimulated by membrane binding. J-Biol-Chem *272*, 3195-9

Bennett, M. K. (1995). SNAREs and the specificity of transport vesicle targeting. Curr Opin Cell Biol *7*, 581-6.

Bennett, M. K., Garcia-Arraras, J. E., Elferink, L. A., Peterson, K., Fleming, A. M., Hazuka, C. D., and Scheller, R. H. (1993). The syntaxin family of vesicular transport receptors. Cell *74*, 863-73.

Benz, J., Bergner, A., Hofmann, A., Demange, P., Gottig, P., Liemann, S., Huber, R., and Voges, D. (1996). The structure of recombinant human annexin VI in crystals and membrane-bound. J-Mol-Biol *260*, 638-43

Bernardini, M. L., Mounier, J., d'Hauteville, H., Coquis-Rondon, M., and Sansonetti, P. J. (1989). Identification of icsA, a plasmid locus of Shigella flexneri that governs bacterial intra- and intercellular spread through interaction with F-actin. Proc Natl Acad Sci U S A *86*, 3867-71.

Bianchi, R., Garbuglia, M., Verzini, M., Giambanco, I., and Donato, R. (1994). Calpactin I binds to the glial fibrillary acidic protein (GFAP) and cosediments with glial filaments in a Ca(2+)-dependent manner: implications for concerted regulatory effects of calpactin I and S100 protein on glial filaments. Biochim-Biophys-Acta *1223*, 361-7

Bianchi, R., Giambanco, I., Ceccarelli, P., Pula, G., and Donato, R. (1992). Membrane-bound annexin V isoforms (CaBP33 and CaBP37) and annexin VI in bovine tissues behave like integral membrane proteins. FEBS-Lett *296*, 158-62

Biener, Y., Feinstein, R., Mayak, M., Kaburagi, Y., Kadowaki, T., and Zick, Y. (1996). Annexin II is a novel player in insulin signal transduction. Possible association between annexin II phosphorylation and insulin receptor internalization. J-Biol-Chem *271*, 29489-96

Blackwood, R. A., and Ernst, J. D. (1990). Characterization of Ca2(+)-dependent phospholipid binding, vesicle aggregation and membrane fusion by annexins. Biochem-J *266*, 195-200

Blanchard, S., Barwise, J. L., Gerke, V., Goodall, A., Vaughan, P. F., and Walker, J. H. (1996). Annexins in the human neuroblastoma SH-SY5Y: demonstration of relocation of annexins II and V to membranes in response to elevation of intracellular calcium by membrane depolarisation and by the calcium ionophore A23187. J-Neurochem *67*, 805-13

Block, M. R., Glick, B. S., Wilcox, C. A., Wieland, F. T., and Rothman, J. E. (1988). Purification of an N-ethylmaleimide-sensitive protein catalyzing vesicular transport. Proc Natl Acad Sci U S A *85*, 7852-6.

Bock, J. B., Klumperman, J., Davanger, S., and Scheller, R. H. (1997). Syntaxin 6 functions in trans-Golgi network vesicle trafficking. Mol Biol Cell *8*, 1261-71.

Bokoch, G. M., Wang, Y., Bohl, B. P., Sells, M. A., Quilliam, L. A., and Knaus, U. G. (1996). Interaction of the Nck adapter protein with p21-activated kinase (PAK1). J Biol Chem *271*, 25746-9.

Bommert, K., Charlton, M. P., DeBello, W. M., Chin, G. J., Betz, H., and Augustine, G. J. (1993). Inhibition of neurotransmitter release by C2-domain peptides implicates synaptotagmin in exocytosis. Nature *363*, 163-5.

Bomsel, M., de Paillerets, C., Weintraub, H., and Alfsen, A. (1988). Biochemical and functional characterization of three types of coated vesicles in bovine adrenocortical cells: implication in the intracellular traffic. Biochemistry *27*, 6806-13.

Bootman, M. D., and Berridge, M. J. (1996). Subcellular Ca2+ signals underlying waves and graded responses in HeLa cells. Curr Biol *6*, 855-65.

Borovikov, Y. S., Norman, J. C., Price, L. S., Weeds, A., and Koffer, A. (1995). Secretion from permeabilised mast cells is enhanced by addition of gelsolin: contrasting effects of endogenous gelsolin. J Cell Sci *108*, 657-66.

Brambilla, R., Zippel, R., Sturani, E., Morello, L., Peres, A., and Alberghina, L. (1991). Characterization of the tyrosine phosphorylation of calpactin I (annexin II) induced by platelet-derived growth factor. Biochem-J *278*, 447-52

Brewster, J. L., de Valoir, T., Dwyer, N. D., Winter, E., and Gustin, M. C. (1993). An osmosensing signal transduction pathway in yeast. Science *259*, 1760-3.

Broadie, K., Prokop, A., Bellen, H. J., O'Kane, C. J., Schulze, K. L., and Sweeney, S. T. (1995). Syntaxin and synaptobrevin function downstream of vesicle docking in Drosophila. Neuron *15*, 663-73.

Brose, N., Petrenko, A. G., Sudhof, T. C., and Jahn, R. (1992). Synaptotagmin: a calcium sensor on the synaptic vesicle surface. Science *256*, 1021-5.

Brown, D. A., and London, E. (1997). Structure of detergent-resistant membrane domains: does phase separation occur in biological membranes? Biochem Biophys Res Commun *240*, 1-7.

Burger, A., Berendes, R., Liemann, S., Benz, J., Hofmann, A., Gottig, P., Huber, R., Gerke, V., Thiel, C., Romisch, J., and Weber, K. (1996). The crystal structure and ion channel activity of human annexin II, a peripheral membrane protein. J-Mol-Biol *257*, 839-47

Burgoyne, R. D., and Morgan, A. (1990). Evidence for a role of calpactin in calcium-dependent exocytosis. Biochem-Soc-Trans *18*, 1101-4

Burgoyne, R. D., Cambray Deakin, M. A., and Norman, K. M. (1989). Developmental regulation of tyrosine kinase substrate p36 (calpactin heavy chain) in rat cerebellum. J Mol Neurosci *1*, 47-54.

Burridge, K., and Phillips, J. H. (1975). Association of actin and myosin with secretory granule membranes. Nature *254*, 526-9.

Calvert, C. M., Gant, S. J., and Bowles, D. J. (1996). Tomato annexins p34 and p35 bind to F-actin and display nucleotide. Plant Cell *8*, 333-42.

Cande, W. Z. (1990). Centrosomes: composition and reproduction. Curr Opin Cell Biol *2*, 301-5.

Caohuy, H., Srivastava, M., and Pollard, H. B. (1996). Membrane fusion protein synexin (annexin VII) as a Ca2+/GTP sensor in exocytotic secretion. Proc-Natl-Acad-Sci-U-S-A *93*, 10797-802

Carpenter, C. L., Auger, K. R., Chanudhuri, M., Yoakim, M., Schaffhausen, B., Shoelson, S., and Cantley, L. C. (1993). Phosphoinositide 3-kinase is activated by phosphopeptides that bind to the SH2 domains of the 85-kDa subunit. J Biol Chem *268*, 9478-83.

Carter, C., Howlett, A. R., Martin, G. S., and Bissell, M. J. (1986). The tyrosine phosphorylation substrate p36 is developmentally regulated in embryonic avian limb and is induced in cell culture. J Cell Biol *103*, 2017-24.

Casey, K. A., Maurey, K. M., and Storrie, B. (1986). Characterization of early compartments in fluid phase pinocytosis: a cell fractionation study. J Cell Sci *83*, 119-33.

Cesarman, G. M., Guevara, C. A., and Hajjar, K. A. (1994). An endothelial cell receptor for plasminogen/tissue plasminogen activator (t-PA). II. Annexin II-mediated enhancement of t-PA-dependent plasminogen activation. J-Biol-Chem *269*, 21198-203

Chalfie, M., Tu, Y., Euskirchen, G., Ward, W. W., and Prasher, D. C. (1994). Green fluorescent protein as a marker for gene expression. Science *263*, 802-5.

Chandler, C. E., and Herschman, H. R. (1983). Binding, sequestration, and processing of epidermal growth factor and nerve growth factor by PC12 cells. J Cell Physiol *114*, 321-7.

Chandler, D. E. (1984). Comparison of quick-frozen and chemically fixed sea-urchin eggs: structural evidence that cortical granule exocytosis is preceded by a local increase in membrane mobility. J Cell Sci *72*, 23-36.

Chapman, E. R., An, S., Edwardson, J. M., and Jahn, R. (1996). A novel function for the second C2 domain of synaptotagmin. Ca2+- triggered dimerization. J Biol Chem *271*, 5844-9.

Chapman, E. R., Hanson, P. I., An, S., and Jahn, R. (1995). Ca2+ regulates the interaction between synaptotagmin and syntaxin 1. J Biol Chem *270*, 23667-71.

Chasserot Golaz, S., Vitale, N., Sagot, I., Delouche, B., Dirrig, S., Pradel, L. A., Henry, J. P., Aunis, D., and Bader, M. F. (1996). Annexin II in exocytosis: catecholamine secretion requires the translocation of p36 to the subplasmalemmal region in chromaffin cells. J-Cell-Biol *133*, 1217-36

Cheek, T. R., Jackson, T. R., O'Sullivan, A. J., Moreton, R. B., Berridge, M. J., and Burgoyne, R. D. (1989). Simultaneous measurements of cytosolic calcium and secretion in single bovine adrenal chromaffin cells by fluorescent imaging of fura-2 in cocultured cells. J Cell Biol *109*, 1219-27.

Cheney, R. E., and Willard, M. B. (1989). Characterization of the interaction between calpactin I and fodrin (non-erythroid spectrin). J-Biol-Chem *264*, 18068-75

Chiang, Y., Davis, R. G., and Vishwanatha, J. K. (1996). Altered expression of annexin II in human B-cell lymphoma cell lines. Biochim-Biophys-Acta *1313*, 295-301 *LHM: This title is currently taken by UCL: Medical Sciences ISSN: 0006-3002.

Chung, C. Y., and Erickson, H. P. (1994). Cell surface annexin II is a high affinity receptor for the alternatively spliced segment of tenascin-C. J-Cell-Biol *126*, 539-48

Clary, D. O., Griff, I. C., and Rothman, J. E. (1990). SNAPs, a family of NSF attachment proteins involved in intracellular membrane fusion in animals and yeast. Cell *61*, 709-21.

Clerk, A., and Sugden, P. H. (1997). Activation of p21-activated protein kinase alpha (alpha PAK) by hyperosmotic shock in neonatal ventricular myocytes. FEBS Lett *403*, 23-5.

Cole, S. P., Pinkoski, M. J., Bhardwaj, G., and Deeley, R. G. (1992). Elevated expression of annexin II (lipocortin II, p36) in a multidrug resistant small cell lung cancer cell line. Br-J-Cancer *65*, 498-502

Concha, N. O., Head, J. F., Kaetzel, M. A., Dedman, J. R., and Seaton, B. A. (1992). Annexin V forms calcium-dependent trimeric units on phospholipid vesicles. FEBS-Lett *314*, 159-62

Cossart, P. (1998). Interactions of the bacterial pathogen Listeria monocytogenes with. Folia Microbiol *43*, 291-303.

Craxton, M., and Goedert, M. (1995). Synaptotagmin V: a novel synaptotagmin isoform expressed in rat brain. FEBS Lett *361*, 196-200.

Creutz, C. E. (1981). cis-Unsaturated fatty acids induce the fusion of chromaffin granules aggregated by synexin. J-Cell-Biol *91*, 247-56

Creutz, C. E., Moss, S., Edwardson, J. M., Hide, I., and Gomperts, B. (1992). Differential recognition of secretory vesicles by annexins. European Molecular Biology Organization Course "Advanced Techniques for Studying Secretion". Biochem-Biophys-Res-Commun *184*, 347-52

Creutz, C. E., Pazoles, C. J., and Pollard, H. B. (1978). Identification and purification of an adrenal medullary protein (synexin) that causes calcium-dependent aggregation of isolated chromaffin granules. J-Biol-Chem *253*, 2858-66

Creutz, C. E., Pazoles, C. J., and Pollard, H. B. (1979). Self-association of synexin in the presence of calcium. Correlation with synexin-induced membrane fusion and examination of the structure of synexin aggregates. J-Biol-Chem *254*, 553-8

Creutz, C. E., Zaks, W. J., Hamman, H. C., Crane, S., Martin, W. H., Gould, K. L., Oddie, K. M., and Parsons, S. J. (1987). Identification of chromaffin granule-binding proteins. Relationship of the chromobindins to calelectrin, synhibin, and the tyrosine kinase substrates p35 and p36. J-Biol-Chem *262*, 1860-8

Crowe, W. E., Altamirano, J., Huerto, L., and Alvarez-Leefmans, F. J. (1995). Volume changes in single N1E-115 neuroblastoma cells measured with a fluorescent probe. Neuroscience *69*, 283-96.

Cudmore, S., Cossart, P., Griffiths, G., and Way, M. (1995). Actin-based motility of vaccinia virus. Nature *378*, 636-8.

Cudmore, S., Reckmann, I., Griffiths, G., and Way, M. (1996). Vaccinia virus: a model system for actin-membrane interactions. J Cell Sci *109*, 1739-47.

Dai, J., Ting-Beall, H. P., and Sheetz, M. P. (1997). The secretion-coupled endocytosis correlates with membrane tension changes in RBL 2H3 cells. J Gen Physiol *110*, 1-10.

Daniels, R. H., Hall, P. S., and Bokoch, G. M. (1998). Membrane targeting of p21-activated kinase 1 (PAK1) induces neurite outgrowth from PC12 cells. Embo J *17*, 754-64.

Daro, E., van der Sluijs, P., Galli, T., and Mellman, I. (1996). Rab4 and cellubrevin define different early endosome populations on the pathway of transferrin receptor recycling. Proc Natl Acad Sci U S A *93*, 9559-64.

de Bruin, W. C., Leenders, W. P., Moshage, H., and van Haelst, U. J. (1996). Species specificity for HBsAg binding protein endonexin II. J-Hepatol *24*, 265-70 issn: 0168-8278.

de la Fuente, M., and Ossa, C. G. (1997). Binding to phosphatidyl serine membranes causes a conformational change in the concave face of annexin I. Biophys-J *72*, 383-7

de la Fuente, M., and Parra, A. V. (1995). Vesicle aggregation by annexin I: role of a secondary membrane binding site. Biochemistry *34*, 10393-9

Delouche, B., Pradel, L. A., and Henry, J. P. (1997). Phosphorylation by protein kinase C of annexin 2 in chromaffin cells stimulated by nicotine. J-Neurochem *68*, 1720-7

Demange, P., Voges, D., Benz, J., Liemann, S., Gottig, P., Berendes, R., Burger, A., and Huber, R. (1994). Annexin V: the key to understanding ion selectivity and voltage. Trends Biochem Sci *19*, 272-6.

Desjardins, M., Celis, J. E., van Meer, G., Dieplinger, H., Jahraus, A., Griffiths, G., and Huber, L. A. (1994). Molecular characterization of phagosomes. J-Biol-Chem *269*, 32194-200

Dharmawardhane, S., Sanders, L. C., Martin, S. S., Daniels, R. H., and Bokoch, G. M. (1997). Localization of p21-activated kinase 1 (PAK1) to pinocytic vesicles and cortical actin structures in stimulated cells. J Cell Biol *138*, 1265-78.

Diakonova, M., Gerke, V., Ernst, J., Liautard, J. P., van der Vusse, G., and Griffiths, G. (1997). Localization of five annexins in J774 macrophages and on isolated phagosomes. J-Cell-Sci *110*, 1199-213

Dillon, S. T., Rubin, E. J., Yakubovich, M., Pothoulakis, C., LaMont, J. T., Feig, L. A., and Gilbert, R. J. (1995). Involvement of Ras-related Rho proteins in the mechanisms of action of Clostridium difficile toxin A and toxin B. Infect Immun *63*, 1421-6.

Dold, F. G., Sanger, J. M., and Sanger, J. W. (1994). Intact alpha-actinin molecules are needed for both the assembly of actin into the tails and the locomotion of Listeria monocytogenes inside infected cells. Cell Motil Cytoskeleton *28*, 97-107.

Doyle, T., and Botstein, D. (1996). Movement of yeast cortical actin cytoskeleton visualized in vivo. Proc Natl Acad Sci U S A *93*, 3886-91.

Drust, D. S., and Creutz, C. E. (1988). Aggregation of chromaffin granules by calpactin at micromolar levels of calcium. Nature *331*, 88-91

Drust, D. S., and Creutz, C. E. (1991). Differential subcellular distribution of p36 (the heavy chain of calpactin I) and other annexins in the adrenal medulla. J-Neurochem *56*, 469-78

Dubois, T., Oudinet, J. P., Mira, J. P., and Russo Marie, F. (1996). Annexins and protein kinases C. Biochim-Biophys-Acta *1313*, 290-4

Durrbach, A., Louvard, D., and Coudrier, E. (1996). Actin filaments facilitate two steps of endocytosis. J-Cell-Sci *109*, 457-65

Eberhard, D. A., Brown, M. D., and VandenBerg, S. R. (1994). Alterations of annexin expression in pathological neuronal and glial reactions. Immunohistochemical localization of annexins I, II (p36 and p11 subunits), IV, and VI in the human hippocampus. Am-J-Pathol *145*, 640-9

Elferink, L. A., Peterson, M. R., and Scheller, R. H. (1993). A role for synaptotagmin (p65) in regulated exocytosis. Cell *72*, 153-9.

Emans, N., Gorvel, J. P., Walter, C., Gerke, V., Kellner, R., Griffiths, G., and Gruenberg, J. (1993). Annexin II is a major component of fusogenic endosomal vesicles. J-Cell-Biol *120*, 1357-69

Erikson, E., and Erikson, R. L. (1980). Identification of a cellular protein substrate phosphorylated by the avian sarcoma virus-transforming gene product. Cell *21*, 829-36.

Erikson, E., Tomasiewicz, H. G., and Erikson, R. L. (1984). Biochemical characterization of a 34-kilodalton normal cellular substrate of pp60v-src and an associated 6-kilodalton protein. Mol Cell Biol *4*, 77-85.

Ernst, J. D., Hoye, E., Blackwood, R. A., and Mok, T. L. (1991). Identification of a domain that mediates vesicle aggregation reveals functional diversity of annexin repeats. J-Biol-Chem *266*, 6670-3

Favier Perron, B., Lewit Bentley, A., and Russo Marie, F. (1996). The high-resolution crystal structure of human annexin III shows subtle differences with annexin V. Biochemistry *35*, 1740-4

Fernando, K. C., and Barritt, G. J. (1996). Pinocytosis in 2,5-di-tert-butylhydroquinone-stimulated hepatocytes and evaluation of its role in Ca2+ inflow. Mol Cell Biochem *162*, 23-9.

Fielding, P. E., and Fielding, C. J. (1995). Plasma membrane caveolae mediate the efflux of cellular free cholesterol. Biochemistry *34*, 14288-92

Fiorentini, C., Arancia, G., Paradisi, S., Donelli, G., Giuliano, M., Piemonte, F., and Mastrantonio, P. (1989). Effects of Clostridium difficile toxins A and B on cytoskeleton organization in HEp-2 cells: a comparative morphological study. Toxicon *27*, 1209-18.

Fischer, M., Kaech, S., Knutti, D., and Matus, A. (1998). Rapid actin-based plasticity in dendritic spines. Neuron *20*, 847-54.

Fox, M. T., Prentice, D. A., and Hughes, J. P. (1991). Increases in p11 and annexin II proteins correlate with differentiation in the PC12 pheochromocytoma. Biochem-Biophys-Res-Commun *177*, 1188-93

Frischknecht, F., Cudmore, S., Moreau, V., Reckman, I., Rottger, S., and Way, M. (1999). Tyrosine phosphorylation is required for actin-based motility of vaccinia but not *Listeria* or *Shigella*. Curr Biol *9*, 89-92.

Fruman, D. A., Meyers, R. E., and Cantley, L. C. (1998). Phosphoinositide kinases. Annu Rev Biochem *67*, 481-507.

Fukuda, M., Aruga, J., Niinobe, M., Aimoto, S., and Mikoshiba, K. (1994). Inositol-1,3,4,5-tetrakisphosphate binding to C2B domain of IP4BP/synaptotagmin II. J Biol Chem *269*, 29206-11.

Futter, C. E., Felder, S., Schlessinger, J., Ullrich, A., and Hopkins, C. R. (1993). Annexin I is phosphorylated in the multivesicular body during the processing of the epidermal growth factor receptor. J-Cell-Biol *120*, 77-83

Galcheva-Gargova, Z., Derijard, B., Wu, I. H., and Davis, R. J. (1994). An osmosensing signal transduction pathway in mammalian cells. Science *265*, 806-8.

Garbuglia, M., Bianchi, R., Verzini, M., Giambanco, I., and Donato, R. (1995). Annexin II2-p11(2) (calpactin I) stimulates the assembly of GFAP in a calcium- and pH-dependent manner. Biochem-Biophys-Res-Commun *208*, 901-9

Geisow, M., Childs, J., Dash, B., Harris, A., Panayotou, G., Sudhof, T., and Walker, J. H. (1984). Cellular distribution of three mammalian Ca2+-binding proteins related to Torpedo calelectrin. EMBO-J *3*, 2969-74

Geppert, M., Goda, Y., Hammer, R. E., Li, C., Rosahl, T. W., Stevens, C. F., and Sudhof, T. C. (1994). Synaptotagmin I: a major Ca2+ sensor for transmitter release at a central synapse. Cell *79*, 717-27.

Gerke, V., and Moss, S. E. (1997). Annexins and membrane dynamics. Biochim Biophys Acta *1357*, 129-54.

Gerke, V., and Weber, K. (1984). Identity of p36K phosphorylated on Rous sarcoma virus transformation with a protein purified from brush borders; calcium dependent binding to brush non-erythroid spectrin and F-actin. EMBO-J *3*, 227-233.

Gerke, V., and Weber, K. (1985). The regulatory chain in the p36-kd substrate complex of viral tyrosine-. Embo J *4*, 2917-20.

Glenney, J. (1986a). Phospholipid-dependent Ca2+ binding by the 36-kDa tyrosine kinase. J Biol Chem *261*, 7247-52.

Glenney, J. (1986b). Two related but distinct forms of the Mr 36,000 tyrosine kinase substrate (calpactin) that interact with phospholipid and actin in a Ca2+-dependent manner. Proc-Natl-Acad-Sci-U-S-A *83*, 4258-62

Glenney, J. R., Jr. (1985). Phosphorylation of p36 in vitro with pp60src. Regulation by Ca2+ and phospholipid. FEBS-Lett *192*, 79-82

Glenney, J. R., Jr., and Tack, B. F. (1985). Amino-terminal sequence of p36 and associated p10: identification of the site of tyrosine phosphorylation and homology with S-100. Proc Natl Acad Sci U S A *82*, 7884-8.

Glenney, J. R., Jr., Tack, B., and Powell, M. A. (1987). Calpactins: two distinct Ca++-regulated phospholipid- and actin-binding proteins isolated from lung and placenta. J-Cell-Biol *104*, 503-11

Glenney, J., and Zokas, L. (1988). Antibodies to the N-terminus of calpactin II (p35) affect Ca2+ binding and phosphorylation by the epidermal growth factor receptor in vitro. Biochemistry *27*, 2069-76

Gomperts, B. D., Barrowman, M. M., and Cockcroft, S. (1986). Dual role for guanine nucleotides in stimulus-secretion coupling. Fed Proc *45*, 2156-61.

Goodson, H. V., Valetti, C., and Kreis, T. E. (1997). Motors and membrane traffic. Curr Opin Cell Biol *9*, 18-28.

Gottlieb, T. A., Ivanov, I. E., Adesnik, M., and Sabatini, D. D. (1993). Actin microfilaments play a critical role in endocytosis at the apical but not the basolateral surface of polarized epithelial cells. J-Cell-Biol *120*, 695-710

Gould, K. L., Cooper, J. A., and Hunter, T. (1984). The 46,000-dalton tyrosine protein kinase substrate is widespread, whereas the 36,000-dalton substrate is only expressed at high levels in certain rodent tissues. J Cell Biol *98*, 487-97.

Graham, M. E., Gerke, V., and Burgoyne, R. D. (1997). Modification of annexin II expression in PC12 cell lines does not affect Ca(2+)-dependent exocytosis. Mol-Biol-Cell *8*, 431-42

Grandori, C., and Hanafusa, H. (1988). p60c-src is complexed with a cellular protein in subcellular compartments involved in exocytosis. J Cell Biol *107*, 2125-35.

Greenberg, M. E., Brackenbury, R., and Edelman, G. M. (1984). Changes in the distribution of the 34-kdalton tyrosine kinase substrate during differentiation and maturation of chicken tissues. J Cell Biol *98*, 473-86.

Greene, L. A., and Tischler, A. S. (1976). Establishment of a noradrenergic clonal line of rat adrenal pheochromocytoma cells which respond to nerve growth factor. Proc Natl Acad Sci U S A *73*, 2424-8.

Hackstadt, T. (1996). The biology of rickettsiae. Infect Agents Dis *5*, 127-43.

Hajjar, K. A., Jacovina, A. T., and Chacko, J. (1994). An endothelial cell receptor for plasminogen/tissue plasminogen activator. I. Identity with annexin II. J-Biol-Chem *269*, 21191-7

Han, J., Lee, J. D., Bibbs, L., and Ulevitch, R. J. (1994). A MAP kinase targeted by endotoxin and hyperosmolarity in mammalian. Science *265*, 808-11.

Handel, S. E., Rennison, M. E., Wilde, C. J., and Burgoyne, R. D. (1991). Annexin II (calpactin I) in the mouse mammary gland: immunolocalization by light- and electron microscopy. Cell-Tissue-Res *264*, 549-54

Hanson, P. I., Roth, R., Morisaki, H., Jahn, R., and Heuser, J. E. (1997). Structure and conformational changes in NSF and its membrane receptor. Cell *90*, 523-35.

Harder, T., and Gerke, V. (1993). The subcellular distribution of early endosomes is affected by the annexin II2p11(2) complex. J-Cell-Biol *123*, 1119-32

Harder, T., and Gerke, V. (1994). The annexin II_2p11_2 complex is the major protein component of the triton X-100-insoluble low-density fraction prepared from MDCK cells in the presence of Ca2+. Biochim-Biophys-Acta *1223*, 375-82

Harder, T., Kellner, R., Parton, R. G., and Gruenberg, J. (1997). Specific release of membrane-bound annexin II and cortical cytoskeletal elements by sequestration of membrane cholesterol. Mol-Biol-Cell *8*, 533-45

Harder, T., Thiel, C., and Gerke, V. (1993). Formation of the annexin II2p112 complex upon differentiation of F9 teratocarcinoma cells. J-Cell-Sci *104*, 1109-17.

Harricane, M. C., Caron, E., Porte, F., and Liautard, J. P. (1996). Distribution of annexin I during non-pathogen or pathogen phagocytosis by confocal imaging and immunogold electron microscopy. Cell-Biol-Int *20*, 193-203

Helgadottir, A., Halldorsson, H., Magnusdottir, K., Kjeld, M., and Thorgeirsson, G. (1997). A role for tyrosine phosphorylation in generation of inositol phosphates and prostacyclin production in endothelial cells. Arterioscler Thromb Vasc Biol *17*, 287-94.

Hertogs, K., Leenders, W. P., Depla, E., De Bruin, W. C., Meheus, L., Raymackers, J., Moshage, H., and Yap, S. H. (1993). Endonexin II, present on human liver plasma membranes, is a specific binding protein of small hepatitis B virus (HBV) envelope protein. Virology *197*, 549-57

Hong, K., Duzgunes, N., and Papahadjopoulos, D. (1981). Role of synexin in membrane fusion. Enhancement of calcium-dependent fusion of phospholipid vesicles. J-Biol-Chem *256*, 3641-4

Hooper, N. M. (1998). Membrane biology: do glycolipid microdomains really exist? Curr Biol *8*, R114-6.

Hopkins, C. R., Gibson, A., Shipman, M., and Miller, K. (1990). Movement of internalized ligand-receptor complexes along a continuous endosomal reticulum [see comments]. Nature *346*, 335-9.

Hopkins, C. R., Gibson, A., Shipman, M., Strickland, D. K., and Trowbridge, I. S. (1994). In migrating fibroblasts, recycling receptors are concentrated in narrow tubules in the pericentriolar area, and then routed to the plasma membrane of the leading lamella. J Cell Biol *125*, 1265-74.

Hosoya, H., Kobayashi, R., Tsukita, S., and Matsumura, F. (1992). Ca(2+)-regulated actin and phospholipid binding protein (68 kD-protein) from bovine liver: identification as a homologue for annexin VI and intracellular localization. Cell Motil Cytoskeleton *22*, 200-10.

Huang, J. D., Brady, S. T., Richards, B. W., Stenolen, D., Resau, J. H., Copeland, N. G., and Jenkins, N. A. (1999). Direct interaction of microtubule- and actin-based transport motors [In Process Citation]. Nature *397*, 267-70.

Hubaishy, I., Jones, P. G., Bjorge, J., Bellagamba, C., Fitzpatrick, S., Fujita, D. J., and Waisman, D. M. (1995). Modulation of annexin II tetramer by tyrosine phosphorylation. Biochemistry *34*, 14527-34

Huber, R., Romisch, J., and Paques, E. P. (1990a). The crystal and molecular structure of human annexin V, an anticoagulant protein that binds to calcium and membranes. EMBO-J *9*, 3867-74

Huber, R., Schneider, M., Mayr, I., Romisch, J., and Paques, E. P. (1990b). The calcium binding sites in human annexin V by crystal structure analysis at 2.0 A resolution. Implications for membrane binding and calcium channel activity. FEBS-Lett *275*, 15-21

Ibata, K., Fukuda, M., and Mikoshiba, K. (1998). Inositol 1,3,4,5-tetrakisphosphate binding activities of neuronal and non-neuronal synaptotagmins. Identification of conserved amino acid substitutions that abolish inositol 1,3,4,5-tetrakisphosphate binding to synaptotagmins III, V, and X. J Biol Chem *273*, 12267-73.

Ikebuchi, N. W., and Waisman, D. M. (1990). Calcium-dependent regulation of actin filament bundling by lipocortin-85. J-Biol-Chem *265*, 3392-400

Inouye, S., and Tsuji, F. I. (1994). Aequorea green fluorescent protein. Expression of the gene and fluorescence characteristics of the recombinant protein. FEBS Lett *341*, 277-80.

Isacke, C. M., Trowbridge, I. S., and Hunter, T. (1986). Modulation of p36 phosphorylation in human cells: studies using anti-p36 monoclonal antibodies. Mol-Cell-Biol *6*, 2745-51

Isersky, C., Rivera, J., Segal, D. M., and Triche, T. (1983). The fate of IgE bound to rat basophilic leukemia cells. II. Endocytosis of IgE oligomers and effect on receptor turnover. J Immunol *131*, 388-96.

Jackle, S., Beisiegel, U., Rinninger, F., Buck, F., Grigoleit, A., Block, A., Groger, I., Greten, H., and Windler, E. (1994). Annexin VI, a marker protein of hepatocytic endosomes. J-Biol-Chem *269*, 1026-32

Janmey, P. A. (1994). Phosphoinositides and calcium as regulators of cellular actin assembly. Annu Rev Physiol *56*, 169-91.

Jiang, B. H., Zheng, J. Z., and Vogt, P. K. (1998). An essential role of phosphatidylinositol 3-kinase in myogenic differentiation. Proc Natl Acad Sci U S A *95*, 14179-83.

Jindal, H. K., Chaney, W. G., Anderson, C. W., Davis, R. G., and Vishwanatha, J. K. (1991). The protein-tyrosine kinase substrate, calpactin I heavy chain (p36), is part

of the primer recognition protein complex that interacts with DNA polymerase alpha. J-Biol-Chem *266*, 5169-76

Johnsson, N., and Weber, K. (1990). Structural analysis of p36, a Ca2+/lipid-binding protein of the annexin family, by proteolysis and chemical fragmentation. Eur-J-Biochem *188*, 1-7

Johnsson, N., Marriott, G., and Weber, K. (1988). p36, the major cytoplasmic substrate of src tyrosine protein kinase, binds to its p11 regulatory subunit via a short amino-terminal amphiphatic helix. EMBO-J *7*, 2435-42

Johnsson, N., Vandekerckhove, J., Van Damme, J., and Weber, K. (1986). Binding sites for calcium, lipid and p11 on p36, the substrate of retroviral tyrosine-specific protein kinases. FEBS-Lett *198*, 361-4

Johnstone, S. A., Hubaishy, I., and Waisman, D. M. (1992). Phosphorylation of annexin II tetramer by protein kinase C inhibits aggregation of lipid vesicles by the protein. J-Biol-Chem *267*, 25976-81

Jones, P. G., Fitzpatrick, S., and Waisman, D. M. (1994). Salt dependency of chromaffin granule aggregation by annexin II tetramer. Biochemistry *33*, 13751-60 *LHM: This title is currently taken by UCL: Medical Sciences ISSN: 0006-2960.

Jones, P. G., Moore, G. J., and Waisman, D. M. (1992). A nonapeptide to the putative F-actin binding site of annexin-II tetramer inhibits its calcium-dependent activation of actin filament bundling. J-Biol-Chem *267*, 13993-7

Jost, M., and Gerke, V. (1996). Mapping of a regulatory important site for protein kinase C in the N-terminal domain of annexin II. Biochim Biophys Acta *1313*, 283-9.

Jost, M., Thiel, C., Weber, K., and Gerke, V. (1992). Mapping of three unique Ca(2+)-binding sites in human annexin II. Eur J Biochem *207*, 923-30.

Jost, M., Weber, K., and Gerke, V. (1994). Annexin II contains two types of Ca(2+)-binding sites. Biochem J *3*, 553-9.

Jost, M., Zeuschner, D., Seemann, J., Weber, K., and Gerke, V. (1997). Identification and characterization of a novel type of annexin-membrane interaction: Ca2+ is not required for the association of annexin II with early endosomes. J-Cell-Sci *110*, 221-8

Junker, M., and Creutz, C. E. (1993). Endonexin (annexin IV)-mediated lateral segregation of phosphatidylglycerol in phosphatidylglycerol/phosphatidylcholine membranes. Biochemistry *32*, 9968-74.

Junker, M., and Creutz, C. E. (1994). Ca(2+)-dependent binding of endonexin (annexin IV) to membranes: analysis of the effects of membrane lipid composition and development of a predictive model for the binding interaction. Biochemistry *33*, 8930-40.

Kaczan Bourgois, D., Salles, J. P., Hullin, F., Fauvel, J., Moisand, A., Duga Neulat, I., Berrebi, A., Campistron, G., and Chap, H. (1996). Increased content of annexin II (p36) and p11 in human placenta brush-border membrane vesicles during syncytiotrophoblast maturation and differentiation. Placenta *17*, 669-76 issn: 0143-4004.

Karasik, A., Pepinsky, R. B., Shoelson, S. E., and Kahn, C. R. (1988). Lipocortins 1 and 2 as substrates for the insulin receptor kinase in rat liver. J-Biol-Chem *263*, 11862-7

Kassam, G., Manro, A., Braat, C. E., Louie, P., Fitzpatrick, S. L., and Waisman, D. M. (1997). Characterization of the heparin binding properties of annexin II tetramer. J-Biol-Chem *272*, 15093-100

Kaufman, M., Leto, T., and Levy, R. (1996). Translocation of annexin I to plasma membranes and phagosomes in human neutrophils upon stimulation with opsonized zymosan: possible role in phagosome function. Biochem-J *316*, 35-42

Kawasaki, H., Avila Sakar, A., Creutz, C. E., and Kretsinger, R. H. (1996). The crystal structure of annexin VI indicates relative rotation of the two lobes upon membrane binding. Biochim-Biophys-Acta *1313*, 277-82

Kee, Y., Yoo, J. S., Hazuka, C. D., Peterson, K. E., Hsu, S. C., and Scheller, R. H. (1997). Subunit structure of the mammalian exocyst complex. Proc Natl Acad Sci U S A *94*, 14438-43.

Keller, H. U. (1990). Diacylglycerols and PMA are particularly effective stimulators of fluid pinocytosis in human neutrophils. J Cell Physiol *145*, 465-71.

Keller, H. U., and Niggli, V. (1993). The PKC-inhibitor Ro 31-8220 selectively suppresses PMA- and diacylglycerol-induced fluid pinocytosis and actin polymerization in PMNs. Biochem Biophys Res Commun *194*, 1111-6.

Keller, H. U., and Niggli, V. (1994). Selective effects of the PKC inhibitors Ro 31-8220 and CGP 41,251 on PMN locomotion, cell polarity, and pinocytosis. J Cell Physiol *161*, 526-36.

Keller, H., and Niggli, V. (1995). Effects of cytochalasin D on shape and fluid pinocytosis in human neutrophils as related to cytoskeletal changes (actin, alpha-actinin and microtubules). Eur J Cell Biol *66*, 157-64.

Kim, T. D., Eddlestone, G. T., Mahmoud, S. F., Kuchtey, J., and Fewtrell, C. (1997). Correlating Ca2+ responses and secretion in individual RBL-2H3 mucosal mast cells. J Biol Chem *272*, 31225-9.

Kiss, A. L., and Geuze, H. J. (1997). Caveolae can be alternative endocytotic structures in elicited macrophages. Eur J Cell Biol *73*, 19-27.

Knight, D. E., and Baker, P. F. (1985). Guanine nucleotides and Ca-dependent exocytosis. Studies on two adrenal cell preparations. FEBS Lett *189*, 345-9.

Ko, Y. G., Liu, P., Pathak, R. K., Craig, L. C., and Anderson, R. G. (1998). Early effects of pp60(v-src) kinase activation on caveolae. J Cell Biochem *71*, 524-35.

Koffer, A., Tatham, P. E., and Gomperts, B. D. (1990). Changes in the state of actin during the exocytotic reaction of permeabilized rat mast cells. J Cell Biol *111*, 919-27.

Kohtz, D. S., Hanson, V., and Puszkin, S. (1990). Novel proteins mediate an interaction between clathrin-coated vesicles and polymerizing actin filaments. Eur J Biochem *192*, 291-8.

Konig, J., Prenen, J., Nilius, B., and Gerke, V. (1998). The annexin II-p11 complex is involved in regulated exocytosis in bovine pulmonary artery endothelial cells. J Biol Chem *273*, 19679-84.

Kretsinger, R. H. (1980). Structure and evolution of calcium-modulated proteins. CRC Crit Rev Biochem *8*, 119-74.

Kristoffersen, E. K. (1996). Human placental Fc gamma-binding proteins in the maternofetal transfer of IgG. APMIS Suppl *64*, 5-36.

Kristoffersen, E. K., and Matre, R. (1996). Surface annexin II on placental membranes of the fetomaternal interface. Am-J-Reprod-Immunol *36*, 141-9 issn: 1046-7408.

Kristoffersen, E. K., Ulvestad, E., Bjorge, L., Aarli, A., and Matre, R. (1994). Fc gamma-receptor activity of placental annexin II. Scand-J-Immunol *40*, 237-42

Kryvi, H., Flatmark, T., and Terland, O. (1979). Comparison of the ultrastructure of adrenaline and noradrenaline storage granules of bovine adrenal medulla. Eur J Cell Biol *20*, 76-82.

Kube, E., Becker, T., Weber, K., and Gerke, V. (1992). Protein-protein interaction studied by site-directed mutagenesis. Characterization of the annexin II-binding site on p11, a member of the S100 protein family. J-Biol-Chem *267*, 14175-82

Kubler, E., and Riezman, H. (1993). Actin and fimbrin are required for the internalization step of endocytosis in yeast. Embo J *12*, 2855-62.

Kumble, K. D., Hirota, M., Pour, P. M., and Vishwanatha, J. K. (1992). Enhanced levels of annexins in pancreatic carcinoma cells of Syrian hamsters and their intrapancreatic allografts. Cancer-Res *52*, 163-7

Kyriakis, J. M., and Avruch, J. (1996). Sounding the alarm: protein kinase cascades activated by stress and inflammation. J Biol Chem *271*, 24313-6.

Lamaze, C., Fujimoto, L. M., Yin, H. L., and Schmid, S. L. (1997). The actin cytoskeleton is required for receptor-mediated endocytosis in mammalian cells. J Biol Chem *272*, 20332-5.

Lambert, O., Gerke, V., Bader, M. F., Porte, F., and Brisson, A. (1997). Structural analysis of junctions formed between lipid membranes and several annexins by cryo-electron microscopy. J-Mol-Biol *272*, 42-55

Landry, J., and Huot, J. (1995). Modulation of actin dynamics during stress and physiological stimulation by a signaling pathway involving p38 MAP kinase and heat- shock protein 27. Biochem Cell Biol *73*, 703-7.

Langen, R., Isas, J. M., Hubbell, W. L., and Haigler, H. T. (1998). A transmembrane form of annexin XII detected by site-directed spin labeling. Proc Natl Acad Sci U S A *95*, 14060-5.

Lavoie, J. N., Hickey, E., Weber, L. A., and Landry, J. (1993). Modulation of actin microfilament dynamics and fluid phase pinocytosis by phosphorylation of heat shock protein 27. J Biol Chem *268*, 24210-4.

Lengsfeld, A. M., Low, I., Wieland, T., Dancker, P., and Hasselbach, W. (1974). Interaction of phalloidin with actin. Proc Natl Acad Sci U S A *71*, 2803-7.

Lewis, M. J., Rayner, J. C., and Pelham, H. R. (1997). A novel SNARE complex implicated in vesicle fusion with the endoplasmic reticulum. Embo J *16*, 3017-24.

Lewit Bentley, A., Morera, S., Huber, R., and Bodo, G. (1992). The effect of metal binding on the structure of annexin V and implications for membrane binding. Eur-J-Biochem *210*, 73-7

Li, C., Davletov, B. A., and Sudhof, T. C. (1995). Distinct Ca2+ and Sr2+ binding properties of synaptotagmins. Definition of candidate Ca2+ sensors for the fast and slow components of neurotransmitter release. J Biol Chem *270*, 24898-902.

Liemann, S., and Huber, R. (1997). Three-dimensional structure of annexins. Cell Mol Life Sci *53*, 516-21.

Lin, H. C., Sudhof, T. C., and Anderson, R. G. (1992). Annexin VI is required for budding of clathrin-coated pits. Cell *70*, 283-91

Lin, R. C., and Scheller, R. H. (1997). Structural organization of the synaptic exocytosis core complex. Neuron *19*, 1087-94.

Linial, M. (1997). SNARE proteins--why so many, why so few? J Neurochem *69*, 1781-92.

Littleton, J. T., Stern, M., Schulze, K., Perin, M., and Bellen, H. J. (1993). Mutational analysis of Drosophila synaptotagmin demonstrates its. Cell *74*, 1125-34.

Liu, L., Fisher, A. B., and Zimmerman, U. J. (1995a). Lung annexin II promotes fusion of isolated lamellar bodies with liposomes. Biochim-Biophys-Acta *1259*, 166-72

Liu, L., Fisher, A. B., and Zimmerman, U. J. (1995b). Regulation of annexin I by proteolysis in rat alveolar epithelial type II cells. Biochem-Mol-Biol-Int *36*, 373-81

Liu, L., Tao, J. Q., and Zimmerman, U. J. (1997). Annexin II binds to the membrane of A549 cells in a calcium-dependent and calcium-independent manner. Cell-Signal *9*, 299-304 issn: 0898-6568.

Liu, L., Wang, M., Fisher, A. B., and Zimmerman, U. J. (1996). Involvement of annexin II in exocytosis of lamellar bodies from alveolar epithelial type II cells. Am-J-Physiol *270*, L668-76

Liu, P., Ying, Y., Ko, Y. G., and Anderson, R. G. (1996). Localization of platelet-derived growth factor-stimulated phosphorylation cascade to caveolae. J Biol Chem *271*, 10299-303.

Liu, Y., Brew, K., Carraway, K. L., and Carraway, C. A. (1987). Isolation of a calcium-sensitive, 35,000-dalton microfilament- and liposome-binding protein from ascites tumor cell microvilli: identification as monomeric calpactin. J-Cell-Biochem *35*, 185-204

Liu, Z. Y., Young, J. I., and Elson, E. L. (1987). Rat basophilic leukemia cells stiffen when they secrete. J Cell Biol *105*, 2933-43.

Llinas, R., Sugimori, M., and Silver, R. B. (1992). Microdomains of high calcium concentration in a presynaptic terminal. Science *256*, 677-9.

Lu, W., Katz, S., Gupta, R., and Mayer, B. J. (1997). Activation of Pak by membrane localization mediated by an SH3 domain from the adaptor protein Nck. Curr Biol *7*, 85-94.

Luecke, H., Chang, B. T., Mailliard, W. S., Schlaepfer, D. D., and Haigler, H. T. (1995). Crystal structure of the annexin XII hexamer and implications for bilayer insertion [see comments]. Nature *378*, 512-5

Ma, A. S., Bell, D. J., Mittal, A. A., and Harrison, H. H. (1994a). Immunocytochemical detection of extracellular annexin II in cultured human skin keratinocytes and isolation of annexin II isoforms enriched in the extracellular pool. J-Cell-Sci *107*, 1973-84

Ma, A. S., Bystol, M. E., and Tranvan, A. (1994b). In vitro modulation of filament bundling in F-actin and keratins by annexin II and calcium. In-Vitro-Cell-Dev-Biol-Anim *30a*, 329-35 issn: 1071-2690.

Ma, L., Cantley, L. C., Janmey, P. A., and Kirschner, M. W. (1998a). Corequirement of specific phosphoinositides and small GTP-binding protein Cdc42 in inducing actin assembly in Xenopus egg extracts. J Cell Biol *140*, 1125-36.

Ma, L., Rohatgi, R., and Kirschner, M. W. (1998b). The Arp2/3 complex mediates actin polymerization induced by the small GTP-binding protein Cdc42. Proc Natl Acad Sci U S A *95*, 15362-7.

Machesky, L. M., and Insall, R. H. (1998). Scar1 and the related wiskott-aldrich syndrome protein, WASP, regulate the actin cytoskeleton through the Arp2/3 complex [In Process Citation]. Curr Biol *8*, 1347-56.

Maeda, T., Takekawa, M., and Saito, H. (1995). Activation of yeast PBS2 MAPKK by MAPKKKs or by binding of an SH3-. Science *269*, 554-8.

Mailliard, W. S., Haigler, H. T., and Schlaepfer, D. D. (1996). Calcium-dependent binding of S100C to the N-terminal domain of annexin I. J-Biol-Chem *271*, 719-25

Mailliard, W. S., Luecke, H., and Haigler, H. T. (1997). Annexin XII forms calcium-dependent multimers in solution and on phospholipid bilayers: a chemical cross-linking study. Biochemistry *36*, 9045-50

Malorni, W., Fiorentini, C., Paradisi, S., Giuliano, M., Mastrantonio, P., and Donelli, G. (1990). Surface blebbing and cytoskeletal changes induced in vitro by toxin B from Clostridium difficile: an immunochemical and ultrastructural study. Exp Mol Pathol *52*, 340-56.

Maniatis, T., Fritsch, E. F., and Sambrook, J. (1982). Molecular cloning: A Laboratory Manual: Cold Spring Harbour Press).

Manser, E., Leung, T., Salihuddin, H., Zhao, Z. S., and Lim, L. (1994). A brain serine/threonine protein kinase activated by Cdc42 and Rac1. Nature *367*, 40-6.

Marquez, J. A., Pascual-Ahuir, A., Proft, M., and Serrano, R. (1998). The Ssn6-Tup1 repressor complex of Saccharomyces cerevisiae is involved in the osmotic induction of HOG-dependent and -independent genes. Embo J *17*, 2543-53.

Martin, G. A., Bollag, G., McCormick, F., and Abo, A. (1995). A novel serine kinase activated by rac1/CDC42Hs-dependent. Embo J *14*, 1970-8.

Martys, J. L., Shevell, T., and McGraw, T. E. (1995). Studies of transferrin recycling reconstituted in streptolysin O permeabilized Chinese hamster ovary cells. J Biol Chem *270*, 25976-84.

Masaki, T., Tokuda, M., Fujimura, T., Ohnishi, M., Tai, Y., Miyamoto, K., Itano, T., Matsui, H., Watanabe, S., Sogawa, K., and et al. (1994). Involvement of annexin I and annexin II in hepatocyte proliferation: can annexins I and II be markers for proliferative hepatocytes? Hepatology *20*, 425-35 issn: 0270-9139.

Masiakowski, P., and Shooter, E. M. (1990). Changes in PC12 cell morphology induced by transfection with 42C cDNA, coding for a member of the S-100 protein family. J-Neurosci-Res *27*, 264-9

Massey-Harroche, D., Mayran, N., and Maroux, S. (1998). Polarized localizations of annexins I, II, VI and XIII in epithelial cells of intestinal, hepatic and pancreatic tissues. J Cell Sci *111*, 3007-15.

Massol, P., Montcourrier, P., Guillemot, J. C., and Chavrier, P. (1998). Fc receptor-mediated phagocytosis requires CDC42 and Rac1. Embo J *17*, 6219-29.

Mayor, S., and Maxfield, F. R. (1995). Insolubility and redistribution of GPI-anchored proteins at the cell surface after detergent treatment. Mol Biol Cell *6*, 929-44.

Mayorga, L. S., Beron, W., Sarrouf, M. N., Colombo, M. I., Creutz, C., and Stahl, P. D. (1994). Calcium-dependent fusion among endosomes. J-Biol-Chem *269*, 30927-34

Mazurier, F., Moreau-Gaudry, F., Maguer-Satta, V., Salesse, S., Pigeonnier-Lagarde, V., Ged, C., Belloc, F., Lacombe, F., Mahon, F. X., Reiffers, J., and de Verneuil, H. (1998). Rapid analysis and efficient selection of human transduced primitive hematopoietic cells using the humanized S65T green fluorescent protein. Gene Ther *5*, 556-62.

McNiven, M. A. (1998). Dynamin: a molecular motor with pinchase action. Cell *94*, 151-4.

Meers, P., Bentz, J., Alford, D., Nir, S., Papahadjopoulos, D., and Hong, K. (1988a). Synexin enhances the aggregation rate but not the fusion rate of liposomes. Biochemistry *27*, 4430-9

Meers, P., Hong, K., and Papahadjopoulos, D. (1988b). Free fatty acid enhancement of cation-induced fusion of liposomes: synergism with synexin and other promoters of vesicle aggregation. Biochemistry *27*, 6784-94

Meers, P., Mealy, T., Pavlotsky, N., and Tauber, A. I. (1992). Annexin I-mediated vesicular aggregation: mechanism and role in human neutrophils [published erratum appears in Biochemistry 1993 Feb 9;32(5):1390]. Biochemistry *31*, 6372-82

Meier, R., Thelen, M., and Hemmings, B. A. (1998). Inactivation and dephosphorylation of protein kinase Balpha (PKBalpha) promoted by hyperosmotic stress. Embo J *17*, 7294-7303.

Melan, M. A., and Sluder, G. (1992). Redistribution and differential extraction of soluble proteins in permeabilized cultured cells. Implications for immunofluorescence microscopy. J Cell Sci *101*, 731-43.

Meyer, K., Irminger, J. C., Moss, L. G., de Vargas, L. M., Oberholzer, J., Bosco, D., Morel, P., and Halban, P. A. (1998). Sorting human beta-cells consequent to targeted expression of green fluorescent protein. Diabetes *47*, 1974-7.

Miller, K., Beardmore, J., Kanety, H., Schlessinger, J., and Hopkins, C. R. (1986). Localization of the epidermal growth factor (EGF) receptor within the endosome of EGF-stimulated epidermoid carcinoma (A431) cells. J Cell Biol *102*, 500-9.

Mitchell, M. J., Laughon, B. E., and Lin, S. (1987). Biochemical studies on the effect of Clostridium difficile toxin B on actin in vivo and in vitro. Infect Immun *55*, 1610-5.

Miyamoto, S., Funatsu, T., Ishiwata, S., and Fujime, S. (1993). Changes in mobility of chromaffin granules in actin network with its assembly and Ca(2+)-dependent disassembly by gelsolin. Biophys J *64*, 1139-49.

Mochly-Rosen, D., Khaner, H., Lopez, J., and Smith, B. L. (1991). Intracellular receptors for activated protein kinase C. Identification of a binding site for the enzyme. J Biol Chem *266*, 14866-8.

Mohiti, J., Caswell, A. M., and Walker, J. H. (1995). Calcium-induced relocation of annexins IV and V in the human osteosarcoma cell line MG-63. Mol-Membr-Biol *12*, 321-9 issn: 0968-7688.

Moreau, V., and Way, M. (1998). Cdc42 is required for membrane dependent actin polymerization in vitro. FEBS Lett *427*, 353-6.

Moreau, V., Galan, J. M., Devilliers, G., Haguenauer-Tsapis, R., and Winsor, B. (1997). The yeast actin-related protein Arp2p is required for the internalization step of endocytosis. Mol Biol Cell *8*, 1361-75.

Morgan, A., and Burgoyne, R. D. (1992a). Exo1 and Exo2 proteins stimulate calcium-dependent exocytosis in permeabilized adrenal chromaffin cells. Nature *355*, 833-6

Morgan, A., and Burgoyne, R. D. (1992b). Interaction between protein kinase C and Exo1 (14-3-3 protein) and its relevance to exocytosis in permeabilized adrenal chromaffin cells. Biochem J *286*, 807-11.

Morgan, R. O., and Fernandez, M. P. (1995). Molecular phylogeny of annexins and identification of a primitive homologue in Giardia lamblia. Mol-Biol-Evol *12*, 967-79

Morgenstern, E. (1991). Aldehyde fixation causes membrane vesiculation during platelet exocytosis: a freeze-substitution study. Scanning Microsc Suppl *5*, S109-15.

Moss, S. E. (1995). Ion channels. Annexins taken to task [news; comment]. Nature *378*, 446-7

Mosser, G., Ravanat, C., Freyssinet, J. M., and Brisson, A. (1991). Sub-domain structure of lipid-bound annexin-V resolved by electron image analysis. J-Mol-Biol *217*, 241-5

Muallem, S., Kwiatkowska, K., Xu, X., and Yin, H. L. (1995). Actin filament disassembly is a sufficient final trigger for exocytosis in nonexcitable cells. J Cell Biol *128*, 589-98.

Munn, A. L., Stevenson, B. J., Geli, M. I., and Riezman, H. (1995). end5, end6, and end7: mutations that cause actin delocalization and block the internalization step of endocytosis in Saccharomyces cerevisiae. Mol Biol Cell *6*, 1721-42.

Munz, B., Gerke, V., Gillitzer, R., and Werner, S. (1997). Differential expression of the calpactin I subunits annexin II and p11 in cultured keratinocytes and during wound repair. J-Invest-Dermatol *108*, 307-12

Naka, M., Qing, Z. X., Sasaki, T., Kise, H., Tawara, I., Hamaguchi, S., and Tanaka, T. (1994). Purification and characterization of a novel calcium-binding protein, S100C, from porcine heart. Biochim-Biophys-Acta *1223*, 348-53

Nakamura, N., Lowe, M., Levine, T. P., Rabouille, C., and Warren, G. (1997). The vesicle docking protein p115 binds GM130, a cis-Golgi matrix protein, in a mitotically regulated manner. Cell *89*, 445-55.

Nakata, T., Sobue, K., and Hirokawa, N. (1990). Conformational change and localization of calpactin I complex involved in exocytosis as revealed by quick-freeze, deep-etch electron microscopy and immunocytochemistry. J-Cell-Biol *110*, 13-25

Nalefski, E. A., and Falke, J. J. (1996). The C2 domain calcium-binding motif: structural and functional diversity. Protein Sci *5*, 2375-90.

Nanavati, D., Ashton, F. T., Sanger, J. M., and Sanger, J. W. (1994). Dynamics of actin and alpha-actinin in the tails of Listeria monocytogenes in infected PtK2 cells. Cell Motil Cytoskeleton *28*, 346-58.

Naqvi, S. N., Zahn, R., Mitchell, D. A., Stevenson, B. J., and Munn, A. L. (1998). The WASp homologue Las17p functions with the WIP homologue. Curr Biol *8*, 959-62.

Neurath, A. R., and Strick, N. (1994). The putative cell receptors for hepatitis B virus (HBV), annexin V, and apolipoprotein H, bind to lipid components of HBV. Virology *204*, 475-7

Newman, R., Tucker, A., Ferguson, C., Tsernoglou, D., Leonard, K., and Crumpton, M. J. (1989). Crystallization of p68 on lipid monolayers and as three-dimensional single crystals. J-Mol-Biol *206*, 213-9

Nichols, B. J., Ungermann, C., Pelham, H. R., Wickner, W. T., and Haas, A. (1997). Homotypic vacuolar fusion mediated by t- and v-SNAREs [see comments]. Nature *387*, 199-202.

Nielsen, E. H. (1990). A filamentous network surrounding secretory granules from mast cells. J Cell Sci *96*, 43-6.

Nishida, E., Iida, K., Yonezawa, N., Koyasu, S., Yahara, I., and Sakai, H. (1987). Cofilin is a component of intranuclear and cytoplasmic actin rods induced in cultured cells. Proc Natl Acad Sci U S A *84*, 5262-6.

Norman, J. C., Price, L. S., Ridley, A. J., and Koffer, A. (1996). The small GTP-binding proteins, Rac and Rho, regulate cytoskeletal organization and exocytosis in mast cells by parallel pathways. Mol Biol Cell *7*, 1429-42.

Ohki, S., and Leonards, K. (1982). Effects of proteins on phospholipid vesicle aggregation and lipid vesicle-monolayer interactions. Chem-Phys-Lipids *31*, 307-18 issn: 0009-3084.

Ohnishi, M., Tokuda, M., Masaki, T., Fujimura, T., Tai, Y., Matsui, H., Itano, T., Ishida, T., Takahara, J., Konishi, R., and et al. (1994). Changes in annexin I and II levels during the postnatal development of rat pancreatic islets. J-Cell-Sci *107*, 2117-25

Orci, L., Perrelet, A., and Rothman, J. E. (1998). Vesicles on strings: morphological evidence for processive transport within the Golgi stack. Proc Natl Acad Sci U S A *95*, 2279-83.

Ortega, D., Pol, A., Biermer, M., Jackle, S., and Enrich, C. (1998). Annexin VI defines an apical endocytic compartment in rat liver hepatocytes. J Cell Sci *111*, 261-9.

Ortega, D., Pol, A., Biermer, M., Jackle, S., and Enrich, C. (1997). [Immunohistochemical localization of annexin VI in the endocytic compartment of rat liver hepatocytes]. Gastroenterol Hepatol *20*, 391-7.

Ortega, E., Hazan, B., Zor, U., and Pecht, I. (1989). Mast cell stimulation by monoclonal antibodies specific for the Fc epsilon receptor yields distinct responses of arachidonic acid and leukotriene C4 secretion. Eur J Immunol *19*, 2251-6.

Ottlinger, M. E., and Lin, S. (1988). Clostridium difficile toxin B induces reorganization of actin, vinculin, and talin in cultured cells. Exp Cell Res *174*, 215-29.

Parkin, E. T., Turner, A. J., and Hooper, N. M. (1996). A role for calcium and annexins in the formation of caveolae. Biochem-Soc-Trans *24*, 444S

Parton, R. G., Joggerst, B., and Simons, K. (1994). Regulated internalization of caveolae. J Cell Biol *127*, 1199-215.

Pelham, H. R., Banfield, D. K., and Lewis, M. J. (1995). SNAREs involved in traffic through the Golgi complex. Cold Spring Harb Symp Quant Biol *60*, 105-11.

Penalver, E., Ojeda, L., Moreno, E., and Lagunas, R. (1997). Role of the cytoskeleton in endocytosis of the yeast maltose transporter. Yeast *13*, 541-9.

Pepinsky, R. B., and Sinclair, L. K. (1986). Epidermal growth factor-dependent phosphorylation of lipocortin. Nature *321*, 81-4

Pepinsky, R. B., Sinclair, L. K., Chow, E. P., and O'Brine Greco, B. (1989). A dimeric form of lipocortin-1 in human placenta. Biochem-J *263*, 97-103

Pepinsky, R. B., Tizard, R., Mattaliano, R. J., Sinclair, L. K., Miller, G. T., Browning, J. L., Chow, E. P., Burne, C., Huang, K. S., Pratt, D., and et al. (1988). Five distinct calcium and phospholipid binding proteins share homology with lipocortin I. J-Biol-Chem *263*, 10799-811

Peskin, C. S., Odell, G. M., and Oster, G. F. (1993). Cellular motions and thermal fluctuations: the Brownian ratchet. Biophys J *65*, 316-24.

Peters, C., and Mayer, A. (1998). Ca^{2+}/calmodulin signals the completion of docking and triggers a step of vacuole fusion. Nature *396*, 575-80.

Pevsner, J., Hsu, S. C., Braun, J. E., Calakos, N., Ting, A. E., Bennett, M. K., and Scheller, R. H. (1994). Specificity and regulation of a synaptic vesicle docking complex. Neuron *13*, 353-61.

Pfeiffer, J. R., Seagrave, J. C., Davis, B. H., Deanin, G. G., and Oliver, J. M. (1985). Membrane and cytoskeletal changes associated with IgE-mediated serotonin release from rat basophilic leukemia cells. J Cell Biol *101*, 2145-55.

Phaire-Washington, L., Wang, E., and Silverstein, S. C. (1980). Phorbol myristate acetate stimulates pinocytosis and membrane spreading in mouse peritoneal macrophages. J Cell Biol *86*, 634-40.

Pol, A., Ortega, D., and Enrich, C. (1997). Identification of cytoskeleton-associated proteins in isolated rat liver endosomes. Biochem J *327*, 741-6.

Porte, F., de Santa Barbara, P., Phalipou, S., Liautard, J. P., and Widada, J. S. (1996). Change in the N-terminal domain conformation of annexin I that correlates with liposome aggregation is impaired by Ser-27 to Glu mutation that mimics phosphorylation. Biochim-Biophys-Acta *1293*, 177-84

Powell, M. A., and Glenney, J. R. (1987). Regulation of calpactin I phospholipid binding by calpactin I light-chain binding and phosphorylation by p60v-src. Biochem-J *247*, 321-8

Prasher, D. C., Eckenrode, V. K., Ward, W. W., Prendergast, F. G., and Cormier, M. J. (1992). Primary structure of the Aequorea victoria green-fluorescent protein. Gene *111*, 229-33.

Predescu, D., Predescu, S., McQuistan, T., and Palade, G. E. (1998). Transcytosis of alpha1-acidic glycoprotein in the continuous microvascular endothelium. Proc Natl Acad Sci U S A *95*, 6175-80.

Prepens, U., Just, I., von Eichel-Streiber, C., and Aktories, K. (1996). Inhibition of Fc epsilon-RI-mediated activation of rat basophilic leukemia cells by Clostridium difficile toxin B (monoglucosyltransferase). J Biol Chem *271*, 7324-9.

Protopopov, V., Govindan, B., Novick, P., and Gerst, J. E. (1993). Homologs of the synaptobrevin/VAMP family of synaptic vesicle proteins function on the late secretory pathway in S. cerevisiae. Cell *74*, 855-61.

Puisieux, A., Ji, J., and Ozturk, M. (1996). Annexin II up-regulates cellular levels of p11 protein by a post-translational mechanisms. Biochem-J *313*, 51-5

Purich, D. L., and Southwick, F. S. (1997). ABM-1 and ABM-2 homology sequences: consensus docking sites for actin-based motility defined by oligoproline regions in Listeria ActA surface protein and human VASP. Biochem-Biophys-Res-Commun *231*, 686-91

Qiu, R. G., Chen, J., Kirn, D., McCormick, F., and Symons, M. (1995). An essential role for Rac in Ras transformation. Nature *374*, 457-9.

Ra, C., Furuichi, K., Rivera, J., Mullins, J. M., Isersky, C., and White, K. N. (1989). Internalization of IgE receptors on rat basophilic leukemic cells by phorbol ester. Comparison with endocytosis induced by receptor aggregation. Eur J Immunol *19*, 1771-7.

Radke, K., and Martin, G. S. (1979). Transformation by Rous sarcoma virus: effects of src gene expression on the synthesis and phosphorylation of cellular polypeptides. Proc Natl Acad Sci U S A *76*, 5212-6.

Radke, K., Gilmore, T., and Martin, G. S. (1980). Transformation by Rous sarcoma virus: a cellular substrate for transformation-specific protein phosphorylation contains phosphotyrosine. Cell *21*, 821-8.

Raynal, P., and Pollard, H. B. (1994). Annexins: the problem of assessing the biological role for a gene family of multifunctional calcium- and phospholipid-binding proteins. Biochim-Biophys-Acta *1197*, 63-93

Reeves, S. A., Chavez Kappel, C., Davis, R., Rosenblum, M., and Israel, M. A. (1992). Developmental regulation of annexin II (Lipocortin 2) in human brain and expression in high grade glioma. Cancer-Res *52*, 6871-6

Regnouf, F., Rendon, A., and Pradel, L. A. (1991). Biochemical characterization of annexins I and II isolated from pig nervous tissue. J-Neurochem *56*, 1985-96

Regnouf, F., Sagot, I., Delouche, B., Devilliers, G., Cartaud, J., Henry, J. P., and Pradel, L. A. (1995). "In vitro" phosphorylation of annexin 2 heterotetramer by protein kinase C. Comparative properties of the unphosphorylated and phosphorylated annexin 2 on the aggregation and fusion of chromaffin granule membranes. J-Biol-Chem *270*, 27143-50

Ren, M., Xu, G., Zeng, J., De Lemos-Chiarandini, C., Adesnik, M., and Sabatini, D. D. (1998). Hydrolysis of GTP on rab11 is required for the direct delivery of transferrin from the pericentriolar recycling compartment to the cell surface but not from sorting endosomes. Proc Natl Acad Sci U S A *95*, 6187-92.

Reynolds, T. B., Hopkins, B. D., Lyons, M. R., and Graham, T. R. (1998). The high osmolarity glycerol response (HOG) MAP kinase pathway controls localization of a yeast golgi glycosyltransferase. J Cell Biol *143*, 935-46.

Richard, I. (1995). ? Cell *81*, 27-40.

Rivero-Lezcano, O. M., Marcilla, A., Sameshima, J. H., and Robbins, K. C. (1995). Wiskott-Aldrich syndrome protein physically associates with Nck through Src homology 3 domains. Mol Cell Biol *15*, 5725-31.

Robinson, J. M., Chiplonkar, J., and Luo, Z. (1996). A method for co-localization of tubular lysosomes and microtubules in macrophages: fluorescence microscopy of individual cells. J Histochem Cytochem *44*, 1109-14.

Roseman, B. J., Bollen, A., Hsu, J., Lamborn, K., and Israel, M. A. (1994). Annexin II marks astrocytic brain tumors of high histologic grade. Oncol Res *6*, 561-7.

Rosenblatt, J., Agnew, B. J., Abe, H., Bamburg, J. R., and Mitchison, T. J. (1997). Xenopus actin depolymerizing factor/cofilin (XAC) is responsible for the turnover of actin filaments in Listeria monocytogenes tails. J Cell Biol *136*, 1323-32.

Rosengarth, A., Wintergalen, A., Galla, H. J., Hinz, H. J., and Gerke, V. (1998). Ca2+-independent interaction of annexin I with phospholipid monolayers. FEBS Lett *438*, 279-84.

Rosenqvist, E., Michaelsen, T. E., and Vistnes, A. I. (1980). Effect of streptolysin O and digitonin on egg lecithin/cholesterol vesicles. Biochim Biophys Acta *600*, 91-102.

Roth, D., and Burgoyne, R. D. (1995). Stimulation of catecholamine secretion from adrenal chromaffin cells by 14-3-3 proteins is due to reorganisation of the cortical actin network. FEBS Lett *374*, 77-81.

Roth, D., Morgan, A., and Burgoyne, R. D. (1993). Identification of a key domain in annexin and 14-3-3 proteins that stimulate calcium-dependent exocytosis in permeabilized adrenal chromaffin cells. FEBS-Lett *320*, 207-10

Rothman, J. E. (1994). Mechanisms of intracellular protein transport. Nature *372*, 55-63.

Rothman, J. E., and Orci, L. (1992). Molecular dissection of the secretory pathway. Nature *355*, 409-15.

Rothman, J. E., and Sollner, T. H. (1997). Throttles and dampers: controlling the engine of membrane fusion [see comments]. Science *276*, 1212-3.

Rothman, J. E., and Wieland, F. T. (1996). Protein sorting by transport vesicles. Science *272*, 227-34.

Sagot, I., Regnouf, F., Henry, J. P., and Pradel, L. A. (1997). Translocation of cytosolic annexin 2 to a Triton-insoluble membrane subdomain upon nicotine stimulation of chromaffin cultured cells. FEBS-Lett *410*, 229-34

Sanders, M. C., and Theriot, J. A. (1996). Tails from the hall of infection: actin-based motility of pathogens. Trends Microbiol *4*, 211-3.

Sarafian, T., Aunis, D., and Bader, M. F. (1987). Loss of proteins from digitonin-permeabilized adrenal chromaffin cells essential for exocytosis. J Biol Chem *262*, 16671-6.

Sarafian, T., Pradel, L. A., Henry, J. P., Aunis, D., and Bader, M. F. (1991). The participation of annexin II (calpactin I) in calcium-evoked exocytosis requires protein kinase C. J-Cell-Biol *114*, 1135-47

Schauenstein, K., Schauenstein, E., and Wick, G. (1978). Fluorescence properties of free and protein bound fluorescein dyes. I. Macrospectrofluorometric measurements. J Histochem Cytochem *26*, 277-83.

Schiavo, G., Gmachl, M. J., Stenbeck, G., Sollner, T. H., and Rothman, J. E. (1995). A possible docking and fusion particle for synaptic transmission. Nature *378*, 733-6.

Schlegel, A., Volonte, D., Engelman, J. A., Galbiati, F., Mehta, P., Zhang, X. L., Scherer, P. E., and Lisanti, M. P. (1998). Crowded little caves: structure and function of caveolae. Cell Signal *10*, 457-63.

Schnitzer, J. E., Allard, J., and Oh, P. (1995a). NEM inhibits transcytosis, endocytosis, and capillary permeability: implication of caveolae fusion in endothelia. Am J Physiol *268*, H48-55.

Schnitzer, J. E., Liu, J., and Oh, P. (1995b). Endothelial caveolae have the molecular transport machinery for vesicle budding, docking, and fusion including VAMP, NSF, SNAP, annexins, and GTPases. J-Biol-Chem *270*, 14399-404

Schnitzer, J. E., Oh, P., Pinney, E., and Allard, J. (1994). Filipin-sensitive caveolae-mediated transport in endothelium: reduced transcytosis, scavenger endocytosis, and capillary permeability of select macromolecules. J Cell Biol *127*, 1217-32.

Schwendeman, S. P., Costantino, H. R., Gupta, R. K., Siber, G. R., Klibanov, A. M., and Langer, R. (1995). Stabilization of tetanus and diphtheria toxoids against moisture- induced aggregation. Proc Natl Acad Sci U S A *92*, 11234-8.

Sechi, A. S., Wehland, J., and Small, J. V. (1997). The isolated comet tail pseudopodium of Listeria monocytogenes: a tail of two actin filament populations, long and axial and short and random. J-Cell-Biol *137*, 155-67

Seemann, J., Weber, K., and Gerke, V. (1996a). Structural requirements for annexin I-S100C complex-formation. Biochem-J *319*, 123-9

Seemann, J., Weber, K., and Gerke, V. (1997). Annexin I targets S100C to early endosomes. FEBS-Lett *413*, 185-90

Seemann, J., Weber, K., Osborn, M., Parton, R. G., and Gerke, V. (1996b). The association of annexin I with early endosomes is regulated by Ca2+ and requires an intact N-terminal domain. Mol-Biol-Cell *7*, 1359-74

Senda, T., Okabe, T., Matsuda, M., and Fujita, H. (1994). Quick-freeze, deep-etch visualization of exocytosis in anterior pituitary secretory cells: localization and possible roles of actin and annexin II. Cell-Tissue-Res *277*, 51-60

Senda, T., Yamashita, K., Okabe, T., Sugimoto, N., and Matsuda, M. (1998). Intergranular bridges in the anterior pituitary cell and their possible. Cell Tissue Res *292*, 513-9.

Sheets, E. D., Lee, G. M., Simson, R., and Jacobson, K. (1997). Transient confinement of a glycosylphosphatidylinositol-anchored protein in the plasma membrane. Biochemistry *36*, 12449-58.

Shisheva, A., Doxsey, S. J., Buxton, J. M., and Czech, M. P. (1995). Pericentriolar targeting of GDP-dissociation inhibitor isoform 2. Eur J Cell Biol *68*, 143-58.

Shoji-Kasai, Y., Yoshida, A., Sato, K., Hoshino, T., Ogura, A., Kondo, S., Fujimoto, Y., Kuwahara, R., Kato, R., and Takahashi, M. (1992). Neurotransmitter release from synaptotagmin-deficient clonal variants of PC12 cells. Science *256*, 1821-3.

Siffert, J. C., Baldacini, O., Kuhry, J. G., Wachsmann, D., Benabdelmoumene, S., Faradji, A., Monteil, H., and Poindron, P. (1993). Effects of Clostridium difficile

toxin B on human monocytes and macrophages: possible relationship with cytoskeletal rearrangement. Infect Immun *61*, 1082-90.

Sjolin, C., Movitz, C., Lundqvist, H., and Dahlgren, C. (1997). Translocation of annexin XI to neutrophil subcellular organelles. Biochim-Biophys-Acta *1326*, 149-56

Sjolin, C., Stendahl, O., and Dahlgren, C. (1994). Calcium-induced translocation of annexins to subcellular organelles of human neutrophils. Biochem-J *300*, 325-30

Skehel, J. J., and Wiley, D. C. (1998). Coiled coils in both intracellular vesicle and viral membrane fusion. Cell *95*, 871-4.

Sladeczek, F., Camonis, J. H., Burnol, A. F., and Le Bouffant, F. (1997). The Cdk-like protein PCTAIRE-1 from mouse brain associates with p11 and 14-3-3 proteins. Mol-Gen-Genet *254*, 571-7

Small, J. V., Herzog, M., and Anderson, K. (1995). Actin filament organization in the fish keratocyte lamellipodium. J Cell Biol *129*, 1275-86.

Smith, G. A., Portnoy, D. A., and Theriot, J. A. (1995). Asymmetric distribution of the Listeria monocytogenes ActA protein is required and sufficient to direct actin-based motility. Mol Microbiol *17*, 945-51.

Smith, G. A., Theriot, J. A., and Portnoy, D. A. (1996). The tandem repeat domain in the Listeria monocytogenes ActA protein controls the rate of actin-based motility, the percentage of moving bacteria, and the localization of vasodilator-stimulated phosphoprotein and profilin. J Cell Biol *135*, 647-60.

Smith, R. M., Harada, S., Smith, J. A., Zhang, S., and Jarett, L. (1998). Insulin-induced protein tyrosine phosphorylation cascade and signalling molecules are localized in a caveolin-enriched cell membrane domain. Cell Signal *10*, 355-62.

Smythe, E., Smith, P. D., Jacob, S. M., Theobald, J., and Moss, S. E. (1994). Endocytosis occurs independently of annexin VI in human A431 cells. J-Cell-Biol *124*, 301-6

Sogaard, M., Tani, K., Ye, R. R., Geromanos, S., Tempst, P., Kirchhausen, T., Rothman, J. E., and Sollner, T. (1994). A rab protein is required for the assembly of SNARE complexes in the docking of transport vesicles. Cell *78*, 937-48.

Sollner, T., Bennett, M. K., Whiteheart, S. W., Scheller, R. H., and Rothman, J. E. (1993a). A protein assembly-disassembly pathway in vitro that may correspond to sequential steps of synaptic vesicle docking, activation, and fusion. Cell *75*, 409-18.

Sollner, T., Whiteheart, S. W., Brunner, M., Erdjument-Bromage, H., Geromanos, S., Tempst, P., and Rothman, J. E. (1993b). SNAP receptors implicated in vesicle targeting and fusion. Nature *362*, 318-24.

Solsona, C., Innocenti, B., and Fernandez, J. M. (1998). Regulation of exocytotic fusion by cell inflation. Biophys J *74*, 1061-73.

Song, K. S., Sargiacomo, M., Galbiati, F., Parenti, M., and Lisanti, M. P. (1997). Targeting of a G alpha subunit (Gi1 alpha) and c-Src tyrosine kinase to caveolae membranes: clarifying the role of N-myristoylation. Cell Mol Biol *43*, 293-303.

Sontag, J. M., Aunis, D., and Bader, M. F. (1988). Peripheral actin filaments control calcium-mediated catecholamine release from streptolysin-O-permeabilized chromaffin cells. Eur J Cell Biol *46*, 316-26.

Spector, I., Shochet, N. R., Blasberger, D., and Kashman, Y. (1989). Latrunculins--novel marine macrolides that disrupt microfilament organization and affect cell growth: I. Comparison with cytochalasin D. Cell Motil Cytoskeleton *13*, 127-44.

Spudich, A. (1994). Myosin reorganization in activated RBL cells correlates temporally with stimulated secretion. Cell Motil Cytoskeleton *29*, 345-53.

Spudich, A., and Braunstein, D. (1995). Large secretory structures at the cell surface imaged with scanning force microscopy. Proc Natl Acad Sci U S A *92*, 6976-80.

Stan, R. V., Roberts, W. G., Predescu, D., Ihida, K., Saucan, L., Ghitescu, L., and Palade, G. E. (1997). Immunoisolation and partial characterization of endothelial plasmalemmal vesicles (caveolae). Mol-Biol-Cell *8*, 595-605

Stossel, T. P., Hartwig, J. H., Yin, H. L., Southwick, F. S., and Zaner, K. S. (1984). The motor of leukocytes. Fed Proc *43*, 2760-3.

Stout, A. L., and Axelrod, D. (1989). Evanescent field excitation of fluorescence by epi-illumination microscopy. Applied Optics *28*.

Stutzin, A., Cabantchik, Z. I., Lelkes, P. I., and Pollard, H. B. (1987). Synexin-mediated fusion of bovine chromaffin granule ghosts. Effect of pH. Biochim-Biophys-Acta *905*, 205-12

Sudhof, T. C. (1995). The synaptic vesicle cycle: a cascade of protein-protein interactions. Nature *375*, 645-53.

Sugimori, M., Lang, E. J., Silver, R. B., and Llinas, R. (1994). High-resolution measurement of the time course of calcium-concentration microdomains at squid presynaptic terminals. Biol Bull *187*, 300-3.

Suzuki, H., Komiyama, M., Konno, A., and Shimada, Y. (1998). Exchangeability of actin in cardiac myocytes and fibroblasts as determined by fluorescence photobleaching recovery. Tissue Cell *30*, 274-80.

Suzuki, T., Miki, H., Takenawa, T., and Sasakawa, C. (1998). Neural Wiskott-Aldrich syndrome protein is implicated in the actin- based motility of Shigella flexneri. Embo J *17*, 2767-76.

Swanson, J. A. (1989). Phorbol esters stimulate macropinocytosis and solute flow through macrophages. J Cell Sci *94*, 135-42.

Swanson, J. A., Johnson, M. T., Beningo, K., Post, P., Mooseker, M., and Araki, N. (1999). A contractile activity that closes phagosomes in macrophages. J Cell Sci *112*, 307-316.

Swanson, J. A., Yirinec, B. D., and Silverstein, S. C. (1985). Phorbol esters and horseradish peroxidase stimulate pinocytosis and redirect the flow of pinocytosed fluid in macrophages. J Cell Biol *100*, 851-9.

Symons, M., Derry, J. M., Karlak, B., Jiang, S., Lemahieu, V., McCormick, F., Francke, U., and Abo, A. (1996). Wiskott-Aldrich syndrome protein, a novel effector for the GTPase CDC42Hs, is implicated in actin polymerization. Cell *84*, 723-34.

Tahara, M., Coorssen, J. R., Timmers, K., Blank, P. S., Whalley, T., Scheller, R., and Zimmerberg, J. (1998). Calcium can disrupt the SNARE protein complex on sea urchin egg secretory vesicles without irreversibly blocking fusion. J Biol Chem *273*, 33667-73.

Tanaka, K., Tashiro, T., Sekimoto, S., and Komiya, Y. (1994). Axonal transport of actin and actin-binding proteins in the rat sciatic nerve. Neurosci-Res *19*, 295-302

Temm Grove, C. J., Jockusch, B. M., Rohde, M., Niebuhr, K., Chakraborty, T., and Wehland, J. (1994). Exploitation of microfilament proteins by Listeria monocytogenes: microvillus-like composition of the comet tails and vectorial spreading in polarized epithelial sheets. J-Cell-Sci *107*, 2951-60.

Teo, M., Manser, E., and Lim, L. (1995). Identification and molecular cloning of a p21cdc42/rac1-activated serine/threonine kinase that is rapidly activated by thrombin in platelets. J Biol Chem *270*, 26690-7.

TerBush, D. R., Maurice, T., Roth, D., and Novick, P. (1996). The Exocyst is a multiprotein complex required for exocytosis in Saccharomyces cerevisiae. Embo J *15*, 6483-94.

Teter, K., Chandy, G., Quinones, B., Pereyra, K., Machen, T., and Moore, H. P. (1998). Cellubrevin-targeted fluorescence uncovers heterogeneity in the recycling endosomes. J Biol Chem *273*, 19625-33.

Theriot, J. A., Mitchison, T. J., Tilney, L. G., and Portnoy, D. A. (1992). The rate of actin-based motility of intracellular Listeria monocytogenes equals the rate of actin polymerization. Nature *357*, 257-60.

Thiel, C., Osborn, M., and Gerke, V. (1992). The tight association of the tyrosine kinase substrate annexin II with the submembranous cytoskeleton depends on intact p11- and Ca(2+) binding sites. J Cell Sci *103*, 733-42.

Tilney, L. G., and Portnoy, D. A. (1989). Actin filaments and the growth, movement, and spread of the intracellular bacterial parasite, Listeria monocytogenes. J Cell Biol *109*, 1597-608.

Tilney, L. G., DeRosier, D. J., and Tilney, M. S. (1992). How Listeria exploits host cell actin to form its own cytoskeleton. I. Formation of a tail and how that tail might be involved in movement. J Cell Biol *118*, 71-81.

Tokumitsu, H., Mizutani, A., and Hidaka, H. (1993). Calcyclin-binding site located on the NH2-terminal domain of rabbit CAP-50 (annexin XI): functional expression of CAP-50 in Escherichia coli. Arch-Biochem-Biophys *303*, 302-6

Tooze, J., and Hollinshead, M. (1991). Tubular early endosomal networks in AtT20 and other cells. J Cell Biol *115*, 635-53.

Tressler, R. J., Updyke, T. V., Yeatman, T., and Nicolson, G. L. (1993). Extracellular annexin II is associated with divalent cation-dependent tumor cell-endothelial cell adhesion of metastatic RAW117 large-cell lymphoma cells. J-Cell-Biochem *53*, 265-76

Trotter, P. J., Orchard, M. A., and Walker, J. H. (1995a). Ca^{2+} concentration during binding determines the manner in which annexin V binds to membranes. Biochem-J *308*, 591-8

Trotter, P. J., Orchard, M. A., and Walker, J. H. (1995b). EGTA-resistant binding of annexin V to platelet membranes can be induced by physiological calcium concentrations. Biochem-Soc-Trans *23*, 37S

Tsien, R. Y. (1998). The green fluorescent protein. Annu Rev Biochem *67*, 509-44.

Turpin, E., Russo-Marie, F., Dubois, T., de Paillerets, C., Alfsen, A., and Bomsel, M. (1998). In adrenocortical tissue, annexins II and VI are attached to clathrin coated vesicles in a calcium-independent manner. Biochim Biophys Acta *1402*, 115-30.

Ueda, M., Graf, R., MacWilliams, H. K., Schliwa, M., and Euteneuer, U. (1997). Centrosome positioning and directionality of cell movements. Proc Natl Acad Sci U S A *94*, 9674-8.

Ullrich, B., Li, C., Zhang, J. Z., McMahon, H., Anderson, R. G., Geppert, M., and Sudhof, T. C. (1994). Functional properties of multiple synaptotagmins in brain. Neuron *13*, 1281-91.

Ullrich, O., Reinsch, S., Urbe, S., Zerial, M., and Parton, R. G. (1996). Rab11 regulates recycling through the pericentriolar recycling endosome. J Cell Biol *135*, 913-24.

Upton, A. L. (1994). Annexin II and exocytosis. PhD Thesis, University College, London.

Valentine Braun, K. A., Hollenberg, M. D., Fraser, E., and Northup, J. K. (1987). Isolation of a major human placental substrate for the epidermal growth factor

(urogastrone) receptor kinase: immunological cross-reactivity with transducin and sequence homology with lipocortin. Arch-Biochem-Biophys *259*, 262-82

van Bilsen, M., Reutelingsperger, C. P., Willemsen, P. H., Reneman, R. S., and van der Vusse, G. J. (1992). Annexins in cardiac tissue: cellular localization and effect on phospholipase activity. Mol-Cell-Biochem *116*, 95-101

van der Goot, F. G. (1997). Separation of early steps in endocytic membrane transport. Electrophoresis *18*, 2689-93.

Varma, R., and Mayor, S. (1998). GPI-anchored proteins are organized in submicron domains at the cell surface. Nature *394*, 798-801.

Varticovski, L., Chahwala, S. B., Whitman, M., Cantley, L., Schindler, D., Chow, E. P., Sinclair, L. K., and Pepinsky, R. B. (1988). Location of sites in human lipocortin I that are phosphorylated by protein tyrosine kinases and protein kinases A and C. Biochemistry *27*, 3682-90

Veithen, A., Cupers, P., Baudhuin, P., and Courtoy, P. J. (1996). v-Src induces constitutive macropinocytosis in rat fibroblasts. J Cell Sci *109*, 2005-12.

Vishwanatha, J. K., Chiang, Y., Kumble, K. D., Hollingsworth, M. A., and Pour, P. M. (1993). Enhanced expression of annexin II in human pancreatic carcinoma cells and primary pancreatic cancers. Carcinogenesis *14*, 2575-9

Vitale, M. L., Seward, E. P., and Trifaro, J. M. (1995). Chromaffin cell cortical actin network dynamics control the size of the release-ready vesicle pool and the initial rate of exocytosis. Neuron *14*, 353-63.

Waisman, D. M. (1995). Annexin II tetramer: structure and function. Mol Cell Biochem *150*, 301-22.

Wang, S., and Hazelrigg, T. (1994). Implications for bcd mRNA localization from spatial distribution of exu protein in Drosophila oogenesis. Nature *369*, 400-03.

Wang, W., and Creutz, C. E. (1994). Role of the amino-terminal domain in regulating interactions of annexin I with membranes: effects of amino-terminal truncation and mutagenesis of the phosphorylation sites. Biochemistry *33*, 275-82

Watanabe, T., Inui, M., Chen, B. Y., Iga, M., and Sobue, K. (1994). Annexin VI-binding proteins in brain. Interaction of annexin VI with a membrane skeletal protein, calspectin (brain spectrin or fodrin). J-Biol-Chem *269*, 17656-62

Weber, T., Zemelman, B. V., McNew, J. A., Westermann, B., Gmachl, M., Parlati, F., Sollner, T. H., and Rothman, J. E. (1998). SNAREpins: minimal machinery for membrane fusion. Cell *92*, 759-72.

Weng, X., Luecke, H., Song, I. S., Kang, D. S., Kim, S. H., and Huber, R. (1993). Crystal structure of human annexin I at 2.5 A resolution. Protein-Sci *2*, 448-58 issn: 0961-8368.

Westphal, M., Jungbluth, A., Heidecker, M., Muhlbauer, B., Heizer, C., Schwartz, J. M., Marriott, G., and Gerisch, G. (1997). Microfilament dynamics during cell movement and chemotaxis monitored using a GFP-actin fusion protein. Curr Biol *7*, 176-83.

Wice, B. M., and Gordon, J. I. (1992). A strategy for isolation of cDNAs encoding proteins affecting human intestinal epithelial cell growth and differentiation: characterization of a novel gut-specific N-myristoylated annexin. J-Cell-Biol *116*, 405-22

Willingham, M. C., and Pastan, I. (1985). Ultrastructural immunocytochemical localization of the transferrin receptor using a monoclonal antibody in human KB cells. J Histochem Cytochem *33*, 59-64.

Wilton, J. C., Matthews, G. M., Burgoyne, R. D., Mills, C. O., Chipman, J. K., and Coleman, R. (1994). Fluorescent choleretic and cholestatic bile salts take different paths across the hepatocyte: transcytosis of glycolithocholate leads to an extensive redistribution of annexin II. J-Cell-Biol *127*, 401-10

Witke, W., Podtelejnikov, A. V., Di Nardo, A., Sutherland, J. D., Gurniak, C. B., Dotti, C., and Mann, M. (1998). In mouse brain profilin I and profilin II associate with regulators of the endocytic pathway and actin assembly. Embo J *17*, 967-76.

Wright, J. F., Kurosky, A., and Wasi, S. (1994). An endothelial cell-surface form of annexin II binds human cytomegalovirus. Biochem-Biophys-Res-Commun *198*, 983-9

Wright, J. F., Kurosky, A., Pryzdial, E. L., and Wasi, S. (1995). Host cellular annexin II is associated with cytomegalovirus particles isolated from cultured human fibroblasts. J-Virol *69*, 4784-91

Wu, Y. N., and Wagner, P. D. (1991). Calpactin-depleted cytosolic proteins restore Ca(2+)-dependent secretion to digitonin-permeabilized bovine chromaffin cells. FEBS-Lett *282*, 197-9

Wu, Y. N., Vu, N. D., and Wagner, P. D. (1992). Anti-(14-3-3 protein) antibody inhibits stimulation of noradrenaline (norepinephrine) secretion by chromaffin-cell cytosolic proteins. Biochem J *285*, 697-700.

Wymann, M., and Arcaro, A. (1994). Platelet-derived growth factor-induced phosphatidylinositol 3-kinase activation mediates actin rearrangements in fibroblasts. Biochem J *3*, 517-20.

Xiao, B., Smerdon, S. J., Jones, D. H., Dodson, G. G., Soneji, Y., Aitken, A., and Gamblin, S. J. (1995). Structure of a 14-3-3 protein and implications for coordination of multiple signalling pathways. Nature *376*, 188-91.

Xu, K., Williams, R. M., Holowka, D., and Baird, B. (1998). Stimulated release of fluorescently labeled IgE fragments that efficiently accumulate in secretory granules after endocytosis in RBL- 2H3 mast cells. J Cell Sci *111*, 2385-96.

Yeatman, T. J., Updyke, T. V., Kaetzel, M. A., Dedman, J. R., and Nicolson, G. L. (1993). Expression of annexins on the surfaces of non-metastatic and metastatic human and rodent tumor cells. Clin-Exp-Metastasis *11*, 37-44 issn: 0262-0898.

Young, P. R., McLaughlin, M. M., Kumar, S., Kassis, S., Doyle, M. L., McNulty, D., Gallagher, T. F., Fisher, S., McDonnell, P. C., Carr, S. A., Huddleston, M. J., Seibel, G., Porter, T. G., Livi, G. P., Adams, J. L., and Lee, J. C. (1997). Pyridinyl imidazole inhibitors of p38 mitogen-activated protein kinase bind in the ATP site. J Biol Chem *272*, 12116-21.

Yumura, S., and Fukui, Y. (1998). Spatiotemporal dynamics of actin concentration during cytokinesis and locomotion in Dictyostelium. J Cell Sci *111*, 2097-108.

Zaks, W. J., and Creutz, C. E. (1990). Evaluation of the annexins as potential mediators of membrane fusion in exocytosis. J-Bioenerg-Biomembr *22*, 97-120

Zeile, W. L., Condit, R. C., Lewis, J. I., Purich, D. L., and Southwick, F. S. (1998). Vaccinia locomotion in host cells: evidence for the universal involvement of actin-based motility sequences ABM-1 and ABM-2. Proc Natl Acad Sci U S A *95*, 13917-22.

Zeile, W. L., Purich, D. L., and Southwick, F. S. (1996). Recognition of two classes of oligoproline sequences in profilin- mediated acceleration of actin-based Shigella motility. J Cell Biol *133*, 49-59.

Zhang, L., Marcu, M. G., Nau-Staudt, K., and Trifaro, J. M. (1996). Recombinant scinderin enhances exocytosis, an effect blocked by two scinderin-derived actin-binding peptides and PIP2. Neuron *17*, 287-96.

Zhang, S., Han, J., Sells, M. A., Chernoff, J., Knaus, U. G., Ulevitch, R. J., and Bokoch, G. M. (1995). Rho family GTPases regulate p38 mitogen-activated protein kinase through the downstream mediator Pak1. J Biol Chem *270*, 23934-6.

Zheng, X., and Bobich, J. A. (1998). A sequential view of neurotransmitter release. Brain Res Bull *47*, 117-28.

Zheng, Y., Bagrodia, S., and Cerione, R. A. (1994). Activation of phosphoinositide 3-kinase activity by Cdc42Hs binding to p85. J Biol Chem *269*, 18727-30.

Zhukarev, V., Ashton, F., Sanger, J. M., Sanger, J. W., and Shuman, H. (1995). Organization and structure of actin filament bundles in Listeria- infected cells. Cell Motil Cytoskeleton *30*, 229-46.

Zokas, L., and Glenney, J. R., Jr. (1987). The calpactin light chain is tightly linked to the cytoskeletal form of calpactin I: studies using monoclonal antibodies to calpactin subunits. J-Cell-Biol *105*, 2111-21